BEST AVAILABLE IMAGES

Defective images within this document are accurate representations of the original documents submitted by the applicant.

Defects in the images may include (but are not limited to):

- BLACK BORDERS
- TEXT CUT OFF AT TOP, BOTTOM OR SIDES
- FADED TEXT
- ILLEGIBLE TEXT
- SKEWED/SLANTED IMAGES
- COLORED PHOTOS
- BLACK OR VERY BLACK AND WHITE DARK PHOTOS
- GRAY SCALE DOCUMENTS

IMAGES ARE BEST AVAILABLE COPY.

As rescanning documents *will not* correct images, please do not report the images to the Image Problems Mailbox.

STIC-ILL

QH442.G43
+
mic

From: Helms, Larry
Sent: Friday, March 23, 2001 2:38 PM
To: STIC-ILL
Subject: 09/489394

Please send the following:

Biochem. Biophys. Res. Commun. (1978), 83(4), 1284-90

Can. J. Biochem. (1979), 57(3), 279-85

J. Exp. Med. (1981), 154(5), 1554-69

J. Biochem. (Tokyo) (1978), 83(5), 1249-63

J. Biol. Chem. (1982), 257(7), 3811-18

Biochim. Biophys. Acta (1984), 787(1), 39-44

Mol. Immunol. (1988), 25(10), 1019-24

Nucl. Med. Biol. (1991), 18(7), 695-703

J. Exp. Med. (1992), 176(4), 1191-5

Bioconjugate Chem. (1993), 4(2), 153-65

Gene (1993), 128(2), 203-9

Clin. Diagn. Lab. Immunol. (1997), 4(2), 147-155

Mol. Immunol. (1999), 36(11-12), 777-788

thank you,

Larry

Larry Helms
AU 1642
CM-1
8D08

Gene, 128 (1993) 203–209

GENE 07105

Efficient secretion of murine Fab fragments by *Escherichia coli* is determined by the first constant domain of the heavy chain

(Periplasmic space; 2-phenyloxazolone; recombinant antibody; assembly and expression; stability)

Kaija Alfthan[a], Kristiina Takkinen[a], Dorothea Sizmann[a], Ilkka Seppälä[b], Tiina Immonen[a], Liisa Vanne[a], Sirkka Keränen[a], Matti Kaartinen[b], Jonathan K.C. Knowles*[a] and Tuula T. Teeri[a]

[a]*VTT Biotechnical Laboratory, SF-02151 Espoo, Finland; and* [b]*Department of Bacteriology and Immunology, University of Helsinki, SF-00290 Helsinki, Finland*

Received by R.W. Davies: 17 July 1992; Revised/Accepted: 7 November/19 December 1992; Received at publishers: 18 February 1993

SUMMARY

Fab fragments of IgG1 and IgG3 subclass antibodies which bind to 2-phenyloxazolone (Ox) were produced in *Escherichia coli*. The signal sequences of the Fd and L chains were correctly processed, the fragments were secreted into the periplasmic space and released into the culture medium upon prolonged cultivations. The yields of active Ox IgG1 and Ox IgG3 Fab fragments after one-step purification from the culture medium by affinity chromatography were 2 μg/ml and 0.5 μg/ml, respectively. The majority of the purified Ox IgG1 Fab was properly assembled, but in the case of Ox IgG3, the preparation was found to consist of a complete L chain and C-terminally degraded fragments of the Fd chain. A deletion up to the interchain disulfide bond in the first constant domain (CH1) of the Ox IgG3 Fd chain led to proper assembly of the truncated Fab fragment. The production level of the truncated fragment was comparable to that of the Ox IgG1 Fab and its hapten-binding activity similar to that of the idiotype monoclonal antibody. The temperature stability of the Ox IgG1 Fab was similar to that of the intact antibody. However, both of the Ox IgG3 Fab fragments showed reduced stability, suggesting that the CH1 domain contributes significantly to the thermal stability of the Fab fragment.

INTRODUCTION

The highly selective hapten-binding properties of antibodies (Ab) make them important tools in research, diagnostics and medicine. For many applications, only the antigen-binding domains of Ab are required and the rest of the protein is unnecessary or even deleterious. The microbial expression systems developed in recent years provide valuable alternatives for the production of functional Ab fragments and facilitate considerably the engineering of novel antibodies (for reviews see, e.g., Plückthun, 1991; Winter and Milstein, 1991). A number

Correspondence to: Dr. Kaija Alfthan, VTT Biotechnical Laboratory, PO Box 202, SF-02151 Espoo, Finland. Tel. (358-0) 4565106; Fax (358-0) 4552028; e-mail kaija.alfthan@vtt.fi

*Present address: Glaxo Institute for Molecular Biology, 14 chemin des Aulx, 1228 Plan-les-Ouates, Geneva, Switzerland, Tel. (41-22) 7069928

Abbreviations: *A*, absorbance (1 cm); aa, amino acid(s); Ab, antibody(ies); Ap, ampicillin; bp, base pair(s); cDNA, DNA complementary to RNA; CH1, first constant domain of the immunoglobulin heavy chain; ELISA, enzyme-linked immunosorbent assay; Fab, antigen-binding fragment (Fd and L chains); $F(ab)_2$, bivalent Ab fragment (two Fab fragments); Fc, fragment mediating effector functions; Fd, truncated heavy chain (VH and CH1 domains); Fv, antigen-binding fragment (VH and VL domains); H, heavy chain; IPTG, isopropyl-β-D-thiogalactopyranoside; K_a, affinity constant; L, light chain; LB, Luria-Bertani (medium); mAb, monoclonal Ab; oligo, oligodeoxyribonucleotide; ORF, open reading frame; Ox, 2-phenyloxazolone; PAGE, polyacrylamide-gel electrophoresis; PCR, polymerase chain reaction; PMSF, phenylmethylsulfonyl fluoride; scFv, single-chain Ab; SDS, sodium dodecyl sulfate; VH, variable domain of the heavy chain; VL, variable domain of the light chain.

of different Fab fragments have been expressed in *E. coli* either intracellularly (Cabilly, 1989; Condra et al., 1990; Buchner and Rudolph, 1991) or by co-secretion of the L and Fd chains to the periplasm where the intra- and interdomain disulfide bonds are formed and the chains fold and assemble into an active Fab fragment (Better et al., 1988; Better and Horwitz, 1989; Plückthun and Skerra, 1989; Anand et al., 1991a; Skerra and Plückthun, 1991; Carter et al., 1992). The size of Ab fragments produced in *E. coli* can be further reduced to consist of only one or both of the antigen-binding domains. Examples of such minimized antibody molecules include Fv fragments which consist of the two variable domains (VL, VH) (Skerra and Plückthun, 1988; Glockshuber et al., 1990), single-chain Ab (scFv) with a flexible linker peptide between the VH and VL domains (Bird et al., 1988; Huston et al., 1988; Chaudhary et al., 1989; Anand et al., 1991b; Takkinen et al., 1991) and single VH domains (Ward et al., 1988; Power et al., 1992). Differences in the production levels of the various Ab fragments derived from the same parent mAb in microbes have been reported. In the case of the phosphorylcholine-binding Ab McPC603 a functional Fv fragment was produced and secreted to the periplasm of *E. coli* significantly more efficiently than the corresponding Fab (Skerra and Plückthun, 1991) or scFv fragment (Glockshuber et al., 1990). In our previous study IgM-Fab fragments recognizing 4-hydroxy-5-iodo-3-nitrophenyl acetyl (NIP) were produced in yeast *Saccharomyces cerevisiae* using two different Fd chain constructions. In one, the CH1 domain was intact and in the other six aa from the C terminus were missing. In this case only the longer form allowed secretion of active Fab fragment into the culture medium (Edqvist et al., 1991).

In this study we have produced 2-phenyloxazolone (Ox) binding IgG1 and IgG3 Fab fragments into the culture medium of *E. coli* using the expression system described earlier for the Ox scFv (Takkinen et al., 1991). Two different constructions of the Ox IgG3 were made: in the first one, the CH1 region was complete and in the second most of the CH1 domain was deleted. The production levels and properties of the Ox IgG1 and Ox IgG3 Fab fragments were compared. Based on the results, we suggest that the CH1 domain of the Ox IgG3 Fd chain has properties that do not allow efficient production of a functional Ox IgG3 Fab fragment in *E. coli* and that it is the CH1 domain that largely determines the stability of a Fab fragment.

RESULTS AND DISCUSSION

(a) Expression and production of the Ox Fab fragments

The cDNAs of the Ox Fd and L chains were assembled as a dicistronic operon under the *tac* promoter (Fig. 1).

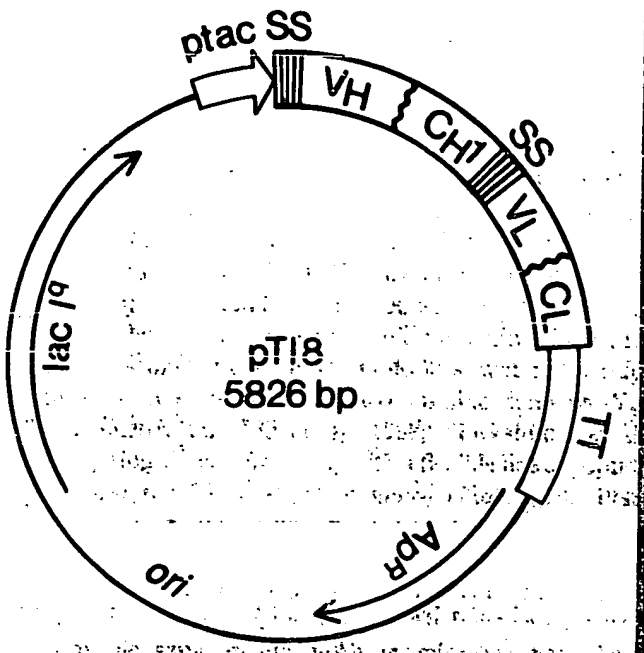

Fig. 1. Plasmid pTI8, the *E. coli* expression vector for the Ox IgG1 Fab fragment. The Fab expression units were cloned into the tightly regulated *E. coli* expression vector containing the *tac* promoter (*ptac*), the transcription termination region (*TT*) derived from pKK223-3 plasmid (Pharmacia), and genes for ampicillin resistance (Ap^R) and *lac* repressor ($lacI^q$) from pMJR156C plasmid (Amersham). The expression constructions were transformed into *E. coli* strain RV308 (Schöner et al., 1985), which was used as the production host. Methods: The mRNAs of the L and H chain of the Ox IgG3 and Ox IgG1 subclass antibodies were isolated from hybridoma cell clones H26 and NQ2-17.4.1, respectively (Kaartinen et al., 1983; 1989). The first strand cDNAs of the H and L chains were synthesized using an oligo(dT) primer and 5 μg of mRNAs (Maniatis et al., 1982). The PCR primers provided with restriction enzyme cleavage sites for the cloning were synthesized according to published mRNA sequences of the Ox H and L chains (Kaartinen et al., 1983; 1989). The cDNA:mRNA hybrids were directly subjected to PCR amplification. The PCR reaction mixture (100 μl) contained 5 μl of the first-strand cDNA synthesis reaction mixture, 10 μl 10 × reaction buffer (100 mM Tris pH 8.0/10 mM $MgCl_2$/50 mM KCl/1 mM β-mercaptoethanol/1 mg gelatin per ml)/16 μl 1.25 mM dNTPs/100 pmol of primers/2.5 units *Taq* polymerase (US Biochemical, Cleveland, OH). The amplification (25 cycles) consisted of denaturation at 94°C for 1 min, annealing at 55°C for 30 s and polymerization at 72°C for 1.5 min. The complete Ox IgG3 and Ox IgG1 Fab fragment expression units were first assembled in the pSP73 plasmid (Promega, Madison, WI, USA). The signal sequence(SS)-coding region of pectate lyase (PelB) of *Erwinia carotovora* (Lei et al., 1987; Better et al., 1988) and the intergenic DNA sequence (Schöner et al., 1986) between the ORFs of the Fd and L chain were cloned from overlapping oligos using the method of Hill et al. (1987). The cDNAs of the Fd and L chains were modified with PCR (Sambrook et al., 1989) to provide them with restriction sites, which allowed precise in frame fusions of the Fab expression units. The Ox IgG3ΔC_H was constructed by deleting an internal *Bam*HI-*Bcl*I fragment from the IgG3 chain constant domain coding region resulting in deletion of 72 aa (aa 134–206) of the Fd chain.

Both the Fd and L chain genes were fused with the pectate lyase (PelB) signal sequence coding region of *Erwinia carotovora* (Lei et al., 1987). The PelB signal sequence has

previously been utilized to obtain efficient periplasmic secretion and subsequent release of antibody fragments into the culture medium (Better et al., 1988; Ward et al., 1988; Takkinen et al., 1991).

Immunoblot analysis under nonreducing conditions (Fig. 2) showed that about half of the produced Ox IgG1 Fd and L chains (23.9 kDa and 23.3 kDa, respectively) were assembled in the periplasmic space of *E. coli* to the Fab fragment (47.2 kDa). The Fab fragment was released already after 3 h induction to the culture medium and the amount was gradually increased during overnight inductions up to 3–5 μg/ml. In the case of the Ox IgG3 sample only a faint band corresponding to the calculated 46.5-kDa Fab was detected in the immunoblot but a major band was migrating at the position of unassociated chains.

The L chains of the Ox IgG1 and Ox IgG3 Fab fragments are identical, and the VH regions differ only by five aa residues within the D-J region. Thus, the major difference between the two Fd chains lies in the aa sequence and in the interchain disulfide bond arrangement of the CH1 domain (Fig. 3). To test whether we could facilitate the disulfide bond formation and perhaps thereby the assembly of the Ox IgG3 Fab in *E. coli*, we deleted most of the C-terminal part of the CH1 region but retained the $Cys^{128}H$ participating in the interchain disulfide bond formation (Fig. 3). Interestingly, the truncated Ox IgG3 Fd chain was now able to assemble to the L chain and form the interchain disulfide bond. The truncated Fab fragment formed (Ox IgG3ΔC_H of

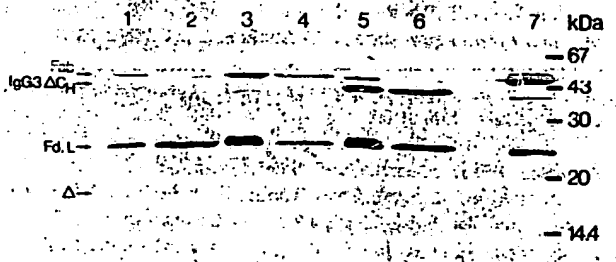

Fig. 2. Immunoblot analysis of the Ox Fab fragments in the periplasmic (PP) extracts and in culture supernatants (S) after 3 h of induction. Equal amounts of the samples were run on a 0.1% SDS-15% polyacrylamide gel under nonreducing conditions (Laemmli, 1970), and then transferred onto a nitrocellulose filter (Towbin et al., 1979). The Ox Fab fragments were detected as described earlier (Takkinen et al., 1991). Lane 1, PP and lane 2, S of *E. coli* producing Ox IgG3 Fab; lane 3, PP and lane 4, S of *E. coli* producing Ox IgG1 Fab; lane 5, PP and lane 6, S of *E. coli* producing IgG3ΔC_H; lane 7, proteolytically produced Ox IgG1 Fab (for digestion and purification see the legend of Fig. 4). Arrows on the left indicate the positions of the Ox IgG1 and Ox IgG3 Fab (Fab), the truncated Ox IgG3 Fab (IgG3ΔC_H), unassociated chains (Fd, L) and the truncated Ox IgG3 Fd chain (Δ). Methods: The RV308 cells were grown at 30°C in LB medium containing 100 μg Ap/ml to an A_{600} of about 1.5 after which IPTG was added to a final concentration of 1 mM. After 3 h of induction the cells were harvested and fractionated according to Sambrook et al. (1989).

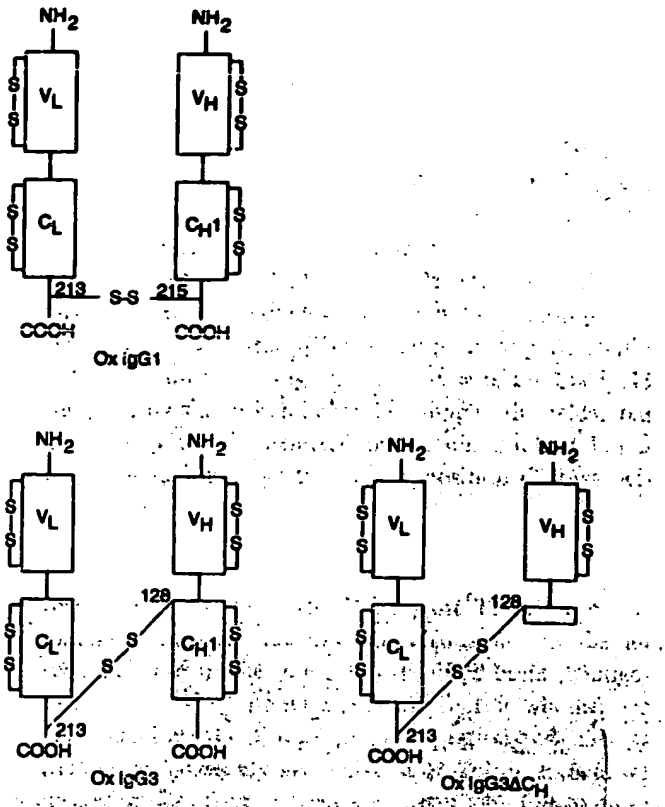

Fig. 3. Schematic presentation of the interchain disulfide bond arrangement in the Ox Fab fragments. In the Ox IgG1 Fab the bond is formed between the L chain Cys^{213} ($Cys^{213}L$) and Cys^{215} of the H chain ($Cys^{215}H$). In the Ox IgG3 the Cys^{128} ($Cys^{128}H$) located in the N terminus of the CH1 domain participates in the interchain disulfide bond formation. The $Cys^{128}H$ is retained in the truncated Ox IgG3 Fd chain.

38.4 kDa) was clearly detected in the immunoblot analysis (Fig. 2). Some unassociated L chain was also observed, whereas the unassociated truncated Fd chain (15.1 kDa) was poorly identified by the antiserum used for immunoblotting and thus was hardly detectable.

As estimated by ELISA from the overnight culture medium of *E. coli* the production levels of active Ox IgG1 Fab and Ox IgG3ΔC_H fragments were 3–5 μg/ml. This is comparable to the levels we have obtained earlier for the corresponding Ox scFv (Takkinen et al., 1991). However, the active Ox IgG3 Fab was produced only up to 1–2 μg/ml. The amounts of functional Ox IgG1 Fab and Ox IgG3ΔC_H fragments released into the culture medium were obtained without optimizing the growth conditions. Immunoblot analysis of the cytoplasmic extracts showed that only less than half of the produced Fd and L chains were secreted to the periplasmic space (data not shown). Thus, by designing a microbial host with good secretory capacities and/or using the more precisely controlled environment in a fermentor the efficiency of production can be further improved. Recently, amounts up to 1–2 mg/ml of secreted and functional Fab

fragments have been obtained in *E. coli* (Carter et al., 1992).

(b) Purification of the Ox Fab fragments

The yields of active Fab fragments after one-step purification by affinity chromatography from the overnight culture medium of *E. coli* were 2 μg/ml for the Ox IgG1 Fab and Ox IgG3ΔC$_H$ and 0.5 μg/ml for the Ox IgG3 Fab preparation. Correct processing of the PelB signal sequence was confirmed by determining the first five N-terminal aa residues of the L and Fd chains using the method of Baumann (1990) (data not shown).

SDS–PAGE analysis of the purified samples under both nonreducing and reducing conditions is shown in Fig. 4. Ox IgG1 and Ox IgG3 Fab fragments digested proteolytically from the corresponding idiotype mAbs were used as controls. In nonreducing conditions the bacterially produced Ox IgG1 Fab was seen as a major band comigrating with the proteolytically produced Ox IgG1 Fab (Fig. 4A). Under reducing conditions the Fd and L chains overlap and only one band was observed (Fig. 4B).

The purified Ox IgG3 Fab preparation analyzed in nonreducing SDS–PAGE gave several bands (Fig. 4A). N-terminal aa sequencing revealed that the 23-kDa band obtained was a correctly processed L chain and no intact Fd chain was detected. Instead, the two smaller bands appearing on the gel contained correct N-termini of the Ox IgG3 Fd chain which indicates C-terminal proteolytic degradation. In another set of experiments three degradation products of the Fd chain were identified (data not shown). A faint band of about 38 kDa observed in the nonreducing gel suggests that a small amount of a fragment composed of the L chain covalently bound to a degraded Fd chain was formed. Production of the Ox IgG3 Fab in the presence of a protease inhibitor mixture containing PMSF (100 μg/ml), aprotinin (2 μg/ml), pepstatin A (1 μg/ml) and EDTA (1 mM) or the use of an *E. coli* strain defective in the main periplasmic protease OmpT (Earhart et al., 1979) did not reduce the observed degradation of the Fd chain (data not shown).

Sensitivity to proteases has been used as an indication of incomplete folding of a protein (Randall and Hardy,

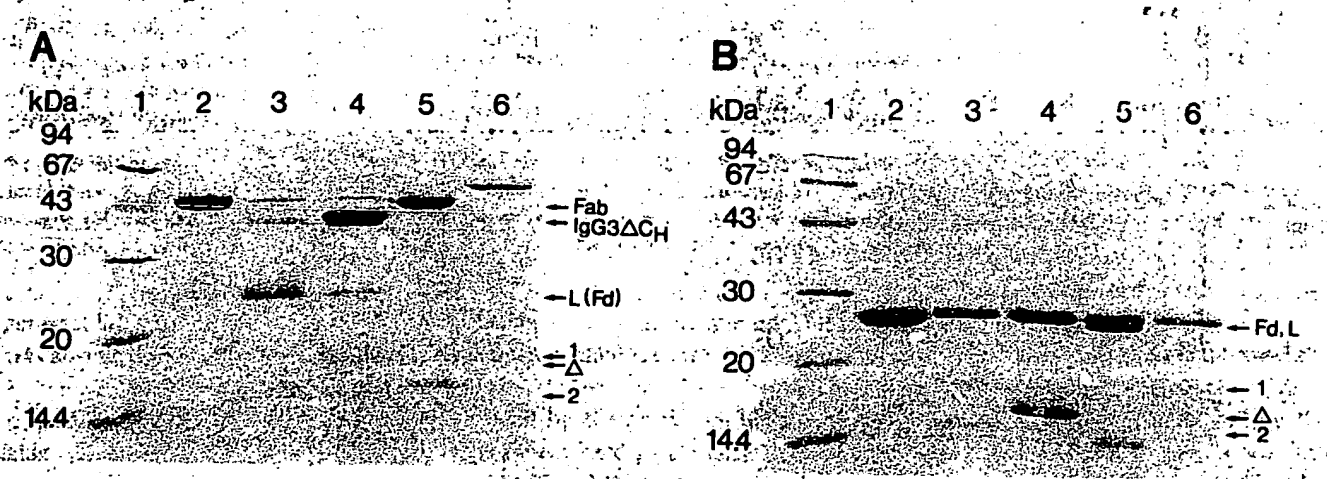

Fig. 4. SDS–PAGE analysis of the purified Ox Fab fragments produced into the culture medium of *E. coli*. For comparison, the Ox Fab fragments produced by papain digestion from the parent mAbs are shown. Equal amounts of the samples were analyzed on 0.1% SDS-15% polyacrylamide gels under nonreducing (A) and reducing (B) conditions. Gels were stained with Coomassie brilliant blue. Lanes: 1, the size markers; 2, Ox IgG1 Fab; 3, Ox IgG3 Fab; 4, Ox IgG3ΔC$_H$; 5, Ox IgG1 Fab produced by papain digestion from the NQ2–17.4.1 antibody; 6, Ox IgG3 Fab produced by papain digestion from the H26 antibody. Arrows on the right margin indicate positions of the Ox IgG1 and Ox IgG3 Fab (Fab), the truncated Ox IgG3 Fab (IgG3ΔC$_H$), unassociated chains (Fd, L), the truncated Ox IgG3 Fd chain (Δ) and the C-terminal degradation products of the Ox IgG3 Fd chain (bands 1 and 2). **Methods**: the Ox Fab fragments produced in *E. coli* were purified in one step by affinity chromatography as described earlier (Takkinen et al., 1991) from 4 liters of induced overnight culture supernatant. Protein concentrations were determined from the A_{280} values using molar extinction coefficients calculated on the basis of the Tyr and Trp content of each Fab fragment (Wetlaufer, 1962). The NQ2–17.4.1 Ab was purified from mouse ascites on a Protein A-Sepharose (Pharmacia) column (0.7 × 8.5 cm) according to the protocol of the manufacturer and digested to F(ab)$_2$ fragment by papain cleavage in 0.1 M acetate/3 mM EDTA buffer pH 5.5 for approx. 8 h at 37°C, using an enzyme:substrate ratio of 1:30. The reaction was stopped by iodoacetamide (15 mM in the reaction mixture). The Fc fragments and undigested Ox IgG1 antibody were removed on the protein A-Sepharose column. The F(ab)$_2$ was reduced to Fab with 10 mM cysteine in 50 mM phosphate/0.9%NaCl buffer pH 7.4 (PBS) for 2 h at 37°C, and the reaction was stopped with iodoacetamide as above. The final purification was done by S300-HR (Pharmacia) size exclusion chromatography (1.5 × 96 cm) using PBS as the buffer system. The H26 Ab was purified from mouse ascites by applying the euglobulin precipitation method described earlier (Goding, 1986; Garcia-Gonzalez et al., 1988). The purified Ox IgG3 Ab was digested to Fab fragments by papain in 0.1 M Tris pH 8.0/0.05 M NaCl/2 mM EDTA for 1.5 h at 37°C, using an enzyme:substrate ratio of 1:100. The reaction was stopped with iodoacetamide as described above. The Fc fragments and undigested Ox IgG3 were removed on a protein A-Sepharose column (0.7 × 8.5 cm). Final purification was done with fast protein liquid chromatography (FPLC) on a Mono Q HR 5/5 column (0.5 × 5.0 cm, Pharmacia) applying a linear gradient (0–100%) of 0.5 M NaCl in 10 mM ethanolamine pH 9.0.

1986), and in this case, the degradation of the Fd chain may indicate incorrect folding of the Ox IgG3 Fab. Disulfide bonds are known to contribute significantly to the folding and stability of proteins. Recently, it was shown that formation of intrachain disulfide bonds in the VH and VL domains of the McPC603 antibody is essential for the functionality of the Ab fragments produced in *E. coli* (Glockshuber et al., 1992), but we have found no reports on the importance of the interchain disulfide bonds in the production of functional Fab fragments of different IgG subclasses in bacteria. Since the Ox IgG3 Fab differs from the Ox IgG1 Fab with respect to the position of the interchain disulfide bond at the CH1 domain (Fig. 3), the failure to produce functional and stable Ox IgG3 Fab in *E. coli* may indicate that the appropriate chaperones or protein disulfide isomerases (PDI) for the formation of a correct interchain disulfide bond are not available in this case. As seen in Fig. 4A, the truncation of the CH1 domain of the Ox IgG3 Fd chain clearly facilitated the proper assembly and folding of both the L chain and the truncated Fd chain into a functional antigen-binding fragment.

The total amount of the degraded Ox IgG3 Fd chains was significantly lower than the amount of the truncated Fd chain of the Ox IgG3ΔC_H as estimated in SDS–PAGE (Fig. 4B). It has been reported that the antibodies of the IgG3 subclass tend to aggregate and selfassociate (Gyotoko et al., 1987; Jiskoot et al., 1991) and there is one report that the site responsible for the aggregation is localized in the Fd fragment (Capra and Kunkel, 1970). Accordingly, precipitation in addition to the observed degradation of the Ox IgG3 Fd chain during the synthesis in *E. coli* cannot be ruled out.

(c) Hapten-binding by the Ox Fab fragments

The affinity constants (K_a) of the Ox Fab fragments were determined by the fluorescence quenching method (Eisen, 1964; Parker, 1978) using the assay conditions described earlier (Takkinen et al., 1991). The K_a value of the Ox IgG1 Fab was 1.8×10^6 M^{-1}, which is close to that of the idiotype NQ2–17.4.1 antibody (1.5×10^6 M^{-1}) (Takkinen et al., 1991). The affinity was retained also in the case of Ox IgG3ΔC_H and the K_a values for the truncated Fab fragment and the corresponding idiotype H26 antibody were 3.7×10^6 M^{-1} and 4.0×10^6 M^{-1} (M.K., unpublished data), respectively. An earlier study by Sen and Beychok (1986) describes proteolytic production of a truncated Fab, consisting of the VH domain and the L chain of a human myeloma protein that binds to riboflavin. In this case the resulting fragment showed two to three orders of magnitude lower affinity than the intact antibody. In our case the CH1 domain did not have any significant contribution to the affinity, as was also observed earlier in the case of the Ox scFv (Takkinen et al., 1991). In this connection our findings support those of Udaka et al. (1990), who expressed two VH proteins specific for the 5-dimethylaminonaphthalene-1-sulfonyl (Dns) group in *E. coli* and associated them with the homologous L chains to form VHL molecules. These recombined proteins were shown to have affinities comparable to those of the corresponding parent monoclonal antibodies. The observed K_a value of the Ox IgG3 Fab preparation (2.9×10^6 M^{-1}) was similar to that of the intact H26 antibody. This is most easily explained by assuming the formation of a mixture of Fab fragments in which the L chain and the degradation products of the Fd chain are held together mainly by noncovalent forces.

(d) Stability of the Ox Fab fragments

Comparison of the temperature stabilities of the different fragments revealed that similar to the NQ2–17.4.1 Ab, the Ox IgG1 Fab was stable up to 60°C (Fig. 5). Both Ox IgG3 fragments were less stable than the Ox IgG1 Fab and began to loose their activity already at 40°C. The temperature stabilities of both the Ox IgG3 Fab and Ox IgG3ΔC_H are very similar to those of the Ox scFv shown in Fig. 5 (Takkinen et al., 1991) and Ox Fv (D.S., manuscript in preparation). All these fragments have either incomplete CH1 domains or this domain is absent. This suggests that the CH1 domain stabilizes the structure of the Fab fragment against thermal denaturation.

(e) Conclusions

(*1*) The Ox IgG1 Fab fragment can be secreted as an active and soluble protein to the periplasmic space and

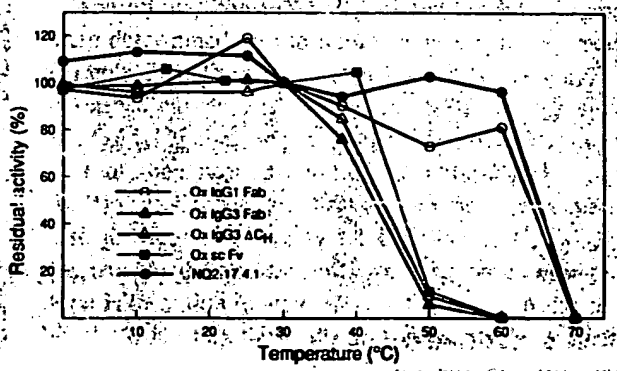

Fig. 5. The temperature stability of the Ox Fab fragments. The experiments were performed as described earlier (Takkinen et al., 1991) except that alkaline phosphatase(AFOS)-labeled goat anti-mouse κ Ab (1:500) (Southern Biotechnology Associates, Inc.) was used for the detection of the bound Fab fragments on the Ox_{19}-BSA coated ELISA plate. The hapten-binding activities at 30°C were defined as 100%. For comparison the stabilities of the Ox scFv (Takkinen et al., 1991) and the NQ2–17.4.1 antibody are shown.

is released to the culture medium of *E. coli*. The amount of active Ox IgG1 Fab fragment found in the culture medium is the same as that seen earlier for the corresponding Ox scFv (Takkinen et al., 1991). Thus, *E. coli* is able to make equal amounts of active Fab and scFv fragments, but the final yields obtained with different antibodies depend on the specific sequence and structure of the fragment produced.

(*2*) The Fd chain of the Ox IgG3 Fab produced in *E. coli* was proteolytically degraded from the C terminus. Truncation of the constant domain of Ox IgG3 Fd chain up to the interchain disulfide bond facilitated proper folding and/or assembly of the chains. The truncated Fab was now able to form a stable and active hapten-binding fragment. This indicates that proper formation of the interchain disulfide bond is important for efficient expression and assembly of functional Fab fragments in *E. coli*.

(*3*) All of the Ox antibody fragments which had truncated or no CH1 domains showed reduced temperature stabilities while the Ox IgG1 Fab was as stable as the intact mAb. It therefore appears that an intact CH1 domain has a major contribution to the thermal stability of a Fab fragment.

ACKNOWLEDGEMENTS

We wish to thank Dr. Marc Baumann, University of Helsinki, for the N-terminal protein sequence analysis, Anna-Marja Hoffrén for revealing us some of the antibody structures by molecular modeling and Kariitta Berg and Pirkko Veijola-Bailey for excellent technical assistance. We would also like to thank Oili Lappalainen for her invaluable secretial help. The financial support of the Technology Development Centre of Finland is gratefully acknowledged.

REFERENCES

Anand, N.N., Dubuc, G., Phipps, J., MacKenzie, C.R., Sadowska, J., Young, N.M., Bundle, D.R. and Narang, S.A.: Synthesis and expression in *Escherichia coli* of cistronic DNA encoding an antibody fragment specific for a *Salmonella* serotype B O-antigen. Gene 100 (1991a) 39–44.

Anand, N.N., Mandal, S., MacKenzie, C.R., Sadowska, J., Sigurskjold, B., Young, N.M., Bundle, D.R. and Narang, S.A.: Bacterial expression and secretion of various single-chain Fv genes encoding proteins specific for a *Salmonella* serotype B O-antigen. J. Biol. Chem. 266 (1991b) 21874–21879.

Baumann, M.: Comparative gas phase and pulsed liquid phase sequencing on a modified Applied Biosystems 477A sequencer. Anal. Biochem. 190 (1990) 198–208.

Better, M., Chang, C.P., Robinson, R.R. and Horwitz, A.H.: *Escherichia coli* secretion of an active chimeric antibody fragment. Science 240 (1988) 1041–1043.

Better, M. and Horwitz, A.H.: Expression of engineered antibodies and antibody fragments in microorganisms. Methods Enzymol. 178 (1989) 476–496.

Bird, R.E., Hardman, K.D., Jacobson, J.W., Johnson, S., Kaufman, B.M., Lee, S.-M., Lee, T., Pope, S.H., Riordan, G.S. and Whitlow, M.: Single-chain antigen-binding proteins. Science 242 (1988) 423–426.

Buchner, J. and Rudolph, R.: Renaturation, purification and characterization of recombinant Fab-fragments produced in *Escherichia coli*. Bio/Technology 9 (1991) 157–162.

Cabilly, S.: Growth at sub-optimal temperatures allows the production of functional, antigen-binding Fab fragments in *Escherichia coli*. Gene 85 (1989) 553–557.

Capra, J.D. and Kunkel, H.G.: Aggregation of γG3 proteins: relevance to the hyperviscosity syndrome. J. Clin. Invest. 49 (1970) 610–621.

Carter, P., Kelley, R.F., Rodrigues, M.L., Snedecor, B., Covarrubias, M., Velligan, M.D., Wong, W.L.T., Rowland, A.M., Kotts, C.E., Carver, M.E., Yang, M., Bourell, J.H., Shepard, H.M. and Henner, D.: High level *Escherichia coli* expression and production of a bivalent humanized antibody fragment. Bio/Technology 10 (1992) 163–167.

Chaudhary, V.K., Queen, C., Junghans, R.P., Waldmann, T.A., FitzGerald, D.J. and Pastan, I.: A recombinant immunotoxin consisting of two antibody variable domains fused to *Pseudomonas* exotoxin. Nature 339 (1989) 394–397.

Condra, J.H., Sardana, V.V., Tomassini, J.E., Schlabach, A.J., Davies, M.-E., Lineberger, D.W., Graham, D.J., Gotlib, L. and Colonno, R.J.: Bacterial expression of antibody fragments that block human rhinovirus infection of cultured cells. J. Biol. Chem. 265 (1990) 2292–2295.

Earhart, C.F., Lundrigan, M., Pickett, C.L. and Pierce, J.R.: *Escherichia coli* K-12 mutants that lack major outer membrane protein *a*. FEMS Microbiol. Lett. 6 (1979) 277–280.

Edqvist, J., Keränen, S., Penttilä, M., Stråby, K.B. and Knowles, J.K.C.: Production of functional IgM Fab fragments by *Saccharomyces cerevisiae*. J. Biotechnol. 20 (1991) 291–300.

Eisen, H.N.: Determination of antibody affinity for haptens and antigens by means of fluorescence quenching. In: Eisen, H.N. (Ed.), Methods in Medical Research, Vol. X. Year Book Medical Publishers, Chicago, 1964, pp. 115–121.

Garcia-Gonzalez, M., Bettinger, S., Ott, S., Olivier, P., Kadouche, J. and Pouletty, P.: Purification of murine IgG3 and IgM monoclonal antibodies by euglobulin precipitation. J. Immunol. Methods 111 (1988) 17–23.

Glockshuber, R., Malia, M., Pfitzinger, I. and Plückthun, A.: A comparison of strategies to stabilize immunoglobulin Fv-fragments. Biochem. 29 (1990) 1362–1367.

Glockshuber, R., Schmidt, T. and Plückthun, A.: The disulfide bonds in antibody variable domains: effects on stability, folding in vitro, and functional expression in *Escherichia coli*. Biochem. 31 (1992) 1270–1279.

Goding, J. W.: Monoclonal Antibodies: Principles and Practice, 2nd ed. Academic Press, London, 1986, pp. 109–110.

Gyotoku, Y., Abdelmoula, M., Spertini, F., Izui, S. and Lambert, P.-H.: Cryoglobulinemia induced by monoclonal immunoglobulin G rheumatoid factors derived from autoimmune MRL/MpJ-*lpr*/*lpr* mice. J. Immunol. 138 (1987) 3785–3792.

Hill, D.E., Oliphant, A.R. and Struhl, K.: Mutagenesis with degenerate oligonucleotides: an efficient method for saturating a defined DNA region with base pair substitutions. Methods Enzymol. 155 (1987) 558–568.

Huston, J.S., Levinson, D., Mudgett-Hunter, M., Tai, M.-S., Novothy, J., Margolies, M.N., Ridge, R.J., Bruccoleri, R.E., Haber, E., Crea, R. and Oppermann, H.: Protein engineering of antibody binding

sites: recovery of specific activity in an anti-digoxin single-chain Fv analogue produced in *Escherichia coli*. Proc. Natl. Acad. Sci. USA 85 (1988) 5879–5883.

Jiskoot, W., Hoven, A.-M.V., De Koning, A.A.M., Leerling, M.F., Reubsaet, C.H.K., Crommelin, D.J.A. and Beuvery, E.C.: Purification and stabilisation of a poorly soluble mouse IgG3 monoclonal antibody. J. Immunol. Methods 138 (1991) 181–189.

Kaartinen, M., Griffiths, G.M., Markham, A.F. and Milstein, C.: mRNA sequences define an unusually restricted IgG response to 2-phenyloxazolone and its early diversification. Nature 304 (1983) 320–324.

Kaartinen, M., Solin, M.-L. and Mäkelä, O.: 'Allelic' forms of immunoglobulin V genes in different strains of mice. EMBO J. 8 (1989) 1743–1748.

Laemmli, U.K.: Cleavage of structural proteins during the assembly of the head of bacteriophage T4. Nature 227 (1970) 680–685.

Lei, S.-P., Lin, H.-C., Wang, S.-S., Callaway, J. and Wilcox, G.: Characterization of the *Erwinia carotovora pelB* gene and its product pectate lyase. J. Bacteriol. 169 (1987) 4379–4383.

Maniatis, T., Fritsch, E.F. and Sambrook, J.: Molecular Cloning. A Laboratory Manual. Cold Spring Harbor Laboratory, Cold Spring Harbor, NY, 1982.

Parker, C.W.: Spectrofluorometric methods. In: Weir, D.M. (Ed.), Handbook of Experimental Immunology, 3rd ed., Chapter 18, Blackwell Scientific Publications, Oxford, 1978.

Plückthun, A.: Antibody engineering: advances from the use of *Escherichia coli* expression systems. Bio/Technology 9 (1991) 545–551.

Plückthun, A. and Skerra, A.: Expression of functional antibody Fv and Fab fragments in *Escherichia coli*. Methods Enzymol. 178 (1989) 497–515.

Power, B.E., Ivancic, N., Harley, V.R., Webster, R.G., Kortt, A.A., Irving, R.A. and Hudson, P.J.: High-level temperature-induced synthesis of an antibody VH-domain in *Escherichia coli* using the PelB secretion signal. Gene 113 (1992) 95–99.

Randall, L.L. and Hardy, S.J.S.: Correlation of competence for export with lack of tertiary structure of the mature species: a study in vivo of maltose-binding protein in *E. coli*. Cell 46 (1986) 921–928.

Sambrook, J., Fritsch, E.F. and Maniatis, T.: Molecular Cloning. A Laboratory Manual, 2nd ed. Cold Spring Harbor Laboratory Press, Cold Spring Harbor, NY, 1989.

Schoner, B.E., Belagaje, R.M. and Schoner, R.G.: Translation of a synthetic two-cistron mRNA in *Escherichia coli*. Proc. Natl. Acad. Sci. USA 83 (1986) 8506–8510.

Schoner, R.G., Ellis, L.F. and Schoner, B.E.: Isolation and purification of protein granules from *Escherichia coli* cells overproducing bovine growth hormone. Bio/Technology 3 (1985) 151–154.

Sen, J. and Beychok, S.: Proteolytic dissection of a hapten binding site. Proteins 1 (1986) 256–262.

Skerra, A. and Plückthun, A.: Assembly of a functional immunoglobulin Fv fragment in *Escherichia coli*. Science 240 (1988) 1038–1041.

Skerra, A. and Plückthun, A.: Secretion and in vivo folding of the Fab fragment of the antibody McPC603 in *Escherichia coli*: influence of disulphides and *cis*-prolines. Prot. Eng. 4 (1991) 971–979.

Takkinen, K., Laukkanen, M.-L., Sizmann, D., Alfthan, K., Immonen, T., Vanne, L., Kaartinen, M., Knowles, J.K.C. and Teeri, T.T.: An active single-chain antibody containing a cellulase linker domain is secreted by *Escherichia coli*. Prot. Eng. 4 (1991) 837–841.

Towbin, H., Staehelin, T. and Gordon, J.: Electrophoretic transfer of proteins from polyacrylamide gels to nitrocellulose sheets: procedure and some applications. Proc. Natl. Acad. Sci. USA 76 (1979) 4350–4354.

Udaka, K., Chua M.-M., Tong, L.-H., Karush, F. and Goodgal, S.H.: Bacterial expression of immunoglobulin VH proteins. Mol. Immunol. 27 (1990) 25–35.

Ward, E.S., Güssow, D., Griffiths, A.D., Jones, P.T. and Winter, G.: Binding activities of a repertoire of single immunoglobulin variable domains secreted from *Escherichia coli*. Nature 341 (1988) 544–546.

Wetlaufer, D. B.: Ultraviolet spectra of proteins and amino acids. Adv. Prot. Chem. 17 (1962) 303–390.

Winter, G. and Milstein, C.: Man-made antibodies. Nature 349 (1991) 293–299.

Preparation, Characterization, and in Vivo Biodistribution Properties of Synthetically Cross-Linked Multivalent Antitumor Antibody Fragments

Margaret E. Schott,* Kevin A. Frazier, Douglas K. Pollock, and Kathryn M. Verbanac†

Bioproducts Laboratory, The Dow Chemical Company, Midland, Michigan 48674. Received September 30, 1992

Two new antibody forms of the general structure $F(ab')_n$ (n = 3 or 4) were prepared and tested in vivo as part of an ongoing search for antibody candidates with improved biodistribution properties for cancer immunotargeting applications. The novel multivalent antibody forms, called $F(ab')_3$-x (tribody, 150 kDa, x = cross-linker) and $F(ab')_4$-x (tetrabody, 200 kDa), were constructed through chemical cross-linking of Fab' subunits derived from murine CC49 IgG, a monoclonal antibody which recognizes the tumor-associated antigen TAG-72. Two new chemical reagents (trismaleimide 1 and tetramaleimide 2) were synthesized for use in cross-linking cysteine sulfhydryl groups present on the hinge region of Fab'. Homogeneous Fab' was prepared by mild reduction of $F(ab')_2$ followed by selective reoxidation of interchain disulfide bonds, leaving a single hinge-region cysteine sulfhydryl group available for modification. For biodistribution studies, the parent $F(ab')_2$ fragment was first radiolabeled via lysine amine modification using the isothiocyanate derivative of the ^{105}Rh(BA-2,3,2-tet)Cl_2 complex. Both new fragment forms were shown to retain antigen binding ability in vitro using a solid-phase immunoassay. Although isolated yields for $F(ab')_3$-x and $F(ab')_4$-x were low (18 and 4%, respectively), sufficient quantities were prepared for preliminary biodistribution studies in Balb/c mice and, in the case of $F(ab')_3$-x, for a 5-day biodistribution study in tumor-bearing nude mice. A large proportion of the ^{105}Rh-labeled $F(ab')_4$-x was found to accumulate in the liver, possibly indicating an upper size limit for the in vivo use of cross-linked fragments. The biodistribution behavior of ^{105}Rh-labeled $F(ab')_3$-x in both Balb/c and nude mice was intermediate between that of IgG and $F(ab')_2$ for all organs studied. Kidney localization was reduced, while blood circulation time and tumor accumulation were slightly increased, for the trivalent species compared with $F(ab')_2$. The unique biodistribution profile of $F(ab')_3$-x suggests the possible use of this multivalent fragment for in vivo tumor targeting applications.

INTRODUCTION

The development of antibodies and antibody-like species with improved biodistribution properties for cancer immunotargeting applications is an area of intense current interest (for recent reviews, see Waldmann, 1991; Koppel, 1990). To date the most thoroughly studied antibody forms include IgG and its proteolytic fragments, $F(ab')_2$ and Fab. Although the smaller fragments have been shown to penetrate tumor tissue more readily than the parent immunoglobulin (Fujimori et al., 1989), both fragments localize extensively to the kidneys, limiting their usefulness particularly when conjugated to radiometals (Sharkey et al., 1990). And while genetically engineered single-chain antigen binding proteins offer the potential advantages of rapid plasma clearance, enhanced tumor penetrance (Milenic et al., 1991; Yokota et al., 1992), and reduced immunogenicity, the amount of sFv actually delivered to tumor sites is low in comparison with the slower clearing IgG. It is evident that no single immunoglobulin form will possess properties that match the requirements of all cancer diagnosis and therapeutic applicatons. The investigation of alternative structural forms should lead to a better understanding of the role of structure as it relates to biodistribution and may aid in the design of useful immunotargeting agents.

Various chemical cross-linking methods have been employed in the preparation of antibody forms possessing two or more antigen binding arms. One method involves the formation of chemical cross-links between lysine amine residues on whole antibodies and/or antibody fragments. This approach is considered nonspecific with respect to location of the chemical bonds formed on the protein surface and can result in heterogeneous product mixtures (Perez et al., 1985). Hetero-cross-linked IgG and Fab fragments have been constructed for the purpose of retargeting cytotoxic cells in vivo (Segal and Wunderlich, 1988). These authors note that since chemically linked hetero-aggregates clear more rapidly from the circulation than monomeric IgG, their use may be limited to in vitro screening applications.

Hetero-cross-linked bivalent and multivalent antibody forms have also been constructed through site-specific reactions involving cysteine sulfhydryl groups obtained through mild reduction of disulfide bonds in the parent immunoglobulins or fragments. Several reports have appeared concerning the preparation of heterobifunctional $F(ab')_2$ species using bismaleimide cross-linkers (Glennie et al., 1987; French et al., 1991; Stickney et al., 1988). These novel fragments were formed through the chemical cross-linking of hinge-region sulfhydryl groups. Heterobifunctional fragments have also been prepared through reformation of hinge-region disulfide bonds via leaving-group chemistry (Brennan et al., 1985) or using a two-step reduction/reoxidation procedure (Staerz and Bevan, 1986). However, thioether bonds may be preferable to disulfide bonds based on evidence of their enhanced stability in vivo (Meares et al., 1988; Stevenson et al., 1989). In a recent study of the relative in vivo stability of radiolabeled $F(ab')_2$ versus bismaleimide-cross-linked $F(ab')_2$, the latter fragments (constructed with three different cross-linkers) showed significantly longer plasma circulation times

* Present address and to whom correspondence should be addressed: Laboratory of Tumor Immunology and Biology, National Cancer Institute, National Institutes of Health, 9000 Rockville Pike, Bldg 10, Room 8B07, Bethesda, MD 20892.

† Present address: Department of Surgery, East Carolina University School of Medicine, Greenville, NC 27858.

1043-1802/93/2904-0153$04.00/0

compared with the native form (Quadri et al., 1992). Whether the plasma half-life of native $F(ab')_2$ is influenced by the number of hinge-region disulfide bonds was not reported.

Bismaleimide cross-linking has also been employed for the preparation of a "chimeric univalent" Fab-IgG (Stevenson et al., 1985). These authors also observed the putative IgG-$(Fab')_2$ species as a byproduct. Fab-IgG (200 kDa), which is univalent and thus capable of evading antigenic modulation on tumor surfaces, appeared to be "catabolized at the slow rate characteristic of autologous IgG". Bismaleimides reagents have also been used to construct the univalent FabFc species (100 kDa), possessing one antigen binding arm and an Fc region, and its bivalent counterpart, bisFabFc (200 kDa; Stevenson et al., 1989). Biodistribution data for these antibody forms were not reported. However, biodistribution studies for a structurally similar fragment called Fab/c, generated by the limited enzymatic digestion of IgG, were recently carried out (Demignot et al., 1990). In Balb/c mice, the half-lives of the catabolic (β) phase of plasma clearance for radioiodinated Fab/c and the parent IgG were identical, as was whole-body clearance. The distribution (α) phase of plasma clearance for Fab/c was steeper than that for IgG, suggesting a more rapid extravasation into tissues. A slightly greater kidney to blood ratio was observed for the Fab/c fragment compared with IgG. In tumor-bearing nude mice, Fab/c localized to tumor tissue but did so to a lesser extent than whole antibody, presumably due to the lower immunoreactivity of the univalent fragment.

The major pathway by which proteins enter the kidney is through glomerular filtration, a process which depends upon several factors including molecular size, shape, and charge (Sumpio, 1981). Proteins smaller than 50 kDa generally cross the glomerulus while intermediate and high molecular weight proteins greater than 60–70 kDa generally do not (Strober and Waldmann, 1974; Demignot et al., 1990). Anionic proteins are hindered to a greater extent than are charge-neutral or cationic proteins, particularly at sizes greater than 25 Å. Charge is less important for small proteins (Maack et al., 1979). The overall charge of a protein (as well as the distribution of charges on the molecule) are also known to influence uptake by the proximal tubules, with cationic proteins being taken up to a greater degree than anionic proteins of the same molecular weight (Christensen et al., 1983; Sumpio, 1981). The low isoelectric point of the immunoglobulin Fc piece (Goding, 1986) probably accounts for its relatively long circulation time compared with the Fab fragment (Waldmann and Strober, 1969), despite the similarity in molecular weight for Fc and Fab. Additionally, the similarity of the biodistribution patterns observed for IgG and its Fab/c fragment (see above), in striking contrast to the biodistribution observed for $F(ab')_2$ (also 100 kDa), suggests a role for Fc in keeping the Fab/c in circulation and out of the kidneys.

On the basis of the known literature concerning kidney handling of macromolecules, the extent of kidney localization for $F(ab')_2$ is surprising. In order to further investigate the role of fragment size on biodistribution, particularly kidney localization and blood-residence lifetime, we prepared two new homologues of the $F(ab')_n$ series, where $n = 3$ (tribody) and $n = 4$ (tetrabody). Because of their higher molecular weights, the tribody (150 kDa) and tetrabody (200 kDa) species would be expected to show decreased kidney localization compared with $F(ab')_2$ or Fab. Additionally, $F(ab')_3$-x seemed an interesting target because it has the same molecular weight as IgG but lacks the Fc region. Although a putative $F(ab')_3$ species was observed previously as a byproduct of Fab' chemical cross-linking (Glennie et al., 1987), its in vivo properties were not reported. The semisynthetic fragments $F(ab')_3$-x (x = cross-linker) and $F(ab')_4$-x were constructed from univalent Fab' subunits derived from CC49 $F(ab')_2$ using the newly designed and synthesized tri- and tetrafunctional maleimide cross-linking reagents 1 and 2 (Figure 1). The murine monoclonal antibody CC49 is an IgG1 that recognizes the tumor-associated antigen TAG-72 and reacts with a high percentage of tumor cells in a wide range of human carcinomas (Muraro et al., 1988). Radiolabeled CC49 efficiently localizes human carcinoma xenografts in vivo in athymic mice (Colcher et al., 1988). We report here the biodistribution patterns of radiolabeled CC49 $F(ab')_3$-x and $F(ab')_4$-x in Balb/c mice and the tumor localization of $F(ab')_3$-x in nude mice bearing LS-174T human tumor xenografts.

EXPERIMENTAL PROCEDURES

General Procedures. All phosphate buffer solutions were 0.1 M sodium phosphate adjusted to the desired pH, except PBS[1] (pH 7.4), which was prepared by reconstitution of a powder obtained from Sigma (St. Louis, MO). Iodoacetamide and DTT were prepared as 0.1 M solutions in pH 7.0 phosphate buffer. Sure/Seal dimethylformamide was obtained from Aldrich (Milwaukee, WI) and stored under a blanket of nitrogen. Centricon-30 concentrator units (30 000 MW cutoff) from Amicon (Beverly, MA) were used on a Du Pont Sorvall RT-6000B centrifuge equipped with an A-384 rotor at 5000–6000 rpm, 16 °C. Protein assays were performed according to the Pierce (Rockford, IL) Coomassie method, with bovine plasma γ-globulin from Bio-Rad (Richmond, CA) as a quantitation standard.

Monoclonal Antibodies. mAb CC49 is a murine IgG1 which was obtained by immunizing mice with purified TAG-72 (Muraro et al., 1988). For the present studies, CC49 IgG was harvested from bioreactor cultures and purified using an AbX column (Bio-Rad) followed by a Superose 12 gel filtration column (Pharmacia, Piscataway, NJ). CC49 $F(ab')_2$ fragments were prepared via enzymatic digestion of the parent IgG using either thiol-activated papain (neutral pH, nonreducing conditions) or using pepsin (pH 3.5) as described by Goding (1986). The progress of the digestion reactions was monitored by GF-250 HPLC until none of the parent IgG remained. The fragments were purified by gel filtration chromatography using a Superose 12 column and stored at −70 °C in 50 mM pH 6.8 phosphate buffer at approximately 5–10 mg/mL.

High Performance Liquid Chromatography. Analytical HPLC was used both for monitoring the progress of reactions and for checking the quality of final preparations. Preparative HPLC was used for the isolation of cross-linked fragment species and was performed on the same columns as the analytical work. HPLC for nonra-

[1] Abbreviations used: BA-2,3,2-tet, 6-[(4-aminophenyl)methyl]-1,4,8,11-tetraazaundecane; PBS, phosphate-buffered saline; TAG-72, tumor associated glycoprotein-72; DMF, dimethylformamide; THF, tetrahydrofuran; DMSO, dimethyl sulfoxide; EDTA, ethylenediaminetetraacetic acid; DTT, dithiothreitol; NEM, *N*-ethylmaleimide; DTNB, 5,5′-dithiobis(2-nitrobenzoic acid); TNB^{2-}, 5-mercapto-2-nitrobenzoic acid anion; BSA, bovine serum albumin; SDS-PAGE, sodium dodecyl sulfate–polyacrylamide gel electrophoresis; ELISA, enzyme-linked immunosorbent assay; IEF, isoelectric focusing; H′ and L, antibody fragment heavy and light chains (H′ is the same as Fd and is used here for clarity).

dioactive samples was performed on a Du Pont GF-250 column at a flow rate of 1.0 mL/min unless otherwise indicated. The mobile phase was 0.2 M pH 7.0 sodium phosphate containing 1 mM EDTA, which was included to slow oxidation of free thiol groups. For isolation and analysis of radiolabeled samples, both a Berthold LB 506A radioisotope flow-through radioisotope detector and a UV detector were employed, and the flow rate was slowed to 0.5 mL/min for $F(ab')_3$-x and 0.3 mL/min for $F(ab')_4$-x.

SDS–PAGE. Discontinuous SDS–PAGE was performed according to the method of Laemmli (1970) using a Bio-Rad Protean II apparatus (Richmond, CA). Nonreducing and reducing (5% β-mercaptoethanol) 10% polyacrylamide gels were run following denaturation of samples at 80 °C for 2 min. Permanent images of Coomassie Blue-stained polyacrylamide gels were obtained using the Electrophoresis Duplicating Paper system from Kodak (Rochester, NY). Autoradiography was performed on dried gels using Kodak X-Omatic cassettes and film. The progress of disulfide bond reduction, disulfide bond formation, and fragment cross-linking could be monitored by nonreducing SDS–PAGE following treatment of an aliquot (10–20 μL) with an equal volume of 0.1 M iodoacetamide for 15 min at room temperature. Use of nonreducing conditions allowed separation of the CC49 fragment H′ and L chains on 10% polyacrylamide gels. Under reducing conditions, H′ and L typically migrated together. In some experiments, cross-linked antibody fragments were subjected to reduction and alkylation prior to SDS–PAGE analysis on nonreducing gels. This procedure allowed visualization of the fragment H′ and L chains as well as cross-linked H′ chains. For example, an aliquot (18 μL) containing the fragment of interest was first treated with 0.2 M DTT (2 μL) in pH 7.0 phosphate buffer for 10–15 min at room temperature and then with an equal volume (20 μL) of 0.1 M iodoacetamide in pH 7.0 phosphate buffer for 30 min.

Immunoreactivity Assay. ELISA antigen binding assays were performed using 96-well polystyrene microtiter plates, which were precoated with TAG-72 prepared from LS-174T human colorectal carcinoma xenografts using a modification of a reported procedure (Johnson et al., 1986). Briefly, xenograft tumors were minced, homogenized in PBS in the presence of protease inhibitors, and centrifuged in two stages to yield a supernatant containing the tumor extract. The filtered homogenate was further purified by gel filtration chromatography on Sepharose CL-4B or CL-6B (Pharmacia) equilibrated with PBS. Fractions containing TAG-72 were identified by a direct-binding assay using radioiodinated antigen-specific antibody. Microtiter plates for ELISA were prepared by coating with TAG-72-enriched fractions (~10% of total protein) followed by blocking with 1% BSA in PBS. For ELISA, antibody fragment samples (50 μL/well) were incubated on precoated microtiter plates at starting concentrations of 10 μg/mL in 1% BSA. Dilutions (1:2) and transfers were performed using a Cetus Pro/Pette (Emeryville, CA). Plates were incubated for 2–3 h at 37 °C or overnight at 4 °C and washed with 0.025% Tween 20 using a Flow Laboratories plate washer, followed by incubation with a 1:200 solution of alkaline phosphatase-conjugated goat anti-mouse κ antibody (Southern Biotech, Birmingham, AL) in 1% BSA (50 μL) for 2–3 h at 37 °C. After washing, plates were treated with a freshly prepared solution of p-nitrophenol phosphate in diethanolamine buffer (100 μL/ Kirkegaard and Perry Laboratories, Gaithersburg, MD). Color development was monitored using a Dynatech MR600 microplate reader, and the reactions were stopped with 2 N NaOH (100 μL) when the absorbance readings were 1.0–1.2.

Preparation of Trismaleimide 1. Trimethyl 1,3,5-benzenetricarboxylate (10.08 g, 40 mmol) was stirred with ethylenediamine (60 mL) at room temperature under a constant stream of nitrogen. The reaction was monitored by TLC (2:2:1 $CHCl_3$/MeOH/concentrated NH_4OH). After 24 h the reaction appeared to be complete. Excess ethylenediamine was removed under reduced pressure on a rotary evaporator. A viscous oil was obtained which was dissolved in methanol (25–30 mL). The solution was then slowly poured into p-dioxane (350–400 mL). A white powder formed as the methanolic solution was added and the solid was collected by filtration. A tan powder (11 g, 32.7 mmol, 82%) was obtained and identified as the tris(amido amine). An additional amount (2.7 g) of impure material was obtained as a thick oil when the p-dioxane/ethanol solution was evaporated. ^1H NMR (d_6-DMSO) ppm: 1.90 (br s, 2 H, NH_2), 2.75 (br t, 2 H), 3.33 (br t, 2 H), 8.40 (s, 1 H), 8.63 (br s, 1 H). ^{13}C NMR (d_6-DMSO) ppm: 41.178, 43.120, 66.310, 79.079, 128.390, 134.975, 165.667.

Maleic anhydride (2.00 g, 20.4 mmol) was added all at once to a vigorously stirred solution of the tris(amido amine) (2.29 g, 6.8 mmol) dissolved in DMF (10 mL). The mixture warmed slightly as the material gradually dissolved. After 2 h a solid began to form again and eventually stirring was impeded. The reaction was left overnight and THF (200 mL) was added and the mixture was stirred rapidly. The white powder (3.2 g) obtained upon filtering the THF/DMF solution was identified as the trismaleamate. ^1H NMR (d_6-DMSO) ppm: 3.25–3.65 (m, 4 H), 6.26 (d, 1 H), 6.46 (d, 1 H), 7.97 (s, 1 H), 8.48 (s, 1 H), 8.80 (br s, 1 H), 9.23 (br s, 1 H). ^{13}C NMR (d_6-DMSO) ppm: 38.510, 38.851, 128.613, 131.962, 132.563, 134.776, 165.360, 165.646, 165.744.

Trismaleamate (1.54 g), anhydrous sodium acetate (1.54 g), and acetic anhydride (5 mL) were heated at 80 °C with stirring for 24 h. The mixture was then poured into ice water and stirred vigorously for 1 h. The solid was collected by filtration and was washed successively with water, anhydrous ethanol, and anhydrous ether. A tan solid (0.40 g) was obtained after drying under vacuum. Proton and carbon spectra confirm the structure as trismaleimide 1. ^1H NMR (d_6-DMSO) ppm: 3.54 (m, 2 H), 3.59 (m, 2 H), 6.95 (s, 2 H), 8.23 (s, 1 H), 8.79 (br s, 1 H). ^{13}C NMR (d_6-DMSO) ppm: 36.970, 37.721, 128.300, 134.442, 134.672, 165.556, 170.912.

Preparation of Tetramaleimide 2. Maleic anhydride (9.8 g, 100 mmol) was added in portions to a stirred mixture of 3,5-diaminobenzoic acid (7.6 g, 50 mmol) and acetic acid (250 mL) at room temperature. Cooling was necessary as the addition proved to be exothermic. The mixture was stirred for 72 h at room temperature and eventually became too thick to stir. Anhydrous ether (500 mL) was added and the mixture was filtered and the solid washed repeatedly with ether. The bismaelamic acid (18.2 g) was obtained as a yellow-green powder and was used directly for the next reaction.

Sodium acetate (15 g) and bismaleamic acid (15 g) were stirred at 80 °C in acetic anhydride (100 mL) and after 0.5 h the mixture set up as a firm solid. Another portion of acetic anhydride (100 mL) was added and the temperature was raised to 100 °C. After 2 h the reaction mixture was cooled, poured into ice water (300 mL), and left stirring overnight. The mixture was filtered and the solid was washed with absolute ethanol followed by anhydrous ether. The off-white powder (9.50 g, 61%) was identified as the

bismaleimide acid by NMR. ^{1}H NMR (d_6-DMSO) ppm: 7.21 (s, 4 H), 7.67 (t, 1 H), 8.00 (d, 2 H), COOH was not observed. ^{13}C NMR (d_6-DMSO) ppm: 126.310, 128.212, 132.238, 132.811, 134.774, 166.033, 169.533.

The bismaleimide acid (0.25 g) was stirred as a slurry in thionyl chloride (5 mL). The mixture was heated to reflux and gas evolution was monitored with a gas bubbler. The reaction mixture was heated overnight, allowing the solid to dissolve gradually. Excess thionyl chloride was removed under reduced pressure and then CCl_4 was added and the solvents were stripped again, yielding a tan solid. The acid chloride was used without further purification. ^{1}H NMR (d_6-DMSO) ppm: 7.24 (s, 4 H), 7.64 (s, 1 H), 8.01 (s, 2 H). ^{13}C (d_6-DMSO) ppm: 126.248, 128.462, 131.920, 132.330, 134.781, 165.745, 169.484.

The acid chloride (130 mg, 0.39 mmol) was added all at once to a room temperature solution of *p*-phenylenediamine (21 mg, 0.19 mmol) and triethylamine (65 μL; 0.45 mmol) in acetonitrile (5 mL). A small amount of heat was generated and a solid quickly formed. The reaction was stirred for 0.5 h and filtered. The solid was washed with water followed by acetonitrile again to yield a tan powder (65 mg). ^{1}H NMR (d_6-DMSO) ppm: 7.23 (s, 4 H), 7.64 (s, 1 H), 7.83 (s, 2 H), 8.08 (s, 2 H), 10.45 (s, 1 H). ^{13}C (d_6-DMSO) ppm: 120.757, 125.080, 127.584, 132.085, 134.723, 136.137, 163.415, 169.387; one aromatic signal was not detected.

Preparation of Fab'. Fab' was prepared from $F(ab')_2$ by mild reduction followed by selective reoxidation of H'–L interchain disulfide bonds. In a typical preparation, 2.0 mg of $F(ab')_2$ in 0.9 mL of pH 7.0 phosphate buffer was treated with 0.2 M DTT (0.1 mL) for 15 min at room temperature. Interchain disulfide bonds were completely reduced under these conditions (Figure 2a). Sephadex G-25 QS-2B "mini-spin" columns from Isolab (Akron, OH) were equilibrated with 0.1 M pH 8.0 sodium phosphate buffer (10 mL) and spun to dryness in a refrigerated RT-6000B centrifuge before use (16 °C, A-384 rotor). Sample aliquots (100 μL) were applied to the tops of the columns, and following a 5-min equilibration period, the columns were spun for 10 min and the eluents collected into snugly fitting capless 1.5-mL Eppendorf tubes (Sarstedt, Princeton, NJ). Samples were left at room temperature for 3 h to allow H'–L disulfide bonds to reform. Pooled samples were treated with the appropriate volume of 0.1 M EDTA in pH 8.0 phosphate buffer to give a final concentration of 1 mM EDTA; samples prepared in this manner were used immediately for cross-linking experiments. Although actual yields of antibody fragments from mini-spin columns were ~80%, theoretical (100%) yields were used for calculating the cross-linker concentrations indicated below. Variations in the above procedure were also tested in order to evaluate the effects of pH, temperature, protein concentration, and mini-spin loading volume on the preparation of Fab'.

Quantitation of Fab' Sulfhydryl Groups. Analyses were performed in order to quantitate the number of free sulfhydryl groups in the hinge region of Fab'. In one method, a sample of $F(ab')_2$ (0.8 mg; from pepsin-digested IgG) was subjected to mild reduction and reoxidation of H'–L disulfide bonds as above and then treated with an equal volume of 20 mM DTNB (Ellman, 1964) to generate the Fab'–TNB adduct. After a few minutes at room temperature, the sample was concentrated on a Centricon-30 unit and residual reagent was removed by the addition of pH 7.0 phosphate buffer (2 × 2 mL) followed by respinning. The sample was then diluted to 1.0 mL with the same buffer and treated with 0.1 M β-mercaptoethanol (10 μL; in pH 7.0 buffer). The yellow color was quantitated by visible absorbance at 412 nm and the concentration of TNB^{2-} anion was determined using an extinction coefficient of 14 150 and applying a correction for the absorbance of the protein (Riddles et al., 1979). The antibody fragment concentration was calculated using the conversion factor of 1.48 per mg/mL at 280 nm (Mandy and Nisonoff, 1963).

Free sulfhydryl groups were also quantitatively evaluated using a modification of a previously reported isoelectric focusing method (Feinstein and Scott, 1972). Fab' prepared as described above (150 μL) was treated for 30 min at room temperature with 0.2 M of 4-iodoacetamidosalicylic acid (Molecular Probes, Eugene, OR) in DMF (3.75 μL) to give a 5 mM final concentration of the alkylating reagent. A control sample was prepared in a similar manner using iodoacetamide. Following alkylation, the samples were diluted to 2.0 mL with pH 7.0 phosphate buffer, concentrated, and respun with additional buffer (2 × 2 mL) on Centricon-30 units. Analysis of the concentrated samples was performed on a pH 3–10 agarose isoelectric focusing gel obtained from FMC (Rockland, ME). Conditions were as follows: 11 °C, 1500 V, 20 mA, 1 W for 10 min followed by 25 W for 25 min on a Bio-Rad apparatus. The gel was fixed and stained using Coomassie Blue according to the manufacturer's protocol. The total number of interchain cysteines for mildly reduced (but not reoxidized) $F(ab')_2$ was evaluated by a modified procedure in which mini-spin columns were pre-equilibrated in pH 7.0 phosphate buffer containing 1 mM EDTA, conditions developed to preserve free sulfhydryl groups during the elution step.

Fluorescence tagging was used to determine the location (H' or L chain) of the Fab' cysteine. An aliquot of Fab' prepared as above (50 μL) was treated with 1 mM 5-fluorescein–maleimide (Molecular Probes) in DMF (5 μL) for 30 min at room temperature. SDS–PAGE was performed under nonreducing conditions and the gel was photographed under long-wavelength UV light prior to staining.

General Procedure for Fab' Cross-Linking. Chemical cross-linking of Fab' with 1 or 2 was performed as follows. A sample of Fab' was prepared as described above, yielding approximately 2 mg (4×10^{-5} mmol based on MW 50 kDa) in pH 8.0 phosphate buffer containing 1 mM EDTA. Next, a solution of 0.33 mM trismaleimide 1 or 0.25 mM tetramaleimide 2 in DMF was added in four aliquots (10 μL each) over a 1-h period to give a final Fab' to cross-linker molar ratio of 3:1 for tribody or 4:1 for tetrabody, the theoretical ratio for complete formation of the respective cross-linked fragments. Analytical GF-250 HPLC was used to monitor progress of the reactions, with or without prior alkylation of sample aliquots using excess iodoacetamide. Small aliquots were also removed periodically and quenched with iodoacetamide prior to SDS–PAGE analysis. Following the 1 h reaction period, 0.1 M NEM in DMF (10 μL) was added to give a final concentration of 1 mM. NEM serves to alkylate unreacted sulfhydryl groups; alternatively, excess iodoacetamide can be used. After 15 min at room temperature the entire sample was concentrated on a Centricon-30 unit and injected onto a GF-250 HPLC column using a slow flow rate (0.5 mL/min for tribody, 0.3 mL/min for tetrabody) to allow isolation of the peak of interest.

Preparation of Radiolabeled Tribody and Tetrabody. Radiolabeled tribody was prepared as described above, except that ^{105}Rh-labeled $F(ab')_2$ (pepsin-digested) was used for generation of the Fab' subunit. Labeling of $F(ab')_2$ was performed according to a published procedure

(Kruper et al., 1988) in which lysing residues were conjugated by reaction with the isothiocyanate derivative of the radiometal complex ^{105}Rh(BA-2,3,2-tet)Cl$_2$. Previous studies had demonstrated the non-site-specific nature of conjugation using this complex in that both the heavy and light chains of IgG are radiolabeled. For preparation of radiolabeled tribody, two identical 2.0-mg samples of ^{105}Rh-labeled F(ab')$_2$ (specific activity ~0.1 mCi/mg) were used to prepare Fab' for cross-linking. Following the cross-linking and NEM alkylation steps, the samples were pooled, concentrated, and diluted to 200 μL with pH 7.0 phosphate buffer. GF-250 HPLC isolation was performed using four separate injections. Pooled fractions corresponding to the tribody were concentrated on a Centricon-30 unit, respun twice with PBS (2 × 2 mL), and diluted to 2.0 mL. The overall yield of tribody from F(ab')$_2$ was 18%, based on the Pierce Coomassie assay. Separate preparations of HPLC-isolated tribody were used for blood clearance and biodistribution studies in Balb/c mice, and for a 5-day study in tumor-bearing nude mice.

Radiolabeled tetrabody was prepared by a similar procedure except that two identical samples of ^{105}Rh-labeled Fab' were treated with four additions of 0.25 mM tetramaleimide in DMF (10 μL each), one aliquot every 15 min. Following the 1 h cross-linking step, samples were treated and isolated as described above for the tribody. The overall yield of tetrabody from F(ab')$_2$ was 4% based on the Pierce Coomassie assay. HPLC-isolated tetrabody was used for a 4-h blood-clearance study in Balb/c mice; the same animals were sacrificed at 24 h to obtain biodistribution data (Table II).

Biodistribution Studies. Female athymic nude mice (nu/nu, CD1 background) were obtained from Charles River (Wilmington, MA) at 5–8 weeks of age. Mice were housed on laminar flow racks in cages with filter bonnets and fed autoclaved rodent diet and sterilized tap water ad libitum. Balb/c female mice were obtained from Charles River (Portage, MI) at 4–5 weeks of age. All animals were acclimated at least 1 week prior to experimental use. LS-174T human colorectal carcinoma cell line (ATCC CL-188) was maintained in tissue culture in minimal essential media supplemented with 1% nonessential amino acids, 2 mM glutamine, and 10% fetal bovine serum. Cultures were harvested weekly with trypsin-EDTA and cell density and viability determined by trypan blue dye exclusion. Athymic nude mice were injected sc with 1 × 10^{-6} LS-174T cells/0.1 mL culture media and screened for tumor growth 11–13 days later. Mice bearing tumor xenografts in the range of 100–300 mg were selected for biodistribution studies and sorted into five groups. Prior to injection, four syringes of radioimmunoconjugate were randomly selected and expelled into counting tubes to serve as injection standards. Animals were lightly anesthetized with Metofane (Pittman Moore, Mundelein, IL) and the radioconjugate of interest (1–2 μCi/50 μL) injected into the tail vein. For early time point blood-clearance studies, mice were anesthetized with ketamine hydrochloride (Ketaset, Fort Dodge Laboratories, Fort Dodge, IA) to enable repeated sampling from the same animals. Blood samples for these studies were obtained by retroorbital puncture using heparinized capillary tubes. At 5, 24, 48, and 120 h postinjection, five animals were anesthetized and exsanguinated. The blood was placed in counting tubes and weighed. The liver, spleen, kidneys, and tumor, when present, were removed, rinsed in PBS, blotted dry, and weighed. These tissues were then placed in counting tubes. The GI tract, remaining carcass, and tail were placed directly in counting tubes. Radioactivity was determined using a "well-type" NaI scintillation detector coupled to a ND66 (Nuclear Data, Schaumberg, IL) γ-ray spectrometer and a Searle Model 1185 automatic sample changer (TM Analytic, Elk Grove Village, IL). Statistical outliers were identified and removed from the data set using the ANOVA program (SAS Institute Inc., Cary, NC).

Trismaleimide, 1

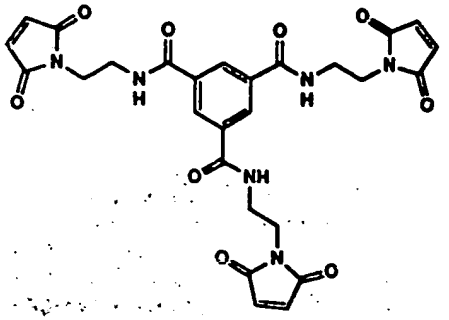

Tetramaleimide, 2

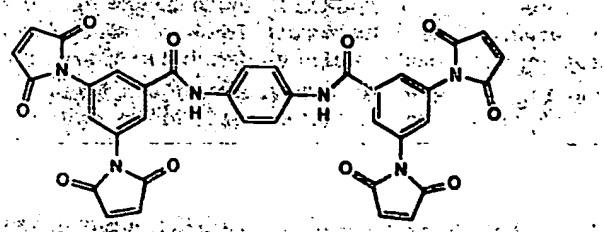

Figure 1. Structures of compounds used for cross-linking Fab' antibody subunits.

RESULTS AND DISCUSSION

Design of Cross-Linkers. A variety of cysteine sulfhydryl modification agents are known from the literature (for a review, see Means and Feeney, 1990). For the present work, we chose the maleimide functionality because of its excellent properties for use in protein covalent modification. These advantages include (a) rapid reactions in the neutral pH range using low, stoichiometric concentrations of protein and reagent, (b) specificity for cysteine sulfhydryl moieties, (c) synthetic accessibility of compounds of interest, and (d) stability of resulting thioether bonds to physiological buffer conditions. Although bromoacetamides are frequently used for modifying sulfhydryl groups on proteins, they are generally less reactive than maleimides (Goldberg et al., 1991) and therefore a greater stoichiometric excess is required. For the cross-linking applications described here, rapid stoichiometric reactions were desirable for obtaining the target immunoconjugates in a straightforward "one-pot" reaction.

Two new compounds, trismaleimide 1 and tetramaleimide 2 (Figure 1), were synthesized as Fab' cross-linking reagents. These multifunctional compounds represent an extension of the series beginning with the bismaleimide reagents previously reported for the preparation of "stabilized" F(ab')$_2$ (Quadri et al., 1992) and bispecific F(ab')$_2$ (Stickney et al., 1988; Glennie et al., 1987). The design of 1 and 2 was influenced by the notion of keeping the structures relatively simple and also taking advantage of known synthetic routes and available starting materials. Compounds 1 and 2 represent a starting point for the preparation of multifunctional antibody fragments; future modifications may be necessary in order to optimize the

structures for Fab′ cross-linking applications. At least one report has appeared on the use of a trifunctional alkylating agent for cross-linking protein subunits (Hiratsuka, 1988). The mustard compound tris(2-chloroethyl)-amine was shown to react with both cysteine sulfhydryl and lysine amine groups in the heavy chain domains of myosin adenosinetriphosphatase. The trifunctional and tetrafunctional reagents described in the present work were expected to be specific for cysteine sulfhydryl groups.

Preparation of 1 was achieved through a multistep procedure involving reaction of the trimethyl ester of 1,3,5-benzenetricarboxylic acid with an excess of ethylene diamine, followed by reaction with maleic anhydride to form a trismaleamate. Reaction of the trismaleamate with sodium acetate in acetic anhydride resulted in cyclization to the symmetrical trismaleimide. Tetramaleimide 2 was prepared using a slightly different approach involving attachment of preformed bismaleimide segments onto a central phenylenediamine moiety. Thus, 3,5-diaminobenzoic acid was converted in two steps to the bismaleimide acid intermediate, followed by formation of the acid chloride, and, finally, reaction with *p*-phenylenediamine to give 2.

Preparation and Characterization of Fab′. The literature contains numerous methods for the preparation of Fab′ from $F(ab')_2$. In many of the reported procedures, however, the quality of Fab′ produced is less than optimal in that polyacrylamide gel analysis shows the presence of small amounts of H′ and L chains remaining after mild reduction of the parent fragment (Glennie et al., 1987). In the present work, a modification of an older method was used for the preparation of Fab′. The original procedure was developed for the preparation of bispecific $F(ab')_2$ (Nisonoff and Rivers, 1961) and involved reduction of interchain disulfides followed by reoxidation of both H′–L and H′–H′ bonds using a stream of oxygen at pH 8. Under these conditions, Fab′ is a likely intermediate since "intramolecular" (H′–L) disulfide bonds within the Fab′ subunit would be expected to form more rapidly than "intermolecular" (H′–H′) disulfide bonds between the Fab′ subunits.

We report here the preparation of Fab′ from the $F(ab')_2$ fragment of monoclonal antibody CC49 (murine IgG1 subclass). A multistep procedure was developed which involved mild reduction of $F(ab')_2$ followed by selective reoxidation of H′–L disulfide bonds. Preparations typically were carried out on a small scale (2 mg per batch). $F(ab')_2$ was first treated with excess dithiothreitol (20 mM) at neutral pH to effect reduction of all interchain disulfide bonds. Preliminary experiments were conducted to examine the influence of pH on the rate of disulfide bond reduction. As expected, reduction proceeded faster with increasing pH over the range of pH 6–8 (data not shown). Use of phosphate buffer at pH 7 allowed complete reduction of fragment interchain disulfides in less than 15 min (Figure 2a).

Following the mild reduction step, excess reducing agent was removed from reaction mixtures by a rapid gel filtration procedure (Meares et al., 1984), performed here using commercially available "mini-spin" columns. This procedure served both to aerate the elution buffer and to exchange the buffered solution to pH 8, conditions which allowed selective reoxidation of H′–L disulfide bonds (Figure 2b). The results show that formation of disulfide bonds between H′ and L chains was virtually complete following a 3-h incubation period at room temperature. Minimal H′–H′ bond formation was observed over the same time period, although incubation for longer periods

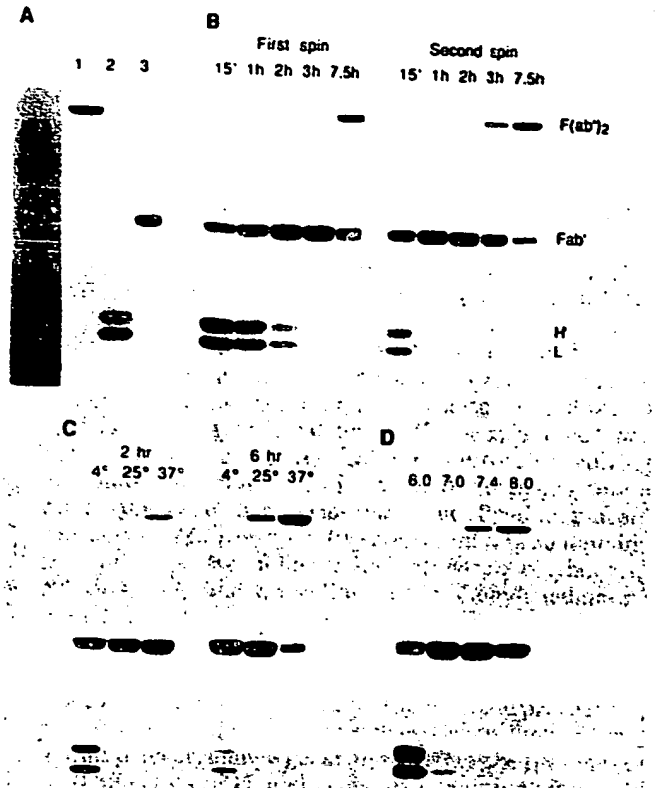

Figure 2. Studies on the preparation of CC49 Fab′ from $F(ab')_2$ by a process of disulfide bond reduction followed by selective reoxidation. In all panels, CC49 $F(ab')_2$ at 2 mg/mL was subjected to mild reduction using dithiothreitol, processed over mini-spin columns and incubated at room temperature (unless otherwise indicated) prior to quenching with excess iodoacetamide (for details see Experimental Procedures). SDS–PAGE analysis was performed on 10% polyacrylamide gels under nonreducing conditions. Molecular weight markers were phosphorylase B (95 kDa), serum albumin (66 kDa), ovalbumin (45 kDa), carbonic anhydrase (31 kDa), and trypsin inhibitor (21.5 kDa). Panel A: Antibody fragment reference standards for reoxidation studies. Lane 1, CC49 $F(ab')_2$; lane 2, $F(ab')_2$ treated with 20 mM DTT for 15 min at room temperature and quenched with iodoacetamide; lane 3, Fab′–pyridyl formed by treatment of mildly reduced fragments with 2,2′-dithiopyridine. Panel B: Time-dependence of disulfide bond reformation following mini-spin processing. $F(ab')_2$ was mildly reduced and aliquots were processed over mini-spin columns at pH 8. Lanes represent aliquots incubated at room temperature for the time periods indicated following one or two mini-spin processing steps. Panel C: Effect of incubation temperature on the rate of disulfide bond formation. $F(ab')_2$ was mildly reduced and processed over mini-spin columns at pH 8, and samples were incubated at various temperatures. Aliquots were quenched with iodoacetamide at postspin times of 2 and 6 h. Panel D: Effect of buffer pH on the rate of disulfide bond formation. $F(ab')_2$ was mildly reduced and processed over mini-spin columns using phosphate buffer adjusted to pH 6.0, 7.0, 7.4, or 8.0. Aliquots were quenched with iodoacetamide following a 6-h incubation time at room temperature.

did lead to significant formation of the unwanted $F(ab')_2$ dimer. These results are consistent with a relatively fast rate of disulfide bond formation between H′ and L chains compared with the rate of disulfide bond formation between Fab′ subunits.

Evidence pointing to the importance of buffer aeration was obtained from the following two experiments. In the first, mildly reduced $F(ab')_2$ was processed sequentially over two mini-spin columns, both at pH 8. Analysis by SDS–PAGE (Figure 2b) revealed that reoxidation of H′ and L chains to Fab′ was completed in approximately half

the time normally required for reoxidation using a single column. In the second experiment, $F(ab')_2$ was subjected to mild reduction using commercially available DTT beads. Samples were then processed over empty mini-spin columns (no resin, filter only) and left at ambient temperature for several hours. SDS-PAGE analysis revealed that disulfide bond formation was slowly significantly in comparison with the results seen with the usual protocol (data not shown).

Examination of the rate of disulfide bond formation as a function of temperature was carried out over the range 4–37 °C at pH 8 (Figure 2c). The results illustrate that disulfide bond formation is speeded up as the temperature is increased, and that nearly complete reformation of disulfide bonds between H′–L and H′–H′ chain pairs is possible when long incubation times and/or elevated temperatures are used (6 h at 37 °C, for example). Examination of the rate of disulfide bond formation as a function of pH was carried out at room temperature using mini-spin processing conditions ranging from pH 6 to 8 (Figure 2d). Not unexpectedly, the rate of disulfide bond formation was enhanced with increasing pH. It was also evident that a range of pH conditions could be used to produce Fab′, with appropriate adjustments in the incubation time.

Additional observations on the rate of disulfide bond formation were as follows. An increase in the protein concentration was observed to result in a higher proportion of the unwanted dimer form of the fragment when reoxidation was carried out at room temperature. Increasing the mini-s; in column loading volume was found to slow reoxidation, presumably due to an increase in amount of DTT which eluted along with the protein fraction. When 1 mM EDTA was included in the mini-spin column elution buffer, disulfide bond formation was slowed dramatically over the pH range 6–8. (This procedure, when carried out at pH 6–7, is useful for the preparation of noncovalently associated H′L pairs). The above results suggest that various combinations of the reoxidation reaction parameters can be used to successfully prepare Fab′ subunits. Conditions selected for the routine preparation of Fab′ were as follows: 2 mg/mL initial concentration of $F(ab')_2$, with pH 8 processing over a mini-spin column (no EDTA present), and a 3-h incubation period at room temperature. Over the course of many experiments, some batch-to-batch variability was noted with respect to the incubation time required for complete H′–L disulfide bond formation, but 3 h appeared to be the average time required.

When EDTA was added to solutions containing Fab′ following the incubation period, subsequent disulfide bond formation was slowed dramatically at pH 8 and to a lesser extent at pH 7 (Figure 3). Therefore, Fab′ containing solutions were routinely made to 1 mM in EDTA following the oxidation step in order to slow dimerization. The presence of a small amount of dimer was not of concern, however, because the dimer could be separated from the higher molecular weight tribody or tetrabody product at a later time by gel filtration chromatography. If desired, the pH of the final solution containing Fab′ could be adjusted to a lower value to further slow dimerization while still allowing rapid reaction of the Fab′ sulfhydryl with the cross-linking reagent. However, the use of a pH 8 buffer was found to be convenient for both the Fab′ reoxidation and for the subsequent cross-linking step.

Following confirmation of the desired 50-kDa species by SDS-PAGE analysis, characterization of Fab′ also involved quantitation of hinge-region sulfhydryl groups.

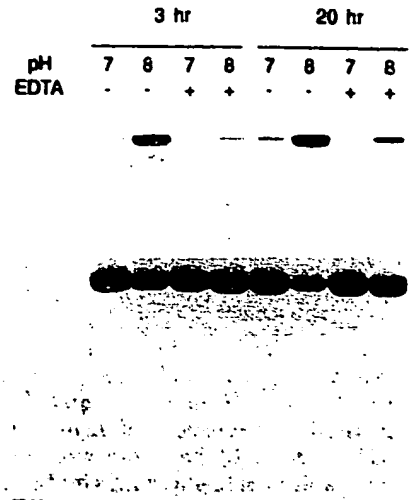

Figure 3. Effect of EDTA on the stability of Fab′. CC49 Fab′ was prepared by the standard protocol, and following the usual 3-h incubation period, the buffer was either adjusted to pH 7 or left at pH 8 in the presence or absence of 1 mM EDTA. The final concentration of Fab′ was approximately 1 mg/mL. Sample aliquots were quenched with iodoacetamide after 3 or 20 h at room temperature.

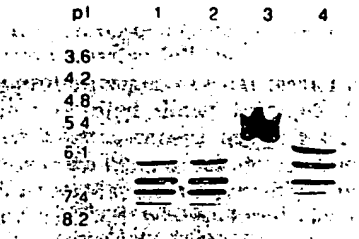

Figure 4. Isoelectric focusing analysis of charge-modified CC49 Fab′ and H′–L pairs. $F(ab')_2$ was mildly reduced and processed over mini-spin columns in one of two ways: At pH 7.0 in the presence of EDTA, to yield the H′L pair (lanes 1 and 3), or at pH 8.0 in the absence of EDTA, to yield Fab′ after the usual 3-h incubation period (lanes 2 and 4). Aliquots were then quenched either with iodoacetamide (lanes 1, 2) or with 4-iodoacetamidosalicylic acid (lanes 3, 4).

Murine IgG is known to possess three disulfide bonds in the hinge region. In published works, determination of free cysteines on Fab′ (prepared by the mild reduction of $F(ab')_2$ from pepsin-digested IgG1) reportedly gave close to the expected value using the colorimetric reagents 2,2′-dithiopyridine (Glennie et al., 1987) and DTNB (Brennan et al., 1985). Quantitation of free sulfhydryl groups on CC49 Fab′ by the latter method gave a TNB^2- to Fab′ molar ratio of 1.1:1. That the ratio was approximately 1:1 and not 3:1 suggests that two of the three hinge region sulfhydryl groups were reoxidized to form an intrachain disulfide bond, leaving one free sulfhydryl group available for subsequent modification.

Sulfhydryl groups on Fab′ were also quantitatively evaluated using a modification of a method reported by Feinstein and Stott (1972). The procedure involves chemical modification of a protein with a negatively charged alkylation reagent such as iodoacetic acid followed by isoelectric focusing analysis. In the present work, a single charge shift was observed by IEF analysis following alkylation of Fab′ with 4-iodoacetamidosalicylic acid (Figure 4, lane 4), indicating the presence of a single hinge-region cysteine. An advantage of using iodoacetamidosalicylic acid compared with iodoacetic acid was its reduced tendency to generate contaminating iodine (a sulfhydryl oxidant) upon storage. Also, iodoacetamidosalicylic acid was found to react more rapidly with Fab′ cysteine sulfhydryl groups (data not shown). In a variation of the

IEF analysis, mini-spin processing was carried out at pH 7 in the presence of 1 mM EDTA. Under these conditions, the newly generated cysteine sulfhydryls were preserved in their reduced state. IEF analysis of charge-modified Fab′ prepared in this manner (actually the noncovalently associated H′L pair) showed a striking shift toward the cathode, indicating charge modification at several cysteine residues (Figure 4, lane 3). This result is consistent with the expected number of sulfhydryls (five) for mildly reduced murine IgG1-derived Fab′. Control samples of Fab′ or the H′L pair which were alkylated with neutral reagents (NEM, iodoacetamide) showed no charge shifts by this analysis. Comparative IEF analysis showed that Fab′ prepared from both papain- and pepsin-digested $F(ab')_2$ gave virtually identical charge shifts following mild reduction and alkylation with 4-iodoacetamidosalicylic acid.

In a qualitative test to further define the location of the free cysteine, Fab′ was treated with an excess of 5-fluorescein–maleimide and analyzed by SDS–PAGE (data not shown). Under nonreducing conditions, a single fluorescent band was observed near 50 kDa. When a sample of fluorescein-modified Fab′ was subjected to mild reduction and alkylation prior to gel analysis, a fluorescent band corresponding to the migration of the H′ chain was observed, consistent with a pattern hinge-region modification.

The air-oxidation procedure described here for the preparation of Fab′ has several advantages over known methods. First, Fab′ is produced as a homogeneous product, with minimal dimer formation and lacking contamination from noncovalently bonded H′ and L chains (which would remain associated under neutral aqueous conditions). The fact that virtually all H′ and L chains are reconnected through disulfide bonds is significant in that no unwanted chemical cross-linking can occur at these sites. For some applications involving "intramolecular" cross-linking of cysteines in mildly reduced IgG, it may be desirable to effect covalent attachment of antibody heavy and light chains with sulfhydryl-specific modification reagents (Packard and Ededin, 1986; Liberatore et al., 1990; Goldberg et al., 1991). However, the successful preparation of $F(ab')_3$-x and $F(ab')_4$-x depends upon selective cross-linking at hinge-region sulfhydryl groups, and not between H′ and L chains.

A second advantage is that preparation of Fab′ is straightforward and does not involve time-consuming dialysis steps, and the entire procedure is completed in under 4 h. The resulting Fab′-containing solution is ready for use in subsequent chemical modification reactions or can be stored frozen for future use. Fab′ can also be prepared by a procedure proposed recently by Glennie and co-workers (1987). In this method, use of 2,2′-dithiopyridine apparently leads both to H′–L disulfide formation and to formation of a mixed disulfide at the hinge region to yield Fab′–pyridyl. The pyridyl group is then selectively removed by treatment with a reducing agent at low pH. In our hands, this method was found to yield a homogeneous preparation of Fab′–pyridyl (Figure 2a) and its reduced counterpart, Fab′ (not shown). However, the method involves additional steps compared with the air-oxidation protocol. Although not explored here, an alternative procedure for Fab′ preparation would be the controlled delivery of air or oxygen to a solution containing the mildly reduced fragment, in the manner reported previously for the preparation of $F(ab')_2$ heterodimers (Nisonoff and Rivers, 1961; Staerz and Bevan, 1986).

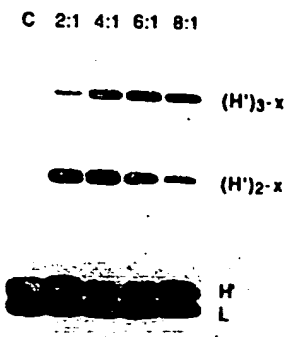

Figure 5. SDS–PAGE analysis of $F(ab')_3$-x preparation trials. CC49 $F(ab')_2$ was subjected to mild reduction, reoxidation, and incubation at pH 8 as described. Aliquots of Fab′ solution were then treated with trismaleimide 1 using the molar ratios indicated (given as 1:Fab′). Following a 1-h reaction period at room temperature, samples were subjected to mild reduction with dithiothreitol and alkylation with excess iodoacetamide to permit visualization of H′ and L chains as distinct bands under nonreducing conditions. Lane C represents control Fab′ with no cross-linker added.

Preparation of Multivalent Cross-Linked Antibody Fragments. Trismaleimide 1 was used for the development of suitable reaction conditions for joining Fab′ subunits. For these experiments, Fab′ was used as a 4×10^{-5} M solution (2 mg/mL) in pH 8 phosphate buffer. The results of a study designed to determine the optimal fragment to cross-linker ratio are shown in Figure 5. In this experiment, individual aliquots of freshly prepared Fab′ were treated with varying concentrations of 1 for 30 min at ambient temperature. Reaction mixtures were analyzed by SDS–PAGE under nonreducing conditions following mild reduction and alkylation, a treatment which allowed separation of the H′ and L bands. The data revealed that a Fab′ to 1 ratio of approximately 4:1 to 6:1 was optimal for tribody formation, as evidenced by an increase in intensity of the band corresponding to the cross-linked H′ chain (H'_3-x, 75 kDa). The observed decrease in the intensity of the H′ band (25 kDa) indicated that nearly all hinge-region sulfhydryl groups were reacted with the cross-linking reagent. Analysis of reaction mixtures by gel filtration HPLC yielded similar results (data not shown). In theory, a Fab′ to 1 ratio of 3:1 should be optimal for complete cross-linking. The discrepancy may be due in part to the loss of protein incurred during the mini-spin elution step (recoveries were ~80%).

One possible explanation for the incomplete formation of $F(ab')_3$-x from Fab′ is that side reactions may occur on non-cysteine residues, leading to the loss of one or more reactive maleimide functionalities (Glennie et al., 1987). This possibility also may explain the presence of small amounts of high molecular weight species that were often observed by SDS–PAGE or gel filtration HPLC. Also, the presence of more than one free cysteine in the hinge region of some Fab′ molecules could lead to unwanted multimeric species. While our analytical results suggested the presence of a single sulfhydryl group on average, the possibility exists that some of the Fab′ molecules were heterogeneous in this respect.

Various other observations from tribody preparation trials are noteworthy. Use of either pepsin or papain-derived fragments gave similar results in small-scale cross-linking reactions. (Due to availability, the former were used for most of the early analytical studies, and the latter were used for preparation of radiolabeled tribody and tetrabody for in vivo studies.) Cross-linking was observed to proceed faster with increasing pH (over the range pH

6–8), although similar product profiles were observed upon completion of the reaction. When a shorter incubation period than 3 h was used for Fab′ formation, the yield of $F(ab')_3$-x was decreased. A likely explanation is that disulfide formation within Fab′ subunits was incomplete, allowing "extra" cysteines on H′ and L chains to participate in cross-linking reactions. Alternatively, a low concentration of unoxidized DTT may have been present following the shorter incubation period, leading to rapid consumption of the cross-linking reagent.

$F(ab')_3$-x was found to be stable over a 6-h period at room temperature when exposed to buffer conditions in the pH range 7.0–8.8. Stability was monitored by SDS–PAGE under nonreducing conditions (data not shown). In contrast, $F(ab')_3$-x was slowly degraded at pH 9.6, as evidenced by the appearance of two new bands near 50 and 100 kDa, presumably the monomeric and dimeric forms of Fab′. (We also observed a pH-related instability for the bismaleimidooctane cross-linked fragment, $F(ab')_2$-x, which was approximately 50% degraded to a 50-kDa product after 24 h at pH 9.6.) Although the maleimide-derived thioether bond is considered to be stable to physiological conditions, it appears to be unstable at high pH, as has been noted previously for maleimide adducts of cysteine (Smyth et al., 1960).

Preparation of Radiolabeled Tribody and Tetrabody. Because of the observed instability of maleimide-cross-linked fragments at high pH, we decided to prepare radiolabeled $F(ab')_3$-x and $F(ab')_4$-x for animal studies using Fab′ generated from prelabeled $F(ab')_2$. This strategy avoided subjecting the unlabeled cross-linked products to the basic conditions (pH ≥ 9) typically required for attachment of the radiometal chelate to lysine residues. Radiolabeled $F(ab')_2$ was prepared via conjugation of lysine amines with the isothiocyanate derivative of the radiometal complex ^{105}Rh(BA-2,3,2-tet)Cl_2 (Kruper et al., 1988). As it possesses both γ- and β-emissions, ^{105}Rh is a candidate for use in cancer immunotargeting applications (Voikert et al., 1991). The stable radiometal chelate complex was favored for biodistribution studies over radioiodine due to the apparent tendency of the latter to dehalogenate in organs (Carrasquillo et al., 1984). Furthermore, it was expected that conjugation of the ^{105}Rh(BA-2,3,2-tet)Cl_2 complex onto lysine residues would lead to no net charge change, since the complex itself was believed to possess an overall charge of +1. This expectation was confirmed by isoelectric focusing analysis.

Radiolabeled $F(ab')_3$-x was prepared by addition of trismaleimide 1 to a freshly prepared sample of ^{105}Rh-labeled Fab′. A final Fab′ to 1 molar ratio of 3:1 was achieved by the addition of several small aliquots of the cross-linking reagent. This procedure was used for the preparative reactions in order to maximize formation of the desired product without risking local high concentrations of the cross-linker, and to prevent overaddition of the reagent. The composition of reaction mixtures was assessed by analytical SDS–PAGE with autoradiographic detection (Figure 6a). Under nonreducing conditions, a band corresponding to $F(ab')_3$-x was observed (150 kDa) along with bands corresponding to dimer and Fab′ monomer (100 and 50 kDa, respectively). Under reducing conditions, a band corresponding to cross-linked H′ chains (75 kDa) was observed, along with a lower molecular weight band presumably corresponding to H'_2-x. Following a brief alkylation step with *N*-ethylmaleimide, ^{105}Rh-labeled $F(ab')_3$-x was isolated by gel filtration chromatography (Figure 7a). HPLC analysis of the isolated product gave a single peak by both UV and radioactivity detection

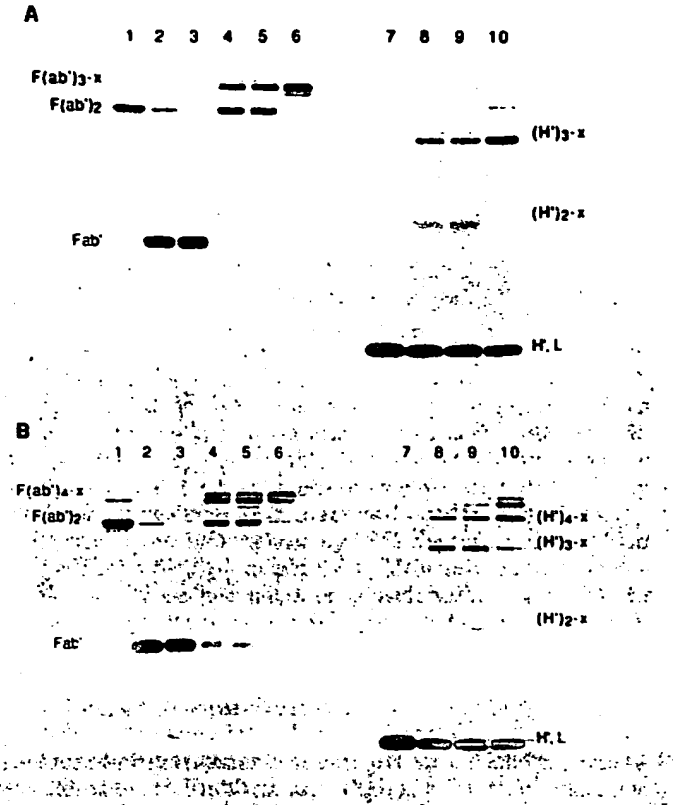

Figure 6. SDS–PAGE autoradiographic visualization of radiolabeled CC49 $F(ab')_3$-x and $F(ab')_4$-x preparations. For the cross-linking reactions, freshly prepared ^{105}Rh(BA-2,3,2-tet)-labeled Fab′ was treated with the theoretical molar excess of either trismaleimide 1 (panel A) or tetramaleimide 2 (panel B) as detailed in Experimental Procedures. Samples were run under nonreducing conditions (lanes 1–6) or reducing conditions (lanes 7–10). Lanes 1 and 7, radiolabeled $F(ab')_2$ starting material; lanes 2 and 3, Fab′ (identical samples in separate reaction vials); lanes 4, 5, 8, and 9, crude reaction mixtures following addition of cross-linker; lanes 6 and 10, GF-250 HPLC-isolated product.

(Figure 7a). The results of SDS–PAGE/autoradiography (Figure 6a) confirmed the purity of the isolated product, and revealed the presence of bands corresponding to H_3-x and L under reducing conditions.

Radiolabeled $F(ab')_4$-x was prepared in a similar manner, except that the final molar ratio of Fab′ to tetramaleimide 2 was 4:1. By SDS–PAGE/autoradiographic analysis, only a small fraction of protein in the reaction mixture corresponded to the desired 200-kDa product (Figure 6b). Other gel bands corresponded to lower molecular weight species including the trimeric, dimeric, and monomeric forms of Fab′. As shown in Figure 7b, HPLC-isolated ^{105}Rh-labeled $F(ab')_4$-x remained contaminated with tribody and unidentified high molecular weight forms. The low isolated yield of tetrabody permitted only a preliminary biodistribution study to be carried out in Balb/c mice. As it is possible that the characteristics of the cross-linking reagent (e.g. hydrophobicity, linker length) may play a role in its ability to react with sulfhydryl groups on Fab′, tetramaleimide 2 may not be an optimal reagent.

Immunoreactivity of the radiolabeled cross-linked fragments was assessed by ELISA (Figure 8). Unconjugated and ^{105}Rh-labeled $F(ab')_2$ showed similar profiles, while both the radiolabeled $F(ab')_3$-x and $F(ab')_4$-x forms showed enhanced binding compared to $F(ab')_2$. A possible explanation for the higher absorbance values observed at low dilution is that the second antibody may be capable of binding to more sites on the cross-linked fragments compared with $F(ab')_2$. Since both ^{105}Rh-labeled $F(ab')_3$-x

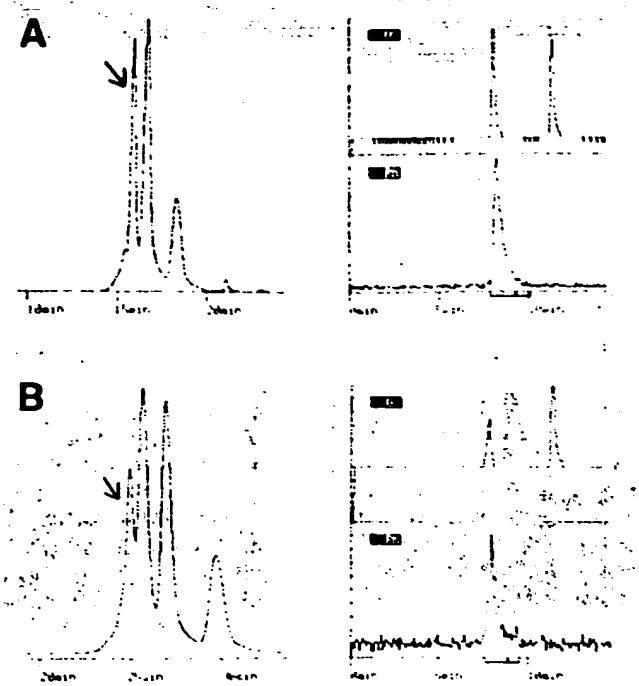

Figure 7. Gel filtration HPLC analysis of radiolabeled $F(ab')_3$-x and $F(ab')_4$-x reaction mixtures and isolated products. ^{105}Rh-labeled CC49 $F(ab')_3$-x (panel A) and $F(ab')_4$-x (panel B) were prepared as described, and product mixtures were subjected to GF-250 isolation. Preparative HPLC profiles with UV detection are shown on the left (note different windows of time shown for the two samples). Arrows indicate the peaks collected. Analytical profiles of the isolated $F(ab')_3$-x and $F(ab')_4$-x products are shown at right, with both UV detection (top) and radioactivity (bottom) detection shown. Flow rates for the isolation of $F(ab')_3$-x and $F(ab')_4$-x were 0.5 and 0.3 mL/min, respectively; the flow rate for analytical runs was 1.0 mL/min. The UV peak near 12 min was probably due to buffer salts.

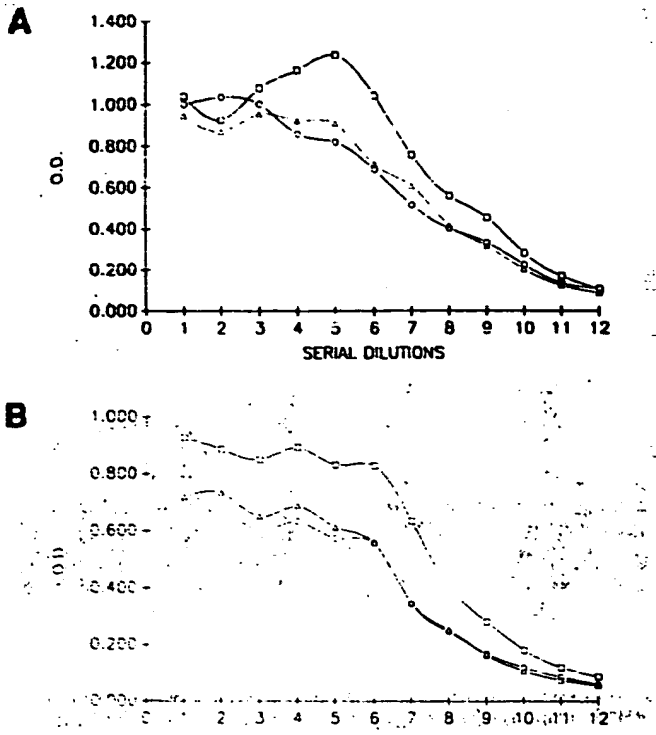

Figure 8. ELISA immunoreactivity analysis of ^{105}Rh-labeled CC49 $F(ab')_3$-x and $F(ab')_4$-x. HPLC-isolated tribody (panel A, squares) and tetrabody (panel B, □) were assessed for immunoreactivity by ELISA and compared in the same assay with unconjugated $F(ab')_2$ (○) and ^{105}Rh-labeled $F(ab')_2$ (△). Starting concentrations for all antibody forms were 10 μg/mL, and partially purified TAG-72 was used as antigen as detailed in Experimental Procedures.

and $F(ab')_4$-x were immunoreactive, it appeared that the cross-linking procedures did not compromise the ability of these forms to bind antigen in a solid-phase assay. (In previous studies, the bismaleimide-cross-linked $F(ab')_2$-x was found to retain full immunoreactivity compared with unmodified $F(ab')_2$).

Animal Biodistribution Studies. A preliminary biodistribution study comparing ^{105}Rh-labeled $F(ab')_2$ and $F(ab')_3$-x was carried out in Balb/c mice. Figure 9a shows early blood values and Table I lists biodistribution data for the same animals at 24 h postinjection. Compared with $F(ab')_2$, $F(ab')_3$-x showed a longer blood residence time and decreased kidney localization. Significantly higher liver, spleen, carcass, and whole-body retention levels were observed for $F(ab')_3$-x. The fact that both $F(ab')_2$ and $F(ab')_3$-x lack the Fc region may correlate with their relatively rapid blood clearance, since this segment is believed to be responsible for the long circulation time of the intact immunoglobin molecule (Waldmann and Strober, 1969).

The biodistribution of ^{105}Rh-labeled $F(ab')_4$-x in Balb/c mice was also studied. Results of a blood sampling study (Figure 9b) indicated that clearance of $F(ab')_4$-x from the circulation was similar to that of $F(ab')_2$ at early time points. Biodistribution data obtained for the same animals at 24 h (Table II) showed significantly greater localization of the radiolabel in the liver for $F(ab')_4$-x compared with $F(ab')_2$. Kidney localization was decreased, while spleen and whole-body retention were increased for the $F(ab')_4$-x. It seems plausible that the extensive accumulation of radiolabel in the liver for $F(ab')_4$-x may account for the relatively low accumulation in other organs. No further animal work was performed with $F(ab')_4$-x due to its high liver localization. Rapid localization of high molecular weight antibody complexes to liver has previously been reported by Coodwin and co-workers (1988).

The results of a 5-day biodistribution study in tumor-bearing nude mice with ^{105}Rh-labeled $F(ab')_3$-x are shown in Figure 10. For purposes of comparison, animal data for radiolabeled IgG and $F(ab')_2$ are also plotted, although these data were obtained in separate experiments (unpublished results). Blood- and whole-body clearance curves for $F(ab')_3$-x were more similar to those of $F(ab')_2$ than IgG, while kidney clearance more closely resembled that of IgG, consistent with the Balb/c result. Tumor accumulation of $F(ab')_3$-x appeared to be greater than that of $F(ab')_2$, although only the final time point was significantly different. Enhanced tumor uptake likely correlates with the longer blood residence time observed for $F(ab')_3$-x (W. Goeckeler, unpublished observations). The liver and spleen data were intermediate between those of IgG and $F(ab')_2$. Tumor to tissue ratios for radiolabeled $F(ab')_3$-x, $F(ab')_2$ and IgG are compared in Table III. At 120 h, the radiolabeled $F(ab')_3$-x gave radiolocation index (RI) values in between those of $F(ab')_2$ and IgG for liver, spleen, and kidney, with the kidney RI value more closely resembling that of $F(ab')_2$. However, the high blood RI value (65.3) achieved for $F(ab')_3$-x at 120 h was higher than for the other two antibody forms.

The kidney results for $F(ab')_3$-x are perhaps not surprising when molecular weight is considered. A species as large as 150 kDa would not be expected to pass through the kidney glomerulus. The fact that $F(ab')_2$ (100 kDa) enters the kidney supports the concept that other properties such as shape may influence the filtration process

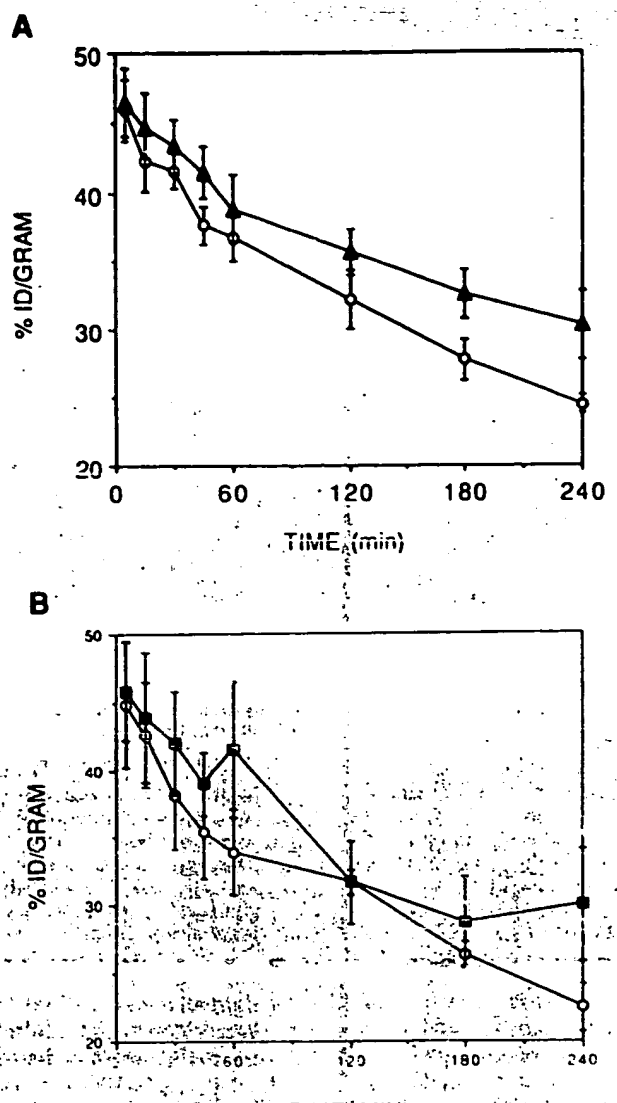

Figure 9. Comparison of blood-clearance curves for ^{105}Rh-labeled CC49 F(ab')$_3$-x and F(ab')$_4$-x Balb c mice. Panel A shows F(ab')$_3$ (○) and F(ab')$_4$-x (▲). Panel B shows F(ab')$_3$ (○) and F(ab')$_4$-x (■). Blood samples were obtained at various times after iv injection of radiolabeled antibody (four or five animals per group).

Table I. Comparison of Biodistribution Data for ^{105}Rh-Labeled F(ab')$_2$ and F(ab')$_3$-x in Balb/c Mice[a]

	% injected dose/g		% injected dose/organ	
tissue	F(ab')$_2$ avg ± SD[b,c]	F(ab')$_3$-x avg ± SD[c,d]	F(ab')$_2$ avg ± SD[b,c]	F(ab')$_3$-x avg ± SD[c,d]
blood	3.07 ± 0.88	10.73 ± 1.53	4.06 ± 1.10	13.47 ± 1.26
liver	8.93 ± 0.19	16.08 ± 1.91	9.30 ± 0.17	15.22 ± 0.56
spleen	5.36 ± 0.42	10.37 ± 1.01	0.60 ± 0.03	1.04 ± 0.17
kidney	63.49 ± 3.97	12.14 ± 1.57	15.47 ± 0.77	2.93 ± 0.23
GI tract	nd	nd	3.84 ± 0.38	5.57 ± 0.67
carcass	nd	nd	21.81 ± 1.01	32.66 ± 2.44
whole-body retention	nd	nd	53.16 ± 1.98	64.32 ± 3.86

[a] Radiolabeled antibody was administered intravenously, and animals were sacrificed at 24 h. [b] n = 5. [c] n = 4, except for blood value where n = 4. [d] nd = no data obtained. [e] SD = standard deviation.

(Sumpio, 1981). A recent investigation (Takakura et al., 1990) of the biodistribution of large and small macromolecules showed that while small species (<10 kDa) generally clear rapidly into the urine, positively charged species are taken up by the liver, and large and negatively charged species exhibit prolonged retention in the circulation. Similar overall results were also reported for synthetic branched polypeptides which differed in size, charge, and side-chain structure (Clegg et al., 1990). The biodistribution results for F(ab')$_3$-x appear to be consistent with these findings. Additionally, since the pI ranges of both the tribody and tetrabody remained unchanged from that of the parent F(ab')$_2$ fragment (pI = 6.5–7.0), it seems unlikely that charge alone played a significant role in the observed biodistribution patterns.

In comparative biodistribution studies carried out previously, we found that native CC49 F(ab')$_2$ and bismaleimide-cross-linked F(ab')$_2$-x showed virtually identical behaviors in tumor-bearing athymic mice. This result contrasts with the observations of Quadri et al. (1992), who observed significantly longer plasma circulation times and enhanced tumor uptake for three different bismaleimide-cross-linked fragments compared with native F(ab')$_2$. One possible explanation for this discrepancy is that the circulation time may be influenced by the number of hinge-region disulfide bonds in the particular F(ab')$_2$ understudy.

Overall, the in vivo behavior of F(ab')$_3$-x reveals a combination of relatively fast blood clearance, low kidney accumulation, and low to moderate tumor uptake when compared with intact IgG, F(ab')$_2$, and Fab (data not shown). These results suggest possible uses for F(ab')$_3$-x in immunotargeting applications where the long blood-residence time of IgG, and the high level of kidney accumulation of F(ab')$_2$ or Fab, are preferably avoided. Additionally, antibody species lacking the Fc region might

Table II. Comparison of Biodistribution Data for ^{105}Rh-Labeled F(ab')$_2$ and F(ab')$_4$-x in Balb/c Mice[a]

	% injected dose/g		% injected dose/organ	
tissue	F(ab')$_2$ avg ± SD[b,e]	F(ab')$_4$-x avg ± SD[c,e]	F(ab')$_2$ avg ± SD[b,e]	F(ab')$_4$-x avg ± SD[c,e]
blood	4.30 ± 1.23	6.12 ± 1.98	4.86 ± 0.92	7.08 ± 2.11
liver	6.68 ± 0.87	29.58 ± 2.23	7.10 ± 0.46	30.09 ± 1.81
spleen	6.08 ± 0.83	16.62 ± 1.46	0.40 ± 0.04	1.16 ± 0.08
kidney	65.37 ± 7.78	9.88 ± 1.02	15.49 ± 0.24	2.40 ± 0.26
GI tract	nd	nd	3.48 ± 0.50	2.81 ± 0.22
carcass	nd	nd	19.50 ± 0.96	17.92 ± 1.50
whole-body retention	nd	nd	48.11 ± 1.97	57.23 ± 3.33

[a] Radiolabeled antibody was administered intravenously, and animals were sacrificed at 24 h. [b] n = 5. [c] n = 4. [d] nd = no data obtained. [e] SD = standard deviation.

Table III. Comparison of Tumor-to-Tissue Ratios for ^{105}Rh-Labeled CC49 F(ab')$_3$-x, F(ab')$_2$, and IgG in Athymic Nude Mice Bearing LS-174T Tumor Xenografts[a]

	RI Values			
organ	5 h	24 h	48 h	120 h
	^{105}Rh-F(ab')$_3$-x			
blood	0.6	3.8	24.3	65.3
liver	1.5	3.3	5.7	6.4
spleen	2.0	4.8	11.1	13.3
kidney	0.8	2.8	6.5	7.1
	^{105}Rh-F(ab')$_2$			
blood	0.9	7.4	31.0	30.0
liver	1.9	4.2	5.3	4.0
spleen	2.9	5.9	8.6	7.5
kidney	0.4	0.6	1.2	1.5
	^{105}Rh-IgG			
blood	0.4	3.7	4.8	8.1
liver	0.8	6.8	9.0	15.2
spleen	1.4	10.1	13.0	21.1
kidney	1.5	18.0	26.7	42.2

[a] Radiolocalization Indices (RI) were calculated as the ratio of % ID/g for tumor divided by % ID/g for normal tissues.

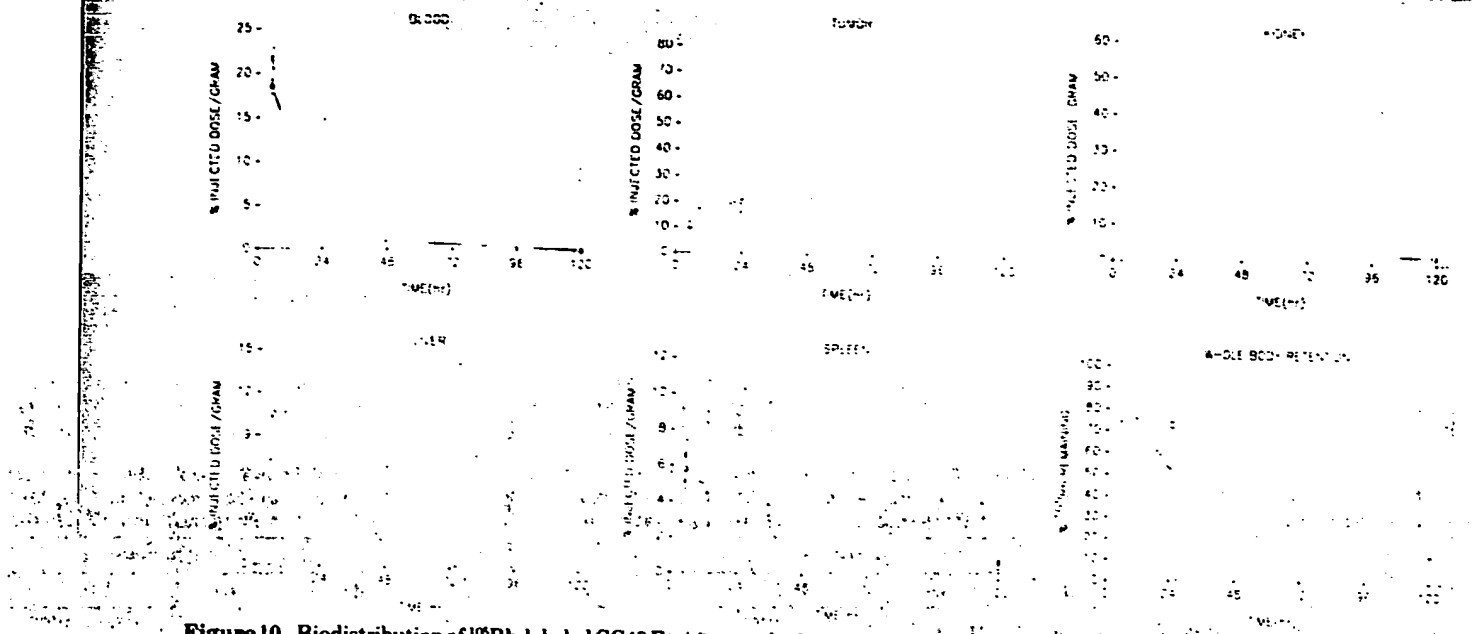

Figure 10. Biodistribution of ^{105}Rh-labeled CC49 F(ab')$_3$-x and other antibody forms in athymic mice bearing LS-174T tumor xenografts. Radiolabeled ^{105}Rh-labeled CC49 IgG (□), F(ab')$_2$ (○), and F(ab')$_3$-x (△) were injected iv in separate but otherwise identical experiments, and five animals were sacrificed at each time point as described in Experimental Procedures.

be expected to show decreased immunogenicity compared with the whole antibody.

SUMMARY AND CONCLUSION

Two new antibody fragment forms, F(ab')$_3$-x and F(ab')$_4$-x, were constructed from Fab' subunits using multifunctional cross-linking reagents. These two species can be considered an extension of the fragment series beginning with Fab' and bismaleimide-cross-linked F(ab')$_2$. Sufficient quantities of the radiolabeled target fragments were prepared for preliminary studies in Balb/c mice, and in the case of F(ab')$_3$-x, for a 5-day study in tumor-bearing nude mice. A large fraction of the radiolabeled tetrabody was found to accumulate in the liver, possibly indicating an upper size limit for the in vivo use of fragments constructed from Fab'. The in vivo behavior of F(ab')$_3$-x in both Balb/c and tumor-bearing nude mice was intermediate between that of IgG and F(ab')$_2$ for all organs studied. Kidney localization was significantly reduced, and blood circulation time and tumor accumulation were slightly increased for the trivalent species compared with F(ab')$_2$. These results are consistent with previous observations that immunoglobulin forms lacking the Fc region clear relatively rapidly from the circulation and that large macromolecules cannot penetrate the kidney glomerulus. On the basis of these results, F(ab')$_3$-x appears to be an interesting new antibody form with potentially useful properties for immunotargeting applications. The methodology developed for the preparation and cross-linking of Fab' subunits should also be applicable to small genetically designed antibody forms bearing a free cysteine moiety. This concept was recently demonstrated by Cumber and co-workers (1992), who introduced a carboxyl-terminal cysteine onto Fv and then used a bismaleimide cross-linker to form the bivalent Fv. Molecules possessing several antigen binding moieties would be expected to show enhanced antigen binding relative to the monovalent and divalent forms. It may also be possible to construct heteromultivalent molecules possessing two or more different antigen-binding specificities.

ACKNOWLEDGMENT

The authors are grateful to W. J. Kruper for providing BA-2,3,2-tet, J. Coleman for providing antibody fragments, V. Treppa for performing antigen binding analysis, and G. Spittka and W. Goeckeler for providing technical assistance during the animal biodistribution experiments. We thank J. Schlom for providing the CC49 producing cell lines.

Note added in proof: A research article concerning a similar subject matter has been published and has just now come to our attention: Tutt, A., Stevenson, G. T., and Glennie, M. J. (1991) Trispecific F(ab')$_3$ derivatives that use cooperative signaling via the TCR/CD3 complex and CD2 to activate and redirect resting cytotoxic T cells. *J. Immunol. 147*, 60–69. While no in vivo biodistribution data was reported in this paper, and different cross-linking compounds were employed, the antibody products were similar to those we described.

LITERATURE CITED

Brennan, M., Davison, P. F., and Paulus, H. (1985) Preparation of bispecific antibodies by chemical recombination of monoclonal immunoglobulin G1 fragments. *Science 229*, 81.

Carrasquillo, J. A., Krohn, K. A., Beaumier, P., McGuffin, R. W., Brown, J. P., Hellstrom, K. E., Hellstrom, I., and Larson, S. M. (1984) Diagnosis of and therapy for solid tumors with radiolabeled antibodies and immune fragments. *Cancer Treat. Rep. 68*, 317.

Christensen, E. I., Rennke, H. G., and Carone, F. A. (1983) Renal tubular uptake of protein: effect of molecular charge. *Renal Fluid Electrolyte Physiol. 13*, F436.

Clegg, J. A., Hudecz, G., Pimm, M. V., Szekerke, M., and Baldwin, R. W. (1990) Carrier design: biodistribution of branched polypeptides with a poly(L-lysine) backbone. *Bioconjugate Chem. 1*, 425.

Colcher, D., Filomena, M. F., Roselli, M., Muraro, R., Simpson-Milenic, D., and Schlom, J. (1988) Radioimmunolocalization of human carcinoma xenografts with B72.3 second generation monoclonal antibodies. *Cancer Res. 48*, 4597.

Cumber, A. J., Ward, S. E., Winter, G., Parnell, G. D., and Warwrzynczak, E. J. (1992) Comparative stabilities in vitro and in vivo of a recombinant mouse antibody FvCys fragment and a bisFvCys conjugate. *J. Immunol. 149*, 120.

Demignot, S., Pimm, M. V., and Baldwin, R. W. (1990) Comparison of biodistribution of 791T/36 monoclonal antibody and its Fab/c fragment in balb/c mice and nude mice bearing human tumor xenographs. *Cancer Res. 50*, 2936.

Ellman, G. (1959) Tissue sulfhydryl groups. *Arch. Biochem. Biophys. 82*, 70.

Feinstein, A., and Stott, D. I. (1972) An electrofocusing technique for the analysis of thiol proteins applied to a mixture of intracellular plasmacytoma proteins. *J. Physiol. 226*, 34.

French, R. R., Courtenay, A. E., Ingamells, S., Stevenson, G. T., and Glennie, M. J. (1991) Cooperative mixtures of bispecific $F(ab')_2$ antibodies for delivering saporin to lymphoma in vitro and in vivo. *Cancer Res. 51*, 2353.

Fujimori, K., Covell, D. G., Fletcher, J. E., and Weinstein, J. N. (1989) A modeling analysis of monoclonal antibody percolation through solid tumors. *J. Nucl. Med. 30*, 903.

Glennie, M. J., McBride, H. M., Worth, A. T., and Stevenson, G. T. (1987) Preparation and performance of bispecific $F(ab')_2$ antibody containing thioether linked Fab' fragments. *J. Immunol. 139*, 2367.

Goding, J. W. (1986) Fragmentation of monoclonal antibodies. In *Monoclonal antibodies: Principles and practice, 2nd ed.*, Section 4.5, Academic Press, New York.

Goldberg, M., Knudsen, K. L., Platt, D., Kohen, F., Bayer, E. F., and Wilchek, M. (1991) Specific interchain cross-linking of antibodies using bismaleimides. Repression of ligand leakage in immunoaffinity chromatography. *Bioconjugate Chem. 2*, 275.

Goodwin, D. A., Meares, C. F., McCall, M. J., McTigue, M., and Chaovapong, W. (1988) Pre-targeted immunoscintigraphy with indium-111-labeled bifunctional haptens. *J. Nucl. Med. 29*, 226.

Hiratsuka, T. (1988) Cross-linking of three heavy-chain domains of myosin adenosinetriphosphatase with a trifunctional alkylating agent. *Biochemistry 27*, 4110.

Johnson, V. G., Schlom, J., Paterson, A. J., Bennett, J., Magnani, J. L., and Colcher, D. (1986) Analysis of a human tumor-associated glycoprotein (TAG-72) identified by monoclonal antibody B72.3. *Cancer Res. 46*, 850.

Koppel, G. A. (1990) Recent advances with monoclonal antibody drug targeting for the treatment of human cancer. *Bioconjugate Chem. 1*, 13.

Kruper, W. J., Jr., Pollock, D. K., Fordyce, W. A., Fazio, M. J., and Inbasekaran, M. N. (1988) Functionalized polyamine chelants and rhodium complexes thereof and process for their preparation. Eur. Pat. Appl. No. 88109799.2.

Laemmli, U. K. (1970) Cleavage of structural proteins during the assembly of the head of bacteriophage T4. *Nature (London) 227*, 680.

Liberatore, F. A., Comeau, R. D., McKearin, J. M., Pearson, D. A., Belonga, B. Q., III, Brocchini, S. J., Kath, J., Phillips, T., Oswell, K., and Lawton, R. G. (1990) Site-directed chemical modification and cross-linking of a monoclonal antibody using equilibrium transfer alkylating cross-link reagents. *Bioconjugate Chem. 1*, 36 (and accompanying paper).

Maack, T., Johnson, V., Kau, S. T., Figueiredo, J., and Sigulem, D. (1979) Renal filtration, transport, and metabolism of low-molecular weight proteins: A review. *Kidney Int. 167*, 251.

Mandy, W. J., and Nisonoff, A. (1963) Effect of reduction of several disulfide bonds on the properties and recombination of univalent fragments of rabbit antibody. *J. Biol. Chem. 238*, 206.

Means, G. E., and Feeney, R. E. (1990) Chemic.. modification of proteins: History and applications. *Bioconjugate Chem. 1*, 2.

Meares, C. F., McCall, M. J., Reardan, D. T., Goodwin, D. A., Diamanti, C. I., and McTigue, M. (1984) Conjugation of antibodies with bifunctional chelating agents: Isothiocyanate and bromoacetamide reagents, methods of analysis, and subsequent addition of metal ions. *Anal. Biochem. 142*, 68.

Meares, C. F., McCall, M. J., Deshpande, S. V., DeNardo, S. J., and Goodwin, D. A. (1988) Chelate radiochemistry: Cleavable linkers lead to altered levels of radioactivity in the liver. *Int. J. Cancer Suppl. 2*, 99.

Milenic, D. E., Yokota, T., Filpula, D. R., Finkelman, M. A. J., Dodd, S. W., Wood, J. F., Whitlow, M., Snoy, P., and Schlom, J. (1991) Construction, binding properties, metabolism, and tumor targeting of a single chain Fv derived from the pancarcinoma monoclonal antibody CC49. *Cancer Res. 51*, 6363.

Muraro, R., Kuroki, M., Wunderlich, D., Poole, D. J., Colcher, D., Thor, A., Greiner, J. W., Simpson, J. F., Molinolo, A., Noguchi, P., and Schlom, J. (1988) Generation and characterization of B72.3 second generation (CC) monoclonal antibodies reactive with the TAG-72 antigen. *J. Cancer Res. 48*, 4588.

Nisonoff, A., and Rivers, M. M. (1961) Recombination of a mixture of univalent antibody fragments of different specificity. *Arch. Biochem. Biophys. Acta 93*, 460.

Packard, B., and Edidin, M. (1986) Site-directed labeling of a monoclonal antibody: Targeting to a disulfide bond. *Biochemistry 25*, 3548.

Perez, P. R., Hoffman, W., Shaw, S., Bluestone, J. A., and Segal, D. M. (1985) Specific targeting of cytotoxic T cells by anti-T3 linked to anti-target cell antibody. *Nature 316*, 354.

Quadri, S. M., Lai, J., Vriesendorp, H. M., and Williams, J. R. (1992) Evaluation of stabilized F(ab')2 fragments of monoclonal antiferritin antibody in nude mouse model. *Antibody Immunoconjugate Radiopharm. 5*, 125 (abstract).

Riddles, P. W., Blakeley, R. C., and Zerner, B. (1979) Ellman's reagent: 5,5'-Dithiobis(2-nitrobenzoic acid)—A reexamination. *Anal. Biochem. 94*, 75.

Segal, D. M., and Wunderlich, J. R. (1988) Targeting of cytotoxic cells with heterocrosslinked antibodies. *Cancer Invest. 6*, 83.

Sharkey, R. M., Motta-Hennessy, C., Pawlyk, D., Siegel, J. A., and Goldenberg, D. M. (1990) Biodistribution and radiation dose estimates for yttrium- and iodine-labeled monoclonal antibody IgG and fragments in nude mice bearing human colonic tumor xenografts. *Cancer Res. 50*, 2330.

Smyth, D. G., Nagamatsu, A., and Fruton, J. S. (1960) Some reactions of N-ethylmaleimide. *J. Am. Chem. Soc. 82*, 4600.

Staerz, U. D., and Bevan, M. J. (1986) Hybrid hybridoma producing a bispecific monoclonal antibody that can focus effector T-cell activity. *Proc. Natl. Acad. Sci. U.S.A. 83*, 1453.

Stevenson, G. T., Glennie, M. J., Paul, F. E., Stevenson, F. K., Watts, H. F., and Wyeth, P. (1985) Preparation and properties of FabIgG, a chimeric univalent antibody designed to attack tumour cells. *Biosci. Rep. 119*, 991.

Stevenson, G. T., Pindar, A., and Slade, C. J. (1989) A chimeric antibody with dual Fc regions (bisFabFc) prepared by manipulations at the IgG hinge. *Anti-Cancer Drug Des. 3*, 219.

Stickney, D. R., Frincke, J. M., Slater, J. B., Ahlem, C. N., Merchant, B., and Slater, J. M. (1988) Bifunctional antibody technology: Clinical applications for CEA expressing tumors. Third International Conference on Monoclonal Antibody Immunoconjugates for Cancer, Feb. 4–6 (San Diego).

Strober, W., and Waldmann, T. A. (1974) The role of the kidney in the metabolism of plasma proteins. *Nephron 13*, 35.

Sumpi B. E. (1981) Tubular absorption and catabolism of low molecular weight proteins. Ph.D. Dissertation.

Takakura, Y., Fujita, T., Hashida, M., and Sezaki, H. (1990) Disposition characteristics of macromolecules in tumor-bearing mice. *Pharm. Res. 7*, 339.

Volkert, W. A., Goeckeler, W. F., Ehrhardt, G. J., and Ketring, A. R. (1991) Therapeutic radionuclides: Production and decay property considerations. *J. Nuc. Med. 32*, 174.

Waldmann, T. A. (1991) Monoclonal antibodies in diagnosis and therapy. *Science 252*, 1657.

Waldmann, T. A., and Strober, W. (1969) Metabolism of immunoglobulins. *Prog. Allergy 13*, 1.

Yokota, T., Milenic, D. E., Whitlow, M., and Schlom, J. (1992) Rapid tumor penetrance of a single-chain Fv and comparison with other immunoglobulin forms. *Cancer Res. 52*, 3402.

Biochimica et Biophysica Acta, 787 (1984) 39–44
Elsevier

BBA 31878

THE EFFECTS OF CLEAVAGE OF THE INTER-CHAIN DISULPHIDE BONDS OF RABBIT IgG ON ITS ABILITY TO BIND C1q

JULIE SUTTON, JOHN R. ALDEN and SIMON B. EASTERBROOK-SMITH *

Department of Biochemistry, University of Sydney, Sydney, NSW 2006 (Australia)

(Received December 6th, 1983)

Key words: C1q, IgG; Complement binding; Inter-chain disulfide bond cleavage; (Rabbit)

Immune complexes prepared from rabbit anti-ovalbumin IgG in which the interchain disulphide bonds had been reduced and then blocked with *N*-(iodoacetylaminoethyl)-8-naphthylamine-1-sulphonic acid retained the ability to bind ^{125}I-labelled C1q. This ability was lost when a small alkylating agent (iodoacetamide) was used to block the cleaved disulphide bonds. The ability of the IgG to form insoluble immune complexes was partially compromised when iodoacetamide was used to block the disulphide bonds, but was unimpaired when *N*-(iodoacetylaminoethyl)-8-naphthylamine-1-sulphonic acid was used. These data are consistent with the suggestion that access to the C1q binding site in IgG in immune complexes is modulated by movement of the Fab arms, which may block access to the site.

Introduction

Immunoglobulins trigger the classical complement pathway by activation of complement component C1; C1 is a macromolecular complex with three subcomponents: C1q, C1r, and C1s – C1q is responsible for binding to the immunoglobulin [1]. The effects of cleavage of the interchain -SS- bonds of immunoglobulins on C1 binding have received considerable attention. The binding of C1 to aggregated IgG is markedly reduced when these bonds are cleaved [2]. Conversely, C1 binding to the Fc fragment of IgG [3] and C1q binding to monomeric IgG [4] are both unaffected by cleavage of the immunoglobulin disulphide bonds.

There are several explanations for these observations, including: (a) steric hindrance of the C1 binding site (in the C_{H2} domains of the immunoglobulin molecule [5]) by the Fab arms as a consequence of increased segmental flexibility conferred on the immunoglobulin molecule by cleavage of the interchain disulphide bonds [3]; (b) alterations in the quaternary structure of the C_{H2} domains in aggregated IgG, modulated by the Fab arms and cleavage of the hinge disulphide bond between the immunoglobulin heavy chains [6]; and (c) disruption of the C1 binding site by the alkylating agent used to block the reduced disulphide bond between the heavy chains.

In an attempt to discriminate between these possibilities we have examined the effects of the size of the alkylating agent used to block the reduced interchain disulphide bonds on the ability of rabbit anti-ovalbumin IgG to form insoluble immune complexes and to bind C1q. The results presented below appear to rule out hypothesis (c) above, and may favour the steric hindrance hypothesis of Isenman et al. [2].

* To whom correspondence should be addressed.

Abbreviations: IAEDANS, *N*-(iodoacetylaminoethyl)-8-naphthylamine-1-sulphonic acid; Fc, C-terminal half of the heavy chain portion of IgG; Fab, light-chain and N-terminal half of the heavy chain of IgG; C_{H2} domain, second homology unit of the constant region of the immunoglobulin heavy chain.

Materials and Methods

Proteins. Human C1q was prepared and labelled with ^{125}I (using lactoperoxidase) as in Ref. 7. Anti-ovalbumin rabbit IgG and immune complexes were prepared by the methods of Ref. 8.

Chemicals. Dithiothreitol, iodoacetamide and IAEDANS were obtained from Sigma, St. Louis, U.S.A.

C1q binding assay. The binding of ^{125}I-labelled C1q to immune complexes (prepared at the equivalence antibody : antigen ratio) was measured by the method of Ref. 9 with the following modifications: the buffer was 0.01 M phosphate/0.15 M NaCl/0.5% (w/v) bovine serum albumin; the reaction volume was 0.3 ml, and the incubation time was 40 min.

Reduction and alkylation of IgG. IgG (0.05–0.1 mM) in 0.1 M Tris-HCl/2 mM EDTA (pH 8.0) [2] was reduced with 5 mM dithiothreitol for 1 h at room temperature, followed by alkylation with either iodoacetamide or IAEDANS (2.5-fold molar excess over dithiothreitol) for 1 h in the dark. Dithiothreitol was omitted from control preparations. When IAEDANS was used, excess reagent was removed by adsorption to activated charcoal (10 mg/mg IAEDANS), which was then removed by centrifuging (3000 × *g*, 10 min). The protein samples were then dialysed against 0.01 M phosphate/0.15 M NaCl (pH 7.2) at 4°C. Polyacrylamide gel electrophoresis in the presence of sodium dodecyl sulphate [10] revealed that there was complete cleavage of the interchain disulphide bonds of IgG treated with dithiothreitol, regardless of whether iodoacetamide or IAEDANS was used as alkylating agent. The extent of labelling of the protein with IAEDANS was determined using $\epsilon_{280nm}^{1\%,1cm} = 14.0$ for IgG, and $\epsilon_{343nm} = 6.3\ mM^{-1} \cdot cm^{-1}$, $\epsilon_{280} = 1.2\ mM^{-1} \cdot cm^{-1}$ for the label [11].

Precipitin reaction. The ability of the IgG to form insoluble immune complexes with ovalbumin was determined as in Ref. 8.

Results

Rabbit IgG contains three interchain disulphide bonds; two linking the heavy and light chains, and a single interheavy chain disulphide bond [12]. The C_{H1} domains of rabbit IgG are unusual in that they contain a disulphide bond linking residues 133/4 and 221 [13] which is not found in the C_{H1} domains of other immunoglobulins. The results shown in Fig. 1 indicate that IAEDANS modification of dithiothreitol treated IgG is selective for the three interchain disulphide bonds; only six extra groups are modified in IgG with all the interchain disulphide bonds reduced, compared to IgG with intact disulphide bonds.

The results shown in Fig. 2 show the effects of cleavage of the interchain disulphide bonds of IgG on its ability to form insoluble complexes with antigen. When the bulky alkylating agent, IAEDANS, was used, cleavage of the bonds had little effect on either the percentage of the immunoglobulin precipitated as insoluble immune complexes or on the shape of the precipitin curve (Fig. 2B). However, when the small alkylating agent, iodoacetamide was employed, cleavage of the disulphide bonds altered both the percentage of the immunoglobulin precipitated as insoluble immune complexes, and the shape of the precipitin curve (Fig. 2A).

When the dependence of C1q binding on immune complex concentration was examined, the results shown in Fig. 3 were obtained. Immune

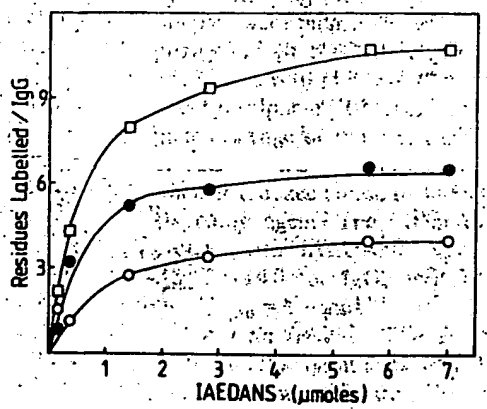

Fig. 1. The dependence of extent of modification of IgG on IAEDANS concentration. IgG was treated with the indicated IAEDANS concentrations after reduction with 5 mM dithiothreitol in a final volume of 0.5 ml; (□——□), as in Materials and Methods. Dithiothreitol was omitted from the control (○——○). The difference in modification between the experimental and control samples was calculated for each IAEDANS concentration (●——●).

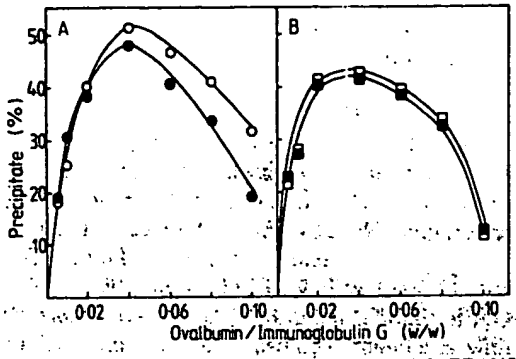

Fig. 2. Precipitin curves for iodoacetamide and IAEDANS-treated IgG. The percentage of input anti-ovalbumin IgG able to form insoluble immune complexes was determined as Ref. 8. Iodoacetamide-treated IgG with (●——●) and without (O——O) cleaved disulphide bonds. IAEDANS-treated IgG with (■——■) and without (□——□) cleaved disulphide bonds. The levels of IAEDANS labelling were 8.2 and 2.1 residues/IgG, respectively.

complexes prepared from IgG in which the reduced interchain disulphide bonds had been blocked with iodoacetamide had a markedly reduced ability to bind C1q (Fig. 3A). However, immune complexes prepared from IgG in which the reduced disulphide bonds had been blocked by IAEDANS had a slightly greater ability to bind C1q than control immune complexes prepared

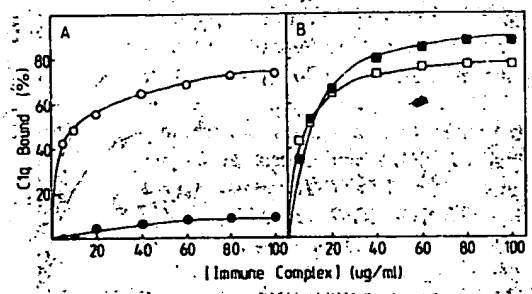

Fig. 3. The effect of varying immune complex concentration on C1q binding. The binding of ^{125}I-labelled C1q (0.5 μg/ml $1.5 \cdot 10^5$ cpm/μg) to immune complexes prepared from the IgG used in the experiment of Fig. 2 at the indicated concentrations was measured as in Materials and Methods. (A) Immune complexes prepared from iodoacetamide treated with (●——●) and without (O——O) cleaved disulphide bonds. (B) Immune complexes prepared from IAEDANS-treated IgG with (■——■) and without (□——□) cleaved disulphide bonds.

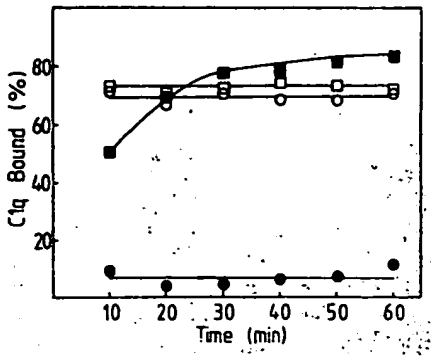

Fig. 4. Time-course for C1q binding to immune complexes. The binding of ^{125}I-labelled C1q (0.16 μg/ml, $1.5 \cdot 10^5$ cpm/μg to immune complexes (60 μg/ml) prepared from the IgG used in the experiment of Fig. 2 was measured at the indicated times as in Materials and Methods. The immune complexes were prepared from iodoacetamide-treated IgG with (●——●) and without (O——O) cleaved disulphide bonds, and from IAEDANS-treated IgG with (■——■) and without (□——□) cleaved disulphide bonds.

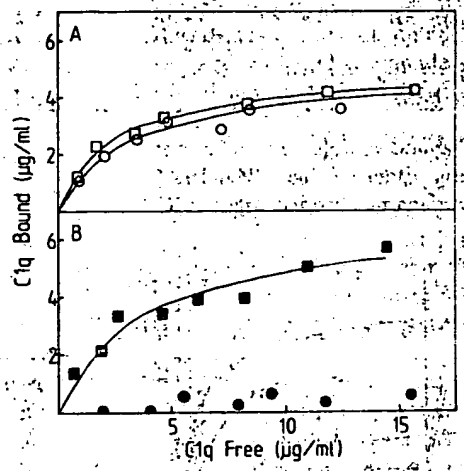

Fig. 5. The effect of varying C1q concentration on C1q binding. The ^{125}I-labelled C1q bound to immune complexes (40 μg/ml) prepared from the IgG used in the experiment of Fig. 2 was measured as in Materials and Methods using an input ^{125}I-labelled C1q concentration range of 2–20 μg/ml. (A) Immune complexes prepared from iodoacetamide (O——O) or IAEDANS- (□——□) treated IgG with intact disulphide bonds. (B) Immune complexes prepared from iodoacetamide- (●——●) or IAEDANS- (■——■) treated IgG with cleaved disulphide bonds. The lines shown were obtained by non-linear regression analysis [15] on the data assuming that C1q binding to the immune complexes was a non-cooperative (Michaelis-Menten) process.

from IgG with intact interchain disulphide bonds (Fig. 3B). These differences did not arise from failure of the C1q : immune complex binding process to come to equilibrium, as the results shown in Fig. 4 shows that the 40 min incubation used in the experiments of Fig. 3 was sufficient to allow the binding process to reach equilibrium.

When the dependence of C1q binding on C1q concentration was determined, the results shown in Fig. 5 were obtained. In the case of immune complexes prepared from IgG with intact disulphide bonds (Fig. 5A), treatment with IAEDANS compared to treatment with iodoacetamide had no significant effect on the amounts of C1q bound to the immune complexes at saturating levels of free C1q (0.123 ± 0.007 μg/μg immune complex, 0.121 ± 0.004 μg/μg immune complex respectively, $P > 0.5$, 10 d.f.* [14]), nor was there a significant effect on the functional dissociation constants for the binding process (3.1 ± 0.6 μg/ml, 2.3 ± 0.3 μg/ml, $P > 0.2$, 10 d.f.). These dissociation constants fall in the range of 1.5–7.8 μg/ml reported by the other investigators [8,9].

In the case of immune complexes prepared from IAEDANS-treated IgG, there was no significant difference between the functional dissociation constants for C1q binding to IgG with intact or cleaved disulphide bonds (2.3 ± 0.3 μg/ml, 3.5 ± 1.0 μg/ml, $P > 0.2$, 11 d.f.). However, the immune complexes prepared from IgG with cleaved disulphide bonds bound more C1q at saturating levels of free C1q than immune complexes with intact disulphide bonds (0.163 ± 0.02 μg/μg immune complex, 0.121 ± 0.007 μg/μg immune complex, respectively, $P < 0.05$, 11 d.f.)

This observation raises the possibility that the differences in C1q binding to immune complexes prepared from IgG with cleaved disulphide bonds (Figs. 3, 5B) could be artefactual, in that the naphthalene sulphonate groups of IAEDANS could provide new binding sites for C1q. The presence of such nonspecific binding sites could mask the loss of the normal binding site following cleavage of the interchain disulphide bonds.

In order to test this possibility, immune complexes were prepared from IgG (with intact disulphide bonds) in which up to seven residues had been labelled with IAEDANS. The capacities of these immune complexes for C1q are given in Table I. Immune complexes prepared from IAEDANS-treated IgG had up to 20% greater capacities for C1q than immune complexes prepared from iodoacetamide-treated IgG. It is known that C1q can bind nonspecifically to both charged and hydrophobic surfaces [16–18]. The increased capacities of the immune complexes prepared from IAEDANS-treated IgG may reflect such nonspecific binding, involving the naphthalene sulphonate groups of IAEDANS. However, it is probably unlikely that this nonspecific binding could account for the differences shown in Figs. 3 and 5B.

TABLE I

IMMUNE COMPLEX CAPACITIES FOR C1q

IgG was treated with either IAEDANS ('Experimental') or iodoacetamide ('Control') at the indicated concentrations for 2 h at 37°C as in Materials and Methods. The number of residues labelled with IAEDANS per molecule of IgG was determined from the absorbance of the protein at 343 and 280 nm. The binding of ^{125}I-labelled C1q ($4 \cdot 10^3$ cpm/μg 2–20 μg/ml) to 40 μg/ml immune complexes (prepared from the protein samples at the equivalence antibody : antigen ratio) was then determined and the capacity of the immune complexes for C1q established by non-linear regression analysis [15] on the primary data.

Reagent concentration (mM)	Residues labelled	Capacity (μg/μg immune complex)	
		Experimental	Control
0	0	–	0.100 ± 0.009
10	1.9	0.156 ± 0.015	0.131 ± 0.013
20	5.6	0.122 ± 0.005	0.108 ± 0.008
28	7.0	0.12 ± 0.01	0.11 ± 0.02

Discussion

The data shown in Fig. 1 indicate that IAEDANS is able to react only with the reduced interchain disulphide bonds of rabbit IgG. This observation may be compared with the work of Press [2], who showed that treatment of reduced rabbit IgG with iodoacetamide under these conditions led to labelling of the extra intraheavy chain disulphide bond in the C_{H1} domain of IgG [13] as well as labelling of the interchain disulphide bonds. This discrepancy may arise from differences in alkylating agents employed. It is possible that the

* d.f., degrees of freedom.

large reagent, IAEDANS, used in this study, may not be able to gain access to the reduced intrachain disulphide bond.

The observation that immune complexes prepared from IgG in which the interchain disulphide bonds have been blocked with iodoacetamide have a markedly impaired ability to bind C1q presents a significant deviation from the demonstration that IgG with cleaved disulphide bonds is able to bind C1q, in the absence of antigen [4].

This deviation may arise from the fact that the modified immunoglobulin was present as an insoluble immune complex in the present investigation. An electron microscopy study [6] has shown that cleavage of the interchain disulphide bonds of rabbit IgG has little effect on the shape of the molecule, in the absence of antigen. However, structural changes were apparent when the modified IgG was complexed with a bivalent hapten.

These observations may have two consequences. Firstly, the retention of gross native structure of modified IgG in the absence of antigen [6] suggests that it would not be unreasonable to suppose that the protein would retain full C1q binding ability, as was demonstrated experimentally [4]. Secondly, the changes in the structure of the modified IgG in the presence of a bivalent hapten [6], may be compared with the effects of blocking the cleaved disulphide bonds of IgG with iodoacetamide on its ability to form insoluble immune complexes (Fig. 2).

A possible explanation of these data is that the increased flexibility conferred upon the IgG by cleavage of the interchain disulphide bonds, which has been demonstrated in both structural [6] and fluorescence depolarisation [19] studies, may lead to an alteration of the complex equilibria [20] of the antibody-antigen interaction in such a way as to alter the proportion of insoluble immune complexes formed at some antibody : antigen ratios. The increased flexibility conferred on the molecule may allow the Fab arms to interact with the antigenic protein in such a way as to block access to the C1q binding site (cf. Fig. 3). This concept of 'steric blockade' [21] has been invoked to account for the failure of intact human IgG_4 to bind C1 [6], and for compromised effector functions in IgG molecules lacking a hinge region [21].

In the case of IgG in which the interchain disulphide bonds have been blocked with IAEDANS, the observation that this procedure has little effect on the ability of the modified protein to form insoluble immune complexes (Fig. 2) is consistent with the hypothesis that incorporation of the bulky naphthalene sulphonate moiety of IAEDANS into the disulphide bonds may minimise the increased flexibility of the Fab arms. Thus, the modified protein would be able to form insoluble immune complexes in a manner similar to unmodified IgG, and the absence of 'steric blockade' may permit access to the C1q binding sites of these complexes.

However, the latter conclusion cannot be drawn unequivocally from the data presented above. It is possible that when the interchain disulphide bonds of IgG are blocked with IAEDANS, the attached naphthalene sulphonate groups may provide a new nonspecific C1q binding site. Although this possibility cannot be eliminated, the observation that labelling of up to seven residues in IgG with IAEDANS leads to only a 20% increase in the capacity of the IgG (as immune complex) for C1q (Table 1) suggests that the differences between blocking the disulphide bonds with IAEDANS and iodoacetamide cannot arise solely from generation of new nonspecific binding sites for C1q in the former case.

The presence of the 'extra' intrachain disulphide bond in the C_{H1} domains of rabbit IgG [13], provides a second complication in the interpretation of the data presented above. It has been suggested [22] that it is the integrity of this bond, rather than the interchain disulphide bond, which is essential for C1q binding to rabbit IgG. As this bond can be blocked by iodoacetamide [22] and appears to be inaccessible to IAEDANS (Fig. 1), it is possible that the retention of C1q binding ability in IAEDANS-modified IgG may arise because the extra disulphide bond is not blocked. It is difficult to assess the significance of this possibility, as the effects of reduction and alkylation of rabbit IgG depend critically on the conditions of the reduction [22]. However, when the effects of reduction and alkylation of IgG using the protocol used in this study were examined, it was concluded that it was the integrity of the interheavy chain disulphide bond of rabbit IgG that was essential for C1 binding [2].

References

1 Porter, R.R. and Reid, K.B.M. (1979) Adv. Prot. Chem. 33, 1–71
2 Press, E.M. (1975) Biochem. J. 149, 285–288
3 Isenman, D.E., Dorrington, K.J. and Painter, R.H. (1975) J. Immunol. 114: 1725–1729
4 Goers, J.W., Ziccardi, R.J., Schumaker, V.N. and Glovsky, M.M. (1977) J. Immunol. 118, 2182–2191
5 Colomb, M. and Porter, R.R. (1975) Biochem. J. 145, 177–183
6 Seegan, G.W., and Smith, C.A. and Shumaker, V.N. (1979) Proc. Natl. Acad. Sci. U.S.A. 76 907–911
7 Tenner, A.J., Lesaure, P.H. and Cooper, N.R. (1981) J. Immunol. 127, 648–653
8 Emanuel, E.J., Brampton, A.D., Burton, D.R., and Dwek, R.A. (1982) Biochem. J. 205, 361–372
9 Lin, T. and Fletcher, D.S. (1978) Immunochemistry 15, 107–117
10 Fairbanks, G., Stech, T.L. and Wallach, D.F.H. (1971) Biochemistry 10, 2606–2617
11 Hudson, E.N. and Weber, G. (1973) Biochemistry 12, 4154–4161
12 Beale, D. and Feinstein, A. (1976) Q. Rev. Biophys. 9, 135–180
13 O'Donnell, I.J., Frangione, B. and Porter, R.R. (1970) Biochem. J. 116, 261–268
14 Cleland, W.W. (1967) Adv. Enzymol. 21, 1–32
15 Duggleby, R.G. (1981) Anal. Biochem. 110, 19–25
16 Cooper, N.R. and Morrison, D.C. (1978) J. Immunol. 120, 1862–1868
17 Loos, M. and Thesen, R. (1978) J. Immunol. 121, 24–28
18 Alving, C.R., Richards, R.L. and Guirguis, A.A. (1977) J. Immunol. 118, 342–347
19 Chan, L.M. and Cathou, R.E. (1977) J. Mol. Biol. 112, 653–656
20 Steensgaard, J., Maw Liu, B., Cline G.B. and Moller, N.P.H. (1977) Immunology 32, 445–456
21 Klein, M., Haeffner-Cavaillon, N., Isenman, D.E., Rivat, C., Navia, M.A., Davies, D.A. and Dorrington, K.J. (1981) Proc. Natl. Acad. Sci. U.S.A. 78, 524–528
22 Johnson, B.A. and Hoffmann, L.G. (1981) Mol. Immunol. 18, 181–188

THE JOURNAL OF BIOLOGICAL CHEMISTRY
Vol. 257, No. 7, Issue of April 10, pp. 3811-3818, 1982
Printed in U.S.A.

Nucleation-controlled Polymerization of Human Monoclonal Immunoglobulin G Cryoglobulins*

(Received for publication, June 29, 1981)

Paul Vialtel‡, David I. C. Kells, Les Pinteric, Keith J. Dorrington, and Michel Klein

From the Department of Biochemistry and Pathology, University of Toronto, Toronto, Canada, M5S 1A8 and the Laboratory of Immunology, Toronto Western Hospital, Toronto, Canada, M5T 2S8

The kinetics of the polymerization of human monoclonal cryoimmunoglobulins at low temperature was investigated in temperature jump experiments by monitoring the changes in turbidity resulting from the scattering of incident light by the polymers. Above a critical concentration between 2 and 3 mg/ml, depending on the ionic strength, the kinetics were characterized by a concentration-dependent lag phase and initial rate of self-assembly. Under equilibrium conditions which favored polymerization, the only stable intermediate detected by analytical ultracentrifugation was the dimer. Although purified monomers were unable to self-associate at 4 °C, addition of trace amounts of autologous dimers promoted polymerization. The apparent rate of polymerization was shown to be slow ($k = 4.7 \times 10^{-4}$ $M^{-1} \cdot s^{-1}$), and the process was governed by an equilibrium constant of 4.6×10^4 M^{-1}. The initial rate of self-assembly was proportional to the product of the monomer concentration and the concentration of promoter (i.e. dimer). The rate of depolymerization was three orders of magnitude greater than the rate of polymerization and was proportional to the concentration of polymers present. These results suggest that the polymerization of monoclonal cryoimmunoglobulins is a nucleation-controlled process in which dimerization is the rate-limiting step. Kinetic studies on the polymerization of Fab and $F(ab')_2$ fragments from cryoimmunoglobulins and a comparison of cryogel ultrastructure by electron microscopy suggested that the interaction site between monomers is located in the Fab region. Since the polymerization of monomers was only induced by autologous dimers and not dimers from other cryoimmunoglobulins, it was concluded that the hypervariable regions play a specific role in the condensation reaction. The fact that one cryoimmunoglobulin has a well defined antibody activity against streptolysin O argued against a low temperature-induced auto-anti-idiotype mechanism. Reduction of the interchain disulfide bonds of the Fab fragments abolished their ability to polymerize, probably by inducing a conformational change a considerable distance away in the variable domains of the molecules.

Cryoglobulins are a clinically important group of immunoglobulins that reversibly precipitate or form gels upon cooling. Previous immunochemical analyses of purified human cryoglobulins have shown that they may be formed either of polymers of monoclonal immunoglobulins (monoclonal cryoglobulins) or of immune complexes (mixed cryoglobulins) (4, 12, 19). Correlations have been established between the immunochemical type of cryoglobulins and the clinical symptoms as well as the underlying disease (4).

Monoclonal cryoglobulins are associated with lymphoproliferative diseases and are responsible for severe cutaneous and vascular lesions. Previous studies have shown that cryoprecipitation of the monoclonal proteins is dependent upon initial protein concentration, temperature, pH, and dielectric constant of the solvent (12, 17, 20). Nevertheless the molecular events underlying cryoprecipitation remain poorly understood. Temperature-induced conformational changes have been proposed as the initial step in polymerization at low temperature for some monoclonal cryoglobulins (17, 20, 31), but such temperature-dependent transitions could not be detected for some others (21, 32). Recently, it has been postulated that cryoprecipitation results from a cooperative intermolecular association occurring via a nucleation event (32). Temperature-dependent molecular mechanisms of this type have been described previously for the self-assembly of tubulin (13), actin (15), flagellin (2), and for the concerted gelation of deoxyhemoglobin S (1). The concerted polymerization of these proteins consists of a rate-limiting nucleation step followed by a growth process. In such systems, the addition of a small amount of high polymers promotes or accelerates the polymerization of the monomeric molecules (13, 24).

The sites responsible for the monomer-monomer interaction at low temperature are probably located in the variable regions of the heavy (V_H) and/or light (V_L) chains. Isolated Fc regions of IgG1 or IgM cryoglobulins did not cryoprecipitate (22, 30), whereas the peptic $F(ab')_2$ fragments of IgG and IgA cryoglobulins retain this property (28, 30). A papain Fab fragment from one IgG cryoglobulin exhibited a temperature-dependent self-association (29). Furthermore, it has been shown that the variable domain of two λ Bence-Jones cryoglobulins were responsible for the thermal behavior of the parent light chain dimer. Modification of the tertiary structure associated with the interchain disulfide bridge at the COOH terminus of the dimer could modulate the cryoprecipitability associated with the variable domains (17).

In the study reported here, we have analyzed the temperature-induced self-assembly of an IgG1 monoclonal cryoglobulin, with anti-streptolysin O antibody activity, as well as its depolymerization in order to determine whether the kinetic pathway is consistent with a nucleated polymerization mechanism. Furthermore, we have attempted to localize the region of the molecule involved in the intermolecular interactions between self-associated monomers.

* This work was supported by grants from the Medical Research Council of Canada (MT 4259) and from the Arthritis Society (7-264-80). The costs of publication of this article were defrayed in part by the payment of page charges. This article must therefore be hereby marked "*advertisement*" in accordance with 18 U.S.C. Section 1734 solely to indicate this fact.

‡ Supported under the terms of the Canada-France Exchange Agreement. Present address, Service de Nephrologie et des Maladies Metaboliques, Centre Hospitalier et Universitaire de Grenoble, 38043 Grenoble, France.

MATERIALS AND METHODS

Isolation and Purification of Cryoglobulins and Normal Immunoglobulins—Monoclonal human cryoglobulins (IgG1κ Cac, IgG2κ Zie, and IgG3κ Pav) were isolated from the sera of myeloma patients by several successive cycles of precipitation at 4 °C and solubilization at 37 °C. The cryoprecipitates were extensively washed after each cycle in 10 mM Tris-HCl/0.15 M NaCl, pH 7.8, containing 0.2% sodium azide (Buffer TBS). Noncryoprecipitating monoclonal IgG and polyclonal normal human IgG were prepared by ammonium sulfate precipitation followed by ion exchange chromatography on DEAE-cellulose (DE-52, Whatman) equilibrated in 20 mM NaCl, 10 mM Tris-HCl, pH 7.8.

Preparations of Immunoglobulin Subunits—Fab and Fc fragments were prepared by solid phase tryptic cleavage, according to Ellerson *et al.* (7). $F(ab')_2$ fragments were prepared by peptic digestion as described by Nisonoff *et al.* (23). Monoclonal immunoglobulins at 10 mg/ml were mildly reduced at 37 °C with 10 mM dithioerythritol (Sigma) in Buffer TBS, pH 8.6, for 30 min under nitrogen, and alkylated with 24 mM iodoacetamide (Sigma) or with [^{14}C]iodoacetamide (Amersham Corp.). Heavy and light chains were separated by gel filtration on a column of Sephadex G-100 equilibrated in 1 M acetic acid and were renatured by extensive dialysis against 4 mM Na-acetate buffer, pH 5.4 (36). Hinge peptides were obtained by tryptic-peptic digestion of ^{14}C-labeled H chains and analyzed by high voltage electrophoresis according to Frangione *et al.* (9).

Covalent and Noncovalent Reassembly of IgG1κ Cac—The noncovalent reassociation of reduced and alkylated H and L chains was achieved by dialyzing an equimolar mixture of H and L chains in 1 M acetic acid against 4 mM acetate buffer, pH 5.4, at room temperature. The reassembled molecules were concentrated and dialyzed against Buffer TBS at room temperature. The oxidative reassembly of the molecule was achieved in two ways. IgG1κ Cac was reduced at 7 mg/ml with 10 mM dithioerythritol at 37 °C and reoxidized by dialysis against Buffer TBS, pH 8.6, at room temperature. Alternatively, H and L chains were separated from the reduced but not alkylated molecule as previously described, recombined, and then renatured and reoxidized by progressive dialysis against Buffer TBS, pH 8.6, in the presence of a disulfide interchange system (oxidized and reduced glutathione), as described by Petersen and Dorrington (25).

Preparation of Cryoglobulin Polymers—Cold-induced polymerization of IgG1κ Cac and IgG3κ Pav was achieved by cooling a solution of resolubilized proteins at 25 mg/ml from 40 °C to 22 °C. Alternatively, nonspecific aggregation of cryoglobulins and normal polyclonal IgG was achieved by heating protein solutions at 10 mg/ml for 10 min at 63 °C. The polymer-containing samples were then fractionated on a Sephacryl S-300 superfine (Pharmacia Fine Chemicals) column equilibrated in Buffer TBS at room temperature. The column was calibrated with standards of known molecular weight (IgM pentamer, IgM monomer, $F(ab')_2$, and albumin). Chemically cross-linked oligomers of IgG1κ Cac were prepared by treating a 15 mg/ml solution of cryoglobulin monomer with 10 mM dimethyl suberimidate (Pierce Chemical Co.) for 30 min at room temperature. The reaction was stopped by the addition of ethanolamine.

Electrophoresis and Immunological Techniques—The purity of the monoclonal and polyclonal proteins and their fragments was assessed by electrophoresis, immunoelectrophoresis, and immunodiffusion, using monospecific and polyvalent antisera and by sodium dodecyl sulfate-polyacrylamide electrophoresis in 7.5% gels containing 0.1% sodium dodecyl sulfate. When cryoglobulins were to be tested, immunoelectrophoresis and immunodiffusion were carried out at 37 °C. The molecular weight of cross-linked oligomers was determined by SDS-polyacrylamide gel electrophoresis in 4% gels.

Analytical Ultracentrifugation—Sedimentation coefficients of native cryoglobulins, cryoglobulin oligomers, and cryoglobulin fragments were measured in a Beckman model E analytical ultracentrifuge operated at 60,000 rpm with a titanium rotor at 37 °C to prevent cryoprecipitation or at lower temperatures in order to monitor the cold-induced formation of high molecular weight components. Sedimentation was followed using schlieren optics at protein concentrations above 2 mg/ml and with the photoelectric scanning system at 280 nm for concentrations below 2 mg/ml. Sedimentation coefficients were calculated in the usual way (5).

Turbidity Measurements—The kinetics of cold-induced polymerization of monomeric cryoglobulins was followed by monitoring changes in the absorbance at 330 nm resulting from the scattering of incident light due to the formation of polymers. Measurements were carried out on a Cary 118 spectrophotometer using full scale settings of 0.02 to 2 absorbance units. The temperature of the experimental cell (pathlength, 0.438 or 1.0 cm) was maintained at 4 °C by using thermostated cell holders connected to a circulating water bath (Lauda K2/R), and the temperature was continuously monitored with a Yellow Springs Instrument Co. model 42SC telethermometer equipped with a small nylon-covered thermistor probe. During preliminary studies, a wavelength scan of several solutions of cryoglobulin at different concentrations, polymerized by incubation at 4 °C for 38 h, indicated that the absorbance was proportional to λ^{-2} for IgG1κ Cac and $\lambda^{-0.2}$ for IgG3κ Pav. In another series of experiments, 1-ml aliquots of solutions of IgG1κ Cac at different concentrations were polymerized in the cold, and absorbance at 330 nm was measured at 4 °C. The polymers were centrifuged in the cold at 60,000 × *g*, and the quantity of cryoprecipitate was calculated from the residual absorbance in the supernatant as previously described. Under these conditions, it was shown that $A_{330\,nm}$ is an exponential function of the total protein concentration and is proportional to the quantity of high polymers found at 4 °C for protein concentrations ranging from 2–20 mg/ml.

Kinetics of Polymerization and Depolymerization—Temperature jump experiments were performed to determine the rates of polymerization and depolymerization of IgG1κ Cac and its fragments. To initiate polymerization, 2.0 ml of cryoglobulin in Buffer TBS was warmed to 37 °C for 1 h, rapidly filtered (Millipore filter, 0.45 μm), and immediately placed in a prechilled cuvette maintained at 4 °C. Thermal equilibration was reproducibly reached in 10 ± 1 min. In order to study the polymerization of cryoglobulin monomers promoted by the addition of oligomers, increasing quantities of a solution containing oligomers were added at 37 °C to the cryoglobulin solution so that the final protein concentration would be held constant at 3.5 mg/ml. The solution was then rapidly placed in the prechilled cuvette and the kinetics recorded. To study the kinetics of depolymerization, samples of polymerized cryoglobulin, maintained at 4 °C, were injected with a prechilled syringe into the experimental cell which had been prewarmed at a predetermined temperature so that the final temperature observed after addition of 1 ml of the cold cryoglobulin solution would be identical with that of the cell holder in which the cell was placed. Using this technique, the time required to obtain thermal equilibration was 10–15 s, irrespective of the amplitude of the temperature jump. The cell compartment was flushed with air throughout the experiment in the presence of anhydrous calcium sulfate in order to prevent condensation.

Initial rates of polymerization and depolymerization were determined graphically.

Electron Microscopy—The native IgGκ Cac and its proteolytic fragments were allowed to gel at 4 °C. About 1 ml of each gel was shaken by a sharp blow, and gel fragments of approximately 1 mm^3 were transferred into cold fixative containing 3% glutaraldehyde. Fixation was allowed to proceed overnight and was followed by extensive washing in three changes of 0.1 M cacodylate buffer, pH 7.4, at 4 °C. The gel fragments were then post-fixed with 1% OSO_4 in the previous buffer for 1 h at 4 °C. After this second fixation, the samples were washed and dehydrated in solutions of increasing ethanol concentrations and finally embedded in Epon. Ultrathin sections of about 50 nm were cut and stained on the grids with uranyl acetate followed by lead citrate. Sections were made conductive with a carbon layer about 5 nm thick in a high vacuum evaporator and were examined in a Philips EM 200 electron microscope equipped with an anticontamination device.

RESULTS

Immunochemical Characterization of Monoclonal Cryoglobulins—The IgG1κ Cac used in the present study has a well documented antibody activity against streptolysin O (34). The V region subgroups of its γ and κ chains were determined by sequence analysis and were shown to be V_HIII and V_κII, respectively. The V region subgroups of the IgG2κ Zie were V_HIII and V_κI, whereas PAV IgG3κ Pav belongs to the V_HIII and V_κI variable frameworks. The ^{14}C-labeled hinge peptides, obtained by tryptic-peptic digestion of the H chains of the IgGs were identical with their normal counterparts, as judged by mobility in high voltage electrophoresis performed at two pH values (6.5 and 3.5).

The general physical-chemical parameters influencing the cryoprecipitation of IgG1κ cryoglobulins have been previously reported (16, 20). The optimal pH for cryoprecipitation for

the three cryoglobulins was near 7.4, and the amount of precipitate decreased when the ionic strength increased above physiological conditions. The IgG1κ and the IgG3κ gave a cryogel when cryoprecipitation was induced by cooling an aggregate-free solution of these proteins at high molar concentrations (10^{-4} M). The IgG2κ cryoglobulin crystallized.

Ultrastructural Studies—Electron microscopy of the cryogels obtained with the native IgG1κ Cac and its $F(ab')_2$ and Fab fragments revealed a periodic tubular structure.

The native IgG gave well aligned bundles of microtubules with a periodic structure and, in cross-section, the annuli were formed of a double ring with an external diameter of 30 nm and an internal diameter of 11 nm. These rods, following gel disruption, were homogeneous in diameter but varied in length. These tubular structures tended to form tangled bundles of long filaments. In contrast, the proteolytic fragments yielded disordered microtubules which in cross-section were formed of a single annulus composed of 12–14 globular subunits with an external diameter of 19 nm. Although a similar structure was observed for the Fab cryogel, the ring structures appeared to be more fragile and to have an external diameter significantly smaller than that observed with the native cryoglobulin or its $F(ab')_2$ fragment (Fig. 1).

Kinetics of Cold-induced Polymerization—The kinetics of the cold-induced polymerization of the IgG1κ cryoglobulin at 4 °C was studied under physiological conditions at different protein concentrations (Fig. 2*A*). As described under "Materials and Methods," the absorbance at 330 nm was linearly proportional to the mass concentration of IgG polymers formed at low temperatures, and changes in light scattering were used to monitor the cryoprecipitation phenomenon. Turbidimetric measurements have been successfully used to monitor the temperature-dependent polymerization reactions of different proteins, such as tubulin (13) and cryoglobulins (32, 33). Below a critical concentration of approximately 2 mg/ml, no cryoprecipitation was observed with IgG1κ Cac. Above this critical concentration, a monotonic increase in absorbance was observed after a short concentration-dependent lag phase following thermal equilibration (10 min for the lowest cryoglobulin concentration). The duration of the initial lag phase decreased as the protein concentration increased and correspondingly, the initial rate of the reaction determined graphically after the lag period increased. As shown in Fig. 2*B*, the polymerization phenomenon at 4 °C was completely reversible at 37 °C during three successive cycles of temperature change. At long reaction times, the observed decrease in absorbance results from the sedimentation of high polymers. Therefore, since the final $A_{330\,nm}$ value could not be precisely determined, the order of the reaction could not be established. Furthermore, for a fixed molar concentration of cryoglobulin, the initial rate varied when different preparations of the same cryoglobulin were compared under identical experimental conditions. Nevertheless, the occurrence of a critical concentration below which polymerization did not occur and the existence of a lag phase are suggestive of a slow thermodynamically unfavorable initiation process for self-nucleating polymerization.

Analytical ultracentrifugation analysis of a sample of native cryoglobulin at 9 mg/ml warmed to 37 °C for an hour showed the presence of two distinct peaks. The major peak corresponded to the IgG monomer ($s_{20,w}$ = 6.7) and a second peak corresponding to the presence of less than 10% of a species corresponded to the dimer ($s_{20,w}$ = 9) (Fig. 3*A*). This observation suggested that dimer formation might be the nucleation event which promoted the growth of large polymers.

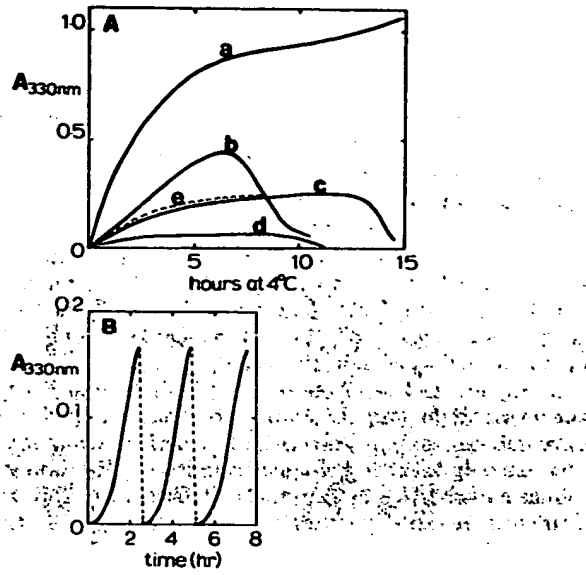

FIG. 2. **Kinetics of the cold-induced polymerization.** *A*, changes in turbidity at 330 nm as a function of time for various solutions of native IgG Cac at different concentrations in Buffer TBS. Protein concentrations in mg/ml were: *a*, 6.4; *b*, 4.2; *c*, 2.9; *d*, 2.2; *e*, IgG1κ Cac reduced and reoxidized at 2.9 mg/ml in Buffer TBS. The temperature was maintained at 4 °C after the initial temperature jump. *B*, reversibility of the cold-induced self-association. A sample of native IgG Cac at 5.7 mg/ml in Buffer TBS was polymerized at 4 °C for 2 h (——) and subsequently depolymerized by rapid rewarming to 37 °C (– – –). Cycles of polymerization-depolymerization were repeated twice.

FIG. 1. **Electron micrographs of longitudinal and cross-sections of cryogels obtained with the intact IgG Cac cryoglobulin (*a*, *b*), its Fab (*c*, *d*), and $F(ab')_2$ (*e*, *f*) proteolytic fragments.** *Solid bars* represent a distance of 100 nm in *a*, *c*, and *e*, and of 50 nm in *b*, *d*, and *f*. Bundles of aligned IgG fibers and the corresponding double-ring structures are shown in *a* and *b*, respectively. In *d*, the *arrow* indicates the presence of structures compatible with loose Fab annuli.

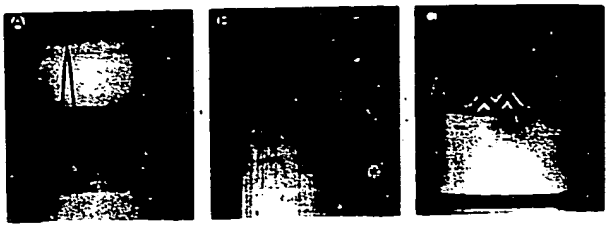

FIG. 3. **Analysis of different preparations of IgG Cac in Buffer TBS in the analytical ultracentrifuge at 37 °C using schlieren optics.** *A*, native cryoglobulin at 6.8 mg/ml; *B*, cryoglobulin monomers of 5.9 mg/ml (fraction *III* in Fig. 4); *C*, monomer-dimer mixture at 2.2 mg/ml (fraction *II* in Fig. 4). Photographs were taken 26, 28, and 30 min after the rotor attained 60,000 rpm, respectively. The bar angles were 50° in *A* and *B* and 40° in *C*.

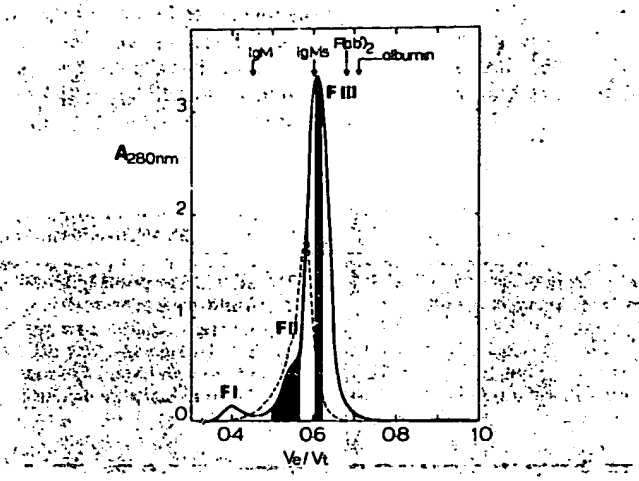

FIG. 4. **Chromatography of native cryoglobulins, which had been warmed at 40 °C for 1 h prior to application, on a column (2.6 × 111 cm) of Sephacryl S-300 at room temperature (flow rate = 30 ml/h).** ——, elution profile of IgG1 Cac; – – –, elution profile obtained with IgG3 Pav. The *filled areas* correspond to the pools of dimer (fraction *II*) and monomer (fraction *III*) used in subsequent experiments.

A nucleation event was further supported by the following experiments. The polymerization of the native IgG1κ at 16 mg/ml was induced by lowering the temperature from 37 °C to 20 °C in less than 5 min. This relatively small drop in temperature was chosen in order to induce a slow polymerization. The turbidity of the solution was continuously monitored at 330 nm, and 0.5-ml aliquots were withdrawn every second hour during the initial polymerization phase and analyzed at 20 °C in the analytical ultracentrifuge. High polymers responsible for the light scattering sedimented to the bottom of the ultracentrifuge cell, and the dimer was the only stable intermediate detected in significants amounts during polymerization (data not shown).

Since the approach to equilibrium of the polymerization reaction seemed to involve a dimer as the stable intermediate acting as a putative promoter, it was necessary to isolate a preparation of aggregate-free monomer capable of polymerizing onto preformed oligomers as well as preparations of oligomers of various sizes which could be assessed for their ability to initiate the growth process. To this end, a solution of solubilized native cryoglobulin at 15 mg/ml was cooled to room temperature and applied to a calibrated Sephacryl S-300 column. The elution profile (Fig. 4) showed a distinct peak of high polymers, larger than IgM, followed by a major peak of monomer eluting at $V_e/V_t = 0.6$, characterized by a marked shoulder (fraction II) on its ascending limb corresponding to a V_e/V_t smaller than that of 8 S IgM. As shown in Fig. 4, the fractions corresponding to the first peak (fraction I), the shoulder (fraction II), and the descending portion of the monomer peak (fraction III) were concentrated and analyzed by analytical ultracentrifugation at 37 °C in Buffer TBS. The high molecular weight fraction consisted of a heterogenous population of polymers as judged by UV scanning at 2 mg/ml (data not shown). The schlieren pattern of fraction II concentrated to 5 mg/ml revealed the presence of symmetrical peaks with sedimentation rates of 6.7 S and 9 S (Fig. 3*C*). The first component was identified as monomer (48%) and the second as dimer (52%) in slow equilibrium with the monomer. The descending portion of the monomer peak isolated by gel filtration was concentrated to 8 mg/ml and was shown to be totally devoid of oligomers (Fig. 3*B*). Both the polymer and dimer preparations were able to cryoprecipitate in the cold. In contrast, the monomer preparation was unable to precipitate at 4 °C within the time course of the polymerization experiments. When this preparation was concentrated to over 20 mg/ml (*i.e.* half the serum concentration of the native monoclonal cryoglobulin), a small amount of cryoprecipitate was observed after 1 week at 4 °C.

Rate of Polymerization as a Function of Initiator and Monomer Concentrations—When high molecular weight polymers were added at 37 °C to a final mass concentration of 1% to a solution of monomer at a concentration as low as 2 mg/ml, the low temperature-induced polymerization was restored.

One characteristic of a self-nucleated condensation polymerization is that the initial rate of polymerization is directly proportional to the concentration of the initiator (13, 24). In order to test this prediction and to determine the minimal size of the promotor, increasing quantities of native dimer were added to a fixed concentration of monomer (Fig. 5*A*), and the temperature was reduced to 4 °C. No change in A_{330nm} was observed in the absence of dimer, whereas a typical condensation polymerization reaction was observed upon addition of increasing concentrations of dimer. Above a critical concentration of dimer, the initial lag period rapidly decreased, and the initial rate of the reaction increased as a linear function of the dimer concentration. Similar findings were observed with IgG3κ Pav. (Fig. 5*B*). The various samples were allowed to stand at 4 °C for 1 week, and the cryoprecipitates formed were collected by centrifugation; the amount of cryoglobulin contained in the precipitate or remaining in the supernatant was determined spectrophotometrically after dilution in 0.25 M acetic acid. The data clearly indicated that the quantity of cryoprecipitate could only be accounted for if co-precipitation of the monomer had occurred.

An additional prediction of a condensation-polymerization reaction is that the initial rate of elongation is directly proportional to the monomer concentration above a critical concentration (13, 24). In order to verify this property, a fixed quantity of purified dimer was added at 37 °C to increasing concentrations of monomer. The mixture was then rapidly cooled, and the polymerization reaction was monitored at 330 nm. As shown in Fig. 6, the initial rate of polymerization, determined graphically for two different initiator concentrations (1.7×10^{-6} and 1.1×10^{-6} M, respectively), increased as a linear function of the molar concentration of monomer. A 1.54-fold increase in the dimer concentration resulted in a 1.58-fold increase in both the slope and the *y* intercept of the curve obtained for the lowest seed concentration.

Assuming that the polymerization-depolymerization reaction occurs at the end of the linear polymer of cryoglobulin, the initial rate of assembly is the sum of the rates of polymerization and depolymerization and can be described by the following equation

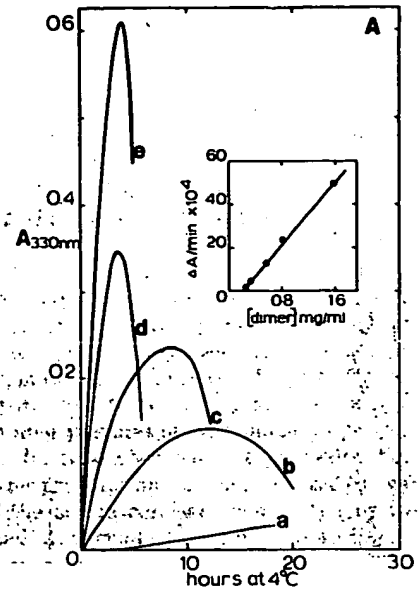

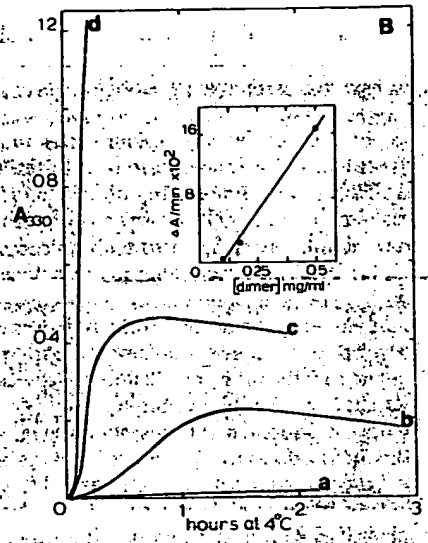

FIG. 5. Kinetics of cryoglobulin polymerization at 4 °C in the presence of different initial concentrations of autologous dimers. *Insets* show the dependence of the initial rates of assembly on the dimer concentration. *A*, IgG1 Cac at 5.6 mg/ml in Buffer TBS in the presence of the following concentrations of dimer: *a*, 0.24; *b*, 0.32; *c*, 0.54; *d*, 0.8; *e*, 1.6 mg/ml. *B*, IgG3 Pav monomer at 2.5 mg/ml in 50 mM NaCl, 20 mM Tris-HCl buffer, pH 7.8, with the following concentrations of dimer: *a*, 0.025; *b*, 0.1; *c*, 0.175; *d*, 0.5 mg/ml. Initial rates of polymerization could be determined graphically only for curves *b*, *c*, and *d*.

$$-\frac{d[M]}{dt} = \frac{cdA_{330\,nm}}{dt} = k_+[M][D] - k_-[D]$$

where $[M]$ and $[D]$ represent the monomer concentration and the number concentration of dimer, respectively, and k_+ and k_- are the apparent rate constants for polymerization and depolymerization, respectively. The constant c is a proportionality constant relating the $A_{330\,nm}$ units to monomer units polymerized. This proportionality constant was estimated to be 0.7 $A_{330\,nm}$ units/μM of monomers polymerized (see "Materials and Methods"). According to the preceding equation, the y intercept in Fig. 6 corresponds to $-(1/c)\cdot k_-[D]$, and the slope is given by $(1/c)k_+[D]$. Therefore, the first order rate constant for depolymerization (k_-) and the second order rate

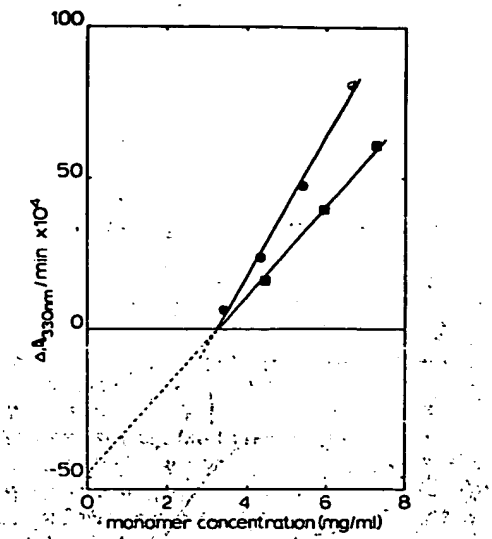

FIG. 6. The initial rate of assembly kinetics as a function of cryoglobulin monomer concentration. The experiments were carried out at 4 °C at two different concentrations of autologous dimer: 0.51 mg/ml (●—●) and 0.35 mg/ml (■—■), respectively. The initial rates of polymerization were calculated from the increase in A_{330} with time after the temperature was rapidly lowered to 4 °C.

constant for polymerization (k_+) could be determined graphically and were found to be 1.02×10^{-5} s^{-1} and 4.72×10^{-4} M^{-1} s^{-1}, respectively, at 4 °C. The equilibrium constant $K = k_+/k_-$ was, therefore, 4.6×10^4 M^{-1}. The monomer concentration at which the rate of polymerization is equal to the rate of depolymerization corresponds to the x intercept and was found to be 2.17×10^{-5} M (*i.e.* 3.25 mg/ml) and independent of the promotor concentration. This point represents the equilibrium monomer concentration M_e at which $d[M]/dt = 0$. Thus, $M_e = k_-/k_+ = 1/K$, where K is the equilibrium association constant (*i.e.* 4.6×10^4 M^{-1}). When similar polymerization reactions were carried out at lower ionic strength (*i.e.* 50 mM *versus* 150 mM NaCl) which was known to enhance the cryophenomenon, the equilibrium monomer concentration was decreased to about 6.7×10^{-6} M (1 mg/ml), and the initial rates of polymerization were increased by one order of magnitude (data not shown).

Specificity of the Cold-induced Polymerization—In order to test the specificity of the polymerization of the IgG1κ monomer onto autologous native dimers used as promoters, we tested the ability of other initiators to induce the nucleation-controlled reaction at low temperature. Soluble high molecular weight polymers obtained by heat aggregation of either the autologous cryoglobulin or polyclonal IgG were prepared by gel filtration. Cross-linked IgG1κ oligomers were obtained by reacting IgG1κ monomers at 10 mg/ml with suberimidate. Under optimal conditions, 50% of the monomer was covalently cross-linked in the form of dimers, trimers, or tetramers, as judged by SDS-polyacrylamide gel analysis (data not shown). None of these preparations was able to initiate the temperature-dependent polymerization, even at appropriate initiator concentrations (*i.e.* over 10%). Furthermore, 10% IgG1κ Cac dimers were unable to initiate the polymerization of two other monomers (IgG2κ Zie and IgG3κ Pav) known to cryoprecipitate in the presence of their autologous dimers.

It was also shown that the polymerization reaction is Fc independent. Both the $F(ab')_2$ and Fab fragments were able to form gel through a nucleation-controlled polymerization in the cold albeit at higher concentrations than the parent molecule (Fig. 7). It was possible to demonstrate that the addition of as little as 1% of IgG1κ Cac dimers induced an instantaneous

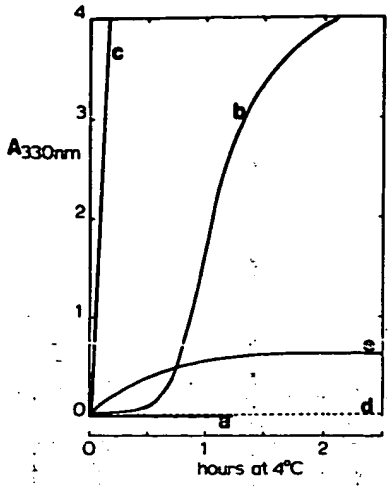

FIG. 7. Kinetics of polymerization for the Fab and $F(ab')_2$ fragments of IgG1 Cac at 4 °C. Fab at 10 (*a*), 17 (*b*), and 24 (*c*) mg/ml in Buffer TBS; $F(ab')_2$ at 3.9 mg/ml in Buffer TBS (*d*) and at the same concentration in the presence of 0.08 mg/ml of IgG1 Cac dimer (*e*).

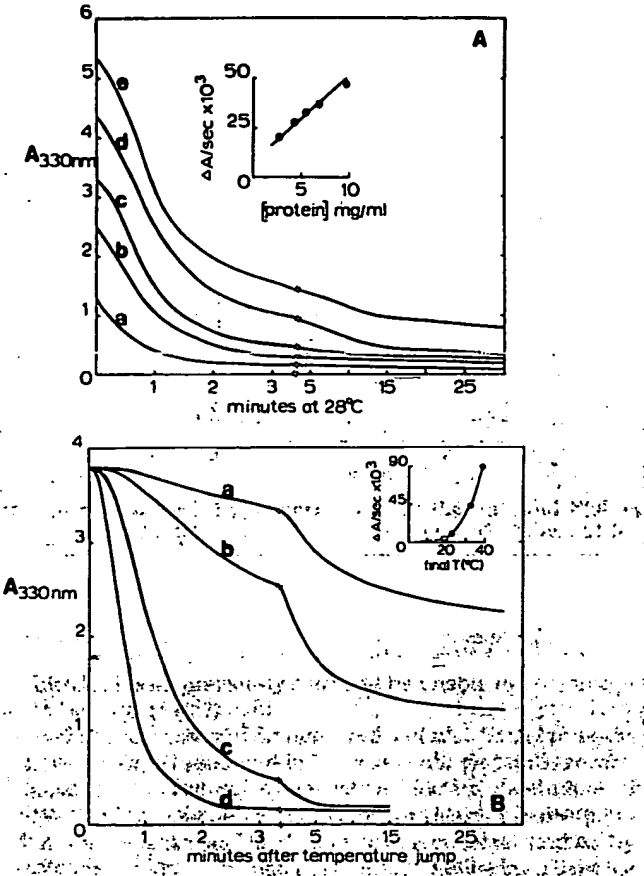

FIG. 8. Kinetics of cryoglobulin depolymerization. *A*, samples of IgG Cac at different concentrations in Buffer TBS were polymerized at 4 °C and subsequently depolymerized at 28 °C. The depolymerization kinetics were obtained by continuous recording of the absorbance at 330 nm following a rapid temperature jump from 4–28 °C. *Inset* shows the dependence of the initial rate of polymerization on the total cryoglobulin concentration. The initial rate was graphically determined after the lag phase (approximately 15 s) corresponding to thermal equilibration. Cryoglobulin concentration in mg/ml was: *a*, 2.85; *b*, 4.3; *c*, 5.7; *d*, 7.2; *e*, 10. *B*, dependence of the depolymerization kinetics on the amplitude of the temperature jump. A sample of IgG Cac at 6 mg/ml in Buffer TBS was polymerized at 4 °C and subsequently depolymerized by rapidly raising the temperature to: *a*, 19 °C; *b*, 23 °C; *c*, 33 °C; *d*, 38 °C. *Inset*, initial rate of depolymerization as a function at the final temperature.

polymerization of a 3.9 mg/ml solution of $F(ab')_2$ monomers which had been previously shown to be unable to cryoprecipitate at 4 °C (Fig. 7).

Depolymerization of Cryoglobulin Tubular Structures—As shown in Fig. 2*B*, the cold-induced assembly is totally reversible at 37 °C. The depolymerization kinetics of solutions of cryoglobulins containing various quantities of tubular polymers of an unequal length and diameter were studied by temperature jump experiments (Fig. 8*A*). Following a brief lag phase of 10–15 s, corresponding to the time required for thermal equilibration, the rate of disassembly was about three orders of magnitude faster than the rate of polymerization. If the initial part of the reaction corresponding to the lag phase was ignored, the kinetics approximately followed pseudo-first order kinetics with a single relaxation time of 27 s. Nevertheless, curve-fitting analysis using a computer program showed that the reaction was more complex since the experimental data could not be accounted for by the sum of three first order processes (data not shown). The initial rate of depolymerization was directly proportional to the mass concentration of polymer determined at 4 °C (Fig. 8*A*). In a second series of experiments, it was shown that the initial rate of depolymerization for a fixed concentration of polymers increased with the amplitude of the temperature jump (Fig. 8*B*).

Molecular Localization of the Site of Monomer-Monomer Interaction—The previously described experiments strongly suggest that the self-nucleating event is indeed the dimerization of the cryoglobulin monomer. This dimerization step is thermodynamically unfavorable. It was not possible to demonstrate any temperature-dependent conformational changes in the intact IgG molecule or its Fab fragment. The temperature-dependent changes observed by circular dichroism for Fab Cac were not significantly different from those observed for the Fab fragment of a noncryoprecipitating monoclonal IgG1κ (data not shown). By difference spectroscopy, we showed that lowering the temperature of a solution of IgG1κ Cac or its Fab fragment induced red-shifted difference spectra. However, it was shown that the changes in molar absorbance at two different fixed wavelengths varied as a linear function of the temperature, as expected for a solvent effect and not a conformational change (data not shown).

It has been clearly shown that the Fab and $F(ab')_2$ fragments of the molecule are capable of cryoprecipitating and forming tubular structures similar to the parent molecule. This implies that the region involved in the polymerization is contained within the Fab fragment. It should be stressed that higher molar concentrations of Fab fragments were required to initiate the formation of a cryogel, whereas $F(ab')_2$ fragments had an ability to cryoprecipitate comparable to that of the intact IgG. The fact that only autologous dimers can induce the specific nucleation of both the IgG monomer (Fig. 5*A*) and the $F(ab')_2$ fragment (Fig. 7) strongly suggests that the region involved in monomer-monomer association is restricted to the complementarity-determining segments of the V regions. Mild reduction of the inter-H-L disulfide bridge of the native IgG and its proteolytic fragments completely abolished this specific interaction. When this bridge was reoxidized in the absence of dissociation of the H and L chains, the cryoprecipitability of the molecule was restored (Fig. 2*A*). In contrast, the recombinant molecules obtained by noncovalent reassociation and reoxidation of isolated H and L chains were unable to polymerize even at 7 mg/ml, and the addition of

autologous dimers to the reduced and alkylated molecule could not trigger polymerization.

DISCUSSION

Although the mechanism of cold-induced polymerization of monoclonal cryoglobulins had not been elucidated, results from previous experiments suggested that the precipitation at low temperatures of these proteins might be a nucleation-controlled event (32, 33). The objectives of the present study were 2-fold: 1) to test for a condensation-polymerization mechanism in order to establish a model for the *in vitro* assembly of monoclonal cryoglobulins, and 2) to localize the region of the molecule involved in the monomer-monomer interaction promoted at low temperatures. The study of two monoclonal cryoglobulins of different subclasses (IgG1κ, IgG3κ) in parallel has clearly shown that cold-induced polymerization is indeed mediated by a nucleation event. The existence of a critical concentration below which the IgG1κ cryoglobulin does not polymerize and a concentration-dependent lag phase and initial rate are strongly suggestive of such a mechanism. Similar observations have been made for a monoclonal IgG2κ cryoglobulin (32, 33). It has been shown that a solution of cryoglobulin monomer, freed of oligomers by gel filtration, is unable to polymerize even at high concentrations, but that the addition of trace amounts of soluble polymers (seeds) at 37 °C initiates the polymerization at 4 °C. It was further demonstrated that the smallest species capable of acting as a promoter is the native dimer obtained by cryoprecipitation of the monomer at 4 °C. The kinetic predictions for a nucleation-controlled polymerization have been confirmed in the case of monoclonal cryoglobulins by the following findings. Under equilibrium conditions favoring polymerization, the only stable intermediate detectable by analytical ultracentrifugation is the dimer. No other discrete oligomeric species smaller than the large tubular structures are found in significant amounts. At a fixed concentration of monomer, the initial rate of polymerization is directly proportional to the concentration of dimer added. At a fixed concentration of dimer, the initial rate of assembly increases in direct proportion to the concentration of cryoglobulin monomer. The dimeric promoter depolymerizes upon dilution when the concentration of monomer is below the critical concentration. Finally, the initial rate of depolymerization following a temperature jump at 28 °C is directly proportional to the polymer concentration.

Taken together, these results suggest that the cold-induced condensation polymerization of monoclonal cryoglobulins can be described as follows.

1) The dimerization of cryoglobulin monomers constitutes a thermodynamically unfavorable nucleation event. The rate of dimerization depends on the monomer concentration and is the limiting factor in the polymerization kinetics. This accounts for the concentration dependence of the lag phase and of the initial rate of the reaction. This finding explains the irreproducibility of the kinetic data obtained with different preparations of the same molecule which usually contain variable amounts of oligomers and why they depend on the techniques which have been used to isolate, solubilize, and centrifuge the cryoglobulin solution. Nevertheless, the detailed mechanism of the dimerization process remains unclear. The formation of dimers has been shown to be necessary for the cold-induced assembly of an IgG1 Fab fragment (29) and for that of a cryoprecipitating human λ chain (17). Although a thermal transition has been proposed to explain the initial step of the polymerization pathway (17, 20, 31) circular dichroism and difference spectroscopy studies performed on both the native IgG and its Fab fragment at various temperatures failed to detect significant conformational changes. A similar observation has also been reported by other groups (21, 32). Conversely, as reported in this paper, a decrease in ionic strength resulted in a marked increase in the rate of polymerization and a significant decrease in the monomer critical concentration. However, a conformational change occurring in a limited region of the molecule which would not affect the spatial orientation of aromatic chromophores could be missed by these methods of detection. It has been established that an increase in ionic strength can reversibly abolish the monomer-monomer interactions at low temperatures (17, 21). These results indicate that electrostatic interactions between Fab fragments are an essential feature of the phenomenon, and since these electrostatic interactions are temperature independent, it is reasonable to assume that a redistribution of charged amino acid side chains have been induced at low temperature.

2) This rate-limiting nucleation event initiates the thermodynamically favorable temperature-dependent elongation of the tubular structures, as judged by the electron microscopic studies of the cryoglobulin. These growth processes are nevertheless slow, with an apparent forward rate constant for the elongation step of 4.7×10^{-4} M^{-1} s^{-1}. They probably result from the addition of monomeric subunits, initially onto the dimer and subsequently at the extremities of the growing microtubule. Further interactions between tubular structures lead to the alignment of microtubules into well ordered bundles or to the formation of entangled filaments. These results are analogous to those reported by Wilson and Makinen (40) for the fiber-to-crystal transition of deoxygenated sickle cell hemoglobin. These authors showed that gels consist of randomly oriented groups of fibers in contrast to the well ordered network of filaments in deoxy Hb S crystals. It is likely that the high viscosity of the gel phase has impeded the crystallization process of the two monoclonal cryoglobulins used in our study. In that respect, it is noteworthy that the crystallization of four human cryoglobulins (IgG1κ Dob (35), IgG1κ Kol (6), IgG1λ Mcg, and IgG2κ Zie (8)) has allowed their three-dimensional analysis by x-ray diffraction. Nevertheless, because of these multiple intermicrotubule interactions, any rigorous analysis of the kinetics of polymerization of cryoglobulins becomes extremely complex.

3) The depolymerization step is exceedingly rapid as compared to the polymerization step, and it has not been possible to elucidate the mechanism in detail because of the complexity of the reaction, due to the fact that the initial solution of tubular polymers is not homogeneous. Although the putative depolymerization by release of monomer from the ends of the tubule should obey zero order kinetics, a pseudo-first order rate will be superimposed due to the time-dependent disappearance of tubular structures heterogeneous in length. This explains why the initial rate of depolymerization is apparently a linear function of the initial mass concentration of polymers.

It has been clearly demonstrated by ultrastructural studies and by the use of proteolytic fragments that the cryophenomenon is Fab dependent. One remarkable finding is that the cryogel structure of the $F(ab')_2$ fragment is similar to that of the parent molecule, although the external diameter of $F(ab')_2$ tubules is significantly smaller than that of IgG rods (19 nm *versus* 30 nm). IgG microtubules are formed of two concentric tubes, the smaller one being approximately the size of $F(ab')_2$ cross-sections. Therefore, the difference of about 11 nm in external diameter may be accounted for by the lack of the Fc fragment (7 nm), assuming that the IgG molecules are radially arranged within the tube, Fabs forming the internal tube and Fcs the external one. Lateral associations between aligned IgG microtubules might result from Fc-Fc interactions (26), since these well ordered structures are not seen in the cryogels of

proteolytic fragments. The dimensions of the annular section of the hollow $F(ab')_2$ rods are similar to those previously reported in the literature for other monoclonal cryoglobulins or cryocrystals (3, 14, 27, 37, 39). The observation that the Fab fragment can form similar structures, but with a slightly different and more fragile organization, indicates that multivalency is an important factor for stabilization of these supramolecular structures. This Fab-Fab interaction has been clearly demonstrated in the crystal lattice of IgG2 Zie cryoglobulin by electron microscopy (27). These results invalidate the hypothesis that a structural anomaly of the hinge (*i.e.* deletion (35) or extra S-S bond (33)) forms the molecular basis for the unusual thermal properties of monoclonal cryoglobulin (32, 33). Furthermore, the hinge peptides of the three cryoglobulins used in the present study were normal, and the three-dimensional structure of the normal hinge region of Kol IgG1 cryoglobulin has recently been established by high resolution x-ray diffraction analysis (18).

In addition, we have shown that the nucleation-controlled polymerization is a phenomenon specifically and exclusively inducible by autologous native promoters. This crucial finding clearly indicates that hypervariable regions are directly involved in the recognition sites between cryoglobulin monomers and that aggregation of the cryoglobulin, chemical modification of lysine groups by bifunctional cross-linking agents, or transient acid denaturation of the polypeptide chains results in an irreversible loss of the thermal properties of the molecule, probably by modifying the limited region(s) involved in the phenomenon. Confirming our previous experiments on a cryoprecipitating human λ chain (17), a change in the tertiary structure of the molecule due to the cleavage of the COOH-terminal causes inter H-L disulfide bridge-induced conformational changes at a distance in the variable region of the Fab fragment leading to a loss of its thermal sensitivity. Recently, it has been shown that some monoclonal cryoglobulins may express an autoantibody activity directed against themselves. Along this line, the possible anti-IgG activity of some monoclonal IgG cryoglobulin has been previously reported (11, 37), and a cryoprecipitating monoclonal IgM with cold agglutinin activity has been shown to react with its own *N*-acetylneuraminosyl residues (38). In IgG Kol crystals, the hypervariable segments of one molecule are in close contact with the hinge peptide of a neighboring molecule, as in an antigen-autoantibody complex (18). More recently, the presence of anti-idiotypic antibodies in mixed cryoglobulins has been suggested (10). In the cases of IgG1 Cac cryoglobulin, it is most improbable that this molecule, selected for this study because of its known anti-streptolysin O activity, is also an auto-anti-idiotype. Therefore, the polymerization of monomers is probably mediated by lateral surface interactions between Fab fragments.

Acknowledgment—We are thankful to Kathy Horne for her assistance in measuring the circular dichroism spectra.

REFERENCES

1. Adachi, K., Segal, R., and Asakura, T. (1980) *J. Biol. Chem.* 255, 7595–7603
2. Asakura, S., and Iino, T. (1972) *J. Mol. Biol.* 64, 251–268
3. Bogaars, H. A., Kalderon, A. E., Cummings, F. J., Kaplan, S., Melnicoff, I., Park, C., Diamond, J., and Calabresi, P. (1973) *Nat. New Biol.* 245, 117–118
4. Brouet, J. C., Clauvel, J. P., Danon, F., Klein, M., and Seligmann, M. (1974) *Am. J. Med.* 54, 775–788
5. Chervenka, C. M. (1970) in *A Manual of Methods for the Analytical Centrifuge*, p. 23, Beckman Instruments, Inc., Palo Alto, California
6. Colman, P. M., Deisenhofer, J., and Huber, R. (1976) *J. Mol. Biol.* 100, 257–282
7. Ellerson, J. R., Yasmeen, D., Painter, R. H., and Dorrington, K. J. (1976) *J. Immunol.* 116, 510–517
8. Ely, K. R., Colman, P. M., Abola, E. E., Hess, A. C., Peabody, D. S., Parr, D. M., Connell, G. E., Laschinger, C. A., and Edmundson, A. B. (1978) *Biochemistry* 17, 820–823
9. Frangione, B., Milstein, C., and Franklin, E. C. (1969) *Nature* 221, 149–151
10. Geltner, D., Franklin, E. C., and Frangione, B. (1980) *J. Immunol.* 125, 1530–1535
11. Grey, H. M., Kohler, P. F., Terry, W. D., and Franklin, E. C. (1968) *J. Clin. Invest.* 47, 1875–1884
12. Grey, H. M., and Kohler, P. F. (1973) *Semin. Hematol.* 10, 87–112
13. Johnson, K. A., and Borisy, G. G. (1977) *J. Mol. Biol.* 117, 1–31
14. Kalderon, A. E., Bogaars, H. A., Diamond, I., Cummings, F. J., Kaplan, S. R., and Calabresi, P. (1977) *Cancer (Phila.)* 39, 1475–1481
15. Kasai, M., Asakura, S., and Oosawa, F. (1962) *Biochim. Biophys. Acta* 57, 22–31
16. Klein, M., Danon, F., Brouet, J. C., Signoret, Y., and Seligmann, M. (1972) *Eur. J. Clin. Biol. Res.* 17, 948–957
17. Klein, M., Kells, D. I. C., Tinker, D. O., and Dorrington, K. J. (1977) *Biochemistry* 16, 552–560
18. Marquart, M., Deisenhofer, J., Huber, R., and Palm, W. (1980) *J. Mol. Biol.* 141, 369–391
19. Meltzer, M., and Franklin, E. C. (1966) *Am. J. Med.* 40, 828–836
20. Middaugh, C. R., Thomas, G. J., Jr., Prescott, B., Aberlin, M. E., and Litman, G. W. (1977) *Biochemistry* 16, 2986–2994
21. Middaugh, C. R., Gerber-Jenson, B., Hurvitz, A., Paluszek, A., Scheffel, C., and Litman, G. W. (1978) *Proc. Natl. Acad. Sci. U. S. A.* 75, 3440–3444
22. Middaugh, C. R., Kehoe, J. M., Prystowsky, M. B., Gerber-Jenson, B., Jenson, J. C., and Litman, G. W. (1978) *Immunochemistry* 15, 171–187
23. Nisonoff, A., Wissler, F. C., Lipman, L. N., and Woernley, D. L. (1960) *Arch. Biochem. Biophys.* 89, 230–244
24. Oosawa, F., and Asakura, S. (1975) in *Thermodynamics of the Polymerization of Proteins*, pp. 1–194, Academic Press, New York
25. Petersen, J. G. L., and Dorrington, K. J. (1974) *J. Biol. Chem.* 249, 5633–5641
26. Pinteric, L., Painter, R. H., and Connell, G. E. (1971) *Immunochemistry* 8, 1041–1045
27. Pinteric, L., and Parr, D. (1974) *Proc. Microsc. Soc. Can.* 1, 36–37
28. Pruzanski, W., Jancelewicz, Z., and Underdown, B. (1973) *Clin. Exp. Immunol.* 15, 181–191
29. Saha, A., Edwards, M. A., Sargent, A. U., and Rose, B. (1968) *Immunochemistry* 5, 341–356
30. Saha, A., Chowdhury, P., Sambury, S., Smart, K., and Rose, B. (1970) *J. Biol. Chem.* 245, 2730–2736
31. Salck, P. H., and Clem, W. (1975) *Immunochemistry* 12, 29–39
32. Scoville, C. D., Abraham, G. N., and Turner, D. H. (1979) *Biochemistry* 18, 2610–2615
33. Scoville, C. D., Turner, D. H., Lippert, J. L., and Abraham, G. N. (1980) *J. Biol. Chem.* 255, 5847–5852
34. Seligmann, M., Danon, F., Basch, A., and Bernard, J. (1968) *Nature* 220, 711–712
35. Silverton, E. W., Navia, M. A., and Davies, D. R. (1977) *Proc. Natl. Acad. Sci. U. S. A.* 74, 5140–5144
36. Stevenson, G. T., and Dorrington, K. J. (1970) *Biochem. J.* 118, 703–712
37. Stoebner, P., Renversez, J. C., Groulade, J., Vialtel, P., and Cordonnier, D. (1979) *Am. J. Clin. Pathol.* 71, 404–410
38. Tsai, C. M., Zopf, D. A., Yu, R. K., Wistar, R., and Ginsburg, V. (1977) *Proc. Natl. Acad. Sci. U. S. A.* 74, 4591–4594
39. White, J. C., Adam, B. A., Lau, K. S., Horne, R. W., and Parkhouse, R. M. E. *J. Pathol.* 120, 25–33
40. Wilson, S. M., and Makinen, M. W. (1980) *Proc. Natl. Acad. Sci. U. S. A.* 77, 944–948

J. Biochem. **83**, 1249–1263 (1978)

Ionization and Reactivities of the Thiol Groups Which Participate in the Formation of Interchain Disulfide Bonds of Bence Jones Proteins and an Fab(t) Fragment[1]

Yoko TANAKA, Takachika AZUMA, and Kozo HAMAGUCHI

Department of Biology, Faculty of Science, Osaka University, Toyonaka, Osaka 560

Received for publication, November 17, 1977

The pK values and reactivities of the thiol groups which participate in the formation of interchain disulfide bonds in Bence Jones proteins and the Fab(t) fragment of a myeloma protein (Jo) (IgGl, κ) were determined by means of the reactions with chloroacetamide and DTNB, and of spectrophotometric titration. The two thiol groups of partially reduced type κ Bence Jones protein dimers had the same pK values (pK=9.76 at 0.2 ionic strength and 25°C) and the same true second-order rate constants ($\bar{k}$) toward chloroacetamide ($\bar{k}=18.8\times10^{-2}$ M$^{-1}\cdot$s^{-1}). The two thiol groups of partially reduced type λ Bence Jones protein dimers had different pK values but the variation of the pK values among the specimens was small (pK_1=8.5–8.6 and pK_2=9.5–9.7 at 0.2 ionic strength and 25°C). The spectrophotometric titration of partially reduced Nag protein (type λ) also showed that the two thiol groups have different pK values. The pK values of two thiol groups of the partially reduced Fab(t) fragment were determined as 8.51 and 9.76 at 0.2 ionic strength and 25°C. The effect of ionic strength on the pK values of the thiol groups of partially reduced Nag protein and the pK values of the thiol groups in partially reduced Ta protein (type κ) and in a hybrid molecule formed between partially reduced Ta protein and partially reduced and alkylated H chains indicated that the difference in pK values did not arise from electrostatic interaction between the two thiol groups, but that the pK values are intrinsically different. The true rate constants, $\bar{k}_1$ and $\bar{k}_2$, of the two thiol groups of type λ Bence Jones proteins varied with the specimen ($\bar{k}_1=1.9$–5.7×10^{-2} M$^{-1}\cdot$s^{-1} and $\bar{k}_2=18.5$–25.0×10^{-2} M$^{-1}\cdot$s^{-1}). The $\bar{k}_1$ and $\bar{k}_2$ values for Jo-Fab(t) were 7.21×10^{-2} and 23.1×10^{-2} M$^{-1}\cdot$s^{-1}, respectively. On the basis of these pK values and reactivities, we discuss the reformation of the interchain disulfide bonds from partially reduced Bence Jones proteins and immunoglobulins in the presence of oxidized glutathione.

[1] This work was supported in part by a grant from the Ministry of Education, Science and Culture of Japan. Abbreviations: DTNB, 5,5′-dithiobis(2-nitrobenzoic acid); DTT, dithiothreitol; EDTA, ethylenediaminetetraacetic acid; GSSG, oxidized glutathione; SDS, sodium dodecyl sulfate.

Bence Jones proteins are free light chains (L chains) of myeloma proteins (monoclonal immunoglobulins) and are synthesized in the plasma cells, like the parent immunoglobulins. Bence Jones proteins exist in three forms, stable dimers (disulfide-bonded dimers), dissociable dimers (noncovalent dimers), and stable monomers. The stable dimer consists of two monomers which are linked by a disulfide bond between cysteinyl residues at the carboxyl termini (type κ) or at the penultimate positions (type λ). The thiol groups of the cysteinyl residues of dissociable dimers and stable monomers are not free but form mixed disulfides with low molecular weight thiol compounds (*1–3*). The thiol groups of IgM_s (a subunit of IgM), which participate in the formation of inter-subunit disulfide bonds, are also blocked with a thiol compound of low molecular weight in the cells (*4*). These findings suggest that the interchain and inter-subunit disulfide bonds in immunoglobulins and Bence Jones proteins are formed in the cells by thiol-disulfide interchange reaction with a low molecular weight disulfide compound.

Previously, Kishida *et al.* (*5*) studied the formation of disulfide bonds from Bence Jones proteins and IgG, in which interchain disulfide bonds are reduced, in the presence of oxidized glutathione (GSSG). They showed that both stable and dissociable dimers are formed from partially reduced type λ Bence Jones proteins, but only dissociable dimers are formed from partially reduced type κ Bence Jones proteins. They also found that the yields of the stable dimers are different depending on the specimen of type λ Bence Jones proteins, but the interchain disulfide bonds of IgG are formed completely under the same conditions. Such a variation in the formation of interchain disulfide bonds among these proteins seems to reflect differences in the pK values and nucleophilicities of the thiol groups, because only thiolate anion participates as a nucleophile in the thiol-disulfide interchange reaction.

In the present paper, we report the ionization behavior and reactivities of the thiol groups in Bence Jones proteins and the Fab(t) fragment of a myeloma protein (IgG1, κ) examined in terms of the reaction with chloroacetamide and discuss the formation of interchain disulfide bonds from partially reduced Bence Jones proteins and immunoglobulins.

MATERIALS AND METHODS

Proteins—Bence Jones proteins and a myeloma protein Jo (IgG1, κ) were prepared by the methods described previously (*6*). Normal human IgG (Fraction II) was obtained from Sigma Chemical Co. Trypsin and soybean trypsin inhibitor were purchased from Worthington Biochemical. Preparation of the Fab(t) fragment of Jo protein was carried out according to the mthod described previously (*7*).

Reagents—Dithiothreitol (DTT), N-acetyl-L-cysteine, chloroacetamide, iodoacetamide, 5,5'-dithiobis-(2-nitrobenzoic acid) (DTNB), and sodium dodecyl sulfate (SDS) were products of Nakarai Chemical Co. Ethylenediaminetetraacetic acid (EDTA) was obtained from Wako Pure Chemicals Co. Oxidized and reduced glutathiones were purchased from Sigma Chemical Co.

Reduction of Interchain Disulfide Bonds—About 1–2% protein in 0.02 M Tris-HCl buffer containing 0.2 M KCl (pH 8.2) was allowed to react with 20 mM DTT for 30 min at room temperature. Under these conditions, no intrachain disulfide bonds of Bence Jones proteins and Fab(t) were reduced. We refer to this procedure as partial reduction. After the reaction the protein was separated from the residual reagent on a column of Sephadex G-25 equilibrated with 0.1 M KCl–1 mM EDTA.

Preparation of a Hybrid Molecule from Partially Reduced and Alkylated Normal H Chains and a Partially Reduced Bence Jones Protein—Partial reduction of normal human IgG was carried out as described above. The reduction was terminated by the addition of iodoacetamide to a final concentration of 44 mM followed by incubation for 20 min at room temperature. The reaction mixture was applied to a column of Sephadex G-25 equilibrated with 0.01 M acetate buffer at pH 5.5 to separate the protein from the excess reagents. The protein solution eluted was made 1 M with respect to propionic acid at 4°C and left to stand for 2 h and then subjected to gel filtration on a column of Sephadex G-100 equilibrated with 1 M propionic acid. The fractions containing the H chains were pooled and dialyzed against 0.01 M acetate buffer at pH 4.5 for renaturation. The H chains thus renatured were mixed with Ta protein (type κ),

which had been partially reduced but not alkylated, and the mixture was subjected to successive steps of dialysis against the following buffers: 0.01 M acetate buffer at pH 5.5, 0.01 M acetate buffer at pH 5.5 containing 0.15 M KCl, and 0.01 M Tris-HCl buffer at pH 8.0 containing 0.15 M KCl. During the dialysis, the H chains assembled with Ta protein and gave a hybrid molecule. It was purified by gel filtration on a column of Sephadex G-200 equilibrated with 0.01 M Tris-HCl buffer at pH 8.0 containing 0.15 M KCl. Before the reaction with chloroacetamide, the hybrid was treated with DTT.

Kinetics of the Reaction with Chloroacetamide—To 2.5 ml of 0.1–0.2% partially reduced protein was added 0.5 ml of a chloroacetamide solution at 25°C. The concentration of chloroacetamide was changed from 5 to 100 mM, depending on the experiment. A sample of 0.3 ml of the reaction mixture was taken at times from 1 to 30 min after the start of the reaction and the extent of alkylation was determined by titration of the remaining free thiol groups with DTNB. Since the rate of reaction of the thiol groups with DTNB was more rapid than that of the reaction with chloroacetamide, the titration of thiol groups was carried out without removing chloroacetamide from the reaction mixture. The pH was controlled with Tris-acetate buffer (below pH 9.0) and borate buffer (pH 9.0–10.8). The ionic strength of the solutions was adjusted by the addition of KCl. The control experiment was done under the same conditions except for the absence of chloroacetamide.

Kinetics of the Reaction with DTNB—A solution of partially reduced protein (2.8 ml) was mixed rapidly with DTNB solution (100 μl) in a silica cell at 25°C. The change in the absorbance at 412 nm was recorded. The concentration of DTNB in the stock solution was determined by titration with a standard solution of reduced glutathione. Tris-acetate buffer was used and the ionic strength of the reaction mixture was adjusted by the addition of KCl.

Spectrophotometric Titration of the Thiol Groups—Ultraviolet difference spectra of partially reduced Nag protein (type λ) and partially reduced and alkylated Nag protein were recorded with a Cary 118 spectrophotometer with a thermostated cell holder. All solutions were filtered through a 0.22 μm Millipore filter. Four quartz cells of 1-cm path length were used. On the reference beam side, one cell contained a mixture of 2.5 ml of an aqueous solution of partially reduced Nag protein (or partially reduced and alkylated Nag protein) and 0.2 ml of buffer solution at the reference pH (7.2), and the other cell contained a mixture of 2.5 ml of water and 0.2 ml of buffer solution at the desired pH. On the sample beam side, one cell contained a mixture of 2.5 ml of an aqueous solution of partially reduced Nag protein (or partially reduced and alkylated Nag protein) and 0.2 ml of buffer solution at the desired pH, and the other cell contained a mixture of 2.5 ml of water and 0.2 ml of buffer solution at the reference pH. All the solutions contained 0.1 M KCl and 1 mM EDTA. Comparison of the difference spectrum of partially reduced Nag protein with that of partially reduced and alkylated Nag protein at the same pH gives the titration curve of the thiol groups in the former protein.

Thiol-Disulfide Interchange Reaction in the Presence of GSSG—A solution of a partially reduced protein at a given pH was mixed with GSSG and the mixture was incubated at 25°C. In the kinetic experiments, a sample of 100 μl was taken from the reaction mixture at an appropriate time and was added to a solution of iodoacetamide to terminate the thiol-disulfide interchange reaction. In order to determine the final extent of formation of interchain disulfide bonds, the reaction mixture was incubated for either 24 or 72 h. The extent of formation of interchain disulfide bonds was determined by SDS-polyacrylamide gel electrophoresis. The amount of free thiol groups remaining was also determined by titration with DTNB after removing glutathione from the reaction mixture by dialysis. The final concentrations of protein and GSSG in the reaction mixture were 2×10^{-4} M and 1 mM, respectively. The buffer solutions used were acetate (pH 5–5.5), phosphate (pH 6–7), EDTA (pH 7–7.5), Tris-HCl (pH 7–8.5), and glycine-KOH (above pH 8.5). All the buffer solutions except for EDTA buffer contained 1 mM EDTA. The ionic strength of the buffer solutions was controlled by the addition of KCl.

Titration of Free Thiol Groups with DTNB—The amount of free thiol groups was determined by titration with DTNB at pH 8.0 in 0.1 M Tris-HCl buffer containing 1 mM EDTA. The absorbance at 412 nm was measured with a Hitachi 323 auto-

matic recording spectrophotometer. A value for the molar extinction coefficient of reduced DTNB of 13,600 (*8*) was used to convert the absorbance at 412 nm to SH content.

SDS-Polyacrylamide Gel Electrophoresis—SDS-polyacrylamide gel electrophoresis was carried out at pH 7.5 in 7.5% polyacrylamide gel according to the method described by Weber and Osborn (*9*), but 2-mercaptoethanol was omitted. Before electrophoresis, samples were incubated with 1% SDS containing 25% glycerol for 24 h at room temperature (for Bence Jones proteins) or for 1 min at 100°C (for Jo-Fab(t)). After the run, the gels were stained with 0.25% Coomassie brilliant blue and destained with 5% methanol–7.5% acetic acid. Densitometric scanning of the gel was carried out at 600 nm using a Fuji Riken FD-4 densitometer.

pH Measurements—A Radiometer PHM 26c pH meter was used.

RESULTS

Kinetics of Alkylation of Partially Reduced Bence Jones Proteins and Fab(t) with Chloroacetamide—Figure 1 shows semilogarithmic plots of the disappearance of the thiol groups of partially reduced Bence Jones proteins and Jo-Fab(t) against the reaction time at several pH values. Since an excess of reagent over thiol groups was used, all runs followed pseudo first-order kinetics, and the rate constants were determined from the slopes. The observed second-order rate constant (k_{obs}) can be calculated from the pseudo first-order rate constant and the concentration of chloroacetamide used. The pH profiles of k_{obs} are shown in Fig. 2. In this figure, the values of k_{obs} for N-acetyl-L-cysteine are also included. The values of k_{obs} of all the samples used increased with increasing pH.

Since only the thiolate anion is available for alkylation with chloroacetamide, the pH dependence of k_{obs} can be explained in terms of the change with pH in the degree of ionization of the thiol groups, and the second-order rate constant at a given pH can be expressed by the equation,

$$k_{obs}=\bar{k}-\frac{k_{obs}(H^+)}{K} \quad (1)$$

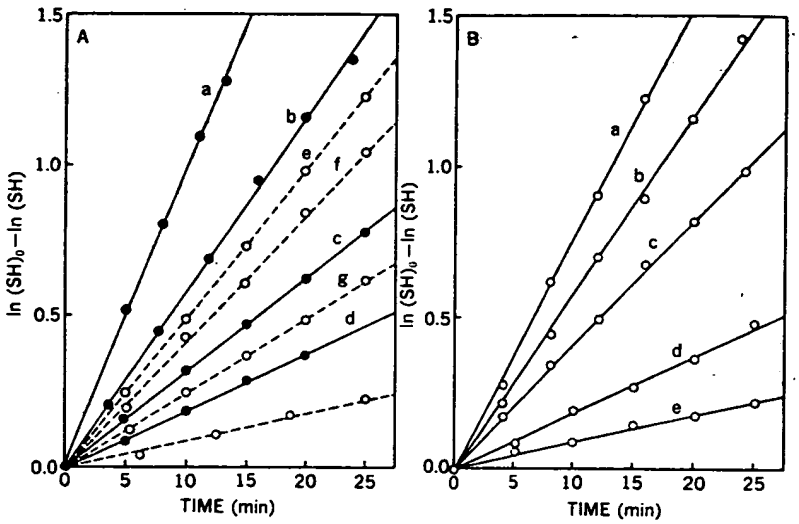

Fig. 1. First-order plots for the alkylation of partially reduced Bence Jones proteins (A) and Jo-Fab(t) (B) with chloroacetamide at 25°C and 0.2 ionic strength. A: Solid and broken lines indicate the plots for Ta protein (type κ) and Nag protein (type λ), respectively. The initial concentrations of Ta and Nag proteins were 8×10^{-5} M. The initial concentrations of chloroacetamide were 10 mM in runs a, b, c, e, f, and g, 25 mM in d, and 20 mM in h. a, pH 10.98; b, pH 9.79; c, pH 9.35; d, pH 8.61; e, pH 10.82; f, pH 9.74; g, pH 9.17; h, pH 8.12. B: The initial concentration of Jo-Fab(t) was 8×10^{-5} M and the concentrations of chloroacetamide were 10 mM in runs a, b, and c and 25 mM in d and e. a, pH 10.52; b, pH 9.82; c, pH 9.34; d, pH 8.10; e, pH 7.66.

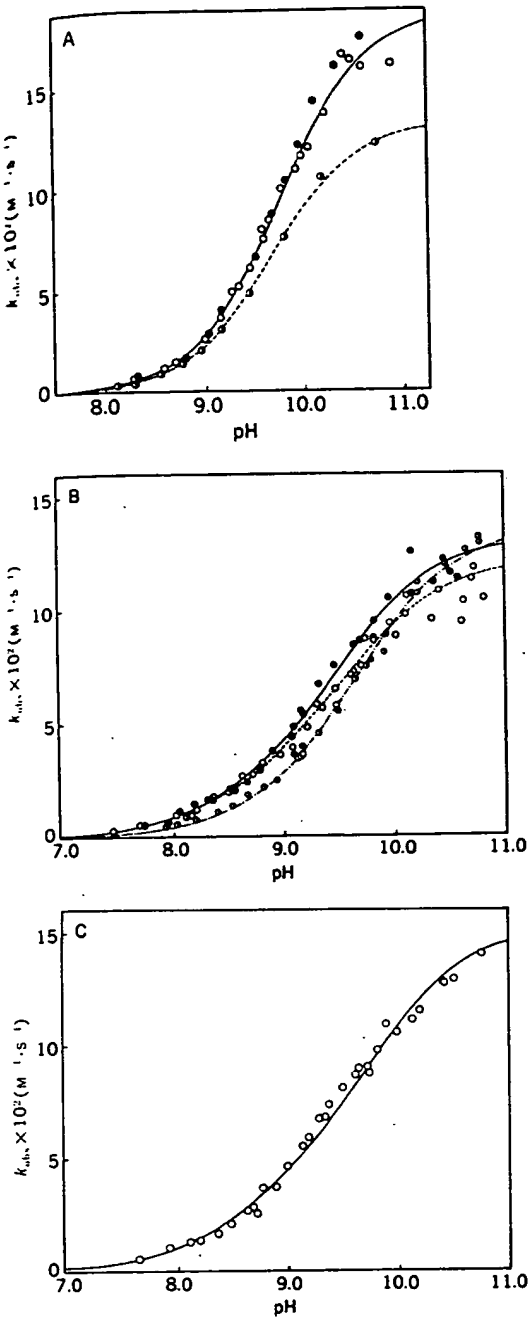

Fig. 2. Effect of pH on the observed second-order rate constant for alkylation with chloroacetamide at 25°C and 0.2 ionic strength. A: Plots for partially reduced type κ Bence Jones proteins and N-acetyl-L-cysteine. ○, Ta protein; ●, Ham protein; ◑, N-acetyl-L-cysteine. B: Plots for partially reduced type λ Bence Jones proteins. ●, Fu protein; ○, Nag protein; ◑, Ni protein. C: Plot for partially reduced Jo-Fab(t). The lines indicate the theoretical curves (see the text).

where K is the ionization constant, $\bar{k}$ is the true second-order rate constant for the alkylation of the thiolate anion, and (H^+) is the activity of protons.

Figure 3 shows the plots of k_{obs} against k_{obs} (H^+) for the data shown in Fig. 2. In the case of type κ Bence Jones proteins (Fig. 3A), this plot gave a straight line and no significant difference was observed between two specimens, Ta and Ham proteins. The values of $\bar{k}$ and pK were determined to be 0.188 ± 0.002 $M^{-1} \cdot s^{-1}$ and 9.76 ± 0.01, respectively. In the case of type λ Bence Jones proteins and Jo-Fab(t), the plots of k_{obs} *vs.* k_{obs} (H^+) were not linear (Figs. 3B and 3C), and the values of $\bar{k}$ and pK could not be obtained directly from these plots.

Bence Jones proteins are an equilibrium mixture of the monomer and dimer, when the two polypeptide chains are not linked by an interchain disulfide bond (*10*, *11*). Under the present experimental conditions, however, the partially reduced Bence Jones proteins used exist mainly as the dimer, which is stabilized by noncovalent interactions. This was confirmed by the observed elution volume on gel filtration of the partially reduced proteins. The dimerization constants were determined to be 10^5 and 10^6 M^{-1} at pH 5.5 for partially reduced and alkylated Ni and Nag proteins, respectively (*11*), and were found to increase with increasing pH (*10*, *11*, Azuma, T., Kobayashi, O., & Hamaguchi, K., to be published). Therefore, at the concentration of Ni and Nag proteins (10^{-4} M) used in the present experiments, more than 90% of the proteins exist as dimers even at pH 5.5. Partially reduced and alkylated Ham and Ta proteins do not show any tendency to dissociate into monomers (*11*, unpublished data). The Fab(t) fragment is composed of the Fd and L chains, which also interact with each other by noncovalent interactions. Therefore, two thiol groups are present in the dimer unit of the partially reduced protein. When these thiol groups are equivalent and independent of each other, the plot of k_{obs} *vs.* k_{obs} (H^+) gives a straight line and the values of $\bar{k}$ and K can be determined directly, as in the case of type κ Bence Jones proteins. On the other hand, when the plot of k_{obs} *vs.* k_{obs} (H^+) is not linear, as in the case of type λ Bence Jones proteins and Jo-Fab(t), the ionization of the two thiol groups must be treated as that of a dibasic acid. The model we

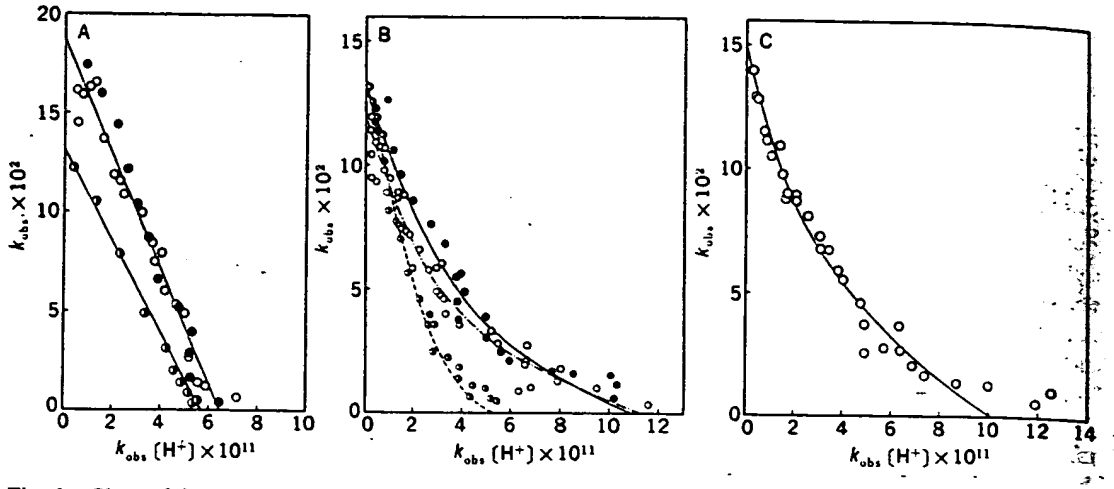

Fig. 3. Plots of k_{obs} *vs.* k_{obs} (H^+) according to Eq. 1. A: Plots for partially reduced type κ Bence Jones proteins and N-acetyl-L-cysteine. ○, Ta protein; ●, Ham protein; ◑, N-acetyl-L-cysteine. B: Plots for partially reduced type λ Bence Jones proteins. ●, Fu protein; ○, Nag protein; ◑, Ni protein. C: Plot for partially reduced Jo-Fab(t). The lines indicate the theoretical curves calculated using the parameters listed in Table I (see the text).

used for the alkylation reaction of the type λ Bence Jones proteins and Jo-Fab(t) is shown in Fig. 4.

If the titration of the two SH groups in the dimer is treated as that of a mixture of two monobasic acids (SH_a and SH_b), the rate of disappearance of the total SH groups ($(SH)_t$) can be expressed by the equation,

$$-\frac{d(SH)_t}{dt}=\frac{1}{2}\left\{-\frac{d(SH_a)}{dt}-\frac{d(SH_b)}{dt}\right\} \quad (2)$$

The observed second-order rate constant, k_{obs}, may be expressed by

$$k_{obs}=\frac{1}{2}\left\{\frac{k_a^*}{1+\frac{(H^+)}{G_a}}+\frac{k_b^*}{1+\frac{(H^+)}{G_b}}\right\} \quad (3)$$

where G_a and G_b are the titration constants and k_a^* and k_b^* the second-order rate constants for SH_a and SH_b.

The macroscopic ionization constants, K_I and K_{II}, and the titration constants are related as follows.

$$K_I=G_a+G_b$$
$$K_IK_{II}=G_aG_b \quad (4)$$

Using a least-squares computer program for the nonlinear function, Eq. 3 was fitted to the experi-

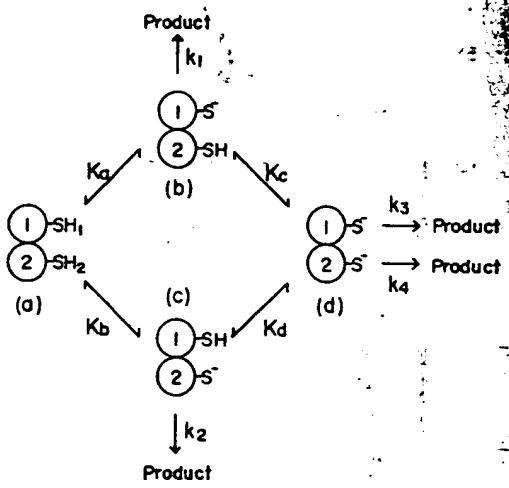

Fig. 4. Scheme for the alkylation of the thiol groups of partially reduced Bence Jones proteins and Jo-Fab(t) with chloroacetamide. The partially reduced protein (a) is composed of two monomers, each of which has a thiol group designated as SH_1 or SH_2. Microscopic ionization constants of the thiol groups corresponding to the respective ionization steps are expressed by K_a, K_b, K_c, and K_d. The thiolate anions of the species, b, c, and d, react with chloroacetamide with true rate constants of k_1, k_2, and k_3 and k_4, respectively.

mental data shown in Fig. 2 and G_a, G_b, k_a*, and k_b* were determined. K_I and K_{II} were also calculated by making use of Eq. 4.

We measured the pH dependence of k_{obs} for Nag protein at ionic strengths 0.05, 0.2, and 0.5 (Fig. 5). The macroscopic ionization constants were pK_I=8.56 and pK_{II}=9.61 at 0.05 ionic strength, pK_I=8.46 and pK_{II}=9.64 at 0.20 ionic strength, and pK_I=8.42 and pK_{II}=9.58 at 0.50 ionic strength.

An increase in the ionic strength from 0.05 to 0.5 decreased the pK_I value by only about 0.1 pH unit. This decrease is in the range expected from the changes in the activities of both protons and thiolate anions with ionic strength (*12*, *13*). Furthermore, the pK_{II} values are less affected by an increase in ionic strength than the pK_I values. These findings indicate that the electrostatic interaction between the two thiol groups may be weak, if there is any. If this is the case, we have for the titration constants $G_a=K_a=K_d$ and $G_b=K_b=K_c$, and we may set k_a* and k_b* equal to the rate constants for the alkylation of the SH on monomer 1 (SH_1) and that on monomer 2 (SH_2), respectively (Fig. 4). We denote the microscopic ionization constants of SH_1 and SH_2 by K_1 and K_2, respectively, and the rate constants for SH_1 and SH_2 by $\bar{k}_1$ and $\bar{k}_2$. The results are summarized in Table I.

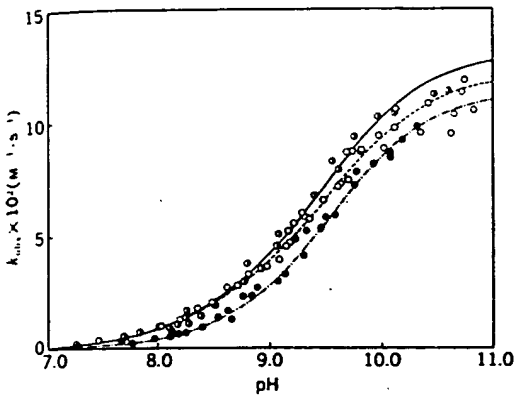

Fig. 5. pH Dependence of the observed second-order rate constant for alkylation of partially reduced Nag protein with chloroacetamide at ionic strengths of 0.05 (●), 0.20 (○), and 0.50 (◑). 25°C.

Table I shows that the thiol groups of all the type λ Bence Jones proteins studied have a pK_1 value of 8.5–8.6 and a pK_2 value of 9.5–9.7. On the other hand, the rate constants of alkylation, especially the $\bar{k}_1$ values, differed from specimen to specimen. In addition, the values of $\bar{k}_1$ were much smaller than the values of $\bar{k}_2$. Variation of ionic strength affected the rate constant but did not significantly affect the ionization constants.

The pK_2 value of Jo-Fab(t) was close to the pK value of type κ Bence Jones proteins. Because the antigenic type of the L chain of Jo-Fab(t) is κ, the pK_2 value of Jo-Fab(t) may correspond to the pK value of the SH group on the L chain and not to the pK value of the SH group on Fd. To confirm this, we examined the alkylation with chloroacetamide of a hybrid molecule formed from partially reduced and alkylated H chains and

TABLE I. The pK values and true rate constants of the thiol groups of partially reduced Bence Jones proteins and Jo-Fab(t) determined by alkylation with chloroacetamide. 25°C.

Samples	Ionic strength	pK		$\bar{k}\times10^2$ ($M^{-1}\cdot s^{-1}$)	
		pK_1	pK_2	$\bar{k}_1$	$\bar{k}_2$
Ta (κ)	0.20	9.76±0.01		18.8±0.3	
Ham (κ)	0.20	9.76±0.01		18.8±0.3	
Fu (λ)	0.20	8.52±0.07	9.54±0.01	5.19±0.15	21.12±0.36
Ni (λ)	0.20	8.57±0.11	9.68±0.01	1.92±0.06	25.06±0.15
Nag (λ)	0.05	8.60±0.19	9.57±0.01	1.91±0.13	20.84±0.35
Nag (λ)	0.20	8.50±0.10	9.61±0.02	5.70±0.17	18.50±0.41
Nag (λ)	0.50	8.45±0.05	9.55±0.01	4.96±0.12	21.14±0.29
Jo-Fab(t)	0.20	8.51±0.05	9.76±0.01	7.21±0.15	23.16±0.38
N-Ac-L-Cys	0.20	9.68±0.01		13.3±0.2	

partially reduced Ta protein (type κ) (see " MATERIALS AND METHODS "). As shown in Fig. 6, the pH dependence of k_{obs} for the hybrid was in good agreement with the pH dependence of k_{obs} for partially reduced Ta protein. This indicates that the thiol group with pK 9.76 corresponds to that of the L chain and that neither the interaction with partially reduced and alkylated H chains nor the interaction with partially reduced H chains affects the pK value of the SH group on the L chain.

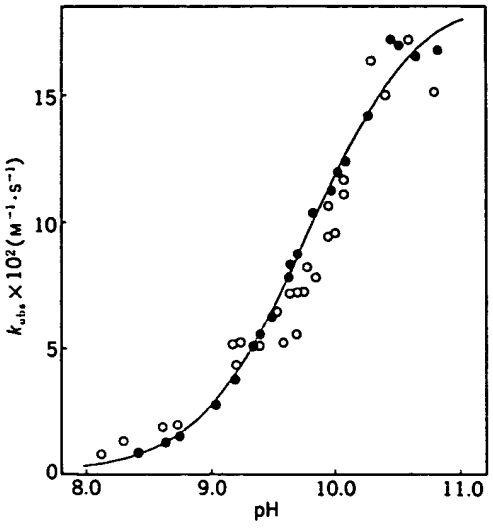

Fig. 6. pH Dependence of the observed second-order rate constants for alkylation of the thiol groups of partially reduced Ta protein in the hybrid molecule with chloroacetamide at 25°C and 0.2 ionic strength (open symbols). The data for partially reduced Ta protein are shown by closed symbols. The solid line represents the theoretical curve for the alkylation of the thiol groups of partially reduced Ta protein constructed using the pK value and the true rate constant listed in Table I (see the text).

Kinetics of the Reaction with DTNB—While the observed rate for the reaction of the thiol groups with chloroacetamide is rather slow near neutral pH, DTNB has a high reactivity toward thiol groups even near neutral pH, and we therefore examined the kinetics of the reaction of the thiol groups of partially reduced Bence Jones proteins with DTNB in the pH range of 7 to 9. The pH dependence of the observed second-order rate constant and the plots of k_{obs} *vs.* k_{obs} (H^+) for type κ proteins are shown in Fig. 7. No difference in the value of k_{obs} was observed among the three specimens. The pK value determined from the slope of the k_{obs} *vs.* k_{obs} (H^+) plot was found to be 9.7, which is in good agreement with the pK value determined from the reaction with chloroacetamide.

The results of the reaction of type λ proteins with DTNB are shown in Fig. 8. Although the plots of k_{obs} *vs.* k_{obs} (H^+) varied from specimen to specimen, their slopes were identical and a pK value of 8.6 was obtained for all the type λ proteins studied. This pK value is in good agreement with

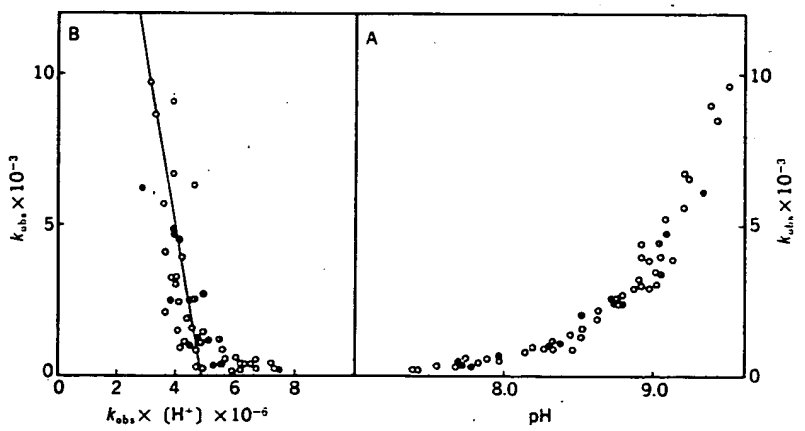

Fig. 7. pH Dependence of k_{obs} for the reaction of the thiol groups of partially reduced type κ Bence Jones proteins with DTNB (A) and plots of k_{obs} *vs.* k_{obs} (H^+) according to Eq. 1 (B). ○, Ta protein; ●, Ham protein; ◑, Tas protein. The reactions were carried out at 25°C and 0.15 ionic strength.

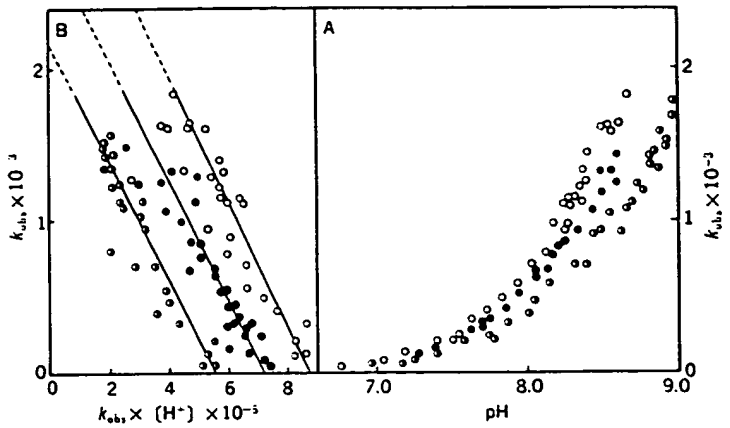

Fig. 8. pH Dependence of k_{obs} for the reaction of the thiol groups of partially reduced type λ Bence Jones protein with DTNB (A) and plots of k_{obs} *vs.* k_{obs} (H^+) according to Eq. 1 (B). ○, Fu protein; ●, Nag protein; ◑, Tod protein. The reactions were carried out at 25°C and 0.15 ionic strength.

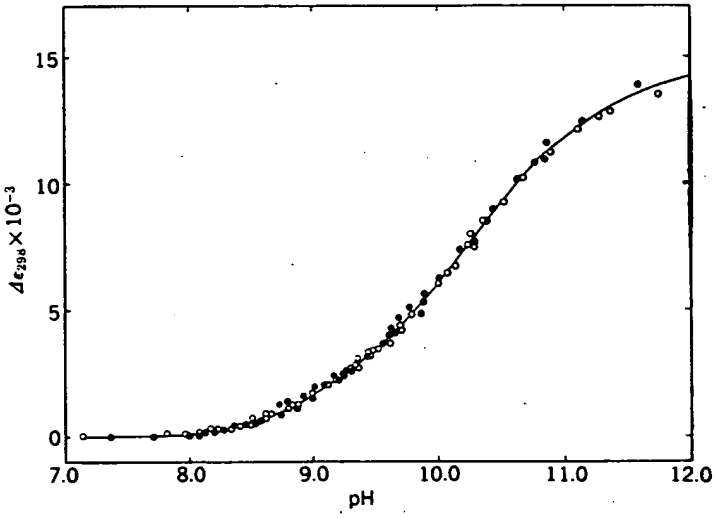

Fig. 9. pH Dependence of the value of $\Delta\varepsilon$ at 298 nm for partially reduced Nag protein (open circles) and partially reduced and alkylated Nag protein (closed circles) at 25°C and 0.2 ionic strength.

pK_1 obtained from the reaction with chloroacetamide. However, the rate constants of the reaction with DTNB were different depending on the specimen.

Spectrophotometric Titration of Thiol Groups—We compared the alkaline difference spectra of partially reduced Nag protein (type λ) with those of partially reduced and alkylated Nag protein. These difference spectra had peaks at 298 and 245 nm. The spectrum obtained by subtracting the difference spectrum of partially reduced and alkylated Nag protein from that of partially reduced Nag protein at the same pH had a peak only at 238 nm with no peak at around 298 nm (not shown). As shown in Fig. 9, the pH dependence curves of the difference in the molar extinction coefficient at 298 nm ($\Delta\varepsilon_{298}$) for the reduced protein and reduced and alkylated protein were identical, and could be

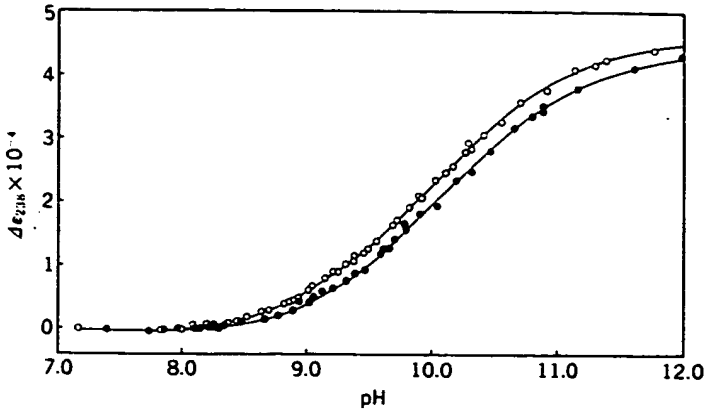

Fig. 10. pH Dependence of the value of $\Delta\varepsilon$ at 238 nm for partially reduced Nag protein (open circles) and partially reduced and alkylated Nag protein (closed circles) at 25°C and 0.2 ionic strength.

explained by the ionization of the tyrosyl residues only. On the other hand, the values of $\Delta\varepsilon_{238}$ for the protein with free thiol groups were larger than those for the alkylated protein (Fig. 10). This indicates that the ionization of both tyrosyl and thiol groups contributes to the change in the absorption at 238 nm.

We calculated the difference in the values of $\Delta\varepsilon_{238}$ by subtracting the value for the alkylated protein from that for the protein with free thiol groups at the same pH, and obtained the titration curve of the thiol groups of partially reduced Nag protein (Fig. 11). The solid line in Fig. 11 is the theoretical curve calculated by assuming that the two thiol groups have pK values of 8.50 and 9.61, that the ionization of the thiol groups is not affected by the mean net charge of the protein molecule, and that the change in the molar extinction coefficient for the ionization of one thiol group is 4,600 $M^{-1} \cdot cm^{-1}$ (*14*). The second assumption was supported by the following findings. The titration data for the thiol groups of Ta protein obtained from the alkylation reaction (Fig. 2A) were analyzed according to the Linderstrøm-Lang equation (*15*),

$$\mathrm{pH} - \log \frac{\alpha}{1-\alpha} = pK_{\mathrm{int}} - 0.868\omega\overline{Z} \qquad (5)$$

where α is the degree of ionization of the thiol groups of Ta protein determined from the pH dependence of the observed rate constant (Fig. 2A), pK_{int} is the negative logarithm of the intrinsic dissociation constant of the thiol group, and

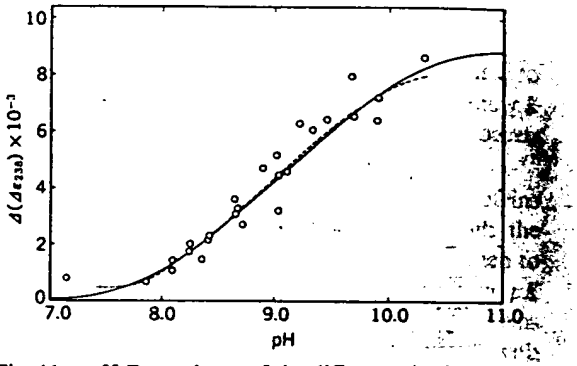

Fig. 11. pH Dependence of the difference in the values of $\Delta\varepsilon_{238}$ ($\Delta(\Delta\varepsilon_{238})$) between partially reduced Nag protein and partially reduced and alkylated Nag protein. The broken line indicates the difference in the value of $\Delta\varepsilon_{238}$ obtained by subtracting the solid line for the reduced and alkylated protein from that for the reduced protein shown in Fig. 10, and circles indicate the difference in the value of $\Delta\varepsilon_{238}$ obtained by directly comparing the $\Delta\varepsilon_{238}$ value for the reduced protein with that for the reduced and alkylated protein at the same pH. The solid line indicates the theoretical cuve (see the text).

$0.868\omega\overline{Z}$ is a term correcting for any electrostatic interaction between protons and the protein molecule of mean net charge $\overline{Z}$. The values of $\overline{Z}$ were obtained by acid-base titration by Azuma *et al.* (*16*). From a plot according to Eq. 5 (Fig. 12), it was found that the pK_{int} value is 9.76 and ω is zero. This means that the ionization of the thiol groups of Ta protein is scarcely affected by the

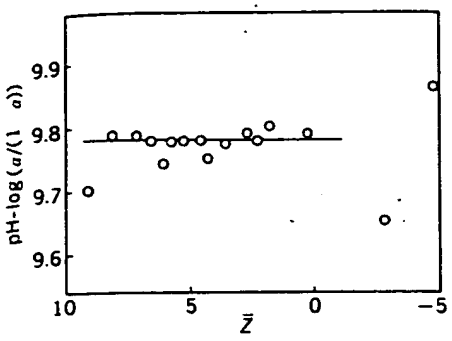

Fig. 12. Plot of the alkylation data for partially reduced Ta protein according to Eq. 5. The degrees of ionization (α) of the thiol groups were calculated from the pH dependence of the observed rate constant shown in Fig. 2A.

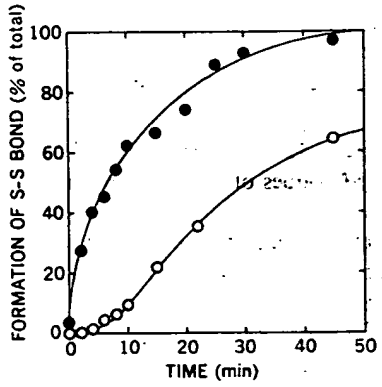

Fig. 13. Kinetics of the formation of interchain disulfide bonds from partially reduced Nag protein (open symbols) and Jo-Fab(t) (closed symbols) in the presence of 1 mM GSSG at pH 8.0, 25°C and 0.2 ionic strength. The extent of interchain disulfide bond formation was determined by SDS-polyacrylamide gel electrophoresis.

change in the mean net charge of the protein molecule.

The agreement between the experimental and theoretical values (Fig. 11) confirms the *pK* values obtained by analysis of the alkylation kinetics (Table I). The titration curve shown in Fig. 11 could not be explained by assuming a single *pK* value.

Formation of the Interchain Disulfide Bond in the Presence of GSSG—Figure 13 shows the kinetics of formation of interchain disulfide bonds from partially reduced Nag protein and Jo-Fab(t) in the presence of 1 mM GSSG at pH 8.0. The formation

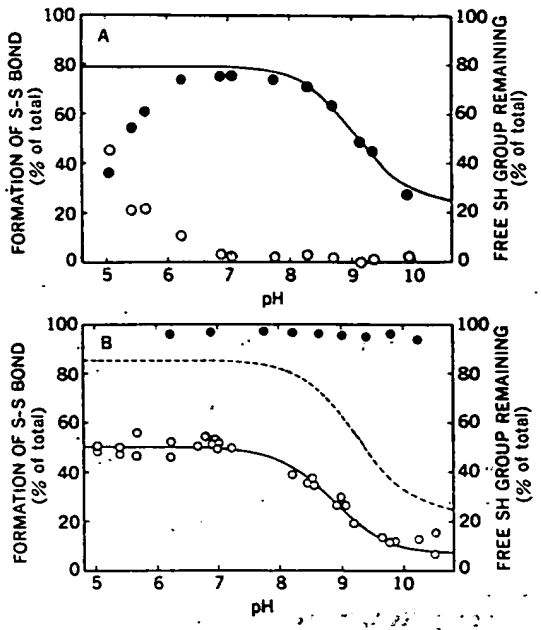

Fig. 14. Effect of pH on the formation of interchain disulfide bonds from partially reduced type λ Bence Jones proteins and Jo-Fab(t) in the presence of 1 mM GSSG at 25°C and 0.2 ionic strength. The partially reduced proteins were allowed to react with GSSG for 24 h (Nag protein and Jo-Fab(t)) or 72 h (Ni protein). After the reaction, the extent of formation of interchain disulfide bonds was determined by SDS-polyacrylamide gel electrophoresis. A: The extent of interchain disulfide bond formation (●) and remaining free thiol groups (○) for Nag protein. Free thiol groups were titrated with DTNB after exclusion of glutathione by dialysis. The solid line represents the theoretical curve for the extent of interchain disulfide bond formation as calculated using Eq. 6. B: The extent of interchain disulfide bond formation from partially reduced Ni protein (○) and Jo-Fab(t) (●). The solid and broken lines represent the theoretical curves for disulfide bond formation from partially reduced Ni protein and Jo-Fab(t), respectively, as calculated using Eq. 6 (see the text).

of the interchain disulfide bond of Jo-Fab(t) was more rapid than that of Nag protein and was complete. The formation of the interchain disulfide bond of Nag protein was not complete, and the extent of dimer formation was about 75%. A lag phase was observed in the early stage of the disulfide formation of Nag protein, but not in the case of Jo-Fab(t).

Figure 14 shows the effect of pH on the

reformation of the inter L-L disulfide bond from partially reduced Nag protein (A) and Ni protein (B). The yields of the dimers were determined after incubation with 1 mM GSSG at 25°C for 24 h for Nag protein and 72 h for Ni protein. The yield of the dimers for Nag protein was constant (75%) between pH 6.5 and 8.0 and decreased outside this pH range. Thiol groups were still titratable for Nag protein incubated for 24 h below pH 6.5. Therefore, the decrease in the yield of dimers for Nag protein below pH 6.5 can be explained in terms of the low rate of thiol-disulfide interchange reactions between thiol groups of Nag protein and GSSG and between free thiol groups and mixed disulfide on Nag protein. A decrease in the yield of dimers in the acidic pH region was not observed for Ni protein after incubation for 72 h. No change with pH in the reformation of the inter L-Fd disulfide bond from partially reduced Jo-Fab(t) was observed (Fig. 14B) and the yield was nearly 100% between pH 6 and 10.

DISCUSSION

Ionization Behavior of the Thiol Groups of Partially Reduced Bence Jones Proteins and Fab(t) —The cysteinyl residue of type κ Bence Jones proteins and human immunoglobulins, which participates in the formation of the interchain disulfide bond, occurs at the carboxyl terminus and is preceded by a glutamyl residue. Therefore, the ionization of the thiol group may be affected by the negative charges on the α- and γ-carboxyl groups, and its *pK* is expected to be higher than that of thiol groups in the absence of neighboring substituent groups carrying negative charges. Indeed, the *pK* value of the thiol groups of type κ Bence Jones proteins was found to be 9.76, which is about 1 pH unit higher than that of glycyl-L-cysteinylglycine (*17*) and is only slightly higher than that of N-acetyl-L-cysteine (Table I). As described in " RESULTS, " partially reduced Bence Jones proteins used in the present work are present as the dimeric form due to noncovalent interactions and contain two thiol groups per dimer unit. However, no differences were detected in the *pK* values and reactivities of the thiol groups of type κ Bence Jones proteins when they were examined in terms of the reactions with chloroacetamide and DTNB. This indicates that the ionizations of the two thiol groups are equivalent and independent.

The ionization behavior of the two thiol groups of type λ Bence Jones proteins is different from that for type κ proteins. The results of the reactions with chloroacetamide and DTNB and of spectrophotometric titration of the thiol groups show that the two thiol groups of type λ Bence Jones proteins have different *pK* values (8.5–8.6 and 9.5–9.7). The results of the alkylation reactions with chloroacetamide of partially reduced Nag protein at various ionic strengths suggest that the two thiol groups of type λ proteins do not interact with each other and that the *pK* values are intrinsically different. The two thiol groups of Jo-Fab(t) also have different *pK* values (8.51 and 9.76). The *pK* value of the thiol group of Ta protein (type κ) was determined to be 9.76 when it combines either with the other partially reduced L chain or with reduced and alkylated H chains. This indicates that the thiol group with a *pK* value of 8.51 corresponds to the thiol groups on Fd, that the thiol group on the L chain and that on the Fd fragment do not interact with each other and that the *pK* values of these groups are intrinsically different.

X-ray crystallographic results for a type λ Bence Jones protein (Mcg) (*18*) show that the two monomers in the Mcg dimer are asymmetric and the spatial arrangement of V_L and C_L domains in one of the monomers is not identical to that of the domains in the other. Segal *et al.* (*19*) showed that the spatial arrangement of V_H and C_H1 domains in an Fab fragment is similar to that of V_L and C_L domains of one of the monomers (monomer 1) in Mcg protein and the arrangement of V_L and C_L domains in the fragment is similar to that of V_L and C_L domains of the other monomer (monomer 2) in Mcg protein. On the basis of these X-ray crystallographic results and the finding that the *pK* values of the thiol groups of partially reduced type λ Bence Jones proteins are very similar to those for partially reduced Jo-Fab(t), we may conclude that the thiol group of monomer 1 ionizes with $pK=8.5$–8.6 and that of monomer 2 with $pK=9.5$–9.7. It is likely that the microenvironments around the two thiol groups are different due to different spatial arrangements of the monomers and thus affect their ionization behavior differently.

As described above, the ionization behavior of the two thiol groups of partially reduced type κ

Bence Jones proteins was different from that for type λ proteins and Jo-Fab(t), as examined in terms of the reaction with chloroacetamide. This suggests that the environments around the thiol groups of type κ proteins differ from those of type λ proteins or Fab(t). No information is available on the three-dimensional structure of type κ Bence Jones proteins.

Reactivities of the Thiol Groups—Lindley (*17*) studied the alkylation reactions of several simple thiol compounds such as glycyl-L-cysteinylglycine, glycyl-L-cysteine, and cysteinyl-L-asparagine and found that the true rate constants ($\overline{k}$) for these compounds are in the range of 0.26 to 0.32 $M^{-1} \cdot s^{-1}$ at 0.1 ionic strength and at 30°C. The value of $\overline{k}$ for N-acetyl-L-cysteine determined in the present study was 0.133 $M^{-1} \cdot s^{-1}$ at 0.2 ionic strength and at 25°C. The thiol groups of type κ Bence Jones proteins have a $\overline{k}$ value of 0.188 $M^{-1} \cdot s^{-1}$ at 0.2 ionic strength and at 25°C and are as reactive as those of these simple compounds.

The two thiol groups of type λ Bence Jones proteins have different reactivities toward chloroacetamide. The values of $\overline{k_2}$ were in the range of 0.18 to 0.25 $M^{-1} \cdot s^{-1}$ at 0.2 ionic strength and at 25°C, which are of the same order of magnitude as those obtained for simple thiol compounds and type κ Bence Jones proteins. On the other hand, the values of $\overline{k_1}$ were small (0.02–0.05 $M^{-1} \cdot s^{-1}$) and varied from specimen to specimen with no significant change of the pK_1 value.[2] The variation of the rate constant depending on the specimen was more apparent in the reaction with DTNB. As shown in Fig. 7, the pK values obtained from the slopes of the k_{obs} *vs.* k_{obs} (H^+) plots were all the same, but the rate constants obtained from the intercepts on the ordinate were different depending on the specimen. The reaction of thiol groups with chloroacetamide proceeds by nucleophilic attack of the thiolate anion on the α-carbon atom of the reagent. In this type of reaction, the ionization constant of the thiol group is a measure of the nucleophilicity, and the thiol group with a higher pK value may react with a higher rate constant (*21*). Thus, it may not be surprising that the reactivities of the thiol groups with pK_1 are lower than those of the thiol groups with pK_2. However, the finding that the values of $\overline{k_1}$ change depending on the specimen with no significant change in pK_1 cannot be explained only by the correlation between pK and reactivity. Steric hindrance must play an important role in the reactivity of thiol groups toward chloroacetamide or DTNB, but not toward protons. In the case of Jo-Fab(t), $\overline{k_1}$ was smaller than $\overline{k_2}$, and the thiol groups of Jo-Fab(t) are similar to those of type λ Bence Jones proteins not only in pK values but also in reactivity toward chloroacetamide.

Formation of the Interchain Disulfide Bond—Kishida *et al.* (*5*) proposed the following scheme to explain the kinetic pattern of interchain disulfide bond formation from partially reduced Bence Jones proteins in the presence of GSSG. In this

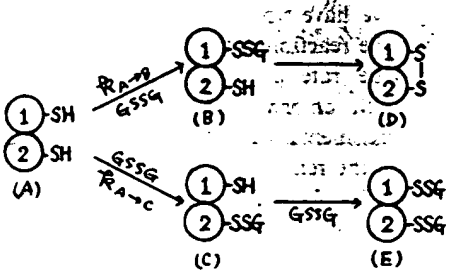

scheme, they assumed that the dimer of a Bence Jones protein consists of two distinct monomers which are designated as monomer 1 and monomer 2, that the reactivities of the two thiol groups in partially reduced Bence Jones protein (A) are different from each other and that two kinds of intermediate, B, in which the SH group on monomer 1 is blocked with GSSG, and C, in which the SH group on monomer 2 is blocked with GSSG, are formed during the reaction. They also assumed that only intermediate B can form a dimer with an inter-monomer disulfide bond (D), while intermediate C cannot. Our present study verified the assumption that the reactivities of the two thiol groups of partially reduced type λ Bence Jones proteins and Jo-Fab(t) are different from each other, and showed that the ionization and reactivity with chloroacetamide differ between the SH

[2] The observed rate constant is expressed as the sum of the observed rate constants for SH_1 and SH_2, $k_{obs} = k_{1,obs} + k_{2,obs}$. The reaction determined experimentally apparently followed first-order kinetics (Fig. 1B). This means that $k_{1,obs}$, which is the product of $\overline{k_1}$ and the ionization degree of SH_1, and $k_{2,obs}$, which is the product of $\overline{k_2}$ and the ionization degree of SH_2, are not different by more than several-fold (*20*).

on monomer 1 and the SH on monomer 2 in type λ Bence Jones proteins and between the SH on L chain and the SH on Fd in Jo-Fab(t).

In the thiol-disulfide interchange reaction, the thiolate anion attacks a sulfur atom of the disulfide bond as a nucleophile. It is, therefore, analogous to the alkylation of a thiol group with chloroacetamide. Thus, the observed rate in each process in the above scheme depends not only on the nucleophilicity but also on the degree of ionization of the thiol groups in the various species. According to the above scheme, the relative amount of the final products, D and E, is determined by the relative rates of the processes, A→B and A→C, because the reaction is of competitive type. The ratio of the amounts of the final products, (D)/(E), can thus be determined by the ratio, $k_{A\to B}/k_{A\to C}$, where $k_{A\to B}$ and $k_{A\to C}$ are the observed rate constants of the reactions A→B and A→C.

The observed rate constant is the product of the degree of ionization and the true rate constant. Although we have no data on the true rate constants for the reaction with GSSG, we can instead use the true rate constants for the alkylation reaction with chloroacetamide obtained in the present experiments, because our primary interest is to obtain the relative amount of the final products, D and E. Thus the ratio (D)/(E) of the final products may be expressed as

$$\frac{(D)}{(E)} = \frac{k_{A\to B}}{k_{A\to C}} = \frac{\alpha_1\overline{k_1}}{\alpha_2\overline{k_2}} \qquad (6)$$

where α_1 and α_2 are the degrees of ionization at a given pH of the thiol group on monomer 1 and that for monomer 2, respectively, in species A.

Using Eq. 6 and the values of pK_1, pK_2, $\overline{k_1}$, and $\overline{k_2}$ shown in Table I, we can estimate the extent of formation of interchain disulfide bonds from partially reduced type λ Bence Jones proteins at pH 8.0. The results are shown in Table II. The calculations fit the experimental data satisfactorily. This indicates that the variation in the yield of the disulfide-bonded dimer for type λ Bence Jones proteins among different specimens and with a change in ionic strength can be explained in terms of the variation of both pK values and the true rate constants of the two thiol groups. We can also estimate the yield of the disulfide-bonded dimer at various pH value using Eq. 6. The theoretical curve for Nag protein and Ni protein (Figs. 14 A and B) are in good agreement with the experimental data. These facts indicate that the formation of interchain disulfide bonds from partially reduced type λ Bence Jones protein in the presence of GSSG proceeds according to the scheme proposed by Kishida *et al.* (5) and that the ratio of the yield of D formed through route A→B→D to that of E formed through route A→C→E is determined by the different pK values and reactivities of the thiol group on monomer 1 and that on monomer 2.

TABLE II. The extent of interchain disulfide bond formation from partially reduced type λ Bence Jones proteins and Jo-Fab(t) in the presence of 1 mM GSSG at pH 8.0 and 25°C. The calculated values were obtained using Eq. 6 (see the text).

Proteins	Ionic strength	S-S bond formation (%)	
		Obsd.	Calcd.
Fu	0.20	83	67
Ni	0.20	45	44
Nag	0.05	45	44
Nag	0.20	72	76
Nag	0.50	70	69
Jo-Fab(t)	0.20	97	82

As shown in Fig. 14B, the yields of disulfide-bonded-Fab(t) from partially reduced Jo-Fab(t) were independent of pH and were nearly 100%. This implies that the product corresponding to E is not formed and the intermediates, B and C, both give the product D at any pH value. The theoretical curve constructed using Eq. 6 is different from the experimental data. Since the pK values and the true rate constants of the thiol groups of Jo-Fab(t) are similar to those for type λ Bence Jones proteins, the two intermediates, B and C, should also be formed from partially reduced Jo-Fab(t) with rates and ratios similar to those for Nag protein. However, as shown in Fig. 13, the formation of the disulfide bond for Jo-Fab(t) proceeds more rapidly than for Nag protein, without a lag phase. This indicates that the rate of intramolecular thiol-disulfide interchange is greater for Fab(t) than for Nag protein and the processes leading to the formation of the inter-

mediates represent rate-limiting steps in the reaction of Fab(t).

In general, the rate of the intramolecular thiol-disulfide interchange reaction is much faster than that of intermolecular reaction owing to the proximity effect (*22*). However, as reported by Kishida *et al.* (*5*), the first-order rate constant of the intramolecular process (B→D) for Nag protein is of an order of magnitude similar to the pseudo first-order rate constants of the intermolecular processes in the presence of 1 mM GSSG. The slow rate of the intramolecular thiol-disulfide interchange reaction may be one of the reasons for the production of two kinds of final products, D and E, from partially reduced type λ Bence Jones proteins in the presence of GSSG. We cannot explain why the rate of the intramolecular reaction is slow for type λ Bence Jones proteins. However, it is likely that the distance between the two thiol groups is not suitable for effective formation of the disulfide bond. The steric factors around the thiol groups may also explain the different behavior in the formation of interchain disulfide bonds of type λ Bence Jones proteins and Fab(t).

As reported by Kishida *et al.* (*5*), no interchain disulfide bond is formed from partially reduced type κ Bence Jones proteins in the presence of GSSG. Our present work shows that the two thiol groups of type κ Bence Jones proteins have the same *pK* values and reactivities toward chloroacetamide. Judging from their high *pK* values, the rate of thiol-disulfide interchange reaction at neutral pH is expected to be slow, but complete absence of formation of interchain disulfide bonds from partially reduced type κ proteins at any pH cannot be explained in terms of their high *pK* values and reactivities. The distance between the two thiol groups may be so great that no disulfide bond is formed.

We thank Dr. T. Isobe, Kobe University School of Medicine, for generous supplies of the serum of patient Jo, and Prof. S. Migita, Kanazawa University, Prof. Y. Sameshima, Kansai Medical School, and Dr. E. Inada, Osaka Police Hospital, for supplies of Bence Jones proteins.

REFERENCES

1. Milstein, C. (1965) *Nature* **205**, 1171–1173
2. Titani, K., Shinoda, T., & Putnam, F.W. (1969) *J. Biol. Chem.* **244**, 3550–3560
3. Kishida, F., Azuma, T., & Hamaguchi, K. (1975) *J. Biochem.* **77**, 481–491
4. Della Corte, E. & Parkhouse, R.M.E. (1973) *Biochem. J.* **136**, 597–606
5. Kishida, F., Azuma, T., & Hamaguchi, K. (1976) *J. Biochem.* **79**, 91–105
6. Azuma, T., Isobe, T., & Hamaguchi, K. (1975) *J. Biochem.* **77**, 473–479
7. Azuma, T. & Hamaguchi, K. (1976) *J. Biochem.* **80**, 1023–1038
8. Ellman, G.L. (1959) *Arch. Biochem. Biophys.* **82**, 70–77
9. Weber, K. & Osborn, M. (1969) *J. Biol. Chem.* **244**, 4406–4412
10. Green, R.W. (1973) *Biochemistry* **12**, 3225–3231
11. Azuma, T., Hamaguchi, K., & Migita, S. (1974) *J. Biochem.* **76**, 685–693
12. Schwabe, K. (1967) *Electrochim. Acta* **12**, 67–93
13. Edsall, J.T. & Wyman, J. (1958) *Biophysical Chemistry* pp. 241–322, Academic Press, New York
14. Donovan, J.W. (1973) in *Methods in Enzymology* (Hirs, C.H. & Timasheff, S.N., eds.) Vol. 27, pp. 525–548, Academic Press, New York
15. Tanford, C. (1972) *Advances in Protein Chemistry* (1962) **17**, 69–165
16. Azuma, T., Hirai, T., Hamaguchi, K., & Migita, S. (1970) *J. Biochem.* **67**, 801–808
17. Lindley, H.L. (1962) *Biochem. J.* **82**, 418–425
18. Schiffer, M., Girling, R.L., Ely, K.R., & Edmundson, A.B. (1973) *Biochemistry* **12**, 4620–4630
19. Segal, D.M., Padlan, E.A., Cohen, G.H., Rudikoff, S., Potter, M., & Davies, D.R. (1974) *Proc. Natl. Acad. Sci. U.S.* **71**, 4298–4302
20. Gutfreund, H. (1972) *Enzymes: Physical Principles* pp. 125–127, John Wiley & Sons Ltd., London and New York
21. Ogilvie, J.W., Tildon, J.T., & Strauch, B.S. (1964) *Biochemistry* **3**, 754–758
22. Jencks, W.P. (1969) *Catalysis in Chemistry and Enzymology* pp. 7–41, McGraw-Hill, Inc., New York

Vol. 83, No. 4, 1978 BIOCHEMICAL AND BIOPHYSICAL RESEARCH COMMUNICATIONS
August 29, 1978 Pages 1284-1290

REDUCED IMMUNOGLOBULIN G ACTIVATES COMPLEMENT SYSTEM WITH DECREASED COOPERATIVITY

J. Keith Wright, Department of Biophysical Chemistry, Biozentrum der Universität Basel, CH-4056 Basel, Switzerland

Received May 22,1978

Summary: Sheep erythrocytes sensitized with intact antibody or reduced and alkylated antibody were lysed by guinea-pig serum indicating that reduced and alkylated antibody bound and activated complement. Reduction of antibody caused erythrocyte lysis to exhibit pseudo-first-order kinetics, while the lysis kinetics of erythrocytes sensitized with intact antibody was sigmoidal. Analysis of erythrocyte lysis by complement according to the von Krogh equation showed that reduction of antibody diminished the von Krogh exponent n from 2.8 to 1.3, while the value of K remained unchanged at 0.17 (complement dilution). These observations suggested that the sole effect of the reduction of antibody inter-heavy-chain and heavy-light chain disulfide bonds was to diminish the cooperativity of antibody-complement interaction.

INTRODUCTION

The role played by the inter-heavy-chain disulfide bond of antibody in the binding and activation of complement figures prominently in two aspects of immunoglobin structure. (i) The disulfide bridge may be required to facilitate the transmission of a conformational change from the antigen binding sites to a distant location where the first complement component C1 would thereafter be bound and activated. (ii) The disulfide bridge may participate in or maintain the structure of a binding site for this complement component.

The various reports of the effect of the reduction of the inter-heavy-chain disulfide bridges in immunoglobulin G and its proteolytic fragments have been contradictory (1-6). The present

0006-291X/78/0834-1284$01.00/0

consensus would appear to favor the interpretation that in the intact immunoglobulin the integrity of said disulfide bonds was indispensable in the antibody-complement interaction. However, recent studies demonstrated that antigen did not function as an allosteric effector in evoking antigen-mediated responses. The structure of the hinge peptide was unaffected by antigen binding (7), and ligands binding exclusively in the F_{ab} or F_c regions were bound independently of one another (8), underscoring the absence of specific interactions between these regions. The function of antigen may merely be the organization of antibody into a multivalent array (cf. 9-10). Since the role of inter-heavy-chain disulfide bridges in such an aggregative model was not obvious, the effect of the reduction of antibody on complement fixation in the classical fixation assay was re-examined.

MATERIALS AND METHODS

The immunoglobulin G fraction of rabbit anti-sheep red blood cell antiserum (BBL) was purified by ammonium sulfate precipitation and chromatography on DEAE Sephadex and Sepharose 6B-CL. A portion of the antibody was reduced: Antibody in 10 mM tris (hydroxymethyl) aminomethane buffer pH 7.4 containing 0.15 M NaCl was reduced for 2 h at 30° in the presence of 10 mM dithioerythritol. The reduction was halted by the addition of iodoacetamide to a final concentration of 20 mM. The solution was dialyzed overnight. The reduction was repeated a second time to eliminate traces of unreduced antibody. As a control, intact antibody was also treated with iodoacetamide. Preparations of intact and reduced and alkylated antibody were examined by gel electrophoresis (11) and in the ultracentrifuge. Complement fixation was measured by a slight modification of the classical technique (12). Sheep erythrocytes (bioMérieux) were sensitized by addition of antibody to suspensions of erythrocytes followed by incubation for 20 min. at 30° with shaking. The final concentrations of erythrocytes and antibody were 5×10^8 cells/ml and 0.5 µM respectively. Complement fixation tests were conducted as follows, 1 ml suspensions of sensitized erythrocytes (10^7 cells/ml) in stoppered plastic tubes were shaken in a water bath at 25°. At appropriate times 0.50 ml of diluted guinea-pig serum kept in ice was added. At the end of the incubation period, all tubes were rapidly cooled in ice and centrifuged. The absorbance of the superna-

tant was read at 413 nm. When the dependence of lysis on complement concentration was studied, aliquots of sensitized erythrocytes were added to complement dilutions held in ice. The samples were then immediately transferred to the 25° water bath. Controls for complement absorbance and spontaneous erythrocyte lysis were included. Erythrocytes treated with nonimmune rabbit serum were employed as controls. Guinea-pig complement (BBL) was always absorbed with packed, unsensitized erythrocytes before use. All dilutions of guinea-pig serum cited refer to the final dilution in the test solution.

RESULTS

Electrophoretic analysis of reduced and alkylated antibody disclosed that the two reductions necessary to eliminate all traces of intact immunoglobulin had led to the reduction of both inter-heavy-chain and heavy-light-chain disulfide bridges. Ultracentrifugal analysis confirmed that the antibody remained undissociated under experimental conditions ($s_{20,w} = 6.6 \times 10^{-13}$ s at 20° and 0.3 μM antibody).

Sheep erythrocytes sensitized with reduced and alkylated antibody were lysed by guinea-pig complement but with altered kinetics (Fig. 1). The time course for erythrocytes sensitized with reduced and alkylated antibody followed a simple pseudo-first-order rate law as evidenced by the linear semilogarithmic plot of intact erythrocytes remaining *vs.* time (Fig. 1).

The dependence of the degree of lysis (y) on the dilution of complement (c) has been traditionally analyzed by the von Krogh equation (cf. 13):

$$\log \frac{y}{1-y} = n \log c + n \log K$$

where *y* is the degree of lysis at a dilution *c* of complement. The constants *n* and *K* are discussed below.

Erythrocytes sensitized with intact or reduced and alkylated

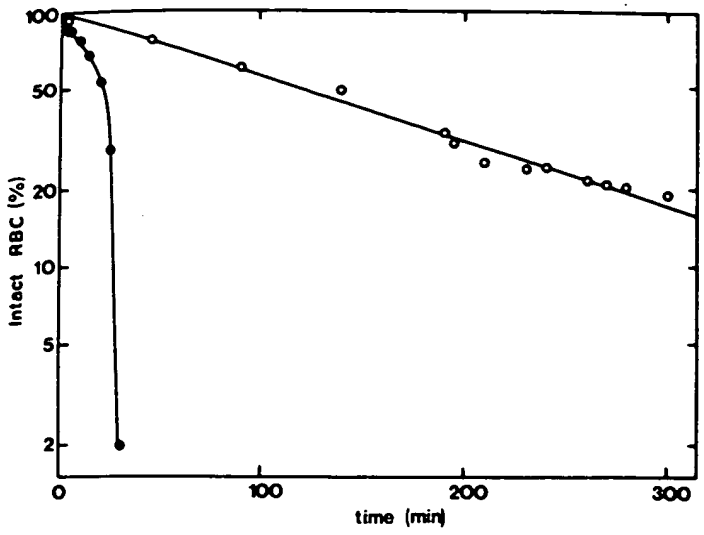

Fig. 1: Effect of antibody disulfide bond reduction on erythrocyte lysis kinetics. Sheep erythrocytes were sensitized with intact or reduced and alkylated antibody. Erythrocytes (6.6×10^6 cells/ml) were treated with guinea-pig complement (1/60 dilution) for the indicated times at 25°. The lysis of erythrocytes sensitized with reduced and alkylated antibody (○) followed pseudo-first-order kinetics, while the lysis of erythrocytes sensitized with intact antibody (●) was sigmoidal.

antibody were lysed with different dependences on complement dilution (Fig. 2). The values of n corresponding to the slope of the logarithmic plot were 2.8 for intact antibody and 1.3 for reduced and alkylated antibody. Contrastingly, the values for K were identical in both instances and corresponded to a 17% final dilution of complement.

DISCUSSION

The experimental observations presented here can be summarized in two points: (i) reduced and alkylated immunoglobulin G bound and activated complement and (ii) the interaction of reduced and alkylated antibody with complement was slightly or not at all cooperative (see below). The implication of the

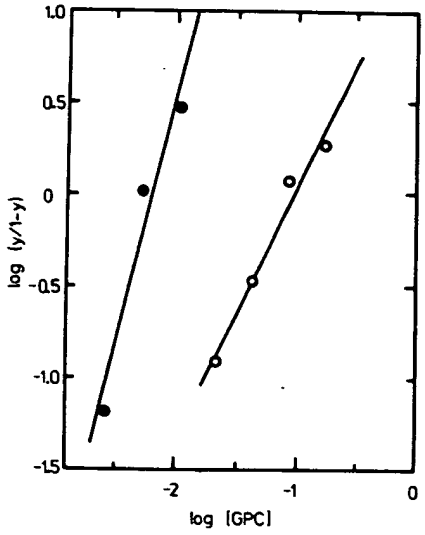

Fig. 2: Effect of antibody disulfide bond reduction on the dependence of lysis on complement concentration. Sensitized erythrocytes (6.6×10^6 cells/ml) were incubated with various dilutions of complement for 60 min. at 25°. Lysis data were analyzed according to the von Krogh plot (see text): $\log(y/1 - y)$ vs. log (GPC), where y is the fraction of cells lysed by the given dilution of guinea-pig-complement (GPC) (log (GPC) = 0 corresponds to undiluted serum. The values of n in the von Krogh equation obtained from least-squares fits to the data were 2.8 for intact antibody (●) and 1.3 for reduced and alkylated antibody (○). The values of K obtained from the intercepts were identical corresponding to a 17% final dilution of guinea-pig complement.

first conclusion is that the inter-heavy-chain disulfide bonds served no essential function in complement (i.e. C1, the first complement component) binding or activation.

The von Krogh equation in the form

$$\frac{y}{1-y} = \left(\frac{c}{K}\right)^n$$

resembles a Hill equation (14, 15). Here n is a kinetic Hill coefficient describing the cooperativity of the system and K is a binding constant under steady-state conditions (cf. the

Michaelis constant, K_m). The effect of reduction of antibody disulfide bonds was to diminish the value of n from 2.8 to 1.3 under the described conditions. The loss of cooperativity in the interaction between antibody and complement was reflected in the value of n near unity (Fig. 2) and the simplification of the lysis kinetics (Fig. 1). The entire effect of disulfide bond reduction resided in this diminished cooperativity, since the value of K was unaltered by reduction (Fig. 2). This observation suggested that the fundamental binding interaction between antibody and C1 remained unaltered. The reduction had a profound effect on the lysis kinetics. This kinetic aspect must be considered in the evaluation of all hemolytic tests, where the apparent cooperativity of the antibody-complement interaction may be changed.

ACKNOWLEDGEMENTS

The excellent technical assistance of Ms. Erna Steffen and the assistance of Mr. Ariel Lustig for ultracentrifugal analysis are gratefully acknowledged.

REFERENCES

1. Schur, P.H. and Christian, G.D. (1964) J. Exp. Med. 120, 531-545.
2. Kehoe, J.M. and Fougereau, M. (1969) Nature 224, 1212-1213.
3. Allan, R. and Isliker, H. (1974) Immunochem. 11 243-248.
4. Press, E.M. (1975) Biochem. J. 149, 285-288.
5. Isenman, D.E., Dorrington, K.J. and Painter, R.H. (1975) J. Immunol. 114, 1726-1729.
6. Lopez de Castro, J.A., Vivanco, F., and Ortiz, F. (1977) Biochem. Biophys. Res. Comm. 78, 1319-1326.
7. Wright, J.K., Jaton, J.-C., and Engel, J. (1978) Eur. J. Immunol., in Press.
8. Wright, J.K., Brandt, D., Jaton, J.-C., and Engel, J. (1978) FEBS Lett., in Press.
9. Metzger, H. (1974) Adv. Immunol. 18, 169-207.

10. Metzger, H. (1978) Adv. Immunol., in Press.

11. Laemmli, U.K. (1970) Nature 227, 680-685.

12. Levine, L., and van Vunakis, H. (1967) Meth. Enz. 9, 928-936.

13. Kabat, E.A., and Mayer, M.M. (1971) in "Experimental Immunochemistry" Charles C. Thomas, Springfield, pp. 135-145.

14. Laidler, K.J., and Bunting, P.S. (1973) in "The Chemical Kinetics of Enzyme Action" Clarendon Press, Oxford, pp. 352-381.

15. Segel, I.H. (1975) in "Enzyme Kinetics" John Wiley and Sons, New York, pp. 360-375.

Brief Definitive Report

Engineered Humanized Dimeric Forms of IgG Are More Effective Antibodies

By Philip C. Caron,* Walter Laird,‡ Man Sung Co,‡ Nevenka M. Avdalovic,‡ Cary Queen,‡ and David A. Scheinberg*

*From the *Department of Medicine, Memorial Sloan-Kettering Cancer Center, New York, New York 10021; and ‡Protein Design Labs, Mountain View, California 94043*

Summary

Humanized IgG1 M195 (HuG1-M195), a complementarity determining region-grafted recombinant monoclonal antibody, is reactive with CD33, an antigen expressed on myelogenous leukemia cells. M195 is in use in trials for the therapy of acute myelogenous leukemia. Since biological activity of IgG may depend, in part, on multimeric Fab and Fc clustering, homodimeric forms of HuG1-M195 were constructed by introducing a mutation in the γ1 chain CH3 region gene to change a serine to a cysteine, allowing interchain disulfide bond formation at the COOH terminal of the IgG. Despite similar avidity, the homodimeric IgG showed a dramatic improvement in the ability to internalize and retain radioisotope in target leukemia cells. Moreover, homodimers were 100-fold more potent at complement-mediated leukemia cell killing and antibody-dependent cellular cytotoxicity using human effectors. Therefore, genetically engineered multimeric constructs of IgG may have advantages relative to those forms that are found naturally.

CDR-grafted humanized mAbs have been constructed to improve immunological effector functions and reduce immunogenicity (1–5). The production of a CDR-grafted, humanized IgG1 construct (HuG1-M195) of the mouse M195 antibody, an anti-CD33 mAb that is specifically reactive with acute myelogenous leukemia (AML) cells and early myeloid progenitors, but not hematopoietic stem cells, has been described (6–9). M195 is currently being evaluated in the therapy of AML (10, 11). HuG1-M195 retains specificity of binding, the capability of internalization into HL60 leukemia cells, and the ability to fix human complement (7). In addition, HuG1-M195 shows superiority over its murine counterpart in its higher avidity and new ability to perform antibody-dependent cellular cytotoxicity (ADCC) with human effector cells against acute myelogenous leukemia cells (7).

The biological activities of IgG depend, in part, on the ability to crosslink antigen on the cell surface and to bind complement or Fc receptors on effector cells via multivalent interactions. Recently, the genetic engineering of a chimeric IgG reactive with a hapten to form a mutant Ig linked together as a covalent dimer, resulted in enhanced complement mediated cytotoxicity (CMC) (12). In an attempt to improve the CMC as well as other biological and immunological properties of the humanized M195 mAb, similar homodimers (Hd-IgG) were genetically designed. A mutation at the COOH end of the CH3 domain of the γ1 H chain was introduced in HuG1-M195 that results in enhanced CMC, and also a dramatic improvement in the ability to perform ADCC against leukemic target cells. In addition, the Hd-IgG shows more rapid modulation with markedly improved retention of targeted radioisotope within the target cells. These Hd-IgG may have therapeutic applications.

Materials and Methods

Construction of Homodimeric IgG (Hd-IgG). The construction of vectors to express humanized M195 L and H chains has been described (6). For expression of Hd-IgG, the H chain expression vector was mutagenized by changing the codon TCT to TGT which resulted in converting amino acid at position 444 of H chain from Ser to Cys (Fig. 1 *A*). The cys allows interchain disulfide bond formation which allows expression of Hd-IgG (Fig. 1 *B*). To allow formation of Hd-IgG, 87 mg of mAb was purified from culture supernatant and concentrated to 10 mg/ml in 0.1 M Tris, pH 8.6. 4 mg of Ellman's reagent (Pierce Chemical Co., Rockford, IL) was added and incubated at room temperature for 1 h to crosslink and then block the excess sulfhydryl sites. The sample was adjusted to 2.5 M NaCl and loaded onto a 50-ml phenyl-Sepharose column equilibrated with 2.5 M NaCl. Monomer antibody was eluted off the column in PBS. Crosslinked material (Hd-IgG) were eluted in 50% propylene glycol in water. SDS-PAGE analysis showed the dimers to be 90% pure.

Cell Surface Modulation. 5×10^6 HL60 cells were incubated at 37°C with 2 μg/ml of HuG1-M195 or Hd-IgG, and aliquots were taken at 0, 60, 150, and 300 min. The cells were washed twice in RPMI and pelleted at 500 *g*, and 50 μl of goat anti-human fluorescein conjugate was added for 30 min, followed by washing twice,

J. Exp. Med. © The Rockefeller University Press • 0022-1007/92/10/1191/05 $2.00
Volume 176 October 1992 1191–1195

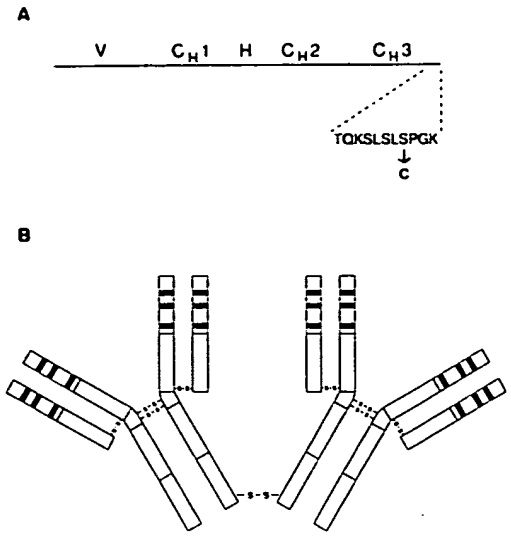

Figure 1. (*A*) Sequence at the site of the mutation of the constant region of the plasmid allowing interchain disulfide bond formation. (*B*) Diagram of homodimeric-HuG1-M195 (Hd-IgG).

and fixing in 0.5% paraformaldehyde before analysis. Ten thousand cells were analyzed on an Epics profile flow cytometer (Coulter Electronics Inc., Hialeah, FL), and the mean fluorescent intensity was measured. Hematopoietic cell lines were grown in RPMI 1640/5% newborn calf serum/10% serum-plus (Hazleton Biologics, Inc., Lenexa, KS).

Internalization Studies. HuG1-M195 or Hd-IgG were labeled with Na-^{125}I (New England Nuclear, Boston, MA) as described previously (8). Internalization of the HuG1-M195 or Hd-IgG was measured from 0 to 48 h by incubating 0.01–2 μg/ml of radiolabeled mAb with 1–2 $\times$ 10^6 HL60 cells/ml in RPMI 1640/2% human Ab serum. Cells were then washed twice in RPMI, and the surface-bound M195 was stripped with 1 ml of 50 mM glycine/150 mM NaCl, pH 2.8 at 24°C for 10 min. The amount (ng) of mAb per million cells remaining after the acid wash (i.e., internalized), or in the supernatant (i.e., cell surface) is shown.

CMC. For CMC assays, 25 μl of 5 $\times$ 10^6 HL60 cells/ml were incubated with 25 μl of diluted rabbit complement and 25 μl of serial dilutions of HuG1-M195 or Hd-IgG at 37°C for 1 h. mAb M31 (IgM anti-CD15) was used as a positive control. Live and dead cells were enumerated using trypan blue. Low toxicity rabbit serum was purchased from Pel-Freeze (Rogers, AR). Complement was used at the maximum concentrations not showing nonspecific lysis of the target cells, usually from 1:6 to 1:9 final dilution.

ADCC. Chromium release assays were conducted using PBMC from human volunteers as effector cells and HL60 cells as positive targets. Target cells were incubated in ^{51}Cr for 90 min and then washed of free ^{51}Cr. HuG1-M195 or Hd-IgG was added at E/T ratios of 10:1, 25:1, and 100:1. Cells were incubated at 37°C for 5 h and harvested using a cell harvester (Skatron, Inc., Sterling, VA), and released ^{51}Cr was counted in a gamma counter (Packard Instrument Co., Downers Grove, IL). Detergent-lysed cells were used as a 100% control. Effector cell only and mAb only treated target cells were used as negative controls. Samples were done in quadruplicate, and SD were always <10% of the mean value. Specific lysis = A – C/B – C; where: A = cpm release in the presence of mAb; B = total cpm released by detergent lysed cells; and C = cpm released in the presence of medium alone.

Results and Discussion

The ability of Hd-IgG to bind to CD33 expressing HL60 cells was determined by radiobinding assays in the presence of excess HL60 cells, as described previously (8). Total immunoreactivity (the fraction of the total radiolabeled Ig capable of binding to antigen) of Hd-IgG nearly doubled to 85% as compared with 50% for the HuG1 in these assays. The increased immunoreactivity may relate to the presence of multiple binding sites that were less likely to be inactivated by radiolabeling. Direct radioimmunoassay showed that binding of both constructs to HL60 cells was saturable and specific. Scatchard analysis of HuG1-M195 showed a slightly lower avidity of binding (K_a = 4.4 $\times$ 10^9 M^{-1}) than that of Hd-IgG (K_a = 6.1 $\times$ 10^9 M^{-1}).

Since direct radiobinding can be affected by damage to the mAb generated during the radioiodination of the Ig, the relative avidities of the HuG1-M195 and Hd-IgG were also compared by competition assays on HL60 cells in the presence of human serum to prevent nonspecific and human Fc receptor binding, as described previously (7). These experiments confirmed the Scatchard analysis that the binding avidities of Hd-IgG and HuG1-M195 were similar.

Cell surface modulation with subsequent internalization of M195 antibody and conjugated isotope has been seen in vitro and in vivo in patients, and is an important aspect of its therapeutic effect in humans for the treatment of AML (10, 11). Although Hd-IgG bound to the cell surface with

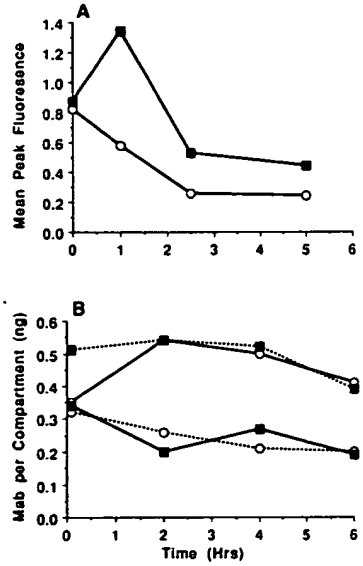

Figure 2. (*A*) Indirect flow cytometric analysis comparing cell surface modulation of HuG1-M195 (■—■) vs Hd-IgG (O—O) over 5 h. (*B*) Internalization and retention of HuG1-M195 in radiobinding experiments on HL60 cells at 37°C over 6 h. Cell surface HuG1 (■---■); cell surface Hd-IgG (O---O); internalized HuG1 (■—■); internalized Hd-IgG (O—O). Radiolabeled mAb at a final concentration of 2 μg/ml was incubated at 37°C with 10^6 HL60 cells/ml in a total volume of 200 μl. Internalization was measured as described in the text. Each time point was done in duplicate, and these results are representative of three independent experiments.

similar avidity as HuG1-M195, we speculated that the oligomerization of the mAb might alter its ability to modulate. The kinetics of modulation were examined by indirect fluorescence flow cytometry on HL60 cells. HuG1-M195 accumulated on the surface of HL60 cells to reach a peak at 1 h, and then slowly modulated (Fig. 2 *A*). By 5 h, 40% of HuG1 remained on the cell surface. In contrast, Hd-IgG was immediately modulated from the cell surface without accumulation first, with 12% of the mAb remaining on the cell surface at 5 h. Thus, Hd-IgG modulated much faster and to a greater degree than HuG1-M195, apparently without requiring the threshold of binding shown by the HuG1-M195.

The fates of the rapidly modulated Hd-IgG and HuG1-M195 were evaluated in the same time period, and internalization was measured by acid washing the cells at various times after ^{125}I-mAb binding to remove residual cell surface mAb (Fig. 2 *B*). Studies done at 0°C showed that neither HuG1-M195 nor Hd-IgG entered the cell. At 37°C, the Hd-IgG at 2 μg/ml rapidly entered the intracellular compartment, with 70% of the radiolabeled mAb being retained inside the cell, and 30% staying on the surface. In contrast, only 30–40% of the HuG1-M195 was retained inside the cell over the same time period with the remainder on the surface.

An extended analysis of internalization out to 48 h showed persistence of the Hd-IgG within cells (Fig. 3). In contrast, HuG1 demonstrated the same pattern of limited internalization as seen in Fig. 2 (not shown). Thus, the rapid modulation resulted in efficient internalization of the radiolabeled Hd-IgG into the cell, and, most importantly, the Hd-IgG was not lost from the cell over long time periods.

Based on integration (areas under the curves) of these internalization data, radiation doses delivered by Hd-IgG to the inside of the cells was more than double that of HuG1 by 48 h. Therefore, presumably in vivo, total radiation doses to target cells would be twice as high for the same added dose and same toxicity. The differences in internalization kinetics may be attributed to the immediate clustering of CD33 achieved by the multivalent Hd-IgG. Such clustering may require time to accumulate with Hug1-M195, thus accounting for the threshold effect, the delay in internalization, and the poor efficiency.

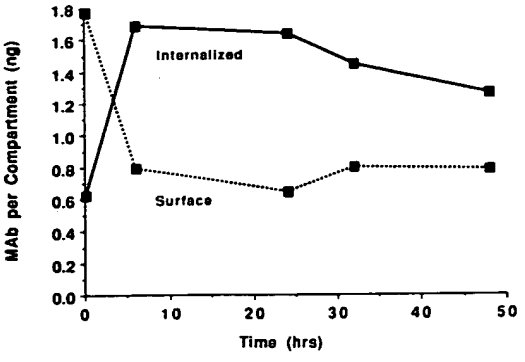

Figure 3. The amounts of radiolabeled Hd-IgG remaining on the surface (■---■) and internalized (■—■) over 48 h. Radiolabeled Hd-IgG at 1 μg/ml was incubated at 37°C with 2 × 10^6 HL60 cells/ml in a final volume of 200 μl, and internalization was measured as described in the text. Each time point was done in triplicate and SD was <10%.

Table 1. *Percent Internalization of HuG1 and Hd-IgG*

mAb Concentration	Percent internalization*	
	HuG1	Hd-IgG
nM		
6.70	43	67
2.23	40	70
0.74	39	64
0.25	41	58
0.08	38	45

* Radiolabeled mAb at concentrations shown were incubated with 2 × 10^6 HL60 cells at 37°C for 4 h in a total volume of 200 μl. Internalization was measured as described in the text. Each time point was done in triplicate and SD was <10% of the mean.

To determine whether mAb concentration affected internalization, HuG1 and Hd-IgG at similar molar concentrations were incubated with HL60 cells for 4 h at 37°C. Hd-IgG showed greater internalization than HuG1 at every concentration (Table 1). Whereas the total amount of bound radioactivity varied with the concentration of mAb added (not shown), the percentage of internalization of mAb did not change over the 2-log range of mAb concentrations. Thus, except possibly at very low concentrations, the percentage of either HuG1 or Hd-IgG internalized into HL60 cells was not dependent on mAb dose.

Although others (13–15) have found that crosslinked IgG bound to Fc receptors more avidly than monomeric Ig, our

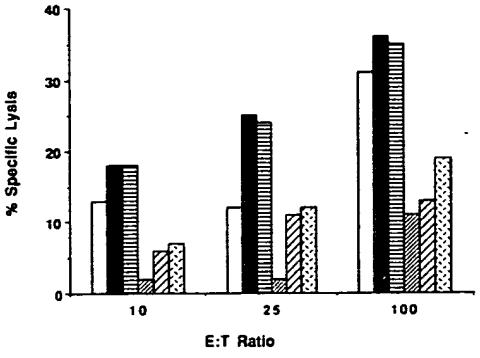

Figure 4. ADCC of HuG1-M195 and Hd-IgG is shown as a function of concentration and E/T ratio. Target HL60 cells were incubated at 37°C with mAb and PBMC as effectors, and ^{51}Cr-release was measured 5-h later as described in the text. Hd-IgG was 100-fold more potent (50 times on a weight basis) and 2–6 times more effective than the HuG1-M195 at ADCC. Hd-IgG at 0.2 μg/ml (▨); Hd-IgG at 1 μg/ml (▨); Hd-IgG at 10 μg/ml (▤); HuG1-M195 at 0.2 μg/ml (▨); HuG1-M195 at 1 μg/ml (▨); HuG1 at 10 μg/ml (▨). Results shown are from a representative experiment that was repeated on three separate days.

system is unique in that binding and internalization occurred via specific Fab binding to antigen and not to Fc receptors. The metabolism of Ig after Fc receptor-mediated internalization has been reported to be both increased and decreased by oligomerization (13, 16, 17).

Hd-IgG was at least 100-fold more potent on a molar basis at cell killing with rabbit complement than the HuG1-M195 (not shown). In this and other experiments, no cytotoxicity of HuG1-M195 was seen below a concentration of .01 μg/ml, whereas Hd-IgG demonstrated a linear increase in cell lysis starting at .001 μg/ml. Since both HuG1-M195 and Hd-IgG have similar avidities of binding, this would not explain the enhanced ability of Hd-IgG to perform CMC. Moreover, the more rapid and efficient internalization of Hd-IgG would argue against its improved ability to perform CMC, since less mAb would be available on the cell surface to fix complement. Although HuG1-M195 (7) and Hd-IgG were capable of fixing human complement and killing AL67 fibroblasts that overexpress CD33, neither HuG1-M195 nor Hd-IgG lysed HL60 cells in the presence of human serum.

Several lines of evidence suggest that the proximity of Fc regions of multimeric IgG may explain its enhanced effectiveness in CMC as compared with monomeric IgG. Binding and activation of C1q requires the formation of doublet IgG on the cell surface (18). Since Hd-IgG intrinsically contains a doublet of Fc regions, it may allow more efficient binding of the polyvalent C1q. The concept that a cluster of IgGs allows for multiple points of C1 attachment (19–21) is consistent with our observations of enhanced CMC here. It has been suggested that another site of attachment to the CH1 domain is needed (22). Hd-IgG may facilitate such spatial rearrangements. Bispecific antibodies capable of binding to two antigens (23) and a chimeric antibody with dual Fc regions (24) were superior to conventional IgG in CMC, presumably because of the increased number of Fc regions and their close arrangement in pairs. A critical number of antigen sites or critical spacing of epitopes on the cell surface has been shown to be necessary for CMC to occur with monovalent IgG (7, 25, 26). Naturally occurring IgG3 mAbs to carbohydrate antigens, which exhibit intermolecular cooperativity through Fc region interactions, show potent complement-mediated effector functions (27). The Hd-IgG described here may achieve this via a genetic mechanism.

Hd-IgG was at least 100 times more potent on a molar basis than HuG1-M195 at ADCC (Fig. 4). Specific lysis with 0.2 μg/ml Hd-IgG was as much as twofold greater than 10 μg/ml HuG1-M195 at the same E/T ratios. Hd-IgG was two- to fivefold more effective over a 50-fold concentration range at each E/T ratio. Chimeric and humanized IgG have shown ADCC where the original murine mAb did not demonstrate that capability (28–30). It is not surprising that homodimeric humanized IgG would be even more effective than monomeric IgG because of the greater ability of dual Fc regions to bring together effectors and targets in close proximity to allow ADCC to occur. IL-2 has been shown to potentiate ADCC against human Tac-positive T cells with humanized anti-Tac mAb (28). We have evidence that IL-2 enhances both HuG1- and Hd-IgG–mediated ADCC against HL60 target cells (31). The combination of other cytokines and Hd-IgG to enhance effector cell function needs to be investigated.

Previously, a human polymeric IgG1 mAb against group B streptococcus, held together by noncovalent interactions, has been described which showed enhanced binding and opsonic activity compared with the original monomeric mAb (32). The demonstrated homophilic interactions with a mouse IgG3 mAb, R24, reactive with GD3 ganglioside, have also led to the suggestion that multimerization of Ig may be a mechanism to enhance antibody-mediated clearance of bacteria (33).

The improvement in internalization of homodimeric M195 IgG should be advantageous for its use as a carrier of radiolabels or toxins, and should allow the delivery of more cytotoxic agent to target cells for each injected dose. Although we are currently able to safely deliver therapeutic levels of radioisotope to leukemia cells in humans in vivo, this change in cellular kinetics should allow the same therapeutic effects with less injected dose. In addition, the markedly improved effector functions and potency of Hd-IgG alone seen in vitro may result in potentially effective cytotoxicity against AML in vivo without conjugated cytotoxins or isotopes.

References

1. Winter, G., and C. Milstein. 1991. Man-made antibodies. *Nature (Lond.)*. 349:293.
2. Hale, G., M.R. Clark, R. Marcus, G. Winter, M.J.S. Dyer,

The authors thank K. Class, M. Curcio, and M. Bull for their technical expertise, and L. Forte for her secretarial assistance.

D.A. Scheinberg is a Lucille P. Markey Scholar. This work is supported by the Lucille P. Markey Charitable Trust, and National Institutes of Health grant R01CA-55349.

Address correspondence to Dr. David A. Scheinberg, Memorial Sloan-Kettering Cancer Center, 1275 York Avenue, New York, NY 10021. Walter Laird is currently at SangStat Medical Corporation, 1505B Adams Dr., Menlo Park, CA 94025.

Received for publication 19 May 1992 and in revised form 7 July 1992.

J.M. Phillips, L. Riechmann, and H. Waldmann. 1988. Remission induction in non-Hodgkins' lymphoma with reshaped human monoclonal antibody CAMPATH-1H. *Lancet (N. Am. Ed.).* 2:1394.

3. Gorman, S.D., M.R. Clark, E.G. Routledge, S.P. Cobbold, and H. Waldmann. 1991. Reshaping a therapeutic CD4 antibody. *Proc. Natl. Acad. Sci. USA.* 8:4181.
4. Queen, C., W.P. Schneider, H.E. Selick, P.W. Payne, N.F. Landolfi, J.F. Duncan, N.M. Avdalovic, M. Levitt, R.P. Junghans, and T.A. Waldmann. 1989. A humanized antibody that binds to the interleukin 2 receptor. *Proc. Natl. Acad. Sci. USA.* 86:10029.
5. Co, M.S., M. Deschamps, R.J. Whitley, and C. Queen. 1991. Humanized antibodies for antiviral therapy. *Proc. Natl. Acad. Sci. USA.* 88:2869.
6. Co., M.S., N.M. Avdalovic, P.C. Caron, M.V. Avdalovic, D.A. Scheinberg, and C. Queen. 1991. Chimeric and humanized antibodies with specificity for the CD33 antigen. *J. Immunol.* 148:1149.
7. Caron, P.C., M.S. Co, M.K. Bull, N.M. Avdalovic, C. Queen, and D.A. Scheinberg. 1992. Humanized M195 (Anti-CD33) monoclonal antibodies: potential for therapy of myelogenous leukemia. *Blood.* 78(Suppl.):54*a*.
8. Tanimoto, M., D.A. Scheinberg, C. Cordon-Cardo, D. Huie, B.D. Clarkson, and L.J. Old. 1989. Restricted expression of an early myeloid and monocytic cell surface antigen defined by monoclonal antibody M195. *Leukemia.* 3:339.
9. Scheinberg, D.A., M. Tanimoto, S. McKenzie, A. Strife, L.J. Old, and B.D. Clarkson. 1989. Monoclonal antibody M195: a diagnostic marker for acute myelogenous leukemia. *Leukemia.* 3:440.
10. Scheinberg, D.A., D. Lovett, C.R. Divgi, M.C. Graham, E. Berman, K. Pentlow, N. Feirt, R.D. Finn, B.D. Clarkson, T.S. Gee, et al. 1991. A phase 1 trial of monoclonal antibody M195 in acute myelogenous leukemia: specific bone marrow targeting and internalization of radionuclide. *J. Clin. Oncol.* 9:478.
11. Schwartz, M.A., D.R. Lovett, A. Redner, C.R. Divgi, M.C. Graham, R.D. Finn, T.S. Gee, M. Andreeff, H.F. Oettgen, S.M. Larson, et al. 1991. Leukemia cytoreduction and marrow ablation after therapy with ^{131}I labeled monoclonal antibody M195 for acute myelogenous leukemia (AML). *Proc. Amer. Soc. Clin. Oncol.* 10:230.
12. B. Shopes. 1992. A genetically engineered human IgG mutant with enhanced cytolytic activity. *J. Immunol.* 148:2918.
13. Strickland, R.W., L.M. Wahl, and D.D. Finbloom. 1988. Dimers of human immunoglobulin G_1 provide an insufficient signal for their degradation by human monocytes. *Clin. Immunol. Immunopathol.* 48:10.
14. Kurlander, R.J., and J. Batker. 1982. The binding of human immunoglobulin G1 monomer and small, covalently crosslinked polymers of immunoglobulin G1 to human peripheral blood monocytes and polymorphonuclear leukocytes. *J. Clin. Invest.* 69:1.
15. Segal, D.M., and E. Hurwitz. 1977. Binding of affinity crosslinked oligomers of IgG to cells bearing Fc receptors. *J. Immunol.* 118:1338.
16. Kurlander, R.J., and J.E. Gartrell. 1983. The binding and processing of monoclonal human IgG1 by cells of a human macrophage-like cell line (U937). *Blood.* 62:652.
17. D.S. Finbloom. 1986. Subcellular characterization of the endocytosis of small oligomers of mouse immunoglobulin G in murine macrophages. *J. Immunol.* 136:844.
18. Borsos, T., and H.J. Rapp. 1965. Complement fixation on cell surfaces by 19S and 7S antibodies. *Science (Wash. DC).* 150:505.
19. Liberti, P.A., D.M. Bausch, and L.M. Schoenberg. 1982. On the mechanism of C1q binding to antibody -I. Aggregation and/or distortion of IgG vs. combining site-transmitted effects. *Mol. Immunol.* 19:143.
20. Yasmeen, D., J.R. Ellerson, K.J. Dorrington, and R. Painter. 1976. The structure and function of immunoglobulin domains. IV. The distribution of some effector functions among $C\gamma2$ and $C\gamma3$ homology regions of human immunoglobulin F. *J. Immunol.* 116:518.
21. Yasmeen, D., J.R. Ellerson, K.J. Dorrington, and R. Painter. 1976. The structure and function of immunoglobulin domains. IV. The distribution of some effector functions among C3 homology regions of human immunoglobulin G. *J. Immunol.* 119:1664.
22. Okada, M., K. Udaka, and S. Utsumi. 1985. Co-operative interaction of subcomponents of the first component of complement with IgG: a functional defect of dimeric Facb from rabbit IgG. *Mol. Immunol.* 22:1399.
23. Wong, J.T., and R.B. Colvin. 1987. Bi-specific monoclonal antibodies: selective binding and complement fixation to cells that express two different surface antigens. *J. Immunol.* 139:1369.
24. Stevenson, G.T., A. Pindar, and C.J. Slade. 1989. A chimeric antibody with dual Fc regions (bis FabFc) prepared by manipulations at the IgG hinge. *Anti-Cancer Drug Des.* 3:219.
25. Circolo, A., and T. Boros. 1982. Lysis of hapten-labeled cells by anti-hapten IgG and complement: effect of cell surface hapten density. *J. Immunol.* 128:1118.
26. Michaelson, T.E., P. Garred, and A. Aase. 1991. Human IgG subclass pattern of inducing complement-mediated cytolysis depends on antigen concentration and to a lesser extent on epitope patchiness, antibody affinity and complement concentration. *Eur. J. Immunol.* 21:11.
27. Greenspan, N.S., and L.J.N. Cooper. 1992. Intermolecular cooperativity: a clue to why mice have IgG3. *Immunol. Today.* 13:164.
28. Junghans, R.P., T.A. Waldmann, N.F. Landolfi, N.M. Avdalovic, W.P. Schneider, and C. Queen. 1990. Anti-Tac-H, a humanized antibody to the interleukin 2 receptor with new features for immunotherapy in malignant and immune disorders. *Cancer Res.* 50:1495.
29. Stevenson, F.K., A.J. Bell, R. Cusack, T.J. Hamblin, C.J. Slade, M.B. Spellerberg, and G.T. Stevenson. 1991. Preliminary studies for an immunotherapeutic approach to the treatment of human myeloma using chimeric anti-CD38 antibody. *Blood.* 77:1071.
30. Liu, A.Y., R.R. Robinson, E.D. Murray, Jr., J.A. Ledbetter, I. Hellström, and K.E. Hellström. 1987. Production of a mouse-human chimeric monoclonal antibody to CD20 with potent Fc-dependent biologic activity. *J. Immunol.* 139:3521.
31. Caron, P.C., D. Saghafi-Ezaz, K.A. Class, M.S. Co, C. Queen, and D.A. Scheinberg. 1992. Cytokine enhancement of humanized M195 (anti-CD33) monoclonal antibody-mediated cellular cytotoxicity against myelogenous leukemia. *Proc. Amer. Assoc. Cancer Res.* 33:346.
32. Shuford, W., H.V. Raff, J.W. Finley, J. Esselstyn, and L.J. Harris. 1991. Effect of light chain V region duplication on IgG oligomerization and *in vivo* efficacy. *Science (Wash. DC).* 252:724.
33. Chapman, P.B., H. Yuasa, and A.N. Houghton. 1990. Homophilic binding of mouse monoclonal antibodies against G_{D3} ganglioside. *J. Immunol.* 145:891.

PERGAMON

Molecular Immunology 36 (1999) 777–788

Molecular Immunology

www.elsevier.com/locate/molimm

Processing of antibodies to the MHC class II antigen by B-cell lymphomas: release of Fab-like fragments into the medium

Gaik Lin Ong, M. Jules Mattes*

Garden State Cancer Center at the Center for Molecular Medicine and Immunology, 520 Belleville Avenue, Belleville, NJ 07922, USA

Received 18 February 1999; accepted 30 June 1999

Abstract

Lym-1, an anti-MHC class II Ab, displayed a unique processing pathway after binding to the surface of Raji B-lymphoma cells, in which Fab-like fragments were gradually released into the medium. The fragments had reduced interchain disulfide bonds. Fragmentation was markedly reduced by inhibitors of intracellular catabolism, namely ammonium chloride, chloroquine and leupeptin. The capacity of the process was high, and fragmentation of approximately 5×10^6 Ab molecules per cell per day was measured directly, in what can be considered to be a minimum estimate. Five other Abs to the MHC class II antigen were tested similarly on Raji and on three other B-cell lymphomas: none showed the same high level of fragmentation seen with Lym-1 binding to Raji, but significant fragmentation did occur with some of the Abs, particularly EDU-1 and L243. The level of fragmentation depended on the cell line as well as on the particular Ab. The other 5 Abs were all catabolized, to low molecular weight material, much more extensively than Lym-1. Part of the difference between Abs can probably be attributed to the fortuitous, preferential labeling of Lym-1 on the light chain, since the data suggest that the Fc fragment is fully degraded while the Fab-like fragment is released into the supernatant. This pathway of Ab processing is likely to be related to the physiology of the MHC class II antigen, which recycles into a mildly proteolytic intracellular compartment.

Keywords: Antibodies to MHC class II; Antibody catabolism; MHC class II antigen recycling

1. Introduction

We have been investigating the processing of radiolabeled Abs bound to B-cell lymphomas and other tumor types (Hanna et al., 1996, 1998; Kyriakos et al., 1992; Mattes et al., 1994; Vangeepuram et al., 1997). In testing an anti-MHC class II Ab, Lym-1, which is currently being used in clinical studies (DeNardo et al., 1997), we observed a unique processing pathway, which is described herein. After binding to the surface of B-cell lymphomas, Fab-like fragments were released in large amounts from the cell. Such fragmentation and release was not observed with many other Abs that have been tested similarly on B-cell lymphomas (Hanna et al., 1996, 1998; Vangeepuram et al., 1997) or carcinomas (Kyriakos et al., 1992; Mattes et al., 1994). Most other Abs, in contrast, remain bound to the cell surface until they are gradually internalized, after which they are promptly catabolized within lysosomes and released as low molecular weight material, probably iodotyrosine (for a conventional iodine label). The unusual processing pathway of Lym-1 probably reflects the unique recycling pathway of the antigen recognized (Watts, 1997), and the fate of the Ab can be considered to provide information about the nature of the intracellular compartments encountered by recycling class II antigens. Five other Abs to MHC class II were also tested, for comparison with Lym-1.

Abbreviations: DTPA, diethylenetriamine pentaacetic acid; TCA, trichloroacetic acid; RAIT, radioimmunotherapy.

* Corresponding author. Tel.: +1-973-844-7013; fax: +1-973-844-7020.

E-mail address: mjmattes.gscancer@worldnet.att.net (M.J. Mattes)

0161-5890/99/$ - see front matter
PII: S0161-5890(99)00084-X

2. Materials and methods

2.1. Antibodies and cell lines

The cell lines and growth conditions were described previously (Hanna et al., 1996; Vangeepuram et al., 1997). The B-cell lymphoma lines included Raji, Ramos, RL, Daudi, SU-DHL-4, SU-DHL-6, Namalwa, BJAB, and NC-37. NC-37 was recently identified as a Raji contaminant by the American Type Culture Collection (A.T.C.C., Rockville, MD), but it has been separated for >20 y, and it is included here because the results obtained with NC-37 were significantly different from the results obtained with Raji. Cell lines were tested routinely for mycoplasma contamination by the Mycotect assay (Gibco BRL, Grand Island, NY), and were negative. Ab Lym-1 is a mouse IgG2a reacting with the human MHC class II antigen (Epstein et al., 1987), and was provided by Dr G. DeNardo, University of California-Davis Medical Center, Sacramento, CA. Its specificity for the β chain of HLA-DR was recently better defined (Rose et al., 1996). It was produced as ascites in mice, then purified by protein A affinity chromatography. The hybridoma clone L243 was obtained from the A.T.C.C., grown as ascites, and purified as described above. Other Abs to class II αβ chains were purchased: TDR31.1 from Ancell (Bayport, MN); YE2/36 and YD1/63.4.10 from Harlan Sera-Lab (Indianapolis, IN); and EDU-1 from BioSource (Camarillo, CA). The $F(ab')_2$ fragment was produced from purified L243 by standard methods (Lamoyi, 1986), and was purified by passing over a protein-A affinity column, then a Bio-Sil G250 HPLC gel filtration column. In analysis by SDS–PAGE, there was one major band at the expected molecular weight, approximately 100,000 Da, with no detectable intact Ab.

2.2. Radiolabeling

^{125}I labeling of Abs was by standard methods, using chloramine-T (Kyriakos et al., 1992). The specific activity was 5–15 mCi/mg, so the molar ratio of ^{125}I:Ab was slightly less than 1:1. Lym-1 was also labeled on the carbohydrate with ^{111}In-benzyl-DTPA, by methods that have been described (Govindan et al., 1995). Briefly, the carbohydrate was oxidized with periodate, then conjugated with amino group-derivatized benzyl-DTPA. The specific activity was 3.8 mCi/mg.

2.3. Ab processing assay

This was previously described in detail (Hanna et al., 1996). Briefly, cells were coated with ^{125}I-labeled Abs for 1 h at 37°C, then washed and incubated under tissue culture conditions for 2–3 days. The specificity of Ab binding was established in every experiment by inhibition with a large excess of unlabeled Ab, and was always >90%. At various times, the cells and supernatant were assayed for cpm, and counts in the supernatant were analyzed by TCA precipitation to determine whether the counts were on intact or degraded Ab. Statistical comparisons were performed with student's *t*-test.

2.4. HPLC gel filtration analysis of culture supernatants

Labeled supernatants were analyzed on a Bio-Sil G250 gel filtration column, with a running buffer of 0.2 M sodium phosphate, pH 6.8, 10 mM NaN_3. Samples were 0.1 ml of spent medium that had been centrifuged and filtered through a 0.22 μm filter. Untreated control Abs were prepared at a similar (but not exactly equal) concentration of radioactivity. Fractions of 0.5 ml were collected and counted. To characterize the peaks observed, the ability of Abs to shift the peaks was determined. Abs used included rabbit anti-mouse IgG (##Z109, 8.7 mg/ml, DAKO, Carpinteria, CA); goat anti-mouse Fab, and goat anti-mouse Fc (##GAM/Fab/7S, 10.0 mg/ml and ##GAM/IgG(Fc)/7S, 10.0 mg/ml, respectively, Nordic Labs/Accurate Scientific, Westbury, NY); and monoclonal rat anti-mouse IgG2a (##LO-MG2A-7-C, 1.0 mg/ml, BioSource, Camarillo, CA). This Ab was stated by the supplier to be Fc-specific. In addition, our control experiments demonstrated that it reacted with whole IgG but not with an $F(ab)'_2$ fragment. To 0.5 ml of supernatant was added 2.5 μl of Ab. After 1 h incubation at 37°C, samples were filtered through a 0.22 μm filter, then applied to the HPLC column.

2.5. SDS–PAGE

Culture supernatants were concentrated by adding 1.5 ml 95% ethanol to 0.5 ml of supernatant. After 30 min at 0–4°C, the precipitate was pelleted for 10 min at 7000 rpm. After discarding the supernatant, the tubes were allowed to air-dry for 10 min, and the precipitates were then resuspended in 0.1 ml sample buffer, and heated for 3 min at 100°C. Unreduced samples were supplemented with 14 mg/ml iodoacetamide to prevent disulfide exchange. Conditions for SDS–PAGE were standard Laemmli conditions, as described previously (Mattes, 1987), using 1.5 mm thick gels. Molecular weight markers were Wide Range Color Markers (##C3437, Sigma Chemicals, St Louis, MO). In order to see distinct bands corresponding to both intact Ab and light chains, a two-phase gel was used consisting of 7.7 cm of 12% acrylamide beneath 3.8 cm of 7% acrylamide, with the usual stacking gel on top. Generally 5000 cpm were run per lane, but this was reduced in cases of low activity, for

which a maximum volume of 100 μl was run. In experiments in which various time points were compared (as in Fig. 3), the volume containing 5000 cpm was determined for one of the samples (usually the earliest) and the same *volume* of the other samples was run. Dried gels were exposed to Kodak BioMax MS film for 1–3 days, with a Kodak BioMax MS intensifying screen. To quantitate bands, they were excised and counted in a γ-counter. In some experiments, cell extracts were analyzed by SDS–PAGE. Cells from wells of 24-well plates were washed once with tissue culture medium, then solubilized in 0.1 ml of phosphate-buffered saline containing 0.5% NP40 and 1 mM Pefabloc (Boehringer Mannheim, Indianapolis, IN) for 20 min at room temperature. After removing insoluble material by centrifugation at 10,000 rpm for 5 min, appropriate number of cpm were added to the standard SDS–PAGE sample buffer. Some bands obtained in unreduced gels were subsequently re-run after reduction. This was done by excising the dried gel section, cutting into approximately 1–2 mm squares, and placing into the sample wells of a second gel. The gel pieces were then allowed to swell in sample buffer containing 12 mg/ml dithiothreitol for 30 min before beginning electrophoresis.

2.6. Use of inhibitors of catabolism

Cells were pretreated with the inhibitors for 30 min at 37°C before application of the Abs. Ammonium chloride was used at a final concentration of 10 mM; chloroquine (Sigma Chemicals) was used at two concentrations, 0.2 and 0.05 mM; and leupeptin (##L2884, Sigma Chemicals) was used at 0.1 mM. The higher concentration of chloroquine slightly affected cell morphology, with less clustering of the cells, but the other conditions tested had no evident effect on cell morphology, viability or growth rate.

2.7. Lym-1 saturation experiments

In these studies, we attempted to saturate the antigen with radiolabeled Lym-1 for prolonged periods (2–3 days), in order to determine the total uptake capacity. To maintain a reasonable level of total radioactivity, the cpm was kept constant while the Ab concentration was adjusted by adding unlabeled Ab. As the Ab concentration is increased, the fraction binding, and being internalized, naturally decreases, due to Ab excess. Thus, it is necessary to adjust the concentrations of labeled and unlabeled Ab in order to obtain near-saturation while the fraction of Ab binding remains adequate for accurate measurement. In these experiments, cells were not pre-coated with Ab, but instead were incubated continuously with Ab for the indicated period. At various times, the supernatant

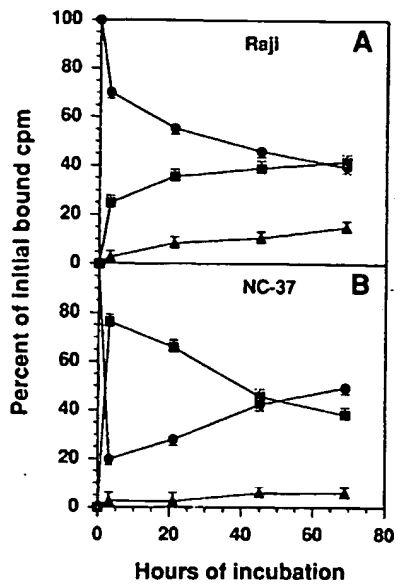

Fig. 1. Processing of ^{125}I-Lym-1 after binding to Raji cells (A) or NC-37 cells (B). At various times, the cpm remaining on the cells (●), released intact (■), or released degraded (▲) were determined. Values shown are means ± standard deviations of duplicates; any standard deviations not seen are too small to be visible above the symbols. The experiments shown are representative of two separate experiments with each cell line

was analyzed for intact and fragmented Ab by SDS–PAGE. To calculate the Ab molecules fragmented per cell, cell counts were obtained at each time point, and the percentage fragmented at each time point was determined by excising and counting bands seen in SDS–PAGE.

3. Results

3.1. Processing of Ab Lym-1 after binding to the cell surface

Lym-1 reacted with only three of the nine B-cell lymphoma lines tested, due to the fact that the Ab recognizes a polymorphic determinant on the MHC class II β chain. Lym-1 reacts with DR10 and with other, unidentified, β chain alleles (Rose et al., 1996). All of the 9 cell lines reacted strongly with other Abs to MHC class II, including L243. Lym-1 processing was initially investigated by an assay that uses TCA precipitation to distinguish between 'intact' and catabolized Ab, and does not analyze the form of high molecular weight, TCA precipitable material. The processing pathway was different depending on the particular cell line. With Raji, the original immunizing cell line (Fig. 1A), a peak of 42% of the bound Ab was released intact within 69 h. The release of intact Ab was initially rapid, with 25% release at 3 h, and after

21 h there was a near plateau. Degraded Ab was released at a low, continuous rate of approximately 4% per day, for the 3-day course of the experiment. This processing pattern is therefore generally similar to results with many other Abs and cell lines, of various histological types (Hanna et al., 1996; Kyriakos et al., 1992), except that there was greater release of intact Ab and less catabolism.

With another positive cell line, NC-37, Lym-1 displayed a unique pattern of release and re-binding of Ab (Fig. 1B). Although it is not uncommon to observe a small decrease in the amount of intact Ab in the supernatant with time, using other Abs, such a decrease is invariably small, <5% of the total bound cpm. Examples of this effect were previously shown (Hanna et al., 1996; Kyriakos et al., 1992), and we generally attribute this decrease to the re-binding and catabolism of Ab that had been released into the medium. A large decrease in the intact Ab in the supernatant from 3 to 69 h, as shown in Fig. 1B, has not been previously described. Moreover, the cell-bound cpm increased from 20% at 3 h to 49% at 69 h; such an increase in cell-bound cpm, after the initial drop, is also unique. These two effects are results of the same process, the rebinding of Ab that was previously released into the medium. We investigated the form in which Lym-1 was retained by the cells, by extraction of cells at various times, from 3 to 69 h, and analysis by SDS–PAGE. The cpm remaining on the cells was predominantly intact IgG in all cases, with no indication of substantial amounts of any distinct catabolite (data not shown). The explanation for this high level of stable re-binding of previously dissociated Ab is not known at this time, but it can be tentatively attributed to gradual accumulation of the Ab in some stable, non-catabolic compartment.

3.2. Release of Fab-like fragments

Since precipitation with 10% trichloroacetic acid does not distinguish between intact Ab, Ab-antigen complexes resulting from antigen-shedding, or large Ab fragments, supernatants from cells coated with ^{125}I-Lym-1, containing relatively large amounts of TCA-precipitable cpm (>20% of the total bound cpm), were analyzed by gel filtration HPLC. With other Abs showing large amounts of TCA-precipitable cpm in the supernatant, which is uncommon, such an analysis showed that the material in the supernatant was free, intact Ab, undoubtediy released due to dissociation of relatively low-avidity Abs ((Vangeepuram et al., 1997); M.J.M., unpublished data). In contrast, the TCA precipitable cpm derived from Lym-1 bound to Raji cells were largely in the form of large fragments of Ab. Analysis of 21–69 h supernatants revealed some intact Ab, but a large fraction of the

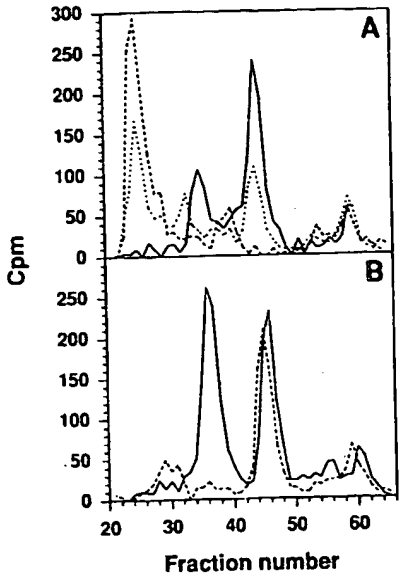

Fig. 2. Gel filtration HPLC analysis of the spent medium obtained from Raji cells that had been coated with ^{125}I-Lym-1, then washed and incubated 21 h under tissue culture conditions. (A) Solid lines, without added Ab; dashed lines, treated with goat anti-mouse Fab; dotted lines, treated with goat anti-mouse Fc. (B) Solid lines, without added Ab; dashed lines, treated with monoclonal rat anti-mouse Fc. Intact IgG elutes at fractions 35–56, and Fab' fragments at fractions 44–46, on this column.

cpm migrated in a peak having a molecular weight of approximately 40–50,000 Da (Fig. 2). Some low molecular weight, fully degraded material, probably iodotyrosine, was also present in the supernatant. This low molecular weight material eluted approximately five fractions later than sodium iodide, due evidently to hydrophobic interaction with the column. To demonstrate that the fragments were a product of cell metabolism, Lym-1 was incubated similarly in either tissue culture medium or spent medium from Raji cells: IgG fragments were not generated in these experiments.

To further characterize the apparent Ab fragment, Abs were added before HPLC to shift the peaks. The Abs tested were polyclonal anti-mouse Fab and anti-mouse Fc, a more broadly reactive anti-mouse IgG, and monoclonal rat anti-mouse Fc. The presumed fragment, as well as the intact Ab, was entirely shifted by both the anti-mouse Fab and the anti-mouse IgG Ab. In contrast, the polyclonal anti-mouse Fc had only a partial effect on the fragment peak, although it efficiently shifted the peak of intact Ab (Fig. 2A). In these experiments, some but not all of the shifted cpm appeared in the void volume peak; we suggest that some of the immune complexes formed were too large to pass through the column. These data demonstrate that the fragment observed was a fragment of IgG, and predominantly Fab-like. However, there was uncertainty regarding the presence of Fc fragments,

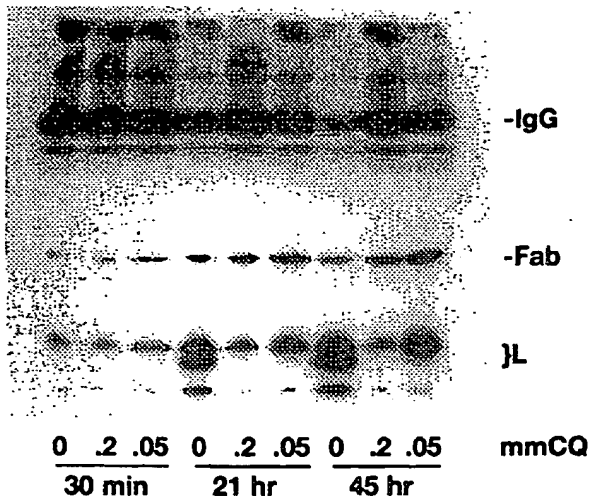

Fig. 3. Fragmentation of ^{125}I-Lym-1 by Raji cells, and its inhibition by chloroquine. Cells coated with ^{125}I-Lym-1 were incubated with or without chloroquine at either 0.2 or 0.05 mM. At various times, the supernatant was analyzed for the presence of Fab-like fragments by SDS–PAGE. The same volume of each of the supernatants was run. Unreduced samples were run on a 7–12% acrylamide gel, as described in Materials and methods. The migration position of IgG, Fab-like fragments, and light chains are indicated. One of the bands in the light chain region is probably the Fd fragment.

since the anti-Fc antiserum did have some effect. It should be noted that this result appears to be inconsistent with the fact that the anti-Fab serum shifted *all* of the fragment, since any Fc present should not be shifted by treatment with anti-Fab'. Our hypothesis, therefore, was that the anti-Fc antiserum might be contaminated by low levels of anti-Fab Abs. This is reasonable because these antisera were made specific by absorption, which typically leaves trace amounts of the unwanted Abs, and because the assay used here is very sensitive to small amounts of Ab. To eliminate the possibility of contaminating Abs, we tested a monoclonal rat anti-mouse Fc: this Ab had no effect on the fragment peak although it efficiently shifted the intact Ab peak (Fig. 2B). We conclude that the fragment generated is Fab-like.

Characterization of the fragment was confirmed and extended by SDS–PAGE analysis. Concentrated supernatants were run without reduction, and with iodoacetamide added to prevent disulfide exchange. The same volume of supernatant at each time point was run. The fragments observed in Lym-1 culture supernatants migrated as a doublet in the region of free light chains (Fig. 3). The simplest explanation of these results, in conjunction with the HPLC data, is that the fragment is Fab-like with interchain bonds reduced. Thus, the doublet observed is probably composed of the light chain and Fd fragment. Only a trace of the Fab-like fragment was present in the supernatant at 3 h, and fragment production was more extensive at 45 h than at 21 h. By 45 h, the majority of the IgG in the medium was converted to the fragment. By excising bands and counting their radioactivity, it was determined that, of the total counts present in the immunoglobulin bands at 45 h (the sum of the intact IgG and the light chain-like doublet), approximately 60% were in the light chain-like doublet. It should also be noted that the amount of intact IgG in the supernatant gradually decreased from 3 to 45 h, as the amount of fragment was increasing (Fig. 3). Based on Figs. 1 and 3, since the total TCA-precipitable cpm in the medium did not change much from 3 to 45 h, it appears probable that the Ab molecules destined for fragmentation are initially released intact from the cells, and are then gradually fragmented after re-binding to the target cells. However, other explanations are also possible, considering that a large fraction of bound Ab, 40%, remains cell-bound over the 3-day experiment.

Similar fragmentation of Lym-1 did not occur with the other two reactive cell lines, SU-DHL-6 and NC-37, or occurred at much lower levels. Supernatants from these cell lines, similar to those described above, were analyzed by both gel filtration HPLC and SDS–PAGE. With NC-37, only a trace of fragments was generated; with SU-DHL-6, small amounts of Fab-like fragments were generated, but much less efficiently than with Raji (data not shown). The lack of fragmentation with SU-DHL-6 can be probably attributed to the fact that the Ab binds weakly, inasmuch as there was a high level of dissociation from this cell line, so Lym-1 probably dissociated before it could be efficiently internalized.

3.3. Effects of catabolic inhibitors

This Ab fragmentation is most likely to occur intracellularly, but it is possible that it could occur on the cell surface. To investigate this point, inhibitors of intracellular proteolysis were tested, namely ammonium chloride, chloroquine and leupeptin. The first two raise the pH of normally acidic intracellular vesicles, and thereby inhibit catabolism, while leupeptin is a specific inhibitor of some proteolytic enzymes. All three produced strong inhibition of Lym-1 fragmentation and release, under conditions in which cell viability was not significantly affected. Representative results, with chloroquine, are included in Fig. 3. The inhibitors not only reduced the production of fragments, but also blocked the gradual decrease in intact IgG in the medium that occurred in control wells, as shown. By calculating the percentage of total IgG that was in the form of fragments, as described above, we estimated that chloroquine produced an approximately 90% inhibition of fragmentation, and similar levels of inhibition were obtained with the other two inhibitors tested.

These data strongly suggests that fragmentation occurs within an intracellular acidic vesicle.

Fig. 3 also demonstrates a 'new' fragment that was more prominent in some of the experiments with inhibitors, but had been only a minor component in earlier experiments. This is the Fab-like band in Fig. 3, having a molecular weight of approximately 50,000 Da. Since this molecular weight is consistent with either free heavy chain or a disulfide-linked Fab, the band was excised and re-run under reducing conditions, on a 12% acrylamide gel. The results indicated clearly that the band was a disulfide-linked Fab, since after reduction it migrated as if approximately 25,000 Da in molecular weight (not shown). Thus, the disulfide-linked Fab appears to be a precursor of the partially reduced Fab, and this intermediate is sometimes increased in the presence of catabolic inhibitors. Despite the presence of this band, it should be emphasized that almost all of the Fab-like fragments released under normal conditions, and most of the Fab-like fragments released in the presence of catabolic inhibitors, were composed of partially reduced subunits in which the interchain disulfide bonds were reduced, and therefore migrated with light chains in SDS–PAGE.

3.4. The capacity for Lym-1 uptake by Raji cells

The above data, together, suggests that the partially reduced Fab-like fragments are transported back to the cell surface, possibly still bound to antigen, where they are released into the supernatant, perhaps due to dissociation. The exposed antigen molecule can then potentially bind another molecule of intact Ab, which binds much more strongly than the monovalent Fab. Given this model, it seems possible that a single antigen molecule could transport many Ab molecules into the cell. To obtain an estimate of the total capacity of this internalization process, experiments were performed with increasing concentrations of Lym-1, up to a near-saturating level of 5 μg/ml. In these experiments, rather than using an initial Ab binding incubation, the cells were simply incubated in the presence of radiolabeled Ab for the duration of the experiment, 2–3 days. At various times, the supernatant was analyzed for the presence of Ab fragments, and the percentage of the total Ab that had been fragmented was calculated. From this data, and the cell counts, the number of Ab molecules fragmented per cell could be calculated. Representative results are shown in Fig. 4, and Fig. 5 displays the results in terms of 'Ab molecules fragmented per cell'. No plateau in the Ab molecules fragmented per cell was observed at the highest Ab concentration tested, indicating that saturation was not reached. The largest amount of fragmentation measured was approximately 10^7 Ab molecules per cell in 2 days. Higher Ab concentrations could not be readily tested, since the fraction of Ab fragmented naturally decreased as the protein dose increased, and this fraction was too low to be measured accurately if the Ab concentration was raised to >5 μg/ml. We speculate that our inability to saturate this uptake process is due to the fact that MHC class II molecules recycle rapidly (Reid and Watts, 1990), and that, therefore, it is experimentally difficult to have a new

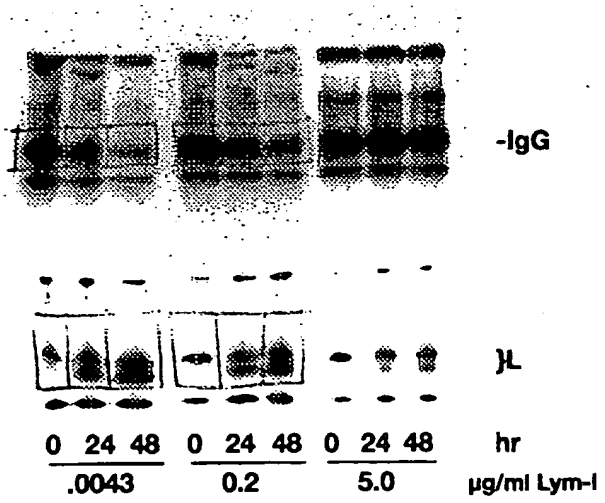

Fig. 4. The capacity of Raji to take up Lym-1, in a prolonged Ab incubation. Cells were incubated with the same amount of radiolabeled Ab, and with varying amounts of unlabeled Ab. At various times, the supernatant was analyzed for intact and fragmented Ab, by analysis on a non-reducing 7–12% acrylamide gel. The migration positions of IgG and light chains are shown. One of the bands in the light chain region is probably the Fd fragment. The lowest Ab concentration, 0.0043 μg/ml, had no unlabeled Ab added. Intermediate Ab concentrations of 0.05 and 1.0 μg/ml were also tested in this experiment, but results are not shown. The bands that were excised, for determination of cpm, are indicated. The intact Lym-1 in the medium is gradually converted to fragments, and the extent of fragmentation is reduced at high Ab concentrations.

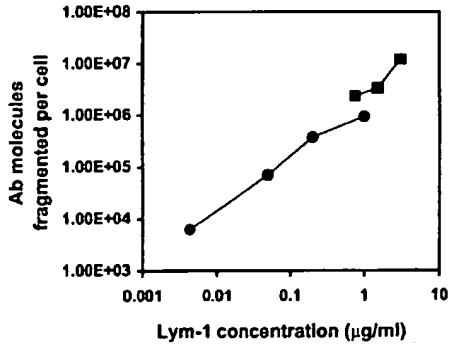

Fig. 5. Summary of the experiments determining fragmentation capacity, using increasing concentrations of Ab. Production of Fab-like fragments was assayed by SDS-PAGE, as described in Materials and methods. The two symbols indicate results of two independent experiments. The values shown are the Ab molecules fragmented in the complete, 2-day, experiment.

intact Ab bind to the antigen molecule each time it appears on the cell surface. Given the presence of 1.1×10^6 Lym-1 binding sites per cell (Epstein et al., 1987), these data suggest that each antigen molecule may be able to transport several Ab molecules into the cell for fragmentation. However, given the uncertainties in these calculations, we cannot rule out the possibility that each antigen molecule transports only a single Ab molecule.

3.5. Tests of other anti-MHC class II Abs

To our knowledge, Lym-1 is not different from other Abs to MHC class II in any basic way, except that it recognizes a polymorphic epitope (Rose et al., 1996), and we would therefore expect other Abs to the same antigen to follow a similar processing pathway. To investigate this point, five other Abs were tested, with Raji target cells. These Abs were tested initially in our standard processing assay. As shown in Fig. 6, all of the Abs had quite high levels of Ab 'dissociation', but were markedly different from Lym-1 in the level of catabolism. While only 12% of Lym-1 was catabolized and released in 45 h, 56% of YD1 was catabolized, and 30–47% was catabolized with three of the other Abs. L243 was most similar to Lym-1, but still had 21% catabolism in 45 h, or almost twice as much as Lym-1. Due to this faster catabolism, together with the similar release of 'intact' Ab, the amount of Ab remaining on the cells was much lower with four of the other Abs than with Lym-1 (Fig. 6). Only L243 was similar to Lym-1 in cellular retention at 45 h.

The 'intact' Ab in the supernatant of Raji cells was further analyzed by gel filtration HPLC and/or SDS–PAGE, for four of the Abs, YD1, YE2/36, EDU-1 and L243. Three of these Abs, all except EDU-1, produced only a trace of Fab-like fragmentation (although such a trace was present and was not seen in the control Ab incubated without cells) (data not shown). With EDU-1, in contrast, a relatively high level of fragmentation was observed by HPLC analysis (Fig. 7). The major fragment was again Fab-like in size, but there were two distinct differences from the fragmentation pattern observed with Lym-1. First, there was never a high level of intact Ab in the medium: at 3 h only a small amount of intact Ab was present, and at 21 h only a trace was present, with the Fab-like peak being the only major protein peak. Secondly, there was much more low molecular-weight catabolic material with EDU-1 than with Lym-1, and at 21 h this peak was much larger than any protein peak. This is consistent with the data in Fig. 6 showing that EDU-1 catabolism was much greater than that of Lym-1. Although the catabolite peak at 21 h was off-scale in Fig. 7, the peak cpm was 1029, and the Fab-like peak was 19% of the catabolite peak. SDS–PAGE analysis of EDU-1 supernatants also showed light-chain-like fragments, similar to those described with Lym-1, and at 21 h more than half of the cpm in immunoglobulin bands were in the Fab-like fragment (data not shown).

Some of the other anti-MHC class II Abs were also tested for fragmentation by other cell lines. Since all of these Abs, unlike Lym-1, react with non-polymorphic epitopes, it was possible to test a wider range of cell lines. Experiments were performed with Ab YD1 binding to NC-37 and SU-DHL-6, and Ab L243 binding to Ramos, RL and Daudi. In general, we observed significant differences in the processing of the same Abs by different B-cell lymphoma lines, particularly in the

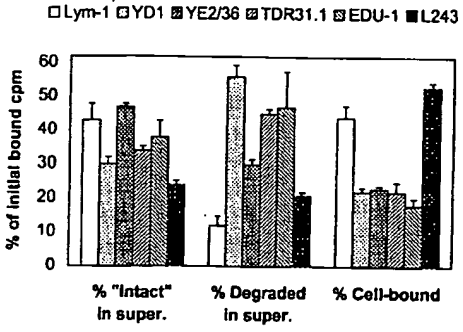

Fig. 6. Processing of six Abs to the MHC class II antigen after binding to the surface of Raji B-lymphoma cells. Values shown are: the peak percentage of initially bound cpm released 'intact' (TCA precipitable) into the medium; the percentage of initially bound cpm released degraded into the medium at 45 h; and the percentage of initially bound cpm remaining cell bound at 45 h. The 'intact' cpm in the medium was sometimes slightly higher at 21 h than at 45 h (due to re-binding of the Ab), which is why the peak value is presented. However, this was a minor effect, always < 5% of the total cpm, and unlike the strong effect shown in Fig. 1B with Lym-1 binding to NC-37. Means ± standard deviations are shown for at least two separate experiments with each Ab, each performed in duplicate.

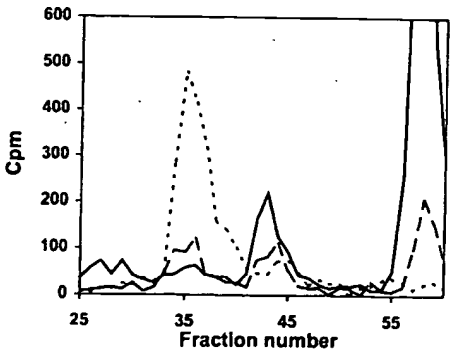

Fig. 7. Gel filtration HPLC analysis of the spent medium obtained from Raji cells that had been coated with ^{125}I-EDU-1, then washed and incubated under tissue culture conditions. Dotted lines, control Ab, prepared at approximately the same concentration of cpm/ml; dashed lines, 0.1 ml of spent medium collected at 3 h; solid lines, 0.1 ml of spent medium collected at 21 h. The peak at fraction 43 is the Fab-like fragment.

catabolic rate (data not shown). Some indication of fragmentation occurred with many Ab/target cell combinations, but generally at a low level. The most extensive Fab-like fragmentation occurred with Ab L243 bound to the Ramos cell line (Fig. 8). Again, the absolute level of fragmentation appeared to be lower than with Lym-1. The fragmentation pattern was similar but not identical to that with Lym-1 on Raji: in addition to the light chain- and Fd-like bands, a prominent band at approximately 50,000 Da was seen, which is very similar to the band noted above in the chloroquine experiments. In the same way as described above, it was demonstrated that this band was composed of a Fab-like fragment (as opposed to free heavy chain). Cutting and counting the bands indicated that 44% of the Ig-related cpm (which includes the bands indicated in Fig. 8), were fragments at 48 h, which is comparable to the percentage obtained with Lym-1 on Raji. There were two other distinct differences from the Lym-1/Raji system: (1) The marked decrease with time in the amount of intact Ab in the medium did not occur with L243; and (2) the level of catabolism was much higher with L243, as shown by the cpm at the dye front in Fig. 8. It is interesting to note that L243 fragmentation was more extensive with Ramos cells than with Raji, although this cannot currently be explained. In conclusion, evidence for fragmentation and release was obtained with two of the five other Abs tested, but Lym-1 bound to Raji cells appears to show more extensive fragmentation than other combinations of Abs and cells.

The possible explanation for the differences between Abs in the extent of fragmentation includes differences in the Ab subclass, the species of origin, and the precise epitope recognized. The epitope recognized was analyzed by competitive binding experiments. ^{125}I-Lym-1 binding to Raji cells was strongly inhibited by L243 and YE2/36, both of which in fact inhibited binding somewhat more effectively than Lym-1 itself, when used at the same concentration. YD1 and EDU-1 showed partial inhibition (data not shown). Thus, the epitope recognized by Lym-1 is not unique, at least according to this assay. We note that this cross-competition was one-way, in that Lym-1 did not significantly inhibit binding of radiolabeled L243. This result suggests that Lym-1 may have a lower avidity than L243, and a relatively low avidity may affect the processing pathway observed.

Another difference that was noted by chance, and that must play some role, is the ^{125}I labeling pattern.

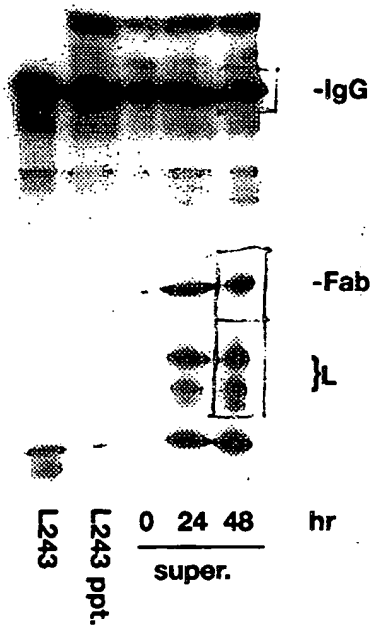

Fig. 8. SDS-PAGE analysis of the spent medium obtained from Ramos cells that had been coated with ^{125}I-L243, then washed and incubated for various periods under tissue culture conditions. Concentrated medium was run unreduced on a 7%/12% resolving gel, as described in Materials and methods. The migration positions of intact IgG, Fab-like fragments, and light chains are indicated. One of the bands in the light chain region is probably the Fd fragment. Supernatants were analyzed at 0, 24, and 48 h. The same volume of each of the supernatants was run. The bands that were excised, for determination of cpm, are indicated. Light-chain-sized and Fab-like fragments were gradually produced, over a 2-day period. The left-most lane shows the control L243 Ab, and the next lane is the same Ab diluted in tissue culture medium and precipitated with ethanol, to mimic conditions used for the spent medium.

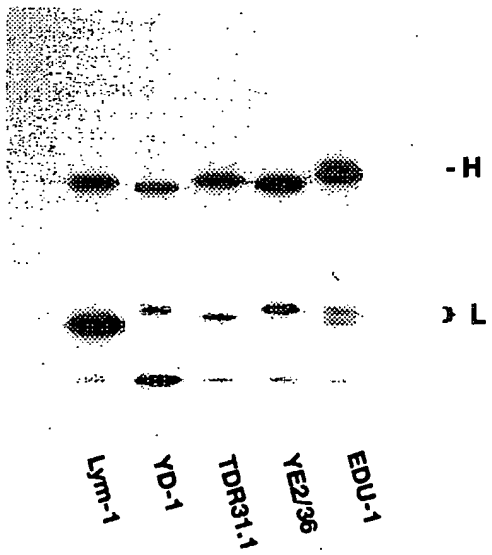

Fig. 9. SDS-PAGE analysis of 5 radioiodinated Ab, reduced and run on an 11% acrylamide gel. The migration positions of the heavy and light chains are shown. Note the differences between Abs in the relative labeling of the light chain vs the heavy chain, with Lym-1 preferentially labeled on the light chain. Ab L243 was analyzed in a separate experiment, not shown here.

More specifically, Lym-1 was labeled predominantly on the light chain, while the other Abs tested were labeled predominantly on the heavy chain (Fig. 9). By excising and counting the heavy and light chain bands, it was determined that 63–72% of the Lym-1 label was on light chains, while this fraction was 36%, 24–37%, 25–26%, 26–27% and 33% for Abs YD-1, YE2/36, TDR31.1, EDU-1 and L243, respectively. This difference was observed repeatedly, using different labeled preparations of the same individual Abs, and must be attributed to randomly dispersed tyrosines that are particularly susceptible to iodination. Since the data presented suggest that only Fab-like fragments are released, the labeling site on the Ab molecule clearly can have an impact on the processing pathway observed. Another possible relevant difference between Abs is in the affinity of the Fab-like fragment for antigen: possibly a high-affinity Fab would not dissociate as readily from the cell surface, so would be less abundant in the supernatant. A prediction from this hypothesis is that Fab-like fragments would be found in cell extracts, and therefore cell extracts were analyzed, at 21 and 45 h, using L243 bound to Raji and Ramos. Bound Fab-like fragments were not observed (data not shown).

3.6. Site-specific labeling of Abs

We have performed two types of experiments to investigate the possibility that the results of processing experiments may depend critically on the location of the radiolabel on the Ab. The first and simplest experiment was to use a $F(ab')_2$ Ab fragment, and this was performed with L243. If the key property of Lym-1 is the predominant labeling on the Fab portion of the molecule (actually the light chain), then it would be predicted that the labeled $F(ab')_2$ fragment of L243 would behave similarly to Lym-1. However, this was not the case. The L243 $F(ab')_2$ was tested on Raji, NC-37 and Ramos, and generally was processed very similarly to the intact Ab in regard to the extent of fragmentation and the release of fragments (data not shown). We can conclude that the difference between Lym-1 and L243 is not due only to the preferential light chain labeling of Lym-1. Another prediction, however, was confirmed, namely that the amount of catabolism of the $F(ab')_2$ fragment to low molecular weight end-products would be reduced (relative to the catabolism of the whole Ab), since the Fc fragment was expected to undergo more complete catabolism than the Fab fragment. This was observed with both cell lines tested, Raji and Ramos. For example, with Ramos cells, 19.8% of the whole Ab bound to Ramos cells was catabolized in 2 days, and this value was reduced by 71%, to 5.8% catabolism in 2 days, when the $F(ab')_2$ fragment was used. (data not shown). This difference was statistically significant ($p < 0.01$).

A second experiment was to specifically label the Fc region by carbohydrate-directed labeling, and this was performed with Lym-1. This is predicted to drastically alter the processing observed, in that there should be no release of detectable Fab-like fragments, and a much greater level of catabolism. Unfortunately, the label which we were equipped to put on the carbohydrate was ^{111}In-benzyl-DTPA, which is a residualizing label. Unlike the conventional ^{125}I label, residualizing labels are trapped within cells after catabolism of the Ab to which they were attached (Shih et al., 1994), although with some very slow release of the label from the cell. Therefore, it would be predicted that this label would gradually accumulate in the cells, as the Lym-1 was fragmented. This result was in fact observed. Furthermore, the supernatant in this experiment contained no detectable Fab-like fragment, when analyzed by both gel filtration HPLC and SDS–PAGE (data not shown), which supports the model suggested.

4. Discussion

The unique processing pathway of Lym-1 is likely to be related to the function of the antigen recognized, which has been recently reviewed (Cresswell, 1994; Watts, 1997). Newly synthesized MHC class II molecules are loaded with antigenic peptides inside the cell, but after reaching the cell surface can recycle, in order to replace the bound peptides with new ones (Pinet et al., 1995; Watts, 1997; Zhong et al., 1997). Thus, the recycling molecules are likely to traverse a mildly proteolytic compartment, which could generate Fab-like fragments from Abs. While many other Abs may undergo a transient conversion to Fab-like fragments, these would normally be rapidly degraded in lysosomes (Grey et al., 1982), and would not be released into the medium. It is the recycling of the class II molecules that brings the Fab fragments (probably still bound to the antigen) back to the cell surface, from where they dissociate into the medium. The monovalent Fab-like fragment will, of course, dissociate much faster than an intact bivalent Ab. The capacity of this pathway was measured directly to be approximately 5×10^6 Ab molecules per cell per day, which, although high, is far (approximately 5-fold) below the rate of internalization of MHC class II molecules on B lymphoblastoid cells estimated by Reid and Watts (1990). This might be attributed to the fact that only a fraction of bound Lym-1 molecules are cleaved on a transit inside the cell and back to the surface. Another explanation may be that not all antigen molecules are bound by Abs before they are interna-

lized. The other unusual aspect of Lym-1 processing, the high level of dissociation of intact Ab followed by re-binding, cannot be readily explained at this time. This was seen most dramatically with NC-37, but also was clearly detected with Raji by SDS–PAGE analysis. While some rebinding occurs with many Abs, it is generally a minor effect (Hanna et al., 1996; Kyriakos et al., 1992).

The release of large fragments of Lym-1 from Raji target cells was described previously by Wang et al. (1989). These authors analyzed only a 6 h time point, and did not characterize the fragments. They also found relatively large amounts of cpm at the void volume of a gel filtration column, in their analysis of the spent medium, which they interpreted to be antigen-Ab complexes. Such large complexes were not observed in our experiments. The reason for this discrepancy is not known, but there were technical differences in the methods used, including different temperatures for the initial Ab binding incubation.

The issue of disulfide bond reduction requires further discussion. We have demonstrated that the fragments of Lym-1 released into the medium have lost virtually all interchain disulfide bonds. The intrachain disulfide bonds are certain to be still intact, although we did not demonstrate this directly, since: (1) Recognition by antibodies indicates that the conformation of the Fab-like fragment is still generally intact; this conformation shields the intrachain bonds from reduction (Stevenson, 1997); and (2) the free light chains and (presumptive) Fd fragments had significantly greater mobility in SDS–PAGE unreduced than after reduction (data not shown), a consequence of the intrachain disulfide bonds. Reduction of accessible disulfide bonds is known to accompany intracellular proteolysis (Pisoni et al., 1990) and the generation of antigenic peptides (Collins et al., 1991), and there is some evidence that reduction can occur in a pre-lysosomal compartment (Ruud et al., 1986, 1988), but we are not aware of previous evidence that recycling class II molecules encounter a reducing environment. Indeed, the data of Reid and Watts (1990) appear to indicate that recycling class II molecules do not encounter a reducing compartment, since the label they used would have been cleaved. Further experiments are required to resolve this discrepancy. It is possible that the pathway observed by Reid and Watts in the presence of primaquine was not a normal pathway, but it is also possible that the pathway observed here, after Ab binding to the class II antigens, is not a normal pathway, since Ab binding may affect the transport of the antigen recognized.

The preferential labeling of the light chain of Lym-1 certainly facilitated the detection of this processing pathway. Considering the evidence that Fab-like fragments are released into the supernatant, while Fc-like fragments are fully catabolized, just as occurs in the standard generation of $F(ab')_2$ fragments from Abs by pepsin digestion (Lamoyi, 1986), predominant light chain labeling would cause enhanced detection of the Fab-like fragments in the supernatant, in comparison to other Abs. Another consequence would be higher levels of low molecular weight (TCA-non-precipitable) catabolites in the supernatant with other Abs than with Lym-1, since this material would be derived preferentially from the Fc region, and this also was observed. It should be noted, however, that light chain vs heavy chain labeling does not completely predict Fab vs Fc labeling, since the heavy chain label could be either in the Fd portion or the Fc portion, and different Abs may vary also in this regard. The report of Nikula et al. (1995) suggested that many Abs iodinate preferentially in the variable region of the heavy chain, but their data were all obtained with a single Ab, and the proposed application to other Abs, based on the tyrosine content of different regions of the Ab, is speculative.

It also seems likely that the Ab subclass, and species of origin, may strongly affect the susceptibility of the Ab to this type of fragmentation (Lamoyi, 1986). Two of the Abs tested were rat mAbs, YD-1 and YE2/36, which are both rat IgG2a. EDU-1 is a mouse IgG2b and TDR31.1 is a mouse IgG1. Only L243 is a mouse IgG2a, like Lym-1. A major effect of Ab subclass on Ab fragmentation to Fab or Fab' fragments is well known (Lamoyi, 1986), and $F(ab')_2$ fragments are produced more rapidly from mouse IgG2a than from mouse IgG1 or IgG2b. Thus, we speculate that Ab subclass differences play some role in the variation between Abs observed. However, since Lym-1 and L243 did not behave identically, Ab subclass is not the only factor involved. Individual Abs of the same subclass sometimes display major differences in fragmentation properties (Lamoyi, 1986). In addition, the epitope specificity of the Ab can affect its processing, as was described with anti-IgM Abs reacting with B-cells (Ruud et al., 1989). The epitope recognized may affect the accessibility of the Ab to proteases, and may also affect the conformation of the bound Ab, especially if the Ab binds bivalently. The conformation, in turn, will affect susceptibility to proteases. Considering that Lym-1 was the only Ab tested that reacts with a polymorphic epitope, it is reasonable to suggest that Lym-1 may be the only Ab that reacts with the variable portion of the class II molecule. However, the competitive binding experiments demonstrated that two of the other anti-class II Abs bound to the same epitope as Lym-1. Still, subtle differences in the epitope recognized cannot be excluded. All of these factors, individually, are likely to impact upon the degree of fragmentation observed. In any case, the results with EDU-1 and L243 demonstrate that Fab-

like fragmentation and release is not limited to the Lym-1/Raji system, although the level observed with Lym-1 and Raji appears to be exceptionally high.

The processing of certain (but not all) anti-IgM Abs by B-cell lines has superficial similarities to the processing of Lym-1, in that large fragments were released into the medium (Ruud et al., 1986, 1989). The fragments present inside the cell were partially reduced, and, although not directly addressed, it is likely that the fragments released into the medium were also partially reduced. However, there are basic differences between these two systems, as follows.

1. With anti-IgM, only a small fraction of the released TCA-precipitable cpm was on the fragment, with the majority being on intact Ab, in contrast to results with Lym-1.
2. The fragments of anti-IgM released were approximately 15,000 Da, smaller than Fab fragments, Fd fragments or light chains.
3. The experiments of Ruud et al. extended for only 4 h, while Lym-1 fragmentation is much slower, and only clearly detected at 21 h.

The release of Lym-1 fragments from target cells must constitute a disadvantage in the use of Lym-1 for RAIT, if the radiolabel is on the Fab-like fragment released. However, despite the high level of dissociation, and despite the generation and release of fragments, a considerable fraction of bound Ab is retained by the target cells for prolonged periods. Thus, Raji retains approximately 40% of the cpm delivered by Lym-1 after 2 days, as shown in Fig. 1. Our data suggest that the uptake and retention by B-cell lymphomas of a radiolabel on Lym-1, or other anti-class II Ab, will depend on the particular Ab, the nature of the label, and the conjugation site on the Ab.

Acknowledgements

We are grateful to Dr S. V. Govindan for carbohydrate-directed labeling of Abs, to Dr H. Karacay for assistance with $F(ab')_2$ purification, to Philip Andrews for assistance with radiolabeling, and to Dr David M. Goldenberg for his support. This work was supported in part by U.S.P.H.S. National Institutes of Health grant No. [CA63624]

References

Collins, D.S., Unanue, E.R., Harding, C.V., 1991. Reduction of disulfide bonds within lysosomes is a key step in antigen processing. J. Immunol. 147, 4054–4059.

Cresswell, P., 1994. Assembly, transport and function of MHC class II molecules. Ann. Rev. Immunol. 12, 259–293.

DeNardo, G.L., Lamborn, K.R., Goldstein, D.S., Kroger, L.A., DeNardo, S.J., 1997. Increased survival associated with radiolabeled Lym-1 therapy for non-Hodgkin's lymphoma and chronic lymphocytic leukemia. Cancer 80, 2706–2711.

Epstein, A.L., Marder, R.J., Winter, J.N., Stathopoulos, E., Chen, F.M., Parker, J.W., Taylor, C.R., 1987. Two new monoclonal antibodies, Lym-1 and Lym-2, reactive with human B-lymphocytes and derived tumors, with immunodiagnostic and immunotherapeutic potential. Cancer Res. 47, 830–840.

Govindan, S.V., Goldenberg, D.M., Griffiths, G.L., Leung, S., Losman, M.J., Hansen, H.J., 1995. Site-specific modifications of light chain glycosylated antilymphoma (LL2) and anti-carcinoembryonic antigen (hImmu-14-N) antibody divalent fragments. Cancer Res. 55, 5721s–5725s (Suppl.).

Grey, H.M., Colon, A.M., Chesnut, R.W., 1982. Requirements for the processing of antigen by antigen-presenting B cells. II. Biochemical comparison of the fate of antigen in B cell tumors and macrophages. J. Immunol. 129, 2389–2395.

Hanna, R., Ong, G.L., Mattes, M.J., 1996. Processing of antibodies bound to B-cell lymphomas and other hematological malignancies. Cancer Res. 56, 3062–3068.

Hanna, R., Ong, G.L., Mattes, M.J., 1998. Correction. Cancer Res. 58, 375.

Kyriakos, R.J., Shih, L.B., Ong, G.L., Patel, K., Goldenberg, D.M., Mattes, M.J., 1992. The fate of antibodies bound to the surface of tumor cells in vitro. Cancer Res. 52, 835–842.

Lamoyi, E., 1986. Preparation of $F(ab')_2$ fragments from mouse IgG of various subclasses. Methods Enzymol. 121, 652–663.

Mattes, M.J., 1987. Biodistribution of antibodies after intraperitoneal or intravenous injection and effect of carbohydrate modifications. J. Nat. Cancer Inst. 79, 855–863.

Mattes, M.J., Griffiths, G.L., Diril, H., Goldenberg, D.M., Ong, G.L., Shih, L.B., 1994. Processing of antibody-radioisotope conjugates after binding to the surface of tumor cells. Cancer 73, 787–793 (Suppl.).

Nikula, T.K., Bocchia, M., Curicio, M.J., Sgouros, G., Ma, Y., Finn, R.D., Scheinberg, D.A., 1995. Impact of the high tyrosine fraction in complementarity determining regions: measured and predicted effects of radioiodination on IgG immunoreactivity. Molec. Immunol. 32, 865 872.

Pinet, V., Vergelli, M., Martin, R., Bakke, O., Long, E.O., 1995. Antigen presentation mediated by recycling of surface HLA-DR molecules. Nature 375, 603–606.

Pisoni, R.L., Acker, T.L., Lisowski, K.M., Lemons, R.M., Thoene, J.G., 1990. A cysteine-specific lysosomal transport system provides a major route for the delivery of thiol to human fibroblast lysosomes: possible role in supporting lysosomal proteolysis. J. Cell Biol. 110, 327–335.

Reid, P.A., Watts, C., 1990. Cycling of cell-surface MHC glycoproteins through primaquine-sensitive intracellular compartments. Nature 346, 655–657.

Rose, L.M., Gunasekera, A.H., DeNardo, S.J., DeNardo, G.L., Meares, C.F., 1996. Lymphoma-selective antibody Lym-1 recognizes a discontinuous epitope on the light chain of HLA-DR10. Cancer Immunol. Immunother. 43, 26–30.

Ruud, E., Blomhoff, H.K., Funderud, S., Godal, T., 1986. Internalization and processing of antibodies to surface antigens on human B cells. Monoclonal anti-IgM antibodies are processed differently than monoclonal antibodies towards non-Ig surface receptors. Eur. J. Immunol. 16, 286–291.

Ruud, E., Kindberg, G.M., Blomhoff, H.K., Godal, T., Berg, T., 1988. Degradation of a monoclonal anti-μ chain antibody in a human surface IgM-positive B cell line starts in prelysosomal vesicle. J. Immunol. 141, 2951–2958.

Ruud, E., Michaelsen, T., Kindberg, G.M., Berg, T., Funderud, S., Godal, T., 1989. Heterogeneity of degradation of B-cell endocy-

tosed monoclonal antibodies reacting with different sIgM epitopes. Scand. J. Immunol. 29, 299–308.

Shih, L.B., Thorpe, S.R., Griffiths, G.L., Diril, H., Ong, G.L., Hansen, H.J., Goldenberg, D.M., Mattes, M.J., 1994. The processing and fate of antibodies and their radiolabels bound to the surface of tumor cells in vitro: a comparison of nine radiolabels. J. Nucl. Med. 35, 899–908.

Stevenson, G.T., 1997. Chemical engineering at the antibody hinge. Chemical Immunol. 65, 57–72.

Vangeepuram, N., Ong, G.L., Mattes, M.J., 1997. Processing of antibodies bound to B-cell lymphomas and lymphoblastoid cell lines. Cancer 80, 2425–2430 (Suppl.).

Wang, B.S., Kelley, K.A., Lumanglas, A.L., Zimmer, A.M., Durr, F.E., 1989. Internalization and shedding of Lym-1 monoclonal antibody following interaction with surface antigens of a cultured human B cell lymphoma. Cell. Immunol. 123, 283–293.

Watts, C., 1997. Capture and processing of exogenous antigens for presentation on MHC molecules. Ann. Rev. Immunol. 15, 821–850.

Zhong, G., Romagnoli, P., Germain, R.N., 1997. Related leucine-based cytoplasmic targeting signals in invariant chain and major histocompatibility complex class II molecules control endocytic presentation of distinct determinants in a single protein. J. Exp. Med. 185, 429–438.

NUCLEAR MEDICINE AND BIOLOGY

INTERNATIONAL JOURNAL OF RADIATION APPLICATIONS AND INSTRUMENTATION PART B

Founder Editor: *The late Professor J. Sternberg*

Publishing Office: Pergamon Press plc, Pergamon House, Bampfylde Street, Exeter EX1 2AH, England [*Tel.* Exeter (0392) 51558; *Fax* 425370]

Subscription and Advertising Offices: North America: Pergamon Press Inc., 395 Saw Mill River Road, Elmsford, NY 10523, U.S.A.

Rest of the World: Pergamon Press plc, Headington Hill Hall, Oxford OX3 0BW, England [*Tel.* Oxford (0865) 794141]

Institutional Subscription Rates 1991. Part B, Nuclear Medicine and Biology: 1-yr, US$340.00; 2-yr, US$646.00. Combined Subscriptions Parts A–E: 1-yr, US$2105.00; 2-yr, US$3999.50. Part A, Applied Radiation and Isotopes: 1-yr, US$655.00; 2-yr, US$1244.50. Part C, Radiation Physics and Chemistry: 1-yr, US$765.00; 2-yr, US$1453.50. Part D, Nuclear Tracks and Radiation Measurements: 1-yr, US$440.00; 2-yr, US$836.00. Part E, Nuclear Geophysics: 1-yr, US$275.00; 2-yr, US$522.50. A personal subscription rate for those whose library subscribes at the regular rate is available on request. Subscription rates for Japan include despatch by air and prices are available on application. All prices are subject to amendment without notice.

Back Issues: Back issues of all previously published volumes, in both hard copy and on microform, are available direct from Pergamon Press offices.

Publication Frequency: 8 issues per annum.

♾™ The text paper used in this publication meets the minimum requirements of American National Standard for Information Sciences—Permanence of Paper for Printed Library Materials, ANSI Z39.48-1984.

Nucl. Med. Biol. Vol. 18, No. 7, pp. 695–703, 1991
Int. J. Radiat. Appl. Instrum. Part B
Printed in Great Britain.

0883-2897/91 $3.00 + 0.00

Direct ^{99m}Tc Labeling of Monoclonal Antibodies: Radiolabeling and *In Vitro* Stability

J. Y. GARRON, M. MOINEREAU, R. PASQUALINI and J. C. SACCAVINI

CIS bio international Compagnie ORIS Industrie, Department of Biomedical Imaging Applications, BP 32, 91192 Gif-sur-Yvette Cedex, France

(Received 30 December 1990)

Direct labeling involves ^{99m}Tc binding to different donor groups on the protein, giving multiple binding sites of various affinities resulting in an *in vivo* instability. The stability has been considerably improved by activating the antibody using a controlled reduction reaction (using 2-aminoethanethiol). This reaction generates sulfhydryl groups, which are known to strongly bind ^{99m}Tc. The direct ^{99m}Tc antibody labeling method was explored using whole antibodies and fragments. Analytical methods were developed for routine evaluation of radiolabeling yield and *in vitro* stability.

Stable direct antibody labeling with ^{99m}Tc requires the generation of sulfhydryl groups, which show high affinity binding sites for ^{99m}Tc. Such groups are obtained with 2-aminoethanethiol (AET), which induces the reduction of the intrachain or interchain disulfide bond, with no structural deterioration or any loss of immunobiological activity of the antibody. The development of fast, reliable analytical methods has made possible the qualitative and quantitative assessment of technetium species generated by the radiolabeling process. Labeling stability is determined by competition of the ^{99m}Tc–antibody bond with three ligands, Chelex 100 (a metal chelate-type resin), free DTPA solution and 1% HSA solution.

Very good ^{99m}Tc–antibody stability is obtained with activated IgG (IgGa) and Fab′ fragment, which makes these substances possible candidates for immunoscintigraphy use.

Introduction

Among the radionuclides currently used in nuclear medicine, ^{99m}Tc is the most suitable element for imaging applications, due to its nuclear properties (radiation energy $E = 140$ keV, half-life = 6.02 h) and its availability from a generator. However, when used in direct-bonding to an antibody, this radioisotope has major disadvantages: ^{99m}Tc is linked to the antibody through sites of two different types (Paik *et al.*, 1985): low-affinity, high-capacity sites (COOH, NH_2... groups) giving unstable *in vivo* compounds which undergo a transchelation process with plasma proteins, and high-affinity, low-capacity sites with no transchelation. Steigman *et al.* (1975), and later Paik *et al.* (1985) have shown the high-affinity sites to be correlated with the presence of free sulfhydryl groups on the antibody. Several authors (Shwarz and Steinstrasser, 1987; Pak *et al.*, 1989; Takhur, 1990), have used controlled reduction reactions to generate such -SH groups, through incubation of antibody with a reducing agent (e.g. dithiothreitol, 2,3-dihydroxybutane-1,4-dithiol, β-mercaptoethanol). This activation technique has been applied to anti-CEA IgG antibody and to Fab′ fragment using 2-aminoethanethiol(AET). ^{99m}Tc antibody labeling was carried out under homogeneous phase conditions, using tin pyrophosphate kit to reduce pertechnetate. At the same time, heterogeneous phase labeling was undertaken, using stannous ion as reducing agent. Simple, fast and reliable analytical techniques were developed to assess radiolabeling efficiency and ^{99m}Tc antibody stability.

Materials and Methods

Antibodies

Anti-carcinoembryonic antigen (aCEA) (whole anti-CEA, IgG: CIS bio international) 10 mg/mL solution in 0.1 M phosphate pH 7.0 buffer. Anti-CEA Fab′ antibody, 10 mg/mL solution in 0.1 M phosphate buffer pH 7.0.

Chemical Antibody Activation

IgG whole antibody was activated by a controlled reduction reaction. To 500 μL of a CEA solution (10 mg/mL) were added 125 μL of 0.5 M phosphate buffer, 5 mM EDTA, pH 6.0, and 50 μL of a 2 M 2-aminoethanethiol (AET, Sigma) in 0.1 M phosphate buffer, 5 mM EDTA, pH 6.0, solution: ([AET]/[IgG] = 3000). After 30 min room temperature, time-activated

IgG (IgGa) solution was purified by gel filtration (using HR 200 Sephacryl 1.6 × 30 cm Pharmacia column) and diafiltered (Filtron, NMWL with 10,000 Da membrane cut-off), then concentrated to 5–10 mg/mL in 0.15 M NaCl. Fab′ fragments were obtained by a controlled reduction reaction of Fab'_2 fragment using AET for 2 h 30 min in the same buffer at a molar ratio [AET]/[Fab'_2] = 2000. After purification using HR200 gel filtration with 0.1 M phosphate buffer, 5 mM EDTA, pH 6.0, Fab′ solution was stored at 4°C in the same buffer at 5–10 mg/mL concentration to prevent any recombination.

Antibody Analysis

Antibodies were analyzed before and after the reduction step, using the following methods:

—High performance gel filtration chromatography system using a TSK 3000 column (30 × 0.75 cm, HPLC System, Pharmacia). 20 μg of antibody samples were eluted with a 0.07 M (0.15 M NaCl) phosphate buffer, pH 7.4, at 1 mL/min flow-rate and monitored by u.v. detection (LKB).

—Antibody concentration was measured by u.v. absorption at 280 nm (Shimadsu u.v. 160 detector).

—SDS–PAGE electrophoresis under nonreducing and reducing conditions, over a 10–15% gradient polyacrylamide gel (Phast System Pharmacia). 10 μL of antibody (1 mg/mL) was loaded on the gel. Following 30 min migration time in 0.2 M Tris–glycine, buffer 0.55% SDS, pH 8.1, the antibody was revealed by the Coomassie blue dye method.

—Number of -SH groups generated was determined using Ellman's method. To 0.01 μmol of antibody, 0.1 μmol of Ellman's reagent was added in 0.1 M bicarbonate buffer, pH 8.0. Sulfhydryl group concentration was determined at 412 nm absorbance using the molar extinction coefficient of the released anion, 13,600 M^{-1} cm^{-1}, pH 8.0. The total labile disulfide bonds (i.e. reducible without denaturation of antibody; Mage and Harrison, 1966) was obtained using AET at concentrations ranging from 2 to 6 M during 30,120 min and 24 h.

—The reaction was also carried out in denaturing conditions (IgG samples were treated with 2.5% SDS, 5% mercaptoethanol at 100°C for 4 min). In this condition other disulfide bonds are available to the reducing agent. The samples were purified by gel filtration (PD10: Pharmacia) and the number of -SH measured.

—To determine antibody immunoreactivity, a sandwich-type technique was used (Kit ELSA 2 CEA; CIS bio international). The method consists of a competition between antibody being evaluated and anti-CEA ^{125}I (from the kit) with respect to CEA antigen. Decreasing quantities (100 μL of 10^{-1}–10^{-8} dilutions obtained from 1 mg/mL solution) of antibody evaluated (IgG, IgGa, Fab'_2, Fab′) were incubated at 37°C for 3 h with 300 μL (10 ng) of anti-CEA ^{125}I and 100 μL (20 units) of antigen. For each dilution, the amount of radioactivity bound to the multifinned stick was counted. The ratio of bound radioactivity to total radioactivity (B/T) was read on the semi-logarithmic curve as a function of the dilution. Antibody titre was given by the dilution value corresponding to 50% inhibition.

Radiolabeling of Intact Antibody and Fab′ Fragment

Homogeneous phase process labeling

^{99m}Tc eluted from the generator (CIS bio international) in the form of pertechnetate ($^{99m}TcO_4^-$) was reduced by stannous ions, the reagent used was a tin pyrophosphate salt in a NaCl isotonic solution, that had been previously lyophilized (Bardy *et al.*, 1975). The initial quantities of tin chloride dihydrate and sodium pyrophosphate decahydrate present in the solution were, respectively, 0.048 and 1.16 mg.

1 mg of antibody (10 mg/mL solution) and $^{99m}TcO_4^-$ solution (final activity = 37 MBq/mL) were added to the vial containing the lyophilized product. The reaction time was 1 h at room temperature and the final volume 1 mL.

Heterogeneous phase process labeling

The reduction system consisted of a 2 mL silica resin (Prolabo Actigel) saturated with stannous ions. This heterogeneous process was developed 10 years ago in our laboratory (Pasqualini *et al.*, unpublished) in order to obtain methylene diphosphonate (MDP) labeled with low stannous ion content. Experiments with ^{117}Sn showed us that MDP was labeled with ^{99m}Tc (3 mg of MDP with 740 MBq) with only 35 μg of stannous ions in the final solution. The uncomplexed technetium (15%) was firmly retained on the silica column. This method also works for DTPA, DMSA and other usual radiopharmaceutical ligands. Basically tin fluoride solution (1 mg of a 5 mg/mL solution in 10^{-2} N HCl) was absorbed on the resin. Stannous ions not taken up by the resin were removed by washing with 0.15 M NaCl solution. A sample containing 1 mg antibody and $^{99m}TcO_4^-$ (37 MBq) was deposited on the column and eluted by 0.15 M NaCl. 0.5 mL fractions were collected and their radioactivity measured with an ionization chamber. The amount of antibody collected in the fractions was measured by absorption at 280 nm after radioactivity decay.

Labeling yield determination

Two techniques were used to identify the various products formed during the reaction. A thin-layer chromatography (ITLCSG Gelman), using methylethylketone (MEK) as solvent, to determine the percentage of unreduced $^{99m}TcO_4^-$. This method, however, did not permit separation of ^{99m}Tc–pyrophosphate from ^{99m}Tc–antibody. This was possible using

: 37°C for 3 h with
^{125}I and 100 μL
ach dilution, the
to the multifinned
· of bound radio-
(B/T) was read on
a function of the
ven by the dilution
inhibition.

ntibody
it

ig

ır (CIS bio inter-
ıte ($^{99m}TcO_4^-$) was
agent used was a
isotonic solution,
zed (Bardy *et al.*,
chloride dihydrate
ıydrate present in
.048 and 1.16 mg.
tion) and $^{99m}TcO_4^-$
'mL) were added
ized product. The
nperature and the

ng

a 2 mL silica resin
annous ions. This
ed 10 years ago in
published) in order
te (MDP) labeled
Experiments with
abeled with ^{99m}Tc
ith only 35 μg of
The uncomplexed
ined on the silica
or DTPA, DMSA
l ligands. Basically
ng/mL solution in
sin. Stannous ions
noved by washing
ample containing
Bq) was deposited
M NaCl. 0.5 mL
heir radioactivity
er. The amount of
was measured by
ctivity decay.

entify the various
ion. A thin layer
ın), using methyl-
to determine the
This method, how-
^{99m}Tc–pyrophos-
was possible using

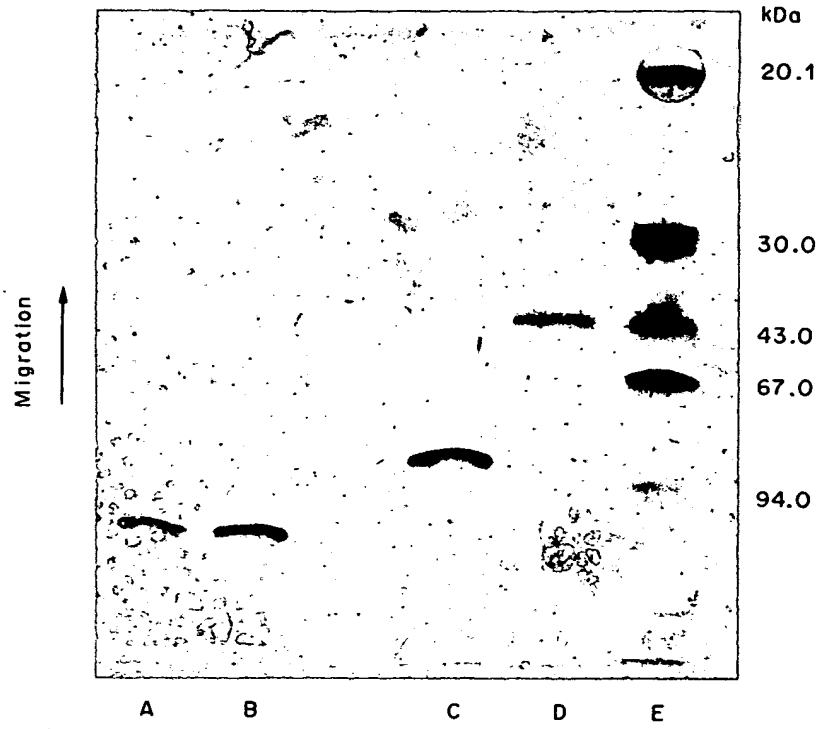

Fig. 1. SDS–PAGE (10–15%) under nonreducing conditions. Gel was Coomassie blue stained. Samples: A, no activated IgG; B, activated IgG (IgGa); C, Fab'_2; D, Fab'; E, LMW calibration kit protein standards.

the centrifugal ultrafiltration technique (Amicon, CF50 or CF25). After centrifugation at 4000 rpm for 20 min, membrane radioactivity was measured. The membrane retained the entire radioactivity associated with antibody. ^{99m}Tc–pyrophosphate and $^{99m}TcO_4^-$ were filtered (10% of ^{99m}Tc radioactivity was absorbed by the membrane).

Radioimmunoreactivity of antibodies labeled with ^{99m}Tc

Radioimmunoreactivity was measured by affinity chromatography on a Sepharose 4B conjugated with carcinoembryonic antigen (CEA) in a ratio of 5000 units for 1 g of Sepharose. 100 μL of the phase were deposited in an Eppendorf tube. 100 μL of 0.05 M phosphate buffer, pH 7.4, and 100 μL of radiolabeled antibody solution (2 ng) were added to the phase. In another tube, nonspecific fixation was calculated by saturation of antigenic sites with cold antibody. After 1 h of stirring, the unfixed fraction was removed by centrifugation at 12,000 rpm. The immunoreactivity percentage was determined by the ratio:

$$\%IR = \frac{\text{radioactivity fixed on the Sepharose}}{\text{total radioactivity}} \times 100.$$

Animal biodistribution

Athymic female nude mice (NMRI/nu–nu/RJ background) were injected (s.c.) in the right flank with an LS174T colorectal carcinoma cells suspension (2.5×10^6 cells in 0.1 mL saline). Two weeks after injection, LS174T tumors had grown up to an average of 0.4 g. Tissue biodistribution was performed after i.v. injection in the tail vein of 4–10 μg of ^{99m}Tc-labeled whole antibody or fragment Fab′ (3.3 MBq). Respectively 2, 6 and 24 h after injection 3 animals were sacrificed, and organs were weighed and counted in a γ counter (Packard 500). Biodistribution data were expressed as percent of injected dose per gram of organ.

Investigation of ^{99m}Tc–Antibody Bond Stability

Competition with the Chelex 100 chelating resin

Chelex 100 is a styrene divinyl benzene copolymer having iminodiacetate functions capable of chelating metal ions (Barker *et al.*, 1979; O'Keef *et al.*, 1980). When in competition with ^{99m}Tc–IgG, ^{99m}Tc–IgGa or ^{99m}Tc–Fab′, Chelex 100 displaces the ^{99m}Tc bound to antibody low-affinity sites. The radioactivity associated with antibody after competition represents the ^{99m}Tc linked to high-affinity sites. Competition studies between ^{99m}Tc–antibody solution and 100 mg of Chelex 100 were undertaken in hemolytic tubes. Prior to use, the resin is converted to sodium salt form by flushing with 0.5 M NaOH, then washing with water. The exchange reaction occurred at two pH levels (7.2 and 8.4) at room temperature in 30 min. Following separation by centrifugation, the radioactivity retained by the resin and present in the supernatant was determined. High-affinity site determination corresponded to the radioactivity present in the supernatant fraction multiplied by the labeling yield.

Competition with DTPA

Diethylene-triamino-pentaacetic acid (DTPA) has a strong chelating effect on ^{99m}Tc. To investigate the transchelating process, ^{99m}Tc–IgG, ^{99m}Tc–IgGa, and ^{99m}Tc–Fab′ (0.5 mg) solutions were incubated for 6 h with a DTPA/antibody at a molar ratio of 1000. The exchange reaction between antibody and DTPA was investigated for pH values from 7.2 to 9.4. Reaction products were analyzed by ITLCSG in acetonitrile:H_2O (3:2) chromatographic system. R_f values are: ^{99m}Tc–antibody = 0.0, ^{99m}Tc–DTPA = 0.5–0.6, $^{99m}TcO_4^-$ = 1.0.

Stability studies in presence of human serum albumin (HSA)

^{99m}Tc–antibody bond stability was measured in competition with 1% HSA solution. 100 μL of antibody (10 mg/mL) was added to 50 μL of 20% HSA solution. The final volume was brought to 1 mL by the addition of 0.15 M NaCl solution. The solution was then incubated at 37°C and 20 μL aliquots were analyzed at different times using high-performance anion-exchange chromatography (mono Q HR5/5; HPLC system, Pharmacia). The solution was eluted with saline gradient: 20 mM Tris buffer, pH 8.0, to 20 mM Tris buffer, 1 M NaCl, pH 8.0, in 15 min, at 1 mL/min flow-rate and monitored by u.v. and radioactivity detectors. In this system IgG and IgGa were eluted at 0.16 M NaCl, and Fab′ at 0.1 M NaCl. HSA was eluted in the form of two peaks corresponding, respectively, to 0.23 and 0.36 M NaCl.

Results

Antibody analysis

HPLC analysis. The elution peaks of native, whole IgG and IgGa were detected at 8.16, 8.51 min for fragment Fab'_2 and at 9.55 min for Fab′.

SDS analysis. The above results were confirmed by electrophoresis, a more sensitive method which showed only one migration band for each antibody form investigated (Fig. 1).

-SH measurement. (a) Under nondenaturing conditions: the average number of sulfhydryl groups generated in 30 min with a ratio of [AET]/[IgGa] = 3000 was 4.30 ± 0.30 per IgG mol and 2.20 ± 0.19 per Fab′ mol. The highest number of labile sulfhydryl groups recovered was 8.0 for a ratio of [AET]/[IgGa] = 9000 at 120 min. (b) Under denaturing conditions: the average number of sulfhydryl groups generated in these conditions was 21.0 per IgG mol.

Immunoreactivity

Results showed that immunoreactivities of whole antibody IgG and IgGa were 16.5 and 18 ng, respectively. Fragment Fab′ and its precursor showed respective immunoreactivities of 134 and 63 ng.

Table 1. Results of direct ^{99m}Tc–antibody labeling using homogeneous phase process

Antibody \ Labeling efficiency (%)	^{99m}Tc-Antibody Tc-Pyro.*	$^{99m}TcO_4^-$*	^{99m}Tc-antibody†	^{99m}Tc-Pyro†	$^{99m}TcO_4^-$†
IgG	95 (94–96)	5.0 (4.0–6.0)	31.6 (30.2–33.8)	63.5 (61.6–65)	4.8 (4.6–5.0)
IgGa	99.1 (98.5–99)	0.9 (0.2–1.5)	98.1 (98–98.4)	0.93 (0.5–1.7)	0.92 (0.27–1.5)
Fab'_2	64.5 (54–62.4)	35.23 (22–46)	29.1 (18–29.6)	41.16 (30–59.8)	29.9 (22.1–37.7)
Fab'	92.2 (99–99.3)	0.86 (0.7–1.0)	98.2 (97.2–94.4)	1.0 (0.56–1.8)	0.68 (0.04–1.0)

The results are expressed as the average and range of triplicate experiments.
*Results obtained on ITLCSG with MEK.
†Results obtained by ultrafiltration on CF50 (whole Ab) or CF25 (fragments) membranes.

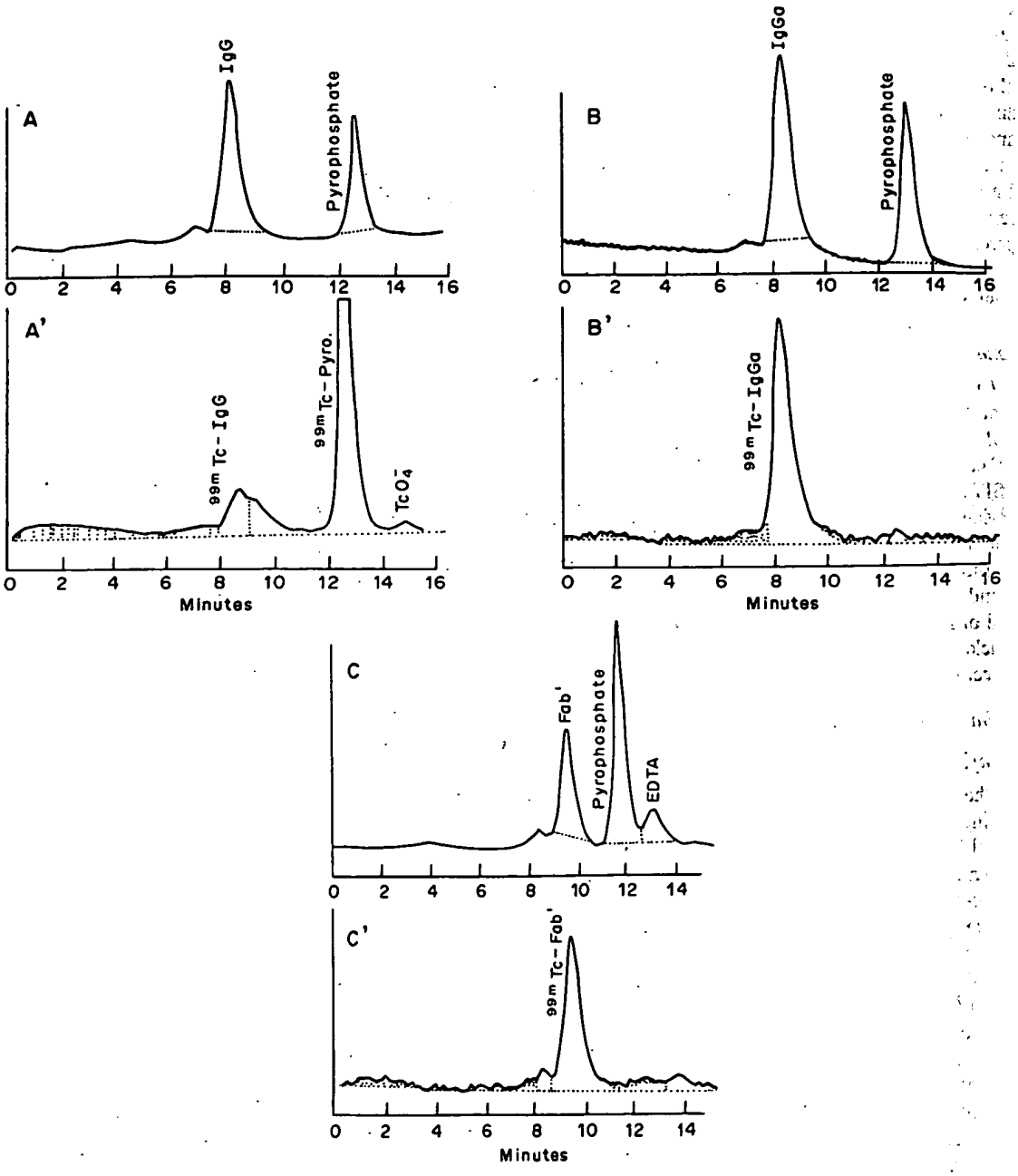

Fig. 2. High performance gel filtration chromatography TSK 3000. Elution in 0.07 M phosphate buffer, pH 7.4: 20 μg antibody injection, 1 mL/min flow-rate. (A) IgG elution profile at 280 nm; (A′) IgG radioactivity elution profile (elution efficiency >95%); (B) IgGa elution profile at 280 nm; (B′) IgGa radioactivity elution profile (elution efficiency >95%); (C) Fab′ elution profile at 280 nm; (C′) Fab′ radioactivity elution profile (elution efficiency >95%).

Table 2. Results of direct ^{99m}Tc–antibody labeling using heterogenous phase process

Antibody \ Labeling efficiency	^{99m}Tc–antibody (%)	$^{99m}TcO_4$ (%)
IgG	98.6 (98.0–99.0)	1.33 (1.0–2.0)
IgGa	99.0 (99.0–99.0)	1.0 (1.0–1.0)
Fab'$_2$	40.6 (39.0–43.0)	59.3 (57.0–61.0)
Fab' in 5 mM EDTA	66.5 (60.0–73.0)	3.0 (2.0–4.0)

The results are expressed as average and range of triplicate experiments.

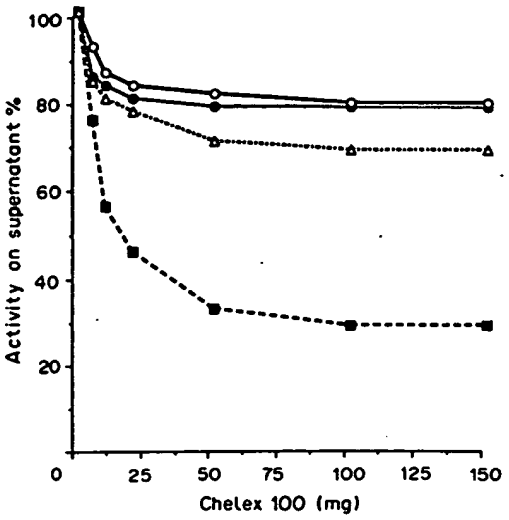

Fig. 3. ^{99m}Tc–antibody bond stability studies by competition with Chelex 100. —○—, ^{99m}Tc–IgCa: heterogeneous or homogeneous process labeling; ··●··, ^{99m}Tc–Fab': homogeneous process labeling; ·–·△·–·, ^{99m}Tc–IgG + ^{99m}Tc–Pyro. + TcO_4^-: homogeneous process labeling; – –■– –, ^{99m}Tc–IgG: heterogeneous process labeling.

Labeling

Labeling of IgG and its fragments with ^{99m}Tc was attempted, using tin pyrophosphate. Concentrations of $SnCl_2 \cdot 2H_2O$ (0.048 mg/mL) and $Na_4P_2O_7 \cdot 10H_2O$ (1.16 mg/mL) were optimized to give the highest labeling efficiency. After 1 h antibody incubation time with reducing agent and $^{99m}TcO_4^-$, ITLCSG chromatography and membrane filtration showed an average labeling of 31.6% for IgG, 98.1% for IgGa, 29% for Fab'$_2$ and 98.2 for Fab' (Table 1). These results were confirmed by HPLC analysis (Fig. 2). Antibody radiolabeling with ^{99m}Tc by elution in a tin saturated silica column gave the following results expressed in Table 2.

The results should be compared with those obtained by the homogeneous phase labeling method using tin pyrophosphate. Labeling efficiency was the same with IgGa. When using the silica labeling method, IgG showed a markedly higher yield (99% instead of 31.6%). Buffer of fragment Fab' contained 5 mM EDTA, this latter chelated ^{99m}Tc (30.5%) when passing over the resin. In the case of Fab'$_2$, labeling efficiency was slightly greater in the heterogenous process labeling, although it remained low.

Effect of ^{99m}Tc labeling on immunoreactivity. Radioimmunoreactivity is not affected by ^{99m}Tc; the values are 90% for ^{99m}Tc–IgGa against 88% for ^{131}I–IgGa. As radiolabeling with ^{131}I is the better-known process, it will be taken as reference (^{131}I–antibody labeling was carried out using the iodogen method). The immunoreactivity of ^{99m}Tc–Fab' was 87% compared to 82% obtained with ^{131}I–Fab'.

^{99m}Tc–antibody bond stability

Competition with iminodiacetate groups. ^{99m}Tc–IgG, ^{99m}Tc–IgGa and ^{99m}Tc–Fab' competition with Chelex 100 resin showed that an equilibrium exchange was reached with 100 mg of resin (Fig. 3). Antibody concentration remained unchanged during incubation with resin. Theoretically the iminodiacetic groups on resin are able to bind heavy metals strongly. Firstly we determined $^{99m}TcO_4^-$ and "reduced" ^{99m}Tc–pyrophosphate absorption. $^{99m}TcO_4^-$ uptake was high with an average of 18% (16–26% range). ^{99m}Tc–pyrophosphate uptake was higher 55% (52–66%) but this was not very surprising because of the known exchange properties of this product.

For ^{99m}Tc–antibody labeling obtained by use of the pyrophosphate kit, the percentages of radioactivity exchange were respectively, 62, 20 and 23% for IgG, IgGa and Fab' (Fig. 3). A second competition displaced only 1% of the radioactivity. Considering the labeling yield achieved, it appeared that, for IgGa and Fab' fragment, the only activity which can be displaced is that associated with the antibody, whereas in the case of IgG, where the labeling efficiency is only 31.6%, the radioactivity uptake by the resin is also due in part to ^{99m}Tc–pyrophosphate and TcO_4^- present in the initial solution. If we take into account the nonspecific absorption ($^{99m}TcO_4^-$, ^{99m}Tc–pyrophosphate) we conclude that Chelex displaced only 5% technetium radioactivity from the IgG.

Table 3. ^{99m}Tc–antibody labeling stability study by competition with 100 mg of Chelex 100. High-affinity sites percent determination

	Labeling using pyrophosphate kit			Labeling using Sn silica column			
Antibody	Eff.*	^{99m}Tc–antibody	HAS†	Eff.*	^{99m}Tc–antibody	HAS†	-SH/Ab
IgG	31.6%	95%	30%	98.6%	30%	29.6%	—
IgGa	98.1%	80%	78.5%	99%	80%	79.2%	4.30 ± 0.30
Fab'	98.2%	75%	73.6%	ND	ND	ND	2.20 ± 0.19

*Labeling efficiency.
†High affinity sites.

Table 4. Biodistribution of ^{99m}Tc radiolabeled antibodies in nude mice, obtained 2, 6 and 24 h after injection

	% Injected dose/g								
	^{99m}Tc-IgG			^{99m}Tc-IgGa			^{99m}Tc-Fab'		
Tissue	2 h	6 h	24 h	2 h	6 h	24 h	2 h	6 h	24 h
Blood	4.20 ± 0.53	2.20 ± 0.55	0.50 ± 0.10	24.7 ± 4.60	21.8 ± 1.71	8.60 ± 0.95	13.2 ± 1.48	3.90 ± 0.53	0.50 ± 0.06
Liver	15.6 ± 5.64	11.0 ± 1.08	4.20 ± 1.53	10.9 ± 1.99	8.80 ± 4.07	5.30 ± 1.35	7.30 ± 0.81	5.60 ± 0.88	2.00 ± 0.50
Kidneys	7.50 ± 1.56	4.90 ± 0.76	1.60 ± 0.76	9.40 ± 1.97	14.8 ± 7.02	6.60 ± 0.90	75.4 ± 8.79	5.20 ± 11.69	20.0 ± 2.72
Tumor	0.60 ± 0.15	1.20 ± 1.13	0.30 ± 0.01	2.70 ± 1.04	3.60 ± 0.81	6.60 ± 2.50	6.30 ± 0.25	4.30 ± 0.16	4.50 ± 1.09
Urinary clearance	38.1 ± 1.17	4.01 ± 4.40	59.9 ± 6.85	12.9 ± 1.65	12.4 ± 1.01	33.6 ± 4.48	36.7 ± 2.47	48.0 ± 5.25	77.5 ± 5.59

Mean ± SD for 3 animals.

For ^{99m}Tc-antibody labeling under heterogeneous phase conditions, study showed the same exchange profile for IgGa, losing about 20% of its radioactivity, whereas the uptake from IgG was 70% (Fig. 3). Percentage calculations for high affinity sites gave 30% for IgG, whereas the percentages were 79 and 73%, respectively, for IgGa and Fab' (Table 3).

Competition in the presence of DTPA. Dissociation of technetium radioactivity from antibody under excess DPTA was greater at pH 8.4 than at pH 7.5. The radioactivity associated to antibody labeled using tin pyrophosphate was (after 6 h of competition) 90% for IgG, 98% for IgGa and 97% for Fab'. When antibody was labeled by the heterogeneous phase reduction method, the values obtained were, 97 and 60%, respectively, for IgGa and IgG.

Competition with HSA. ^{99m}Tc-antibody incubation with HSA at 37°C confirmed the above results, showing a very high stability of ^{99m}Tc-IgGa and ^{99m}Tc-Fab' bonds. 13 and 20% were respectively lost during 6 h competition study. IgG retained only a total of 9% of its initial radioactivity.

In vivo biodistribution

The biodistribution data are summarized in Tables 4 and 5.

The results in Table 5 showed that in mice the time 24 h after injection gave the better tumor/organ ratio. At this time, ^{99m}Tc-IgG and ^{99m}Tc-IgGa disclosed significant differences in tissue radioactivities. For ^{99m}Tc-IgGa we obtained 6.6% of injected dose/g (%ID/g) in tumor and 8.6%ID/g in blood; for ^{99m}Tc-IgG we obtained 0.3%ID/g in tumor and 0.5%ID/g in blood (Table 4). The lowest tumor uptake and blood activity and the highest level of urinary clearance obtained with ^{99m}Tc-IgG demonstrated the lability of the ^{99m}Tc-antibody bond when ^{99m}Tc reacted with intact nonactivated antibody.

The level of tumor uptake was almost the same for ^{99m}Tc-IgGa and ^{99m}Tc-Fab'. The lower blood activity for the latter did not reflect instability of the ^{99m}Tc bond but was the result of a fast fragment Fab' blood clearance. Also for this compound an accumulation in the kidneys of 20%ID/g and a higher urinary excretion of 77%ID/g were noticed.

Discussion

Sulfhydryl groups account for the existence of high affinity sites. A number of methods can be used to improve labeling yield and ^{99m}Tc-antibody bond stability. To avoid the problem of low affinity sites Paik *et al.* (1985) labeled IgG and fragment Fab'_2 with stannous ions in the presence of DTPA. This method has the disadvantage of producing ^{99m}Tc-IgG and ^{99m}Tc-Fab'_2 which are stable in low yield (i.e. 24 and 16%, respectively). The authors then used a two step reaction (Paik *et al.*, 1986) which consists initially of a labeling phase in the presence of stannous ions, and then subsequent competition with free DTPA. The stable labeling percentage thus obtained was 54.5% for Fab'_2 and 70% for IgG. Rhodes *et al.* (1986) used the pre-tinning method, which consists of generating SH groups from the disulfide bridges present on the antibody, by 21-h incubation with the reducing agent (stannous ions); a high degree of labeling stability is shown for IgG (Hawkins *et al.*, 1990).

The method used in our work is based on the generation of -SH groups for IgG and Fab' through a brief controlled reaction. The two antibody radiolabeling investigations performed under homogeneous and heterogeneous processes have shown the efficiency of our quality control to determine the labeling yield and to establish a relation between the sulfhydryl groups and the stability of the ^{99m}Tc-bond.

Heterogeneous phase labeling results indicate that in the absence of complexing anion, even one with low chelating power like pyrophosphate, the IgG labeling is high (98.6%) but very unstable. Following incubation with Chelex 100 resin, the radioactivity

Table 5. Biodistribution of ^{99m}Tc-antibody: g tumor/g organ (T/O) ratio determination

g Tumor/g organ	Tumor/blood			Tumor/liver			Tumor/kidneys		
Time (h)	^{99m}Tc-IgG	^{99m}Tc-IgGa	^{99m}Tc-Fab'	^{99m}Tc-IgG	^{99m}Tc-IgGa	^{99m}Tc-Fab'	^{99m}Tc-IgG	^{99m}Tc-IgGa	^{99m}Tc-Fab'
2	0.15 ± 0.01	0.12 ± 0.03	0.47 ± 0.02	0.05 ± 0.01	0.29 ± 0.07	0.05 ± 0.25	0.07 ± 0.01	0.35 ± 0.07	0.08 ± 0.00
6	0.22 ± 0.01	0.14 ± 0.02	1.11 ± 0.16	0.03 ± 0.01	0.44 ± 0.13	0.76 ± 0.07	0.1 ± 0.00	0.23 ± 0.08	0.08 ± 0.01
24	0.83 ± 0.13	0.86 ± 0.07	6.70 ± 3.00	0.07 ± 0.01	0.90 ± 0.00	2.28 ± 0.24	0.18 ± 0.06	0.81 ± 0.01	0.22 ± 0.01

Mean ± SD for 3 animals.

remaining associated to antibody is only 30%. For IgGa the labeling yield is 98% but only 20% of ^{99m}Tc radioactivity is exchanged with the resin.

Although the presence of pyrophosphate during labeling results in a 31.6% efficiency for IgG, only 5% of the ^{99m}Tc–antibody radioactivity is exchanged after incubation with resin. The labeling yield is high for IgGa 98 and 98.2% for Fab′, and the exchange is low: 20 and 23%. High affinity sites number is identical for both labeling methods, the average percentage for IgG is 30%, a figure comparable with that of Paik *et al.* (1985), whereas it is 79 and 80% for IgGa and Fab′.

The results of competition with HSA show the exchange to be fast in the case of IgG: 20% in 1 h, as compared with 2 and 3% for IgGa and Fab′. After 6 h, an equilibrium is reached: 90% of the ^{99m}Tc–IgG activity is exchanged with HSA, as compared to 13 and 20%, respectively, for IgGa and Fab′.

The stability of the ^{99m}Tc–antibody bond in the presence of DTPA excess at pH 8.4, shows that we have an exchange level of 40% for tin-labeled IgG, as compared with 10% in the case of pyrophosphate-labeled IgG and only 3% for IgGa. Unlike the competition with DTPA, the exchange levels obtained with resin and HSA are very close. The difference can be accounted for by the better chelating agent accessibility when it is present in anionic form (Chelex).

The high tumor uptake for IgGa and Fab′ proves the stable ^{99m}Tc–antibody bond. So the generation of endogenous -SH is realised with no damage to the antibody immunological activity. These results are in agreement with the works of several authors (Schwarz and Steinstrasser, 1987; Pak *et al.*, 1989; Del Rosario and Wahl, 1989). This reaction with a ratio of [AET]/[IgG] = 3000 allows in a short time (30 min) the generation of 50% labile sulfhydryl groups. This amount represents only 20% of total -SH groups available in denaturing conditions. The labeling by tin pyrophosphate kit provides a high degree of stability and does not require post-labeling purification. Our quality control which consists of TLC chromatography and membrane ultrafiltration, is faster than previous methods which required the use of an elaborate molecular gel permeation chromatographic system (Pettit *et al.*, 1980; Rhodes *et al.*, 1982; Dekker *et al.*, 1982). Using the Chelex 100 resin technique, the percentage of high affinity sites, reflecting labeling stability, can be quickly and easily determined.

These results show that it seems quite realistic to introduce the use of ^{99m}Tc-labeled IgGa and Fab′ in routine immunoscintigraphic examinations. Clinical studies are currently in progress.

Acknowledgement—We wish to thank Ms Lecayon and her collaborators who performed the animals studies.

References

Bardy A. Fouye H., Gobin R., Beydon J., De Tovar G., Panneciere C. and Hegesippe M. (1975) Technetium 99m labeling by means of stannous pyrophosphate: application to bleomycin and red blood cells. *J. Nucl. Med.* **16**, 435–437.

Barker R. *et al.* (1979) *Biochem. J.* **177**, 289.

Dekker B. G., Arts C. J. M. and De Ligny C. L. (1982) Gel-chromatographic analysis of ^{99m}Tc-labeled human albumin prepared with Sn II as the reductant. *Int. J. Appl. Radiat. Isot.* **33**, 1331–1357.

Del Rosario R. D. and Wahl R. L. (1989) Site-specific radiolabeling of monoclonal antibodies with biotin/streptavidin. *Nucl. Med. Biol.* **16**, 525–529.

Del Rosario R. D. and Wahl R. L. (1990) Disulfide bond-targeted radiolabeling: tumor specificity of a streptavidin–biotinylated monoclonal antibody complex. *Cancer Res.* (Suppl.) **50**, 804s–808s.

Hawkins E. B., Pant K. D. and Rhodes B. A. (1990) Resistance of direct ^{99m}Tc protein bond to transchelation. *Antibody Immunoconj. Radiopharm.* **3**, 17–25.

Mage M. G. and Harrison E. T. (1966) A comparison of the labile disulfide bonds of rabbit γ G-immunoglobulin fragments. *Archs Biochem. Biophys.* **113**, 709–717.

O'Keef E. T., Hill R. L. and Bell J. E. (1990) *Biochemistry* **19**, 1954.

Paik C., Eckelman W. C. and Reba R. C. (1986) Transchelation of ^{99m}Tc from low affinity sites to high affinity sites of antibody. *Nucl. Med. Biol.* **13**, 359–362.

Paik C. H., Pham L., Hong J. J., Sahami M. S., Head S. C., Reba R. C., Steigman J. and Eckelman W. C. (1985) The labeling of high affinity sites of antibodies with ^{99m}Tc. *Int. J. Nucl. Med. Biol.* **12**, 3–8.

Pak K. Y., Nedelman M. A., Stewart R. and Dean R. T. (1989) A rapid and efficient method for labeling IgG antibodies with Tc-99m and comparison to Tc-99m Fab′ antibody fragments. *J. Nucl. Med.* **30**, 793.

Pak K. Y., Sun L. K., Dean R. T., Ghrayeb J., Nedelman M. and Berger H. J. (1989) Tc-99m labeling of a tumor specific mouse/human chimeric antibody having a human 3 constant region. *J. Nucl. Med.* **30**, 934.

Pettit W. A., Deland F. H., Bennett J. S. and Goldenberg D. M. (1980) Improved protein labeling by stannous tartrate reduction of pertechnetate. *J. Nucl. Med.* **21**, 59–62.

Rhodes B. A., Zamora P. O., Newell K. D. and Valdes E. F. (1986) ^{99m}Tc labeling of murine monoclonal antibody fragments. *J. Nucl. Med.* **27**, 685–693.

Rhodes B. A., Torvestad D. A., Breslow K., Burchiel S. W., Reed K. A. and Austin R. K. (1982) ^{99m}Tc labeling and acceptance testing of radiolabeled antibodies. In *Tumor Imaging Masson* (Edited by Burchiel S. W. and Rhodes B. A.), p. 111.

Schwarz A. and Steinstrasser A. A. (1987) Novel approach to ^{99m}Tc labeled monoclonal antibodies. *J. Nucl. Med.* **28**, 721 (Abstract).

Steigman J., Williams H. P. and Salomon N. A. (1975) The importance of the protein sulfhydryl group in HSA labeling with ^{99m}Tc. *J. Nucl. Med.* **16**, 573.

Thakur M. L. (1990) Radiolabeled blood cells: perspectives and directions. *Nucl. Med. Biol.* **17**, 41–47.

The kinetics of *in vitro* reoxidation and reduction of the inter heavy–light chain disulfide bond in an unusual murine immunoglobulin G myeloma protein lacking inter-heavy chain disulfide bonds

MAIRE E. PERCY,[1] LEBE CHANG,[1] CATHERINE DEMOLIOU,[2] AND REUBEN BAUMAL[3]

Department of Immunology, Research Institute, Hospital for Sick Children, 555 University Avenue, Toronto, Ont., Canada M5G 1X8

Received June 23, 1978

Revised November 15, 1978

Percy, M. E., Chang, L., Demoliou, C. & Baumal, R. (1979) The kinetics of *in vitro* rexoidation and reduction of the inter heavy–light chain disulfide bond in an unusual murine immunoglobulin G myeloma protein lacking inter-heavy chain disulfide bonds. *Can. J. Biochem. 57*, 279–285

After 5 years of subcutaneous transfer in Balb/C mice, our MOPC 173 myeloma tumour line (originally an IgG2a,κ H_2L_2-producer) exclusively synthesized an unusual IgG2b,κ protein lacking inter-heavy (H) chain disulfide bonds. This protein was designated MOPC 173B. On sodium dodecyl sulfate – polyacrylamide gel electrophoresis, it migrated with an apparent molecular weight of 77 000; following complete reduction and alkylation, the mobilities of its constituent H and light (L) chains were found to differ slightly from those of MOPC 173 H_2L_2. MOPC 173B was serologically identical to another typical IgG2b,κ myeloma protein, MOPC 195, and peptide mapping studies showed that it possessed only the inter H–L disulfide bond characteristic of typical IgG2b,κ proteins. In a nondissociating solvent, the sedimentation coefficient of the protein was 6.3S even at concentrations as low as 0.2 mg/ml, indicating that noncovalent interactions existed between two half-molecule subunits. Since this unusual IgG myeloma protein contained only a single category of interchain disulfide bridge, the inter H–L bond, it was an ideal model system for characterization of the kinetics of formation and reduction of interchain disulfide bonds. The kinetics of the glutathione-catalyzed reoxidation of the inter H–L disulfide bridge in MOPC 173B followed an apparent second-order rate equation. In contrast, reduction of its inter H–L bridge under anaerobic conditions with dithioerythritol in excess, was strictly a first-order process and not a simple reversal of the reoxidation. These studies provide the basis for the more complex mathematical models that describe the reoxidation and reduction of typical immunoglobulin molecules.

Percy, M. E., Chang, L., Demoliou, C. & Baumal, R. (1979) The kinetics of *in vitro* reoxidation and reduction of the inter heavy–light chain disulfide bond in an unusual murine immunoglobulin G myeloma protein lacking inter-heavy chain disulfide bonds. *Can. J. Biochem. 57*, 279–285

Après 5 années de transfert sous-cutané à des souris Balb/C, notre lignée tumorale du myélome MOPC 173 (productrice à l'origine d'une IgG2a,κ H_2L_2) synthétise une IgG2b,κ inhabituelle, protéine privée de liaisons disulfure entre les chaînes lourdes (H). Nous désignons cette protéine par MOPC 173B. A l'électrophorèse sur gel de sodium duodécyl sulfate – polyacrylamide, elle se déplace avec un poids moléculaire apparent de 77 000; suite à la réduction complète et à l'alkylation, les mobilités de ses chaînes constituantes H et légères (L) diffèrent quelque peu de celles de la MOPC 173 H_2L_2. Sérologiquement, la MOPC 173B est identique à une autre protéine IgG2b,κ demyélome, la MOPC 195. La cartographie des peptides montre qu'elle ne possède que la liaison disulfure inter H–L caractéristique des protéines IgG2b,κ typiques. Dans un solvant non dissociant, le coefficient de sédimentation de la protéine est de 6.3S et ce, même à ces concentrations aussi faibles que 0.2 mg/mL, preuve de l'existence d'interactions non covalentes entre deux sous-unités de la demi-molécule. Puisque cette protéine IgG inhabituelle ne contient qu'une seule catégorie de pont disulfure interchaines, la liaison inter H–L, elle est un modèle idéal pour caractériser la cinétique de la formation et de la réduction des liaisons disulfure interchaines. La cinétique de la réoxydation catalysée par le

---

ABBREVIATIONS: Ig, immunoglobulin; IgG, immunoglobulin G; H, heavy chain of the Ig molecule; L, light chain of the Ig molecule; κ, light chain of the kappa type; λ, light chain of the lambda type; HL, half molecule; LHHL of H_2L_2, a fully assembled Ig molecule; SDS, sodium dodecyl sulfate; PAGE, polyacrylamide gel electrophoresis; DTE, dithioerythritol; EDTA, ethylenediaminetetraacetic acid.

[1]Present address: Department of Genetics, Research Institute, Hospital for Sick Children, Toronto, Ont., Canada.
[2]Present address: Department of Biochemistry, McMaster University, Hamilton, Ont., Canada.
[3]Present address: Department of Pathology, University of Toronto, Toronto, Ont., Canada.

0008-4018/79/030279-07$01.00/0

glutathion du pont disulfure inter H–L dans la MOPC 173B suit une vitesse d'équation apparente de second ordre. Au contraire, la réduction de son pont inter H–L, dans des conditions anaérobies en présence d'un excès de dithioérythritol, est strictement un processus de premier ordre et non un simple renversement de la réoxydation. Ces résultats servent de base pour les modèles mathématiques plus complexes qui décrivent la réoxydation et la réduction des molécules d'immunoglobine typiques.

[Traduit par le journal]

Introduction

As in other mammalian species, mouse immunoglobulin G consists of two H and two L chains linked by disulfide bonds. There are two categories of interchain disulfide bonds, those joining the H chains (the inter-H bonds) and those linking one L to each H chain (the inter H–L bonds) (1, 2). In the past, the formation of these bonds (covalent assembly) *in vivo* (3, 4) and *in vitro* (5, 6, 7, 8) has been the subject of intensive study. Several possible pathways of interchain disulfide bond formation can lead to fully assembled IgG and one of these pathways may be utilized either predominantly or in parallel with another (3, 6, 7). Recently we described the kinetics of the glutathione-catalyzed *in vitro* reoxidation of several human (6) and mouse (7) myeloma proteins and simulated the kinetics using a simple mathematical model. In the model we assumed that the formation of an interchain disulfide bond followed second-order reaction kinetics, and that formation of the two categories of interchain disulfide bonds proceeded independently and were governed by different rate constants. Within the limits of the experimental error, this simple model appeared to account for the main features of the *in vitro* reoxidation throughout a considerable portion of the time course (6, 7).

In this paper, we examine the kinetics of *in vitro* reoxidation and reduction of a single category of interchain disulfide bond (the inter H–L bond) in an unusual murine IgG myeloma protein lacking inter-H chain disulfide bonds, MOPC 173B.

Materials and Methods

Protein Purification

MOPC 195 (IgG2b,κ) and MOPC 173 (IgG2a,κ) H_2L_2 myeloma proteins were purified from the serum of female Balb/C mice bearing the myeloma tumours subcutaneously, using a combination of ammonium sulfate fractionation, DEAE-cellulose chromatography, and gel filtration on Sephadex G 150 in 0.5 *M* NaCl as described previously (7). Both tumour lines were supplied by Dr. M. Potter.

Following subcutaneous passage in Balb/C mice over a period of 5 years in our laboratory, the MOPC 173 line became the producer of an IgG2b,κ myeloma protein, MOPC 173B, that appeared on SDS-PAGE to be a half-molecule myeloma. MOPC 173B was purified from the serum of tumour-bearing mice using the same procedure as described for MOPC 173 H_2L_2 (7).

Antisera

H and L chain types were determined in immunodiffusion tests using antisera specific for mouse IgG 1, IgG2a, IgG2b, κ, and λ chains (Litton Bionetics, Baltimore, MD).

SDS-PAGE

The phosphate-buffer gel system of Weber and Osborn (5, 9) was used for analysis of the purified proteins, and for identification and quantitation of intermediates in the reoxidation and reduction experiments. The apparent molecular weights of the constituent H and L chains of the completely reduced and alkylated proteins were determined on 12.5% slab gels, using the discontinuous system of Laemmli (10). Proteins were visualized by staining with Coomassie Blue (5).

Sedimentation Velocity Studies

A Spinco model E ultracentrifuge operated at 60 000 rpm was used for all sedimentation velocity experiments. The temperature was maintained at 20 ± 0.01°C. Sedimentation coefficients were obtained for unreduced and partially reduced proteins alkylated with iodoacetamide under the following conditions as described in a previous paper (7): (*i*) at the pH 5 stage of reoxidation following dialysis against 1 *M* acetic acid, and then against 4 m*M* sodium acetate, pH 5; (*ii*) at the pH 8.2 stage of reoxidation following dialyses against 1 *M* acetic acid, 4 m*M* sodium acetate, pH 5, and then against 0.1 *M* Tris–HCl – 0.1 *M* NaCl, pH 8.2. All dialyses were performed at 4°C. In these experiments, the protein concentrations were 0.2 and 3 mg/mL. The schlieren optical system was employed in the latter case, the uv absorption system in the former.

Peptide Mapping

Peptic–tryptic maps of the interchain disulfide bridge peptides were made using the procedure described by Frangione et al. (11).

Reoxidations

In vitro reoxidations were carried out at 21°C as described previously (7) in the presence of 5×10^{-3} *M* disodium EDTA using a mixture of reduced and oxidized glutathione as a disulfide interchange catalyst.

Reductions

Protein solutions (3 mg/mL) in 0.1 *M* Tris–HCl – 0.1 *M* NaCl, pH 8.2, containing 5 m*M* disodium EDTA were reduced in a nitrogen atmosphere with 2 m*M* DTE at 21°C. Reduction was stopped at various times by pipetting 10- to 50-μL aliquots of the protein solution into 0.2 mL of 0.1 *M* iodoacetamide in 0.1 *M* Tris–HCl – 0.1 *M* NaCl, pH 8.2.

Quantitation of the Reoxidation and Reduction Intermediates

Intermediates were resolved in 8 × 0.6 cm cylindrical gel rods as previously described (5, 7). The gels were stained with Coomassie Blue and the proteins were quantitated by densitometry at 580 nm. In all calculations, the staining intensity per weight of protein was assumed to be constant for each intermediate. The quantity of protein in each band was expressed as a percentage of the total absorbance units on the gel, i.e., percent relative absorbance. This procedure eliminated random sampling error (7).

Results

Protein Characterization

On SDS–PAGE the MOPC 173B myeloma protein

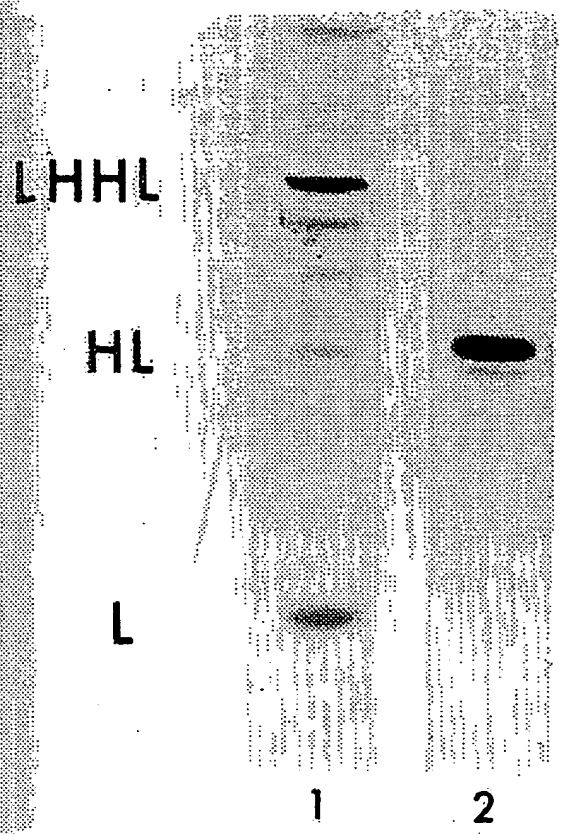

FIG. 1. Analysis of intact MOPC 173B by SDS–PAGE. Slot 1, a partially reoxidized preparation of a typical IgGb,κ protein (MOPC 195), showing the positions of L, HL, and LHHL; slot 2, MOPC 173B (about 15 μg). The bands were visualized by staining with Coomassie Blue.

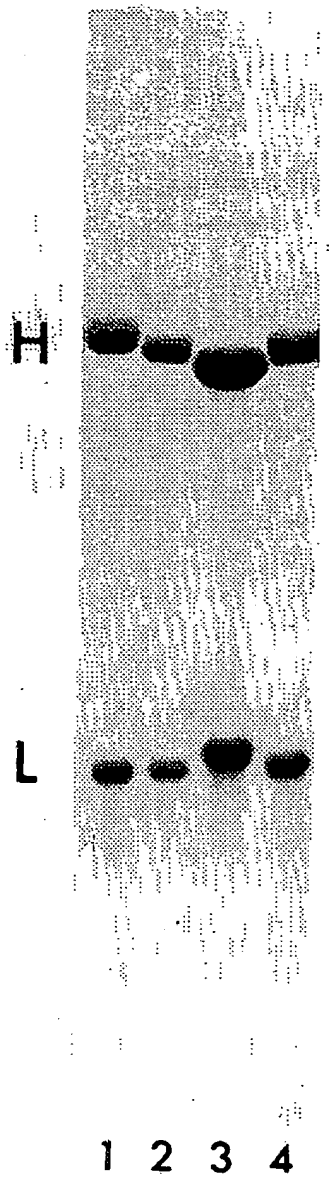

FIG. 2. Analysis of reduced and alkylated mouse IgG myeloma proteins by SDS–PAGE. About 15 μg of each protein were applied to the 12.5% gel, following complete reduction and alkylation. Slot 1, subunits of a typical IgG2b,κ protein (MOPC 195); slots 2 and 4, MOPC 173B; slot 3, MOPC 173 H_2L_2. The mobility differences seen on this gel were reproducible and not caused by concentration differences of the H's and L's. Both the H and L chains of MOPC 173B clearly differ from those of MOPC 173 H_2L_2.

migrated predominantly as a single band with a corresponding molecular weight of 77 000 and comigrated with the half-molecule intermediate formed in *in vitro* reoxidation experiments with a typical IgG2b,κ protein, MOPC 195 (Fig. 1). Like MOPC 195 and the original MOPC 173 H_2L_2 protein (IgG2a,κ), MOPC 173B was shown to contain equimolar proportions of H and L chains (Fig. 2). In contrast with MOPC 173 H_2L_2, which is an IgG2a,κ protein (7), MOPC 173B exhibited a reaction of identity with a typical IgG2b,κ protein, MOPC 195, in immunodiffusion tests with anti-IgG2b and anti-κ antisera. There was no reactivity to the anti-2a serum. As shown in Fig. 2, the H chains of MOPC 173B appeared to be 3000 daltons larger than the H derived from MOPC 173 H_2L_2, and 2500 daltons smaller than the H of MOPC 195 H_2L_2. The L chains of MOPC 173B appeared to be about 2500 daltons smaller than the L chains of MOPC 173 H_2L_2, but identical in size to the L chains of MOPC 195 H_2L_2. These differences in apparent molecular weights were calculated using the following immunoglobulin subunits, completely reduced and alkylated, as markers: MOPC 104E μ, 72 000; IgG EN H, 53 000; IgG EN L, 22 500. IgG EN is a human IgG1,κ myeloma protein that was used in our initial *in vitro* reoxidation experiments (6).

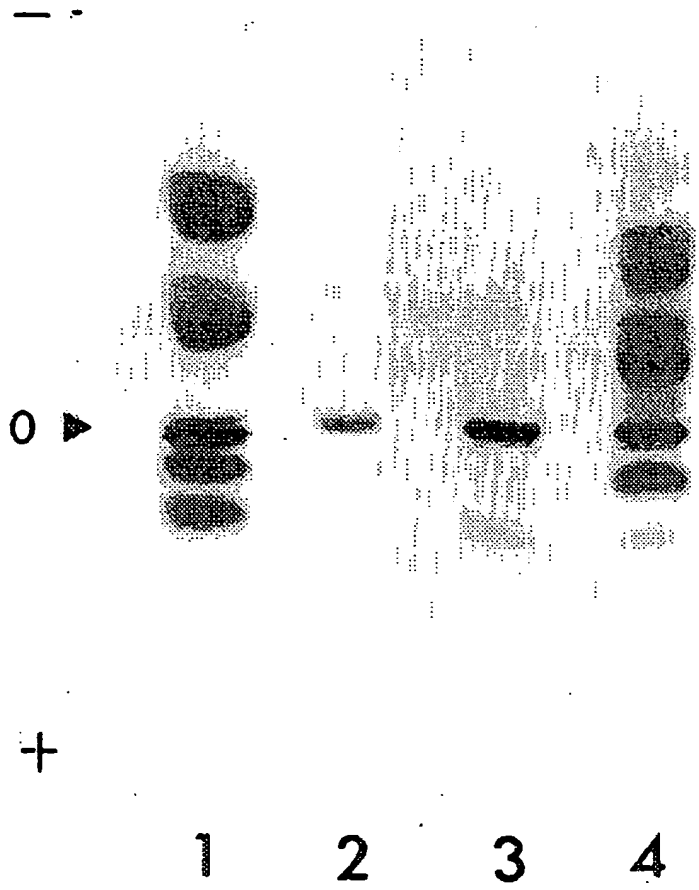

FIG. 3. Interchain disulfide bridge peptides of MOPC 173B and controls. These maps were made using the procedure of Frangione et al. (11). The proteins were partially reduced using conditions that cleaved only interchain bonds, alkylated with ^{14}C iodoacetate, and subjected to digestion with pepsin and trypsin. The digest was then resolved by high-voltage electrophoresis and the one-dimensional map was subjected to autoradiography. Only peptides containing free sulfhydryl groups become labelled using this procedure. Slot 1, MOPC 173 H_2L_2; slots 2 and 3, MOPC 173B; slot 4, MOPC 195 H_2L_2. Identical peptide maps were obtained when the proteins were alkylated with unlabelled iodoacetate prior to the reduction, showing that the radiolabelled peptides were derived from interchain disulfide bonds. The peptides shown in slots 2 and 3 are derived from the inter H–L disulfide bridge of MOPC 173B, the band near the origin from the H chain, the more anodic one from the L chain.

MOPC 173B does not possess any free, titratable SH groups. Peptide mapping studies (Fig. 3) showed that it contains only a single category of interchain disulfide bond linking the H and L chains; the inter-H chain bonds typical of other IgG2b proteins were not detectable. The two peptides derived from the inter H–L bridge in the half-molecule myeloma comigrated with peptides of the same relative intensity from the MOPC 195 H_2L_2 protein (Fig. 3) indicating that the inter H–L bridges in the two proteins are likely identical.

Reoxidation Experiments

The *in vitro* reoxidation system was designed so that noncovalent association between H and L would be established prior to initiation of disulfide bond formation (5). In previous sedimentation velocity experiments with an IgG2b,κ protein, MPC 11, we showed that noncovalent association was complete both at the pH 5 and pH 8.2 stages of reoxidation (7). In the current experiments we found that MOPC 195 H_2L_2 and MOPC 173B were also completely noncovalently associated in sedimentation velocity experiments at the pH 5 and the pH 8.2 stages of reoxidation at concentrations of both 0.2 and 3 mg/mL. In both cases, the sedimentation coefficients of the partially reduced and alkylated proteins did not differ significantly from those of the unreduced, native proteins (MOPC 195 H_2L_2, 6.0 $\pm$ 0.15S; MOPC 173B, 6.3 $\pm$ 0.15S). We showed previously that in the

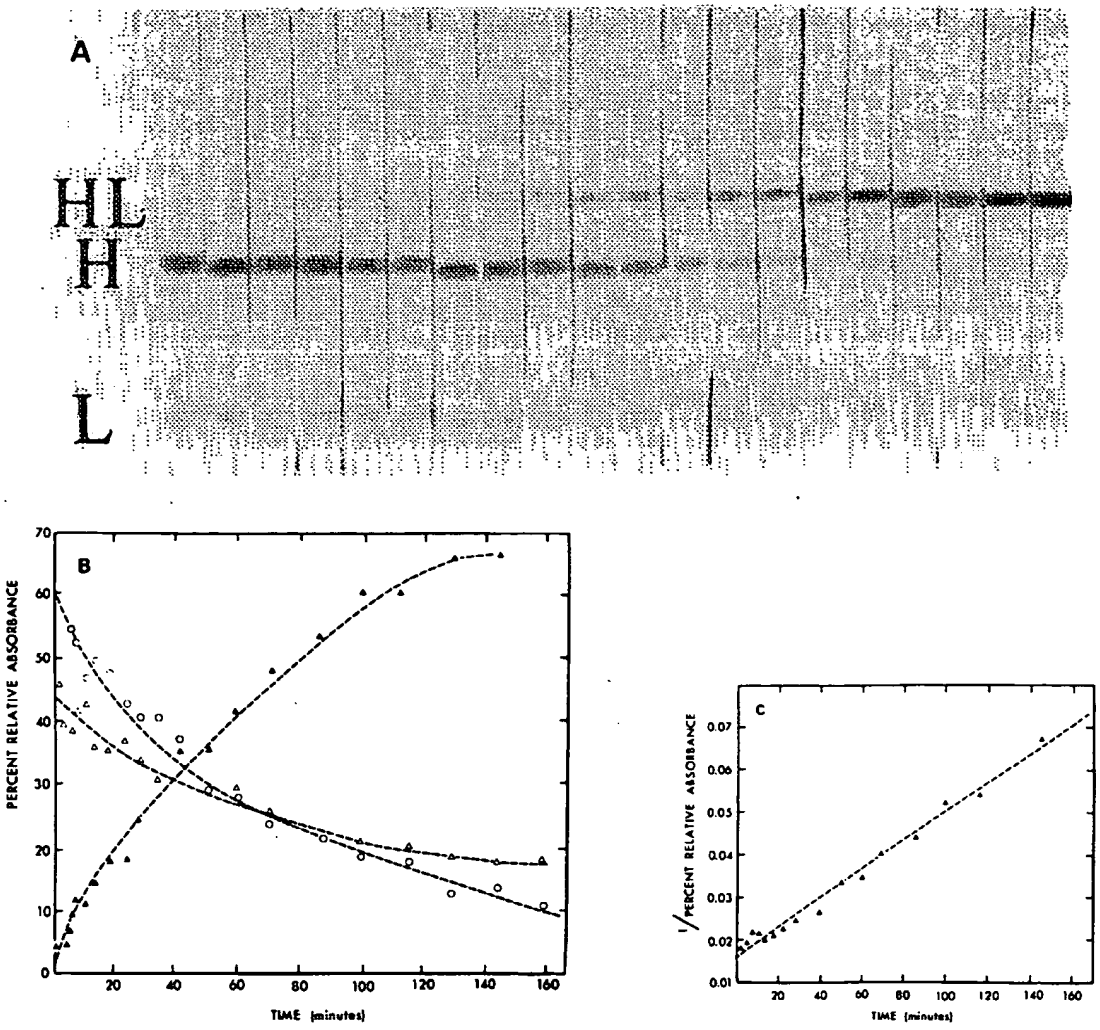

FIG. 4. (A) Resolution of the reoxidation intermediates of MOPC 173B by SDS–PAGE. As indicated in Methods, the protein was partially reduced. Following dissociation and reestablishment of noncovalent association, it was allowed to reoxidize using a mixture of reduced and oxidized glutathione as a disulfide interchange catalyst. The reaction was stopped at various times by the addition of iodoacetamide, and the reaction products were resolved by SDS–PAGE. After being stained with Coomassie Blue, the gels were scanned at 580 nm. Bands of L and H reassemble into HL, with the formation of H_2, H_2L, and H_2L_2 being minimal. Intermediates were analyzed at the times indicated in Fig. 4B. (B) Kinetics of the *in vitro* reoxidation of MOPC 173B. The percentages of the total amount of the protein on each gel in (percent relative absorbance) H (○ - - ○), L (△ - - △), and HL (▲ - - ▲) were plotted as a function of time. (C) A second-order plot of the reoxidation kinetics of MOPC 173B. The reciprocals of the percent relative absorbance of H (from Fig. 4B) were plotted against times of reoxidation. The regression line of best fit, determined using the method of least squares, is 1/percent relative absorbance of H = $(0.000341 \pm 0.000011)t + 0.016$ (correlation coefficient = 0.993).

case of MOPC 173 H_2L_2, noncovalent association was not completely established at the pH 5 stage of reoxidation (7).

The kinetics of the glutathione-catalyzed reoxidation of MOPC 173B are shown in Figs. 4A and 4B. The decrease in free H and L chains is accompanied by an increase in the amount of HL, the formation of H_2, H_2L, and H_2L_2 being minimal. In Fig. 4C we have plotted the reciprocals of the percent relative absorbance of H shown in Fig. 4B as a function of the time of reoxidation. The resulting plot is linear, indicating that reoxidation of the inter H–L bond in MOPC 173B is an apparent second-order reaction. Traditionally, a reaction is classified as second order if the rate of the reaction is proportional to the square of the concentration of one of the reagents, or to the product of the concentration of two species of

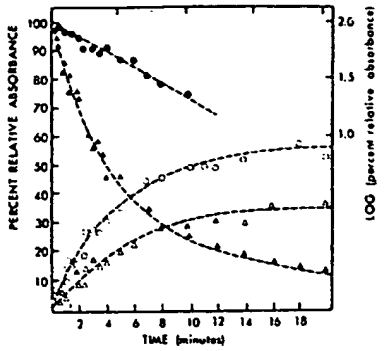

FIG. 5. Kinetics of reduction of MOPC 173B with dithioerythritol. As indicated in Methods, the protein was reduced anaerobically with DTE. The reduction was stopped at various times by the addition of iodoacetamide, and the reaction products were resolved by SDS–PAGE. After being stained with Coomassie Blue, the gels were scanned at 580 nm. The percentages of the total amount of protein on the gel (percent relative absorbance) in H (○- -○), L (△- -△), and HL (▲- -▲) (left-hand ordinate axis) were plotted as a function of the time of reduction. Also, the log (percent relative absorbance of HL) values, (●- -●) (right-hand ordinate axis) were plotted as a function of time. The linearity of this latter function shows that reduction of the H–L disulfide bridge in MOPC 173B is an apparent first-order reaction. The regression line of best fit, determined using the method of least squares, is log (percent relative absorbance of HL) = (− 0.0609 ± 0.0034) t + 1.971 (correlation coefficient = 0.982).

reagents. The second situation leads to the same equations as the first if the two reactants are used up at the same rate, and if their initial concentrations are equal. For those situations, $-dc/dt = Kc^2$ where c is the concentration of the single reagent or of one of the two reagents. In the integrated form $1/c - 1/c^\circ = Kt$, or a plot of $1/c$ versus t gives a straight line (12). In our studies, we have used 'percent relative absorbance of H' in place of 'concentration of H'. Hence we have introduced the term 'apparent' to qualify the order of the reoxidation.

Reduction

The reduction of MOPC 173B was carried out anaerobically using DTE in excess. The kinetics of the reduction of MOPC 173B are shown in Fig. 5. The decrease in amount of HL is accompanied by an increase in the amounts of free H and L chains. When log (percent relative absorbance of HL) was plotted against the time of reduction (solid circles joined by a broken line, right-hand ordinate axis), the function was linear, thus indicating that the reduction process followed simple apparent first-order kinetics. Traditionally, a first-order reaction is one in which the rate of the reaction depends only on the first power of the concentration of a single reacting species. If the concentration of this species is represented by c, and the volume of the system remains essentially constant throughout the reaction, then the first-order rate law can be written as $-dc/dt = Kc$. In the integrated form, $\log c = -K/2.303t + \log c^\circ$. A reaction can therefore be said to be a first-order reaction if a plot of $\log c$ against t gives a straight line (12). As in the reoxidation study, we have used 'percent relative absorbance of HL' in place of 'concentration of HL', and hence have again introduced the term 'apparent' to qualify the order of the reduction.

Discussion

In this paper, we have described an unusual murine IgG2b,κ myeloma protein, MOPC 173B, which possesses only a single category of interchain disulfide bond (the inter H–L bridge), and we have characterized the kinetics of its *in vitro* reoxidation and reduction. This unusual protein was produced by the MOPC 173 line, originally an IgG2a,κ H_2L_2 producer, after 5 years of subcutaneous transfer in Balb/C mice. Analysis of serum samples from these tumour-bearing mice by SDS–PAGE showed a progressive increase in the amount of the 2b,κ protein and a progressive decrease in the amount of 2a,κ parent during this time interval.

On SDS–PAGE, MOPC 173B migrates with an apparent molecular weight of 77 000 and like typical IgG myeloma proteins, it contains an equimolar proportion of H and L chains. The protein contains a typical IgG2b,κ inter H–L disulfide bridge, but inter-H chain cysteinyl residues cannot be detected following reduction and alkylation with radioactive iodoacetate. In immunodiffusion tests, it appears to be a typical IgG2b,κ protein. The L chains of completely reduced MOPC 173B appear to be 2500 daltons smaller than those of MOPC 173 H_2L_2 and its H chains 3000 daltons larger than those of MOPC 173 H_2L_2. In a nondissociating solvent, the sedimentation coefficient is 6.3S indicating that noncovalent forces link two HL subunits into a structure resembling typical IgG.

The origin of MOPC 173B is currently a mystery and requires further investigation. The parent IgG2a H_2L_2-producing MOPC 173 tumour line may have 'switched' to an IgG2b HL-producer. If this is so, it would represent the first documented *in vivo* spontaneous conversion of γ2a to γ2b H chain production. Mutagen-induced conversion of γ2b H chains to H chains of the γ2a serotype have been documented using the *in vitro* tissue culture adapted MPC 11 myeloma cell line (13). A more likely explanation for the MOPC 173B protein is that it originated as a contaminant of the original MOPC 173 line, eventually overgrowing and replacing it. Using SDS–PAGE, half molecules have been found to varying degrees in other mouse myeloma tumour lines. Firstly, in the IgG2b-producing MPC 11 tumour, HL exists together with H_2L_2 and represents an end product of biosynthesis rather than a precursor of the latter (14). Secondly, in the IgA-producing Adj PC6C myeloma, HL subunits are synthesized exclusively, independently of H_2L_2 which is produced by the parent Adj PC6A myeloma tumour (15). Thirdly, we recently purchased some purified MOPC 195 IgG2b from Litton Bionetics, Baltimore, Maryland, and found that on SDS–PAGE the protein existed as a half molecule and was indistinguishable from MOPC 173B on isoelectric focusing, although MOPC 195 that we purified

in our laboratory was typical H_2L_2. Comparative structural studies are presently being carried out with the H and L chains from MOPC 173 H_2L_2 and MOPC 173B to resolve the issue of whether the latter tumour represented a contaminant of the former, or a switch of the MOPC 173 γ2a H chain to the γ2b serotype.

The MOPC 173B myeloma protein has fortuitously proven to be an ideal system for investigation of the kinetics of interchain disulfide bond oxidation and reduction, since it contains only one category of interchain disulfide bond, that linking the H and L chains. When the protein was partially reduced *in vitro*, it reassembled back into a half molecule, with the formation of H_2, H_2L, and H_2L_2 being minimal. In this study, we were thus able to show that using the glutathione-catalyzed *in vitro* reoxidation system devised by Petersen and Dorrington (5), reoxidation of this H–L bridge followed apparent second-order reaction kinetics. This observation therefore provides the experimental basis for the theoretical model that we devised previously to simulate the assembly of typical IgG (6, 7). In this model we made the assumption that formation of both the inter H–L and inter-H bonds followed second-order reaction kinetics, but that the two categories of interchain bonds were characterized by different rate constants. The finding that covalent assembly of a single category of disulfide bond follows an apparent second-order rate equation does not conflict with the observation that the H and L chains are noncovalently bound and are likely not freely interacting. It is important to remember that the order of a reaction and the rate equations are convenient ways of summarizing experimental results and of analytically portraying the experimental data (12) although they can reflect the molecular mechanism of the reaction. We previously suggested that the apparent second-order kinetics reflected the mechanism by which disulfide bond formation was being catalyzed (7).

In contrast with the reoxidation, reduction of the inter H–L bridge in MOPC 173B under anaerobic conditions, using DTE in excess, followed apparent first-order kinetics and was not a simple reversal of the reoxidation. We show in a subsequent paper (Percy, Chang, Demoliou and Baumal, in preparation) that the reduction of both the inter H–L and inter-H categories of disulfide bonds in typical immunoglobulins are also first-order processes, but governed by different rate constants.

Our theoretical models for reoxidation and reduction differ from those presented by Sears et al. (8, 16), who assumed that both the reoxidation and reduction of a disulfide bond followed a zero-order rate equation. However, the experimental reoxidation system used by these investigators cannot be directly compared with ours because it employed a divalent metal ion – O_2 catalyst, rather than a mixture of reduced and oxidized glutathione which catalyzes disulfide bond formation by disulfide interchange. Moreover, the theoretical model developed by Sears et al. was intended to represent changes in numbers of titratable sulfhydryl groups, not of unassembled and partially assembled intermediates, as in our case. However, these authors did not consider the possibility that rate equations other than zero-order reactions would have produced better simulations of their experimental reoxidations and reductions.

Our studies indicate that the *in vitro* covalent assembly and reduction of interchain disulfide bonds in immunoglobulin molecules are basically simple reactions that can be represented by conventional chemical rate laws.

Acknowledgment

This research was supported by grant MA 4596 from the Medical Research Council of Canada.

1. Svasti, J. & Milstein, C. (1972) *Biochem. J. 126*, 837–850
2. De Preval, C., Pink, J. R. & Milstein, C. (1970) *Nature (London) 228*, 930–932
3. Baumal, R., Potter, M. & Scharff, M. D. (1971) *J. Exp. Med. 134*, 1316–1334
4. Percy, J. R., Percy, M. E. & Baumal, R. (1976) *Can. J. Biochem.* 54, 688–698
5. Petersen, J. G. L. & Dorrington, K. J. (1974) *J. Biol. Chem. 249*, 5633–5641
6. Percy, J. R., Percy, M. E. & Dorrington, K. J. (1975) *J. Biol. Chem. 250*, 2398–2400
7. Percy, M. E., Baumal, R., Dorrington, K. J. & Percy, J. R. (1976) *Can. J. Biochem. 54*, 675–687
8. Sears, D. W., Mohrer, J. & Beychok, S. (1975) *Proc. Natl. Acad. Sci. U.S.A. 72*, 353–357
9. Weber, K. & Osborn, M. (1969) *J. Biol. Chem. 244*, 4406–4412
10. Laemmli, U. K. (1970) *Nature (London) 227*, 680–685
11. Frangione, B., Milstein, C. & Franklin, E. C. (1969) *Nature (London) 221*, 151–152
12. Barrow, G. M. (1974) in *Physical Chemistry for the Life Sciences*, pp. 310–315, McGraw-Hill Book Company, New York
13. Morrison, S. L., Baumal, R., Birshtein, B. K., Kuehl, W. M., Preud'homme, J. L., Frank, L., Jasek, T. & Scharff, M. D. (1974) *Cellular Selection and Regulation in the Immune Response* (Edelman, G. M., ed.), pp. 233–244, Raven Press, New York
14. Laskov, R., Lanzerotti, R. & Scharff, M. D. (1971) *J. Mol. Biol. 56*, 327–339
15. Mushinski, J. F. (1971) *J. Immunol. 106*, 41–50
16. Sears, D. W., Mohrer, J. & Beychok, S., (1977) *Biochemistry 16*, 2031–2035

Molecular Immunology, Vol. 25, No. 10, pp. 1019–1024, 1988
Printed in Great Britain.

0161-5890/88 $3.00 + 0.00
Pergamon Press plc

A MOLECULAR-MECHANICS STUDY OF THE CONFORMATION OF THE INTERCHAIN DISULFIDE OF HUMAN IMMUNOGLOBULIN G4 (IgG4)*

MARK E. SNOW† and L. MARIO AMZEL‡
The Laboratory for Molecular Structure and Function, Department of Biophysics, The Johns Hopkins University, School of Medicine, Baltimore, MD 21205, U.S.A.

(*Received* 24 *March* 1988; *accepted* 25 *April* 1988)

Abstract—The conformation of the interchain disulfide bond between the light and the heavy chains of human immunoglobulin G4 (IgG4) was modeled based on the known structure of a human IgG1 Fab. Exploration of a large number of conformations followed by energy minimization using molecular mechanics methods rendered a plausible model for the disulfide. In this model the disulfide adopts the long, *trans-gauche-trans* configuration found in immunoglobulin *intrachain* bridges and not the conformations most commonly observed in other proteins (left-handed spiral or right-handed hook). Heavy chain residues H217 and H218 pack tightly against the disulfide and put restrictions on which sequences can exist in the proposed conformation. Sequence analysis at these positions shows that: (a) all human IgG4 and IgG3 are compatible with the model; (b) IgG2 and human immunoglobulins of other classes cannot adopt the conformation proposed for IgG4.

INTRODUCTION

In most immunoglobulins, the light and heavy chains are covalently linked by an interchain disulfide bridge. While this interchain disulfide always involves the penultimate residue of the L chain (cys L213),§ the residue from the H chain varies, depending on the immunoglobulin class (Nisonoff, 1982). In human IgG1 the intrachain disulfide involves cys 217 of the heavy chain (cys H217), while most other human immunoglobulin classes and subclasses use instead cys H123. The origin of these alternate connectivities of disulfides is not known but is probably related to class and subclass specific biological functions. Knowing the detailed conformation of these interchain disulfides in all immunoglobulin classes is necessary for understanding class specific phenomena and for the formulation of experiments to establish structural correlates of Ig biological functions.

The structure of the disulfide between cys L213 and cys H217 is known from crystallographic studies of Fab fragments (Fig. 1; Poljak *et al.*,1973; for reviews see Amzel and Poljak, 1979; Davis and Metzger, 1983; Padlan, 1977), but no reported structure describes the alternate disulfide between cys H123 and cys L213. It is known, however, that amino acid H123 lies in a bend which, although distant in sequence, is spatially close to the C-terminal sequence of C_H1 and very near to cys L213 (Fig. 1; Poljak *et al.*, 1973).

In this paper, a model is proposed for the alternate disulfide between cys H123 and cys L213 based on an analysis by molecular mechanics methods of the conformations accessible to the disulfide present in IgG4. The study is based on the crystallographically determined structure of a human IgG1 (Saul *et al.*, 1978), the sequence of a human IgG4 (Pink *et al.*, 1970), and modeling procedures and energy equations which have previously been tested on immunoglobulins (Snow, 1986; Snow and Amzel, 1986).

MATERIALS AND METHODS

Sequences and coordinates

The coordinates of the X-ray crystal structure of the human IgG1 Fab New used in this work (Saul *et al.*, 1978) are identical to those in the Brookhaven Protein Data Bank. The sequence of the C_H1 of the human IgG4 (Vin) and its sequence alignment with the IgG1 C_H1 were obtained from Beale and Feinstein (1976). All other sequences are from Kabat *et al.* (1987). All calculations were performed with the Protein Conformation Analysis Package (PCAP) (Snow, 1986; Snow and Amzel, 1986). The regions of the molecule which are spatially near the interchain disulfide and which were consequently included in the modeling procedure were identified using the program LOCATE and visualized on an Evans and

*This work was supported with Supercomputing Grant DMB8605200 from the NSF grant AI20293 from NIH, and contract no. N0004-87-K-0487 of ONR. The Interactive Graphics Facility of the Department of Biophysics was established and is maintained by NIH and NSF grants and by a gift from the Richard-King Mellon Foundation.

†Present address: College of Pharmacy, University of Michigan, Ann Arbor, MI 48109, U.S.A.
‡Author to whom correspondence should be addressed.

§Residue numbering follows that of Fab New in the Brookhaven Protein Data Bank.

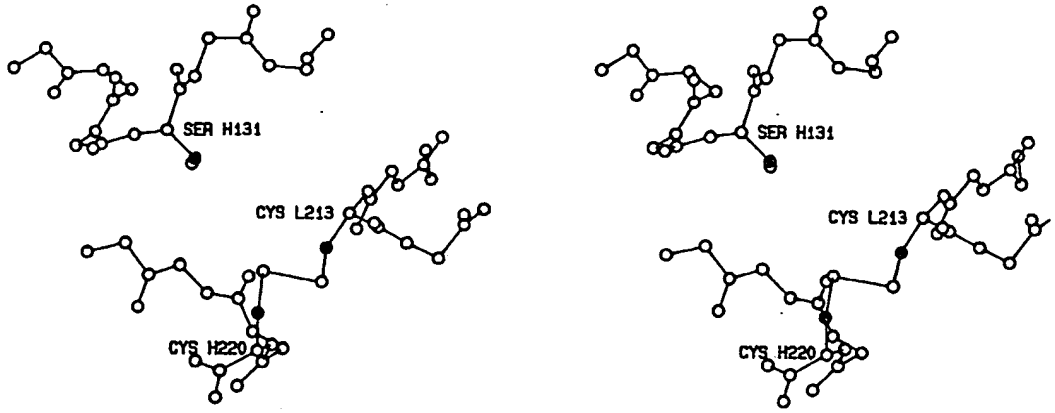

Fig. 1. Structure of the original cys H220 to cys L213 disulfide bond in the IgG1 Fab New. Main chain atoms for residues H129 to H134, H217 to H220 and L211 to L213 are also shown. The β-carbons of cys H220, ser H131 and cys L213 are highlighted (black filled atoms). The position of the residues H131 and L213 are correctly oriented to make the alternate disulfide found in IgG4.

Sutherland PS 330 Graphic System using the Structure Display Module (SDM) of PCAP.

Energy calculations and refinement

All residue replacements, and all energy calculations and refinements were performed using PCAP running on a VAX 8530 (VMS) or on the CRAY XMP of the Pittsburg Supercomputer Center. The functional form and the parameters of the energy equation have been described previously (Snow, 1986; Snow and Amzel, 1986) with the exception of the potential for the disulfide bridge dihedrals.

The functional form of the potential for the disulfide dihedrals was:

$$E_{S-S} = 0.5[1 + \cos(3\chi_1)] + 0.5[1 + \cos(3\chi_2)] + 1.45[1 + \cos(2\chi_3)] + 0.5[1 + \cos(3\chi_2')] + 0.5[1 + \cos(3\chi_1')] \text{ (in kcal/mol.)}.$$

The shape and barrier height of the potential about χ_3 is based on calculations by Perahia and Pullman (1971).

During the first stage of the refinements, a term representing a virtual bond between the alpha carbons of the two residues forming the new disulfide was added to the energy equation. This term serves to pull the disulfide together in fewer refinement cycles than would otherwise be required. Since it is turned off once ∇, the normalized gradient of the energy,* reaches 0.1, and is not used in any subsequent refinements, the results are insensitive to the exact parameterization. The form used for this term was a quadratic potential $1/2\,k(d - d_0)^2$ with $d_0 = 6.2$ Å and $k = 200$ kcal/(mol Å^2).

Generation of disulfide conformations

The region of conformational space accessible to the disulfide was sampled by building the nine conformations which are obtained for all combinations of χ_1 and χ_1' angles of 60°, 180° and −60°. Eighteen structures were obtained by minimizing the energy of each of these nine starting conformations according to two different refinement schemes.

Scheme 1. Using the disulfide virtual bond, refinement was carried to a value of $\nabla = 0.1$. During this refinement, the residues H130–H132 and L212–L214 were allowed to move freely. For residues H128, H129, H133 and H216–H220, the backbone was subject to an 80 kcal/(mol Å^2) penalty for movement while the side-chains were allowed to move freely. At this point the disulfide virtual bond was removed and refinement was carried to a value of 0.05 for ∇ during which backbone atoms of all of the above residues were subject to the penalty for movement and all side-chain atoms were allowed to move freely. Finally refinement was carried to a value of 0.025 for ∇ during which all atoms in the residues L213, L214 and H131 were allowed to move freely.

Scheme 2. Using the disulfide virtual bond, refinement was carried to a value of 0.1 for ∇. For residues L211–L214 and H129–H133, side-chains were allowed to move freely while backbone atoms were subject to a 25 kcal/(mol Å^2) penalty for movement. For residues H128 and H216–H220, side-chains moved freely while backbone atoms were subjected to a penalty of 80 kcal/(mol Å^2) penalty. Refinement to $\nabla = 0.05$ was carried out as in scheme 1 except that one additional residue, L211, was included in the refinement region. Refinement to $\nabla = 0.025$ was as in scheme 1.

*The normalized vector gradient of the energy,

$$\frac{1}{n}\sqrt{\sum \frac{\delta E^2}{\delta \vec{c}_i}},$$

where E is Energy, $\vec{c}$ are the atomic coordinates and n is the number of atoms, is used as a measure of the degree of convergence of a refinement.

Table 1. Conformations for the L213-H131 disulfide bond

Group	Number of cases*	Starting structures: scheme 1 χ_1, χ_1'	Starting structures: scheme 2 χ_1, χ_1'	Final structures† χ_2	χ_3	χ_4	E‡
Ia	8	60, 60	60, 60	174.0	−52.2	−170.6	0.0
		60, 180	60, 180	179.4	−54.5	175.5	
			180, 60	(7.2)	(3.7)	(4.6)	
		−60, 180	−60, 180				
			120, 60				
Ia′	2	180, −60	180, −60	147.0	−68.8	−157.3	34.2
				148.9	−67.0	−155.5	
				(1.2)	(1.3)	(1.3)	
Ib	2	180, 60	−60, −60	−172.5	−107.0	167.7	17.4
				178.7	−101.0	165.2	
				(6.3)	(4.2)	(1.8)	
IIa	8		60, −60	145.9	75.0	151.1	25.4
		180, 180	180, 180	149.5	64.5	156.9	
		−60, 60	−60, 60	(1.6)	(2.7)	(4.4)	
			120, 180				
			120, −60				
			240, 180				
IIb	2	60, −60		−165.3	133.7	−173.9	5.3
		−60, −60		−163.7	138.7	−176.6	
				(1.1)	(3.5)	(1.9)	

*There is a total of 22 structures; eighteen were generated by starting with all staggered combinations of χ_1 and χ_1' and four were selected from structures having χ_1 in an eclipsed configuration. This column contain the number of structures that were classified as belonging to this group. The next two columns contain the initial χ_1 and χ_1' of these structures.

†The first line in each group shows the dihedral angles for the lowest energy structure in the group. The second line shows the mean dihedral angles and the standard deviation. All values in degrees.

‡Conformational energies, in kcal/mol, are for the lowest energy structure in each group, and are measured relative to the lowest energy structure in group Ia.

In addition to the eighteen structures described above, four new structures were generated with χ_1, in an eclipsed configuration. These new starting structures were refined using scheme 2 (Table 1).

RESULTS

The overall modeling strategy (outlined in Table 2) was used to analyze all conformations accessible to the intrachain disulfide. The following section gives further detail for the different steps.

Introduction of the disulfide bond

The disulfide bridge was introduced by replacing serine H131 of Fab New (Fig. 1) with a cysteine and replacing cysteine H220 with a glycine. At this stage residues H133, H217 and H219 were replaced with alanines (shown as glycines in Fig. 1 to facilitate following the chain). Because the disulfide is initially very long (C_α to C_α distance = 7.27 Å), a virtual bond was introduced between the two cysteine α-carbons in order to bring the sulfurs close in fewer refinement

Table 2. Modeling strategy

Step 1	Start with IgG1 coordinates (Fab New) Make the following substitutions ser H123 → cys cys H220 → gly H133, H217, H219 → ala.
Step 2	Generate initial conformations Use all combinations of χ_1, χ_1' equal to −60°, 180° and 60° (staggered)—generates nine conformations. Use some combinations with χ_1 equal to 120° and 240° (eclipsed)—generates four conformations.
Step 3	Refine with scheme 1 Use all staggered conformations—generates nine structures.
Step 4	Refine with scheme 2 Use all staggered conformations—generates nine structures. Use eclipsed conformations—generates four structures.
Step 5	Group conformations (Table 1)
Step 6	Restore side chains Ala residues at positions H133, H217 and H219 were restored to the correct side chains arg, ser and tyr in structures Ia and IIb.
Step 7	Refine structures generated in step 6. Refine the Ia and IIb structures. Compare their energies.

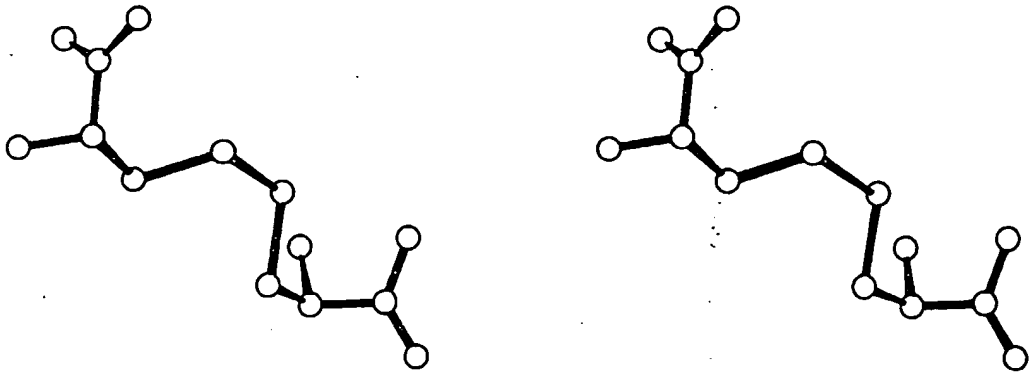

Fig. 2. Proposed conformation of the alternate interchain disulfide bridge. Only the atoms of the two half-cysteins are shown (both atoms bound on each C′ are shown). The orientation is similar to that of Fig. 1 with cys H131 at the top and cys L213 at the bottom.

cycles. This term was used during the initial stage of refinement only.

By building the cysteines with all combinations of χ_1, and χ'_1 equal to 60°, 180° and −60°, and using two different refinement schemes, eighteen refined potential structures for the region were obtained (Table 1). The conformations of the disulfide bridges in these structures fall into five distinct groups. Within each group, slight differences exist in the refined disulfide conformation because of different χ_1 and χ'_1 values and because of positional differences in other residues.

To ascertain whether the conformational space had been samples finely enough, four new structures ($\chi_1 = 120°$, $\chi'_1 = 60°$), (120°, 180°), (120°, 300°) and (240°, 180°) were built and refined using scheme 2. Since each of the new refined structures fell into one of the five groups, no further structures were generated. The conformations that fell in group Ia generally had much lower energy than those in the other groups (Table 1).

Effect of other substitutions

The side-chains of arg H133, ser H217 and tyr H219 were added to the lowest energy structure of group Ia to study the effect of these residues on the disulfide conformation. The new sidechains were built in 10 energetically favorable conformations, and all the resultant structures were refined to minimize their energies. In all cases, very slight changes in the disulfide conformation and conformational energy were found, but in no case did the conformation change enough to be classified as belonging to a new group. This procedure was intended only to explore the effect of the new side-chains on the disulfide conformation, not to model the conformation of the other side-chains accurately.

The side-chains were also added to the lowest energy structure in group IIb, and a similar analysis was performed. Again, no significant changes in conformation were observed. All conformations generated in this test were of higher energy than those from Group Ia, suggesting that conformation Ia is indeed the preferred conformation (Fig. 2).

DISCUSSION

Extent of sampling

Extensive analysis of the conformations accessible to the disulfide bridge was accomplished by starting at all the combinations of χ_1 and χ'_1 angles in staggered configurations (Ponder and Richards, 1987; Moult and James, 1986). In addition, by using two different refinement schemes the structures produced are not biased by the refinement strategy. Since the eighteen structures obtained have only five different disulfide conformations (the five groups in Table 1) it appears that the procedure accomplished an exhaustive sampling of the accessible conformations. The use of two refinement schemes did indeed contribute to the extent of conformational space sampling. Some of the five groups contain structures produced by both refinement schemes but others contain structures produced by only one scheme. In many cases the same initial structure produced different disulfide conformations with each scheme. To further evaluate the extent of sampling of the conformational energy surface, four additional structures each having one of the χ_1 angles in the eclipsed configuration were refined using scheme 2. All four structures after refinement could be clearly assigned to one of the five groups (Table 1). These results were taken as further indications that the procedures used render a quite complete evaluation of the minima of the conformational energy surface.

Disulfide conformation

While most disulfides in globular proteins assume either a left-handed spiral or a right-handed hook conformation, the intrachain beta-barrel spanning disulfides in immunoglobulins tend to be longer and

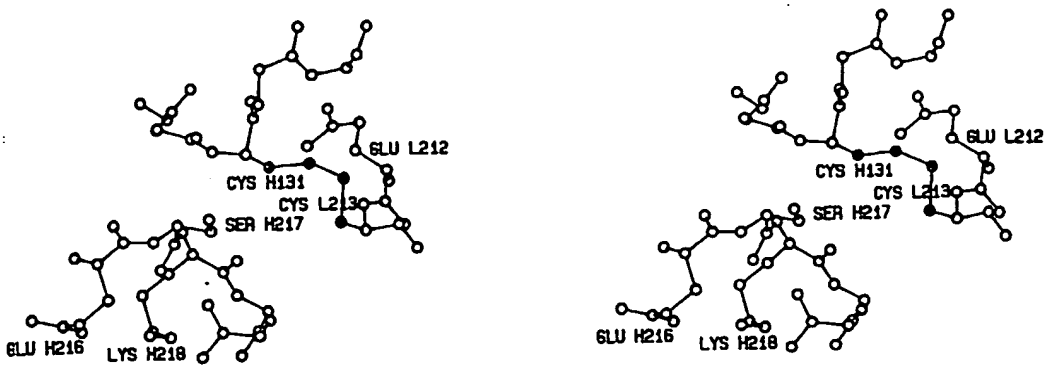

Fig. 3. model of the proposed conformation of the alternate interchain disulfide bridge. Atoms of the main chain residues H129 to H133, H216 to H220 and L212 to L213 are shown. Several important side chains are also included in the drawing. The orientation is similar to that of Fig. 1. The side chains of cys H131 and cys L213 are highlighted.

to have a *trans-gauche-trans* conformation with χ_2 and χ_2' near 180°, χ_3 near +90° or −90° and χ_1 and χ_1' variable (Richardson, 1981; Thornton, 1981). A more recent survey by Katz and Kossiakoff (1986) has categorized many conformations which do not fall into one of these traditional groups.

Although the interchain disulfide does not span a beta-barrel, the disulfide conformation found in this study ($\chi_1 = -40°$, $\chi_2 = 174°$, $\chi_3 = -53°$, $\chi_2' = 171°$ $\chi_1' = 178°$], is except for a slight strain in χ_3, very close to the conformation commonly observed spanning immunoglobulin beta-barrels (Fig. 2) (Richardson, 1981; Thornton, 1981) and falls within the group of immunoglobulins disulfides identified by Katz and Kossiakoff (1986).

Proximity to C-terminus

The ability of cys L213 to form disulfides with cysteines at different positions in different immunoglobulin classes requires significant variability in spatial position of this residue. This variability is possible because of the proximity of cys L213 to the C-terminus of the L chain (residue 214).

Applicability to other sub-classes and classes

The class and subclass dependent biological functions of immunoglobulins do not appear to correlate with the connectivity of the heavy/light interchain disulfide bridge (Nisonoff, 1982). Greater insight can be gained by analyzing the conformation of the disulfides for different classes and subclasses. The calculations in this paper were performed for a specific sequence (human IgG4 Vin) but one can use the results obtained to analyze if other sequences could adopt the same conformation.

Residues which interact strongly with the disulfide bridge are the sidechain of glu L212, backbone atoms of residues H217 and H218, and the side-chain of residue H217 (Fig. 3). Glu H216 and lys H218 both point away from the disulfide while ser H217 packs against it. Since the crucial residues are present in all sequenced IgG4s (Kabat *et al.*, 1987), the model should be applicable to the conformation of this disulfide in IgG4s in general.

A survey of immunoglobulin sequences (sequence data from Kabat *et al.*, 1987) was made to determine if the model might be applicable to the other human IgG subclasses or to other human immunoglobulin classes. The human IgG3 sequences HER, FRO, JON, WIS and SPA show the same sequence pattern, except for glu-leu-lys rather than glu-ser-lys at positions H216–H218. This change could reasonably be accommodated.

Human IgG2 sequences have a number of differences which suggest that the disulfide conformation found in this study would not be a good model for their structure. The residues at H216–H218 are glu-arg-lys, which could not pack against the disulfide (arg is too bulky), and this is followed almost immediately by the inter-H-chain disulfides (IgG1, IgG3 and IgG4 have several more residues before the inter-H-chain disulfides begin). These differences suggest that IgG2s may have a different conformation at the C_H1-hinge interface than other IgG subclasses. This difference in conformation could be responsible for the resistance of unreduced IgG2 to papain digestion. It is also of interest that IgG2 is the only human IgG subclass that does not elicit passive cutaneous anaphylaxis in guinea pigs, and that this effector function has not been previously localized to a particular region of the antibody molecule (Nisonoff, 1982).

In human immunoglobulins IgG, IgM and IgA1 the H chain cysteine involved in the interchain disulfide is at the position observed in IgG2, IgG3 and IgG4, nor that observed in IgG1. An analysis of the surrounding regions indicate that these molecules, like IgG2, could not accommodate the disulfide conformation proposed for IgG3 and IgG4.

Acknowledgements—The authors wish to thank Drs E. E. Lattman, Carl Pabo and B. Frangione for helpful comments and suggestions.


MEDICI
12 B

REFERENCES

Amzel L. M. and Poljak R. J. (1979) Three-dimensional structure of immunoglobulins. *A. Rev. Biochem.* **48**, 961–997.

Beale D. and Feinstein A. (1976) Structure and function of the Constant regions of immunoglobulins. *Q. Rev. Biophys.* **9**, 135–180.

Davis D. R. and Metzger H. (1983) Structural basis of antibody function. *A. Rev. Immun.* **1**, 87–117.

Kabat E. A., Wu T. T., Reid-Miller M., Perry H. M. and Gottesman K. S. (1987) *Sequences of proteins of Immunological Interest.* USHHS Publication.

Katz B. A. and Kossiakoff A. (1986) The crystallographically determined structures of atypical strained disulfides engineered into subtilisin. *J. biol. Chem.* **261**, 15,480–15,485.

Moult J. and James M. N. G. (1986) Algorithm for determining the conformation of polypeptide segments in proteins by systematic search. *Proteins* **1**, 146–163.

Nisonoff A. (1982) *Introduction to Molecular Immunology.* Sinaver Associates, Sunderland, Mass.

Padlan E. A. (1977) Structural basis for the specificity of antigen–antibody reactions and structural mechanisms for the diversification of antigen-binding specificity. *Q. Rev. Biophys.* **10**, 35–65.

Perahia D. and Pullman B. (1971) the conformational energy map for the disulphide bridge in proteins. *Biochem. biophys. Res. Commun.* **43**, 65–68.

Pink J. R. L., Buttery S. H., De Vries G. M. and Milstein C. (1970) Human immunoglobulin Sub-classes. Partial amino acid sequence of the constant region of a gamma-4 chain. *Biochem. J.* **117**, 33–47.

Poljak R. J., Amzel L. M., Avey H. P., Chen B. L., Phizackerley R. P. and Saul F. (1973) Three-dimensional structure of the Fab' fragment of a human immunoglobulin at 2.8A resolution. *Proc. natn. Acad. Sci. U.S.A.* **70**, 3305–3310.

Ponder J. W. and Richards F. M. (1987) Tertiary templates for protein. Use of packing criteria in the enumeration of allowed sequences for different structure classes. *J. molec. Biol.* **193**, 775–791.

Richardson J. S. (1981) The anatomy and taxonomy of protein structure. *Adv. Protein Chem.* **34**, 167–339.

Saul F. A., Amzel L. M., Poljak R. J. (1978) Preliminary refinement and structural analysis of the Fab fragment from human immunoglobulin New at 2.0 angstroms resolution. *J. biol. chem.* **253**, 585–597.

Snow M. E. (1986) *An approach to calculating the structural effect of mutations on the surface residues of proteins: theory and application to the system of immunoglobulins.* Ph.D. Dissertation. The Johns Hopkins University.

Snow M. E. and Amzel L. M. (1986) Calculating three-dimensional changes in protein structure due to amino-acid substitutions: the variable regions of immunoglobulins. *Proteins* **1**, 267–279.

Thornton J. M. (1981) Disulphide bridges in globular proteins. *J. molec. Biol* **151**, 261–267.